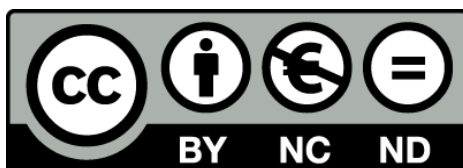


Multimodal MRI Study of Human Brain Connectivity: Cognitive Networks

Roser Sala Llonch

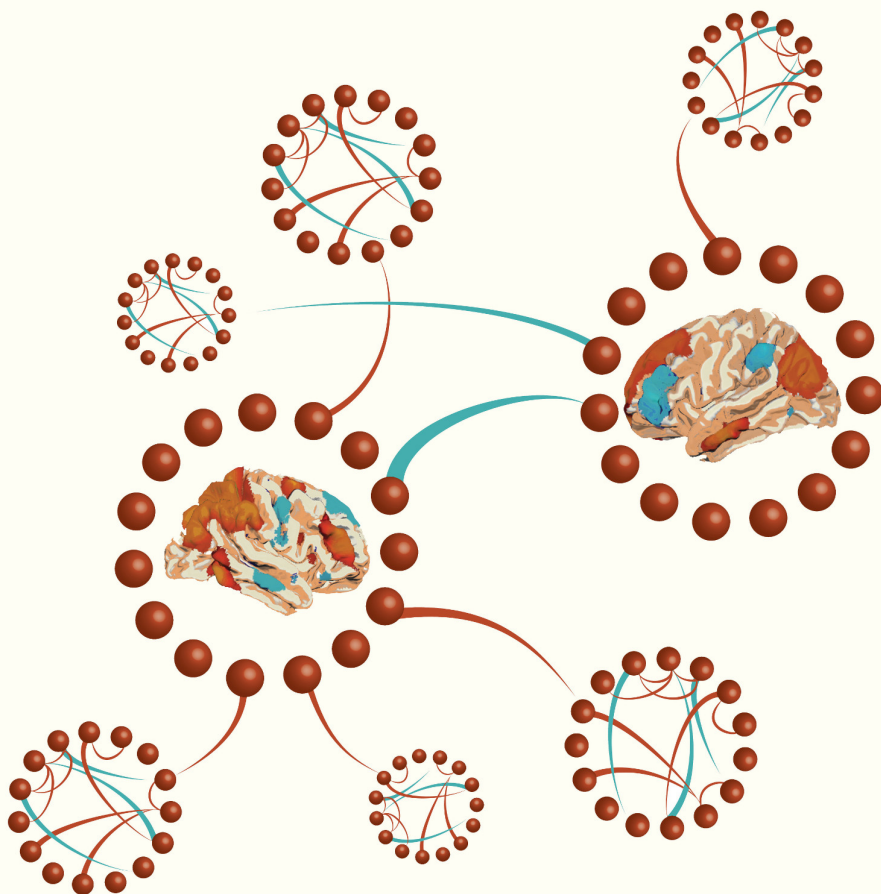


Aquesta tesi doctoral està subjecta a la llicència *Reconeixement- NoComercial – SenseObraDerivada 3.0. Espanya de Creative Commons.*

Esta tesis doctoral está sujeta a la licencia *Reconocimiento - NoComercial – SinObraDerivada 3.0. España de Creative Commons.*

This doctoral thesis is licensed under the *Creative Commons Attribution-NonCommercial-NoDerivs 3.0. Spain License.*

Multimodal **MRI** Study of Human Brain Connectivity: Cognitive Networks



Roser Sala Llonch

Department of Psychiatry and Clinical Psychobiology
University of Barcelona
January 2015

Multimodal MRI Study of Human Brain Connectivity: Cognitive Networks

Thesis presented by:

Roser Sala Llonch

to obtain the degree of doctor from the University of Barcelona in accordance with the
requirements of the international PhD diploma

Supervised by:

Dr. Carme Junqué Plaja, and Dr. David Bartrés Faz

Department of Psychiatry and Clinical Psychobiology

Medicine Doctoral Program

University of Barcelona

2014

A les meves àvies

Barcelona, 13 November 2014

Dr. Carme Junqué Plaja and Dr. David Bartrés Faz, Professors at the University of Barcelona,

CERTIFY that they have guided and supervised the doctoral thesis entitled 'Multimodal MRI Study of Human Brain Connectivity: Cognitive Networks' presented by Roser Sala Llonch. They hereby assert that this thesis fulfils the requirements to present her defense to be awarded the title of doctor.

Signatures,

Dr Carme Junqué Plaja

Dr. David Bartrés Faz

This thesis has been undertaken in the Neuropsychology Group of the Department of Psychiatry and Clinical Psychobiology, Faculty of Medicine, University of Barcelona. The group is a consolidated research group by the *Generalitat de Catalunya* (grants 2009 SGR941 and 2014 SGR98) and it is part of the *Institut d'Investigacions Biomèdiques August Pi i Sunyer* (IDIBAPS).

The present work has been financially supported by a PhD training scholarship of the National Research Program, conferred by the Spanish Government to the PhD candidate (BES-2011-047053). In addition financial support for the studies was also received by the Spanish *Ministerio de Ciencia e Innovación* (grants SAF20090748, PSI2010-16174, and PSI2013-41393), the *Instituto Carlos III* (grants FIS080036 and FIS1200013), and the *Instituto de Mayores y Servicios Sociales* (IM-SERSO, grant 2011/200).

Contents

Foreword	v
Related academic work	vii
Glossary of abbreviations	xiii
Glossary of neuroimaging definitions	xv
1 Introduction	1
1.1 MRI and brain connectivity	1
1.1.1 Diffusion MRI	3
1.1.2 Functional MRI	4
Seed-based correlation	5
Independent Component Analysis (ICA)	6
Whole-brain connectivity approaches using graph-theory	6
1.2 Network-based organization of healthy brains	6
1.3 FMRI during cognitive states	11
1.3.1 Working memory networks	12
1.3.2 Episodic memory networks	12
1.4 FMRI in healthy aging	15
1.4.1 Compensation vs Dedifferentiation	16
Compensation	16
Dedifferentiation	17
1.4.2 Cognitive Models in aging	17
The HAROLD model	17
The CRUNCH model	18

The PASA model	18
1.4.3 Connectivity-related changes in Aging	18
1.5 Alzheimer’s Disease	23
1.5.1 Alzheimer’s disease and task-fMRI	23
1.5.2 Alzheimer’s disease and large-scale networks	24
2 Hypotheses and Objectives	27
3 Methods	29
3.1 Study Sample	29
3.1.1 Subjects included in each study	29
3.2 Acquisition and paradigms	31
3.2.1 MRI sequences	31
Structural T1	31
Diffusion MRI	31
Functional MRI	31
3.2.2 Functional Paradigms	31
Working memory task	31
Episodic memory task	34
3.2.3 Subjects’ selection and clinical/neuropsychological assessment	34
3.3 Analysis of structural MRI	34
3.4 Analysis of Diffusion MRI	35
3.4.1 The DTI approach	35
3.4.2 Tract Based Spatial Statistics	36
3.4.3 Tractography	37
3.5 Analysis of fMRI	37
3.5.1 Data preprocessing for fMRI data	37
3.5.2 Image Registration	38
3.5.3 Model-driven analysis	39
FEAT for task-fmri	39
Seed-based correlation for resting fmri	39
3.5.4 Data-driven analysis	40
Tensor-ICA for task-fMRI	41
Temporal Concatenation ICA and dual-regression for resting-fMRI	42
3.6 Advanced fMRI analysis: whole-brain connectivity	43
3.6.1 Graph Theory	43
3.6.2 Other approaches: FSLNets	47
4 Results	49
5 General Discussion	117

6	Conclusions	127
A	Methodological issues in Graph Theory	129
A.1	Introduction and motivation of the study	129
A.2	Methods	130
A.2.1	Evaluation of different brain parcellations strategies	130
A.2.2	Evaluation of networks at different threshold levels	132
A.3	Results	132
A.3.1	Network metrics	134
A.3.2	Correlations with age	134
B	Resum en català	135
	Acknowledgments	145
	Agraïments	147
	Abstract	149
	References	153

FOREWORD

This thesis, presented for the degree of Doctor by the University of Barcelona, is the result of different studies carried out over a four-year period at the Department of Psychiatry and Clinical Psychobiology of the University of Barcelona. During this period, I have obtained the degree of Master in Neuroscience, which is linked to the Doctorate in Medicine Program (Quality Mention MCD2008-00023; Mention to Excellence MEE2011-0316) at the University of Barcelona.

This thesis follows the published papers format, and it includes four published peer-reviewed papers, one paper that is under review process and one unpublished study. The 6 studies are presented in the following order:

1. Sala-Llonch, R., Peña Gómez, C., Arenaza-Urquijo, E. M., Vidal-Piñeiro, D., Bargalló, N., Junqué, C., and Bartrés-Faz, D. (2012b). Brain connectivity during resting state and subsequent working memory task predicts behavioural performance. *Cortex*, 48(9):1187–96
2. Sala-Llonch, R., Palacios, E.M., Junqué, C., Bargalló, N., and Vendrell, P. Functional and structural connectivity of visuospatial and visuo-perceptual working memory, *Submitted, under revision*.
3. Sala-Llonch, R., Arenaza-Urquijo, E. M., Valls-Pedret, C., Vidal-Piñeiro, D., Bargalló, N., Junqué, C., and Bartrés-Faz, D. (2012a). Dynamic functional reorganizations and relationship with working memory performance in healthy aging. *Frontiers in human neuroscience*, 6(June):152
4. Sala-Llonch, R., Junqué, C., Arenaza-Urquijo, E. M., Vidal-Piñeiro, D., Valls-Pedret, C., Palacios, E. M., Domènech, S., Salvà, A., Bargalló, N., and Bartrés-Faz, D. (2014). Changes in whole-brain functional networks and memory performance in aging. *Neurobiology of aging*, 35(10):2193–202
5. Sala-Llonch et al. Whole-brain network interactions and aging. Relationship with cognition. *in preparation*
6. Sala-Llonch, R., Fortea, J., Bartrés-Faz, D., Bosch, B., Lladó, A., Peña Gómez, C., Antonell, A., Castellanos-Pinedo, F., Bargalló, N., Molinuevo, J. L., and Sánchez-Valle, R. (2013). Evolving brain functional abnormalities in PSEN1 mutation carriers: a resting and visual encoding fMRI study. *Journal of Alzheimer's disease : JAD*, 36(1):165–75

Related Academic Work

List of additional publications of the candidate that are not included in the thesis. These papers are the result of collaborative work with other projects during the time of the thesis:

- 2014 Baggio, H.-C., Segura, B., Sala-Llonch, R., Marti, M.-J., Valldeoriola, F., Compta, Y., Tolosa, E., and Junqué, C. (2014b). Cognitive impairment and resting-state network connectivity in Parkinson's disease. *Human brain mapping*.
- 2014 Vidal-Piñeiro, D., Valls-Pedret, C., Fernandez-Cabello, S., Arenaza-Urquijo, E. M., Sala-Llonch, R., Solana, E., Bargallo, N., Junque, C., Ros, E., and Bartrés-Faz, D. (2014b). Decreased Default Mode Network connectivity correlates with age-associated structural and cognitive changes. *Frontiers in Aging Neuroscience*, 6(256).
- 2014 Baggio, H.-C., Sala-Llonch, R., Segura, B., Marti, M.-J., Valldeoriola, F., Compta, Y., Tolosa, E., and Junqué, C. (2014a). Functional brain networks and cognitive deficits in Parkinson's disease. *Human brain mapping*, 35(9):4620–34.
- 2014 Vidal-Piñeiro, D., Martin-Trias, P., Arenaza-Urquijo, E. M., Sala-Llonch, R., Clemente, I. C., Mena-Sánchez, I., Bargalló, N., Falcón, C., Pascual-Leone, A., and Bartrés-Faz, D. (2014a). Task-dependent activity and connectivity predict episodic memory network-based responses to brain stimulation in healthy aging. *Brain stimulation*, 7(2):287–96.
- 2013 Arenaza-Urquijo, E. M., Molinuevo, J.-L., Sala-Llonch, R., Solé-Padullés, C., Balasa, M., Bosch, B., Olives, J., Antonell, A., Lladó, A., Sánchez-Valle, R., Rami, L., and Bartrés-Faz, D. (2013). Cognitive reserve proxies relate to gray matter loss in cognitively healthy elderly with abnormal cerebrospinal fluid amyloid- β levels. *Journal of Alzheimer's disease : JAD*, 35(4):715–26.
- 2013 García-García, I., Jurado, M. A., Garolera, M., Segura, B., Sala-Llonch, R., Marqués-Iturria, I., Pueyo, R., Sender-Palacios, M. J., Vernet-Vernet, M., Narberhaus, A., Ariza, M., and Junqué, C. (2013). Alterations of the salience network in obesity: a resting-state fMRI study. *Human brain mapping*, 34(11):2786–97.
- 2013 Jovicich, J., Marizzoni, M., Sala-Llonch, R., Bosch, B., Bartrés-Faz, D., Arnold, J., Benninghoff, J., Wiltfang, J., Roccatagliata, L., Nobili, F., Hensch, T., Tränkner, A., Schönknecht, P., Leroy, M., Lopes, R., Bordet, R., Chanoine, V., Ranjeva, J.-P., Didic, M., Gros-Dagnac, H., Payoux, P., Zoccatelli, G., Alessandrini, F., Beltramello, A., Bargalló, N., Blin, O., and Frisoni, G. B. (2013). Brain morphometry reproducibility in multi-center 3T MRI studies: a comparison of cross-sectional and longitudinal segmentations. *NeuroImage*, 83:472–84.
- 2013 Moreno*, F., Sala-Llonch*, R., Barandiaran, M., Sánchez-Valle, R., Estanga, A., Bartrés-Faz, D., Sistiaga, A., Alzualde, A., Fernández, E., Martí Massó, J. F., López de Munain, A., and Indakoetxea, B. n. (2013). Distinctive age-related temporal cortical thinning in asymptomatic granulin gene mutation carriers. *Neurobiology of aging*, 34(5):1462–8.

* (equal contribution)

- 2013 Palacios*, E. M., Sala-Llonch*, R., Junque, C., Roig, T., Tormos, J. M., Bargallo, N., and Vendrell, P. (2013a). Resting-state functional magnetic resonance imaging activity and connectivity and cognitive outcome in traumatic brain injury. *JAMA neurology*, 70(7):845–51.
- * (equal contribution)
- 2013 Palacios*, E. M., Sala-Llonch*, R., Junque, C., Roig, T., Tormos, J. M., Bargallo, N., and Vendrell, P. (2013b). White matter/gray matter contrast changes in chronic and diffuse traumatic brain injury. *Journal of neurotrauma*, 30(23):1991–4.
- * (equal contribution)
- 2013 Palacios, E. M., Sala-Llonch, R., Junque, C., Fernandez-Espejo, D., Roig, T., Tormos, J. M., Bargallo, N., and Vendrell, P. (2013). Long-term declarative memory deficits in diffuse TBI: correlations with cortical thickness, white matter integrity and hippocampal volume. *Cortex*, 49(3):646–57.
- 2013 Pereira, J. B., Junqué, C., Bartrés-Faz, D., Martí, M. J., Sala-Llonch, R., Compta, Y., Falcón, C., Vendrell, P., Pascual-Leone, A., Valls-Solé, J., and Tolosa, E. (2013). Modulation of verbal fluency networks by transcranial direct current stimulation (tDCS) in Parkinson’s disease. *Brain stimulation*, 6(1):16–24.
- 2013 Segura, B., Ibarretxe-Bilbao, N., Sala-Llonch, R., Baggio, H. C., Martí, M. J., Valldeoriola, F., Vendrell, P., Bargalló, N., Tolosa, E., and Junqué, C. (2013). Progressive changes in a recognition memory network in Parkinson’s disease. *Journal of neurology, neurosurgery, and psychiatry*, 84(4):370–8.
- 2012 Bosch, B., Arenaza-Urquijo, E. M., Rami, L., Sala-Llonch, R., Junqué, C., Solé-Padullés, C., Peña Gómez, C., Bargalló, N., Molinuevo, J. L., and Bartrés-Faz, D. (2012). Multiple DTI index analysis in normal aging, amnesic MCI and AD. Relationship with neuropsychological performance. *Neurobiology of aging*, 33(1):61–74.
- 2012 García-García, I., Jurado, M. A., Garolera, M., Segura, B., Marqués-Iturria, I., Pueyo, R., Vernet-Vernet, M., Sender-Palacios, M. J., Sala-Llonch, R., Ariza, M., Narberhaus, A., and Junqué, C. (2012). Functional connectivity in obesity during reward processing. *NeuroImage*, 66C:232–239.
- 2012 Palacios, E. M., Sala-Llonch, R., Junque, C., Roig, T., Tormos, J. M., Bargallo, N., and Vendrell, P. (2012). White matter integrity related to functional working memory networks in traumatic brain injury. *Neurology*, 78(12):852–60.
- 2012 Peña Gómez, C., Sala-Llonch, R., Junqué, C., Clemente, I. C., Vidal, D., Bargalló, N., Falcón, C., Valls-Solé, J., Pascual-Leone, A., and Bartrés-Faz, D. (2012). Modulation of large-scale brain networks by transcranial direct current stimulation evidenced by resting-state functional MRI. *Brain stimulation*, 5(3):252–63.
- 2012 Rami, L., Sala-Llonch, R., Solé-Padullés, C., Fortea, J., Olives, J., Lladó, A., Peña Gómez, C., Balasa, M., Bosch, B., Antonell, A., Sanchez-Valle, R., Bartrés-Faz, D., and Molinuevo, J. L. (2012). Distinct functional activity of the precuneus and posterior cingulate cortex during encoding in the preclinical stage of Alzheimer’s disease. *Journal of Alzheimer’s disease : JAD*, 31(3):517–26.
- 2012 Zubiaurre-Elorza, L., Soria-Pastor, S., Junque, C., Sala-Llonch, R., Segarra, D., Bargallo, N., and Macaya, A. (2012). Cortical thickness and behavior abnormalities in children born preterm. *PloS one*, 7(7):e42148.

- 2011 Arenaza-Urquijo, E. M., Bosch, B., Sala-Llloch, R., Solé-Padullés, C., Junqué, C., Fernández-Espejo, D., Bargalló, N., Rami, L., Molinuevo, J. L., and Bartrés-Faz, D. (2011). Specific anatomic associations between white matter integrity and cognitive reserve in normal and cognitively impaired elders. *The American journal of geriatric psychiatry*, 19(1):33–42.
- 2011 Fortea, J., Sala-Llloch, R., Bartrés-Faz, D., Lladó, A., Solé-Padullés, C., Bosch, B., Antonell, A., Olives, J., Sanchez-Valle, R., Molinuevo, J. L., and Rami, L. (2011b). Cognitively preserved subjects with transitional cerebrospinal fluid β -amyloid 1-42 values have thicker cortex in Alzheimer's disease vulnerable areas. *Biological psychiatry*, 70(2):183–90.
- 2010 Fortea, J., Sala-Llloch, R., Bartrés-Faz, D., Bosch, B., Lladó, A., Bargalló, N., Molinuevo, J. L., and Sánchez-Valle, R. (2010). Increased cortical thickness and caudate volume precede atrophy in PSEN1 mutation carriers. *Journal of Alzheimer's disease : JAD*, 22(3):909–22.
- 2010 Sala-Llloch, R., Bosch, B., Arenaza-Urquijo, E. M., Rami, L., Bargalló, N., Junqué, C., Molinuevo, J.-L., and Bartrés-Faz, D. (2010). Greater default-mode network abnormalities compared to high order visual processing systems in amnesic mild cognitive impairment: an integrated multi-modal MRI study. *Journal of Alzheimer's disease : JAD*, 22(2):523–39.

GLOSSARY OF ABBREVIATIONS

AAL Automated Anatomical Labelling	MNI Montreal Neurological Institute
AD Alzheimer's Disease	MRI Magnetic Resonance Imaging
AMC Asymptomatic Mutation Carriers	MTL Medial Temporal Lobe
AxD Axial Diffusivity	PASA Posterior-Anterior Shift with Aging
BOLD Blood-Oxygen Level Dependent	PET Positron Emission Tomography
CRUNCH Compensation Related Utilization of Neural Circuits Hypothesis	PFC Prefrontal Cortex
CSF Cerebrospinal Fluid	PiB Pittsburgh Compound B
CtrlN Control Network	PMC Posteromedial Cortex
DAN Dorsal Attention Network	PPC Precuneus/Posterior Cingulate
DLPFC Dorsolateral PFC	PSEN1 Presenilin-1
DMN Default Mode Network	RAVLT Rey Auditory Verbal Learning Test
DTI Diffusion Tensor Imaging	RD Radial Diffusivity
E/R Encoding/Retrieval	ROI Region Of Interest
FA Fractional Anisotropy	ROCF Rey Osterrich Complex Figure
FC Functional Connectivity	RSFC Resting State Functional Connectivity
FEF Frontal Eye Fields	rs-fMRI Resting State fMRI
FMRI Functional MRI	RSN Resting State Network
FPN Fronto-parietal network	RT Reaction Time
GLM General Lineal Model	SAL Salience Network
GM Gray Matter	SMA Supplementary Motor Area
HAROLD Hemispheric Asymmetry Reduction in Old Adults	SMC Symptomatic Mutation Carriers
HE Healthy Elders	TBSS Tract Based Spatial Statistics
IC Independent Component	TMT Trail Making Test
ICA Independent Component Analysis	TR Time of Repetition
MCI Mild Cognitive Impairment	TE Time of Echo
MD Mean Diffusivity	WM Working Memory
MPRAGE Magnetization-Prepared Rapid Gradient-Echo	YA Young Adults

GLOSSARY OF NEUROIMAGING DEFINITIONS

- Association matrix** Matrix containing the connectivity of all possible pairs of nodes in a network.
- Axial Diffusivity** Diffusion strength of the main diffusion direction in DTI.
- Binary adjacency matrix** Matrix of connectivity obtained by thresholding the association matrix that can be used for graph theory approaches.
- Brain atlas** Structured representation of the brain. The definition of parcellations can be derived from anatomical or functional data.
- Connectomics** Field within neuroscience that aims to study the brain by estimating the connections between brain regions.
- Clustering** Measure of the cliquishness of connections between nodes from a topological point of view. Measures the number of triangles around a node.
- Cross-sectional study** Observational study that involves data collected from a population at one specific point of time.
- Data-driven analysis** The set of techniques used to obtain patterns that exist in the data regardless of the model
- Default Mode Network** Set of brain regions that are active during resting-state and that deactivate during the performance of goal-directed tasks.
- Diffusion Tensor Imaging** MRI modality that measures random motion of molecules. In brain's white matter is used to estimate the direction of the fibers and to track the major fibre bundles.
- Fractional Anisotropy** Measure of the anisotropy of white matter fibers derived from DTI.
- Functional Connectivity** Estimation of functional connection between regions, direct or indirect.
- Functional Integration** Coordinated activity of different brain units.
- Functional MRI** Sequential acquisition of T2*-weighted MRI volumes during the time-course of a task or a set of events.
- Functional segregation** Existence of specialized neurons and brain units that selectively respond to specific stimuli.
- Graph** A model of a complex system, of any nature, defined by a set of nodes and the edges between them.
- Hemodynamic response** Brain process under which active neurons show increases in oxygen.
- Independent Component Analysis** a data-driven method used to obtain patterns of spatio-temporal independent processes in the data.
- Mediation model** Relationship between an independent variable and a dependent variable through a third variable, known as a mediator variable.
- Model-driven analysis** The set of techniques used to analyze fMRI data that estimate patterns of activity based on the experimental model.
- Partial correlation** a variant of correlation used that estimates the connection between two nodes after removing the effects of all other timeseries.
- Pearson correlation coefficient** Measure of the linear relationship between two variables. It is used between timeseries from different regions to estimate functional connectivity, as well as with any two variables in a population (i.e., a neuroimaging measure and a cognitive measure) to estimate the relationship between them.
- Radial Diffusivity** Diffusion strength at the perpendicular plane of the main diffusion direction in DTI.
- Resting-state fMRI** A specific fMRI acquisition that measures spontaneous temporal fluctuations in brain activity 'at rest'.
- Resting State Functional Connectivity** Measure of the functional connectivity estimated as the temporal synchrony between spontaneous temporal fluctuations at different brain regions.
- Resting State Network** Functional brain networks most commonly estimated from rs-fMRI data.

Skeleton Map created from group-DTI data representing the centres of all tracts common to the group.

Small-worldness characteristic of a network with high clustering and short characteristic path length. Also defined as a network with high global and local efficiency.

Structural Connectivity Estimation of structural links between brain regions.

Topology Properties of a network obtained considering the connectivity between nodes regardless of their physical or anatomical localization.

Tractography Method for identifying anatomical connections in the human brain in-vivo and non-invasively using Diffusion MRI data.

CHAPTER 1

Introduction

1.1 MRI and brain connectivity

For many years, studies of human brain function typically associated specific cognitive capabilities to discrete brain anatomical structures. These evidences were obtained from studies of focal lesions (usually identified postmortem) and with the first in-vivo recordings. More recently, and mostly thanks to Magnetic Resonance Imaging (MRI), the neuroscientific community has moved to the idea that the majority of functions are supported by coordinated activity between distinct, separated brain regions, so that the brain works in networks. These ideas have lead to the definition of *Brain Connectivity* (Catani et al., 2013; Sporns, 2013b) and have motivated the nascent field of *Connectomics* (Smith et al., 2013).

Brain connectivity refers to patterns of links connecting distinct units within the nervous system. It can be studied at different scales, and therefore, units or nodes can be defined as individual neurons, neural populations, or segregated brain regions described by anatomical or functional landmarks. Recent advances on both neuroscience and computational sciences have motivated new approaches for studying brain structure and function from

a complex systems perspective (Sporns, 2013a). These current trends have suggested that connectivity-based methods may provide good tools in order to understand brain functioning in healthy subjects, as well as to study changes during lifespan, or during the timecourse of neurodegenerative diseases.

Although invasive techniques, such as the use of tracers in postmortem samples, have been used to identify brain connections in an accurate and precise way, recent advances in ‘in vivo’ neuroimaging techniques allow the measurement of connectomics in a non-invasive way. However, it is worth mentioning that all neuroimaging techniques are based on inferences, and therefore, they provide an indirect estimation of connectivity, which has to be taken in account when interpreting the results obtained with such approaches (Behrens and Sporns, 2012).

In general terms, in neuroimaging, human brain connectivity can be studied at the structural and functional levels. Brain structural connectivity refers to the presence of fiber tracts directly connecting different brain regions (Basser et al., 1994). The use of *Diffusion MRI* allows investigating structural connections in the brain’s white matter by estimating the directionality of white matter fibers. Functional connectivity can be studied as the temporal correlation between spatially remote neurophysiological events that may or not may have direct physical connection. In this regard, *functional MRI* (fMRI) can be used to measure functional connectivity as the statistical dependence between BOLD fluctuations measured within different brain regions (Behrens and Sporns, 2012; Matthews et al., 2013). fMRI can be obtained during the performance of a cognitive task, or even when subjects are scanned under resting-state condition (Biswal et al., 1995).

It would appear that functional and structural connectivity are two strongly inter-related processes. In this sense, the pattern of structural connections would have a predictive role over functional connectivity and structural connections could be inferred from functional connectivity. Part of these hypotheses have been empirically demonstrated in several multimodal studies (Honey et al., 2009; van den Heuvel et al., 2009). However, there is also some evidence suggesting that these relationships are more complex and that functionally connectivity can be only partially explained by structural connectivity. For example, using animal models, Adachi et al. (2012) studied structural and functional connections in the

macaque and found that some brain regions that were anatomically disconnected showed high levels of functional connectivity. Moreover, it has been demonstrated that the relationship between functional and structural connectivity is not stable across lifespan, and that it exhibits changes during the aging process (Betz et al., 2014). Also in this line, Park and Friston (2013) proposed that the same structural architecture might support a variety of functional networks. One conclusion from these studies is that, although both modalities are highly informative, functional and structural connections should be studied separately, and the transferability of results from structure to function (and viceversa) needs to be taken with caution.

■ **STRUCTURAL CONNECTIVITY**

Refers to the presence of white matter fiber tracts connecting separated brain areas. It can be studied using Diffusion-weighted MRI.

■ **FUNCTIONAL CONNECTIVITY**

Refers to temporal synchrony between regions that do not need to be structurally connected. It can be measured as the coherence or correlation between BOLD signals, derived from fMRI data.

1.1.1 Diffusion MRI

Diffusion-weighted MRI allows the study of the diffusion process of water molecules in the brain (Basser et al., 1994). It provides a unique capability to delineate axonal tracts within the white matter, which was not possible with previous MRI non-invasive techniques (Mori and Zhang, 2006).

One of the key-measures obtained from diffusion MRI is anisotropy, which reflects the preference of each brain voxel for having high directionality. Inside white matter fiber tracts, diffusion is highly anisotropic, due to the presence of myelin sheaths and microstructural components of axons, which help water molecules to follow a trajectory that is parallel to the fiber direction. On the contrary, in brain regions with less organized brain tissues (i.e., gray matter and CSF), the anisotropy is much lower, and water molecules move freely in all directions forming a sphere (Le Bihan, 1991).

One of the most common applications of Diffusion MRI is the so-called *Diffusion Tensor Imaging (DTI)* approach. With DTI, it is possible to measure the differences in anisotropy between brain tissues, based on the calculation of Fractional Anisotropy (FA), which is a metric obtained mathematically (for further details, see Methods in Chapter 3). The FA measure was formalized by Basser and Pierpaoli (1996) and it has values close to 1 in very anisotropic regions, and values around 0 in isotropic tissues. Therefore, it can be further used to generate diffusion maps, which are believed to reflect the degree of myelination and axonal density or fiber integrity (Jones et al., 2013).

Beyond DTI, *Diffusion tractography* is a more complex but more precise technique that can also be performed with Diffusion MRI data. It aims to determine the trajectories of axon bundles traversing the brain's white matter. In order to perform tractography, it is necessary to first estimate the orientation of fibers at every point in the brain. Then, by joining up the estimated directions, it is possible to reconstruct entire pathways or connections between separated brain areas (Behrens et al., 2003a).

1.1.2 Functional MRI

fMRI measures changes in blood-oxygen-dependent (BOLD) signal in the brain across time. In its more traditional application, it has been used to identify areas of increased or decreased neuronal activity during the performance of a task (Logothetis et al., 2001; Logothetis, 2003; Raichle and Mintun, 2006). That is, when fMRI is acquired during the time-course of a goal-directed task, the differences in the BOLD signal level between states can be used to infer the spatial patterns of brain-activated regions under the different task conditions. Task-fMRI requires exposing the subject to different conditions or different cognitive demanding levels. Then, maps of brain activity can be obtained by subtracting the BOLD signal between states or conditions, being one of them usually the baseline condition.

Another popular type of fMRI is the so-called *resting-state fMRI (rs-fMRI)*, which refers to the sequential acquisition of fMRI scans, of duration typically between 5 and 10 minutes, while subjects are asked to lie down, not to fall asleep and not to think in anything particular. The potential of rs-fMRI has been used to identify temporal coherences between spontaneous fluctuations that occur during rest, measured as low-frequency oscillations of

the BOLD signal. In an early study Biswal et al. (1995) used rs-fMRI and described consistent correlations within the regions of the motor network, even in the absence of a task.

Since then, the use of rs-fMRI to study functional connectivity has increased massively and has revealed meaningful low frequency BOLD fluctuations that are correlated across distant brain regions, allowing the study of what has been called Resting-State Functional Connectivity (RSFC). Although, the origin and interpretation of these spontaneous fluctuations are still under debate (Schölvinck et al., 2010). RSFC seems to be highly informative about both brain architecture and brain organization, and it has a high variability in humans, probably reflecting behavioral interindividual differences (Fox et al., 2007). A complete study of human RSFC patterns in the human will be deeply developed in section 1.2 of this introduction.

The analysis of fMRI connectivity covers an elevated number of methodological approaches, and this number increases day-to-day thanks to technical advances and ongoing inter-disciplinary research. Basically, it is possible to differentiate between three main methodologies: seed-based correlation analysis, independent component analysis, and whole-brain approaches using graph theory.

Seed-based correlation

This method consists on identifying whole-brain, voxel-wise connectivity maps of areas showing correlated activity with a seed, which is a delimited brain region (that can be a voxel or a group of voxels) defined *a priori* with data from previous analyses, from the literature or from an atlas. Although seed-based correlation methods usually have an elevated number of confounds and they are highly dependent on the seed definition and the preprocessing applied to the data, they still represent the best approach to answer directly some questions related to connectivity. These methods are the best option to find, for example, correlation patterns from a certain region when there is a strong hypothesis previously formulated, providing a straightforward interpretability (Cole et al., 2010).

Independent Component Analysis (ICA)

ICA is used to find spatio-temporal patterns of synchronized brain activity. It decomposes the data into a set of components, such that all the regions within the same component show synchrony of their temporal oscillations and are independent from the other components (Beckmann and Smith, 2004). In comparison with seed-based correlation, one of its advantages is that it does not require the specification of a priori seeds. In addition, ICA appears as a good approach to identify signals of no-interest, such as artifacts, head motion, physiological noise or CSF-related signals, which can be then easily removed from the data (Griffanti et al., 2014).

Whole-brain connectivity approaches using graph-theory

These kind of studies aim to investigate the overall brain connectivity by describing the brain as a single interconnected network (Bullmore and Sporns, 2009). They belong to the set of higher-level models used to evaluate functional connectivity in a more integrative way than the two methods described above. Graph-theory studies require, in general a first stage in order to parcellate the brain into a set of regions or nodes, and a second stage that finds the relationships between all possible node pairs, defining a 'big' whole-brain network. Once the whole-brain network is defined, it can be studied at different levels of complexity or specificity. For example, it is possible to obtain connectivity characteristics at regional level, and, at the same time, it is possible to obtain parameters reflecting whole-brain organization, including measures such as network efficiency, integration or segregation (Rubinov and Sporns, 2010). Furthermore, using measures of nodal connectivity or centrality it has been possible to define cortical hubs as a key-connected brain regions, that have an special role in controlling connectivity paths across the whole brain (Buckner et al., 2009; Cole et al., 2010; Power et al., 2013).

1.2 Network-based organization of healthy brains

Understanding functional brain organization in normal or healthy brains has become of outstanding interest in neuroscience. It appears as an essential need in order to further de-

fine neuropsychological correlates and potential clinical biomarkers for neurodegenerative diseases or brain damage. In addition, it brings new insight to the design of interventional studies and to track brain changes longitudinally.

The use of resting-state fMRI to study functional connectivity has allowed the identification of a reduced set of networks or connectivity patterns (typically 10-20) named Resting State Networks (RSNs). These networks are commonly identified across subjects (Damoiseaux et al., 2006), and have shown high reproducibility rates (Guo et al., 2012). In addition, RSNs have been associated with networks of brain function (Sadaghiani and Kleinschmidt, 2013).

The most-studied of these RSNs is the Default Mode Network (DMN), which has the specific property of being deactivated during the performance of goal-directed tasks but activated at rest. In a first pioneering study by Shulman et al. (1997) using Positron Emission Tomography (PET), the authors observed a consistent set of regions that were more active during passive than during active conditions, or equivalently, these regions were deactivated during the task performance. Later on, Raichle et al. (2001) performed similar experiments and they proposed empirical and theoretical implications for this baseline brain activity. The existence of these task-related activity decreases, which was first evidenced using PET, was also replicated with task-fMRI studies (Gusnard and Raichle, 2001).

The DMN was further identified in a series of resting-state functional connectivity studies (Greicius et al., 2003; Fox et al., 2005; Fransson, 2005; Damoiseaux et al., 2006; Vincent et al., 2006), and few years after the first Raichle's experiments, Buckner et al. published a review article with the aim to define the anatomy and function of the DMN (Buckner et al., 2008). In this article, they described the DMN as a brain system composed by a set of interacting brain areas functionally connected and distinct from other systems within the brain (such as the visual or motor systems), which participates in internal modes of cognition. By gathering together studies of task-induced deactivations and functional connectivity analyses, they defined the core regions associated with the brain's default network: the ventral/dorsal medial prefrontal cortex, the posterior cingulate and retrosplenial cortex, the inferior parietal lobule and the hippocampal formation (including entorhinal cortex and parahippocampal cortex). Although the number of DMN-related studies with clini-

cal conclusions at that time was still very poor, they already pointed to the idea that the understanding of the DMN would have important implications for brain disease.

From that time onwards, the DMN has been used to characterize brain functioning in healthy young subjects, but also to study brain changes during healthy aging (Andrews-Hanna et al., 2007; Damoiseaux et al., 2008) and changes related to brain disease (Barkhof et al., 2014). The relationship between DMN connectivity and aging as well as its relevance for disease will be discussed in another part of this section.

■ DEFAULT MODE NETWORK

Brain network supporting internal mental states, such as self-referencing and reasoning. It is active during resting-state periods and it deactivates during the performance of the majority of goal-directed tasks. It involves the prefrontal cortex, the posterior cingulate and precuneus, the inferior parietal lobules bilaterally and the hippocampal formation.

Besides the DMN, other networks of intrinsic brain connectivity have been consistently described in healthy populations. The majority of studies agree in a set of 10 RSNs that have also shown a great correspondence with the main task-related networks, covering the full repertory of task-related brain activation patterns. These findings indicate that the human brain has a network-based organization even at rest. In this regard, Smith et al. (2009) used ICA on rs-fMRI data and compared the components with task-patterns averaged from the BrainMap Database (Laird et al., 2005), which assembled results from more than 7000 task-fMRI experiments. They found that the patterns of RSFC could be easily associated with patterns of task-related coactivations from a wide range of cognitive domains.

The high correspondence between rs-fMRI and task-fMRI networks opens new doors to the research community in the sense that rs-fMRI paradigms could be cautiously used instead of task-fMRI to study the status of functional networks. In comparison with task-fMRI, rs-fMRI is easy to acquire and with less confounds, such as task modulations, adaptive changes, or behavioral differences across populations.

The spatial maps of the 10 most commonly defined networks are shown on Figure 1.1. In Table 1.1, a brief description of the areas involved in each network and their associated cognitive functions is provided.

Table 1.1: Summary of main RSNs

Network	Regions	Functions
A Visual Medial	Medial visual Areas	Motion perception.
B Visual Occipital	Visual occipital areas	Cognition-language.
C Visual Lateral	Lateral visual areas	Cognition-space.
D Default Mode	Precuneus and posterior cingulate, bilateral inferior-lateral-parietal, and ventromedial frontal cortex	Introspection and episodic memory, self-referenciing, and deactivaed in goal-directed tasks.
E Cerebellum	Cerebellum	Action-execution and perception-somesthesis-pain.
F Sensorimotor	SMA, sensorimotor cortex, and secondary somatosensory cortex	Bimanual motor tasks, processing of sensory input, and execution of motor functions.
G Salience or executive control or cingulo-opercular	Dorsal anterior cingulate, paracingulate and insula	executive control, salient events, set maintenance action-inhibition.
H Auditory	Superior temporal gyrus, Heschl's gyrus, and posterior insular	action-execution-speech, cognition-language-speech, and perception-audition
I,J Frontoparietal or dorsal attention	Superior parietal and superior frontal areas, intraparietal sulcus and FEF	Voluntary (top-down) orienting, selective atention, and cognition-language

SMA: Supplementary Motor Area; FEF: Frontal Eye Fields.

Apart from the studies that have used ICA to describe the main RSNs, other researchers have focused on higher-level, whole-brain approaches to investigate patterns of RSFC in healthy brains. For example, Crossley et al. (2013) used graph-theory to define a network from rs-fMRI, and they compared this network with a network of task-coactivation patterns obtained from the BrainMap Database. They described a brain structure based on functional connectivity patterns that showed modular organization and which was very similar between task and rest. Concretely, they defined 4 modules that were associated with different functions: the occipital module (perception), the central and sensorimotor module (action),

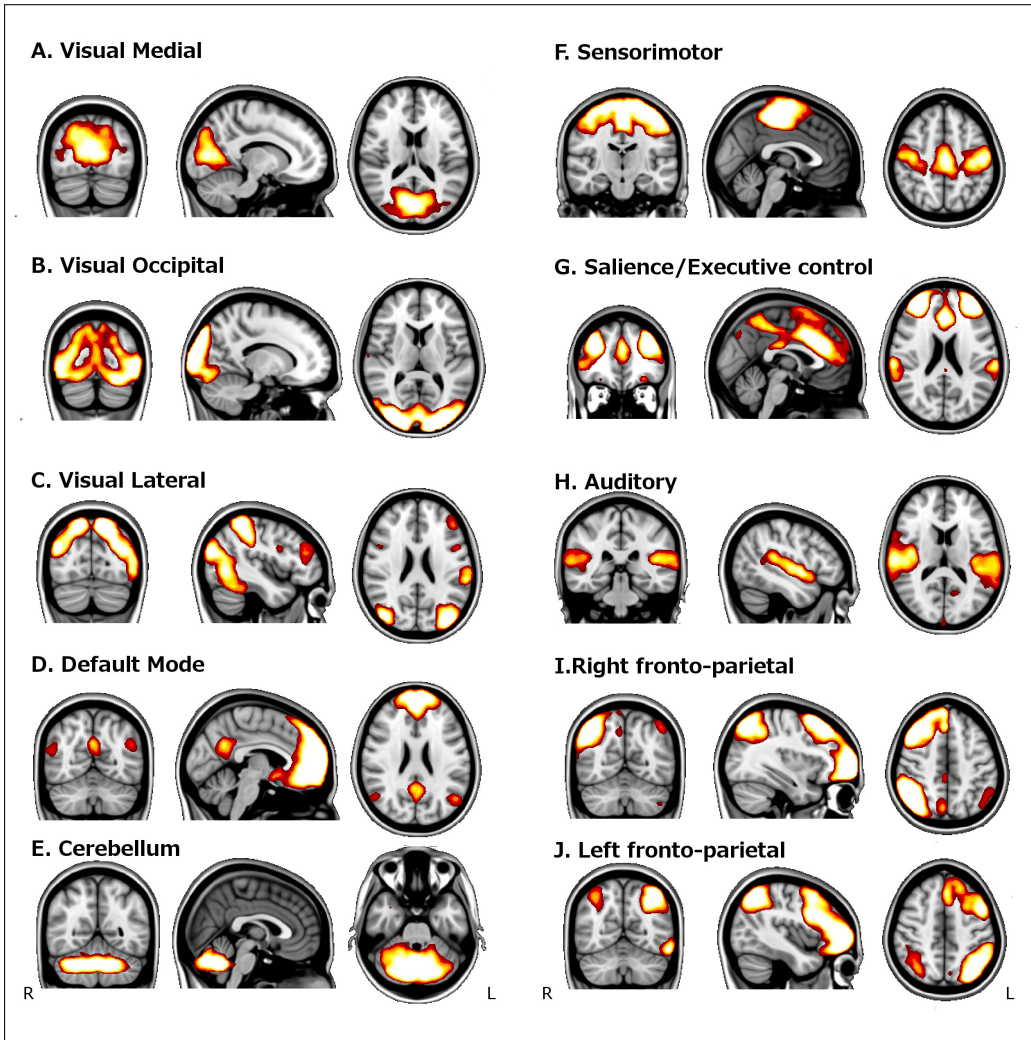


Figure 1.1: Spatial maps of main RSNs. Adapted from (Palacios* et al., 2013a).

the frontoparietal module (executive functions) and the default mode network (emotion). The authors concluded that there is a well-defined network organization in the brain that is equally evidenced at rest and during task performance. In a more recent study, Cole et al. (2014) studied connectivity patterns by creating whole-brain networks from data obtained at rest and while subjects performed a variety of cognitive tasks. They defined an intrinsic network structure obtained from rs-fMRI, which was highly dominant in the resting brain and even during the performance of a task. Interestingly, they also found that this network structure is slightly modulated by task-evoked connectivity changes that were both task-general and task-specific.

■ THE BRAIN AS A GROUP OF NETWORKS

The Human brain has an intrinsic organization based on patterns of functional connectivity that can be observed while subjects are at rest. These patterns can be defined as large-scale networks of isolated brain areas and also by means of interactions between finer brain parcellations.

During the performance of a goal-directed task, the networks involved in the task would shift to active state, without introducing big changes at the organization of the rest of the brain.

1.3 FMRI during cognitive states

Task-related networks can be studied with fMRI by identifying patterns of brain regions that activate and deactivate in synchrony during the performance of a cognitive demanding task. These activation changes are usually evaluated using functional paradigms that can be block-designed or event-related tasks. There has been an increasing effort in order to define and classify networks of task-activity associated with specific cognitive domains. These works have been gathered together, resulting in several meta-analytic publications and leading to the set up of some public databases, such as the BrainMap (Laird et al., 2005, 2013).

One of the most studied domains in fMRI is human memory. In this regard, two of the most differentiable kinds of memory are the working memory and the episodic memory.

1.3.1 Working memory networks

In cognitive neuroscience, Working Memory (WM) refers to the capacity to maintain, manipulate and store information temporarily and involves a set of brain structures and processes to organize and integrate sensory and other information (Baddeley, 1986). WM can be decomposed into processes of memory and attentional control and is one of the functions with clear age-related decline (Park and Reuter-Lorenz, 2009). The use of fMRI during working memory tasks evidenced consistent activation of prefrontal, temporal and parietal cortical regions regardless of the task used and the stimulus modality (D'Esposito et al., 1998; Wager and Smith, 2003; Owen et al., 2005).

The N-back task is one of the most commonly used paradigms to study working memory networks with fMRI (see Owen et al. (2005) for a meta-analysis). It consists on presenting a sequence of stimuli from which the subject is asked to indicate, by means of a response button, when the stimuli presented on the screen is the same that the one presented n items before. The n-back algorithm has the advantage that the cognitive load can be easily controlled by the researcher by changing the number of items (n) to be remembered, allowing for parametrical modeling of working memory. This number usually goes from $n = 1$ to $n = 3$ items. A control condition, 0-back, is often used, in which subjects are asked to indicate each time a specific stimuli appears in the screen. The brain regions that have been reported to consistently reported to be involved in the N-Back task are shown in Figure 1.2.

In N-back tasks, a broad variety of stimuli have been used (for example, verbal vs non-verbal, or identity vs location). In these cases, despite the fact that the main areas of the WM network are commonly activated in all of them, domain-specific activations within brain structures have also been documented (Fuster, 1997; Rottschy et al., 2012).

1.3.2 Episodic memory networks

Episodic memory is defined as the conscious process of remembering experienced events with a particular spatio-temporal context (Tulving, 1987). Brain networks involved in episodic memory function have been studied by identifying areas that show activity increases during successful encoding or successful retrieval trials. FMRI studies have demon-

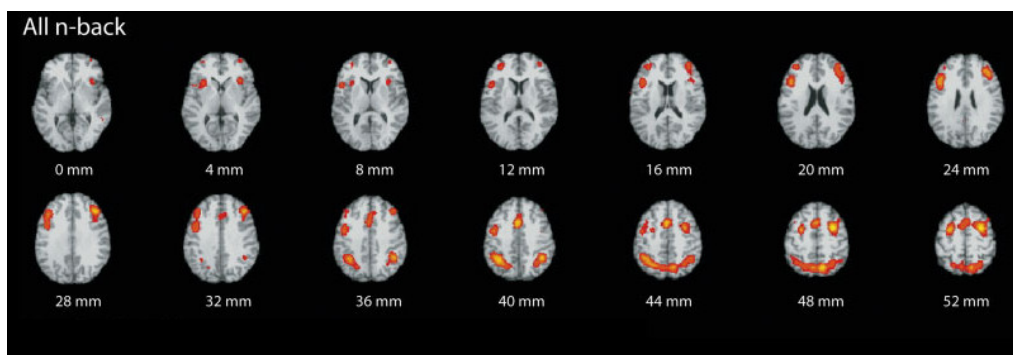


Figure 1.2: Brain regions associated with the N-back paradigm. Adapted from the meta-analysis published by Owen et al. (2005).

strated that there is a memory network highly consistent across different experimental conditions, including a variety of stimuli, or differences in the paradigm. In general, both encoding and retrieval processes are associated with a brain network involving the medial temporal lobe (MTL) and prefrontal and parietal regions (Spaniol et al., 2009).

In a more specific sense, it has been described that the network associated with successful memory encoding includes mainly 5 regions: (1) the left inferior temporal cortex, (2) the bilateral fusiform cortex, (3) the bilateral hippocampal formation (being part of the MTL), (4) the bilateral premotor cortex, and (5) the bilateral posterior parietal cortex (Kim, 2011). These patterns are shown in Figure 1.3.

In addition, the same kind of studies has revealed a set of areas that show consistent deactivations during successful encoding. This pattern of deactivations coincides with the default mode network (DMN), concretely involving the Posteromedial Cortex (PMC), which is also deactivated during the performance of a wide range of cognitive demanding tasks (Raichle et al., 2001). Several studies have indicated that the degree to which the DMN deactivates is directly related to memory performance (Daselaar et al., 2004; Vannini et al., 2011). In the same line, unsuccessful encoding, measured with the forgotten effects (i.e. forgotten > remembered fMRI contrast), has been shown to be held by the activity in the PMC (Kim, 2011).

Intriguingly, it has been observed that there is a region in the PMC that becomes active during successful retrieval process. This region has high overlap with the part of the

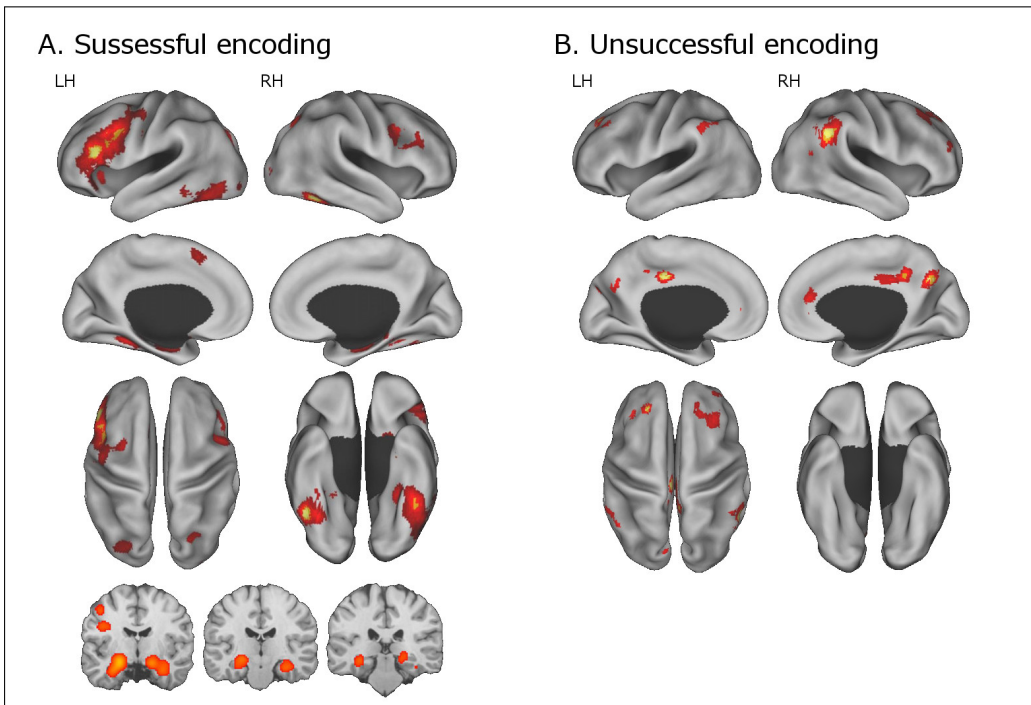


Figure 1.3: Brain regions associated with successful and unsuccessful encoding effects. Adapted from Kim (2011).

PMC that deactivates during encoding. Therefore, memory retrieval is one of the few goal-directed tasks that activate the DMN, which has been interpreted as a result of the implication of self-referential and reflective activity (Gusnard and Raichle, 2001; Buckner et al., 2008). This phenomenon is known as the Encoding/Retrieval (E/R) flip, and it states that successful memory depends on the correct deactivation of the PMC during the codification of items followed by its activation during retrieval (Huijbers et al., 2012; Vannini et al., 2013). The E/R flip has attracted the attention of many researchers because its relevance to neurofunctional changes in aging and neurodegenerative diseases (Miller et al., 2008; Vannini et al., 2008).

■ WORKING MEMORY

Memory capability used to maintain, manipulate and store information during short periods of time. Involves fronto-parietal and temporal networks.

■ EPISODIC MEMORY

Memory capability used to consciously store and retrieve events in a particular context. Its main network involves MTL and prefrontal brain regions.

1.4 FMRI in healthy aging

Some elders are able to maintain their cognitive capabilities at high levels in contrast with other adults who show clear cognitive declines. It has been hypothesized that this variability depends on neurofunctional resources. However, the exact mechanisms that lead to such wide differences are still unclear (Park and Reuter-Lorenz, 2009).

The use of task-fMRI in aging has revealed a complex pattern of brain activity changes characterized by decreases, increases, or no differences between old and young subjects. The diversity of findings depends on many variables, such as the cognitive test used and the level of difficulty (Grady et al., 2006). Nonetheless, there is a relative consensus that there is an age-related increase of brain activity in the prefrontal cortex (PFC) (Turner and Spreng, 2012), while findings as regards reduced activation are localized more heterogeneously in the brain. Regional hyperactivation has been interpreted as compensation, or

attempted compensation; whereas failure to activate has been typically interpreted in relation to cognitive deficits associated to aging.

There are several theories that have been proposed in order to explain the changes observed during the aging process using fMRI (Grady, 2012). In the first place, two main hypotheses have been proposed to explain the nature of the age-related activity increases: the *compensation* and the *dedifferentiation* hypotheses. Furthermore, some theories have emerged in order to understand the spatial localization of these changes and their relation to changes in cognitive abilities. These concepts are summarized in the following two sections.

1.4.1 Compensation vs Dedifferentiation

Compensation

The compensation hypothesis in aging states that older adults are able to recruit higher levels of activity in comparison to young subjects in some brain areas to compensate for functional deficits located somewhere else in the brain. This increased activity is often seen in frontal regions (Turner and Spreng, 2012; Park and Reuter-Lorenz, 2009).

The first studies suggesting compensatory mechanisms appeared early in the literature and used PET during the performance of visuospatial (Grady et al., 1994) or episodic memory (Cabeza et al., 1997; Madden et al., 1999) tasks. Later on, these findings were replicated with fMRI (Cabeza et al., 2002).

However, the term compensation is conditioned by the fact that activity increases would be directly associated with improvements in task performance, and this is not always accomplished. In this regard, some considerations have appeared in order explain these hyperactivations. For example, Cabeza and Dennis (2013) recently suggested that the increased brain activity, which appears when task demands are greater than the cognitive resources, can be classified as: 'attempted compensation', when there are no changes in performance; 'successful compensation', when subjects perform better than those which do not activate; and 'unsuccessful compensation', when subjects perform worse.

Other authors have referred to the 'Partial compensation' hypothesis (de Chastelaine et al., 2011). According to this hypothesis, the effects of additionally activated areas might be

inversely correlated with the functional integrity of the original task-related areas, leading to worse performance.

Dedifferentiation

The term dedifferentiation is described as the loss of functional specificity in the brain regions that are engaged during the performance of a task (Rajah and D'Esposito, 2005). Using fMRI, Park et al. (2004) studied brain activity in the visual cortex during visualization of different stimuli, and they found that, while young subjects exhibited category-specific activation in the ventral visual cortex, old subjects showed less neural-differentiation.

According to this hypothesis, the age-related decreases in brain activity are due to reduced regional process-specificity, whereas activity-increases reflect generalized spreading of activity. In neurobiological terms, it has been suggested that this pattern of changes is caused by a chain of processes which starts from a decline in dopaminergic neuromodulation that produces increases in neural noise, leading to less distinctive cortical representations. At the cortical level, the dedifferentiation phenomenon causes increased variability of intra-network random activity (Li et al., 2001).

1.4.2 Cognitive Models in aging

Besides the two hypotheses presented above, there are different models that have tried to explain the functional and cognitive implications of brain activity changes in aging. Although not exclusively, the main theories are understood under the assumption that activity increases are compensatory.

The HAROLD model

The Hemispheric Asymmetry Reduction in Old Adults (HAROLD) model was introduced by Cabeza (2002). It states that during the performance of a task, the activity pattern observed in older adults is less lateralized than the one observed in young subjects under similar conditions. In their first study, Cabeza et al. used an episodic memory task to demonstrate that low-performing older adults showed an activation pattern very similar to

the activity seen in younger adults, mainly including regions in the right PFC. On the other hand, they found that high-performing older adults also activated the same area in the left PFC. Similar patterns of bilateral activation associated with successful task performance have been described in other studies (Cabeza, 2004).

The CRUNCH model

The compensation-related utilization of neural circuits hypothesis (CRUNCH) defends that, in older adults, higher neural recruitment occurs in cognitive levels that typically imply lower brain activity in younger subjects. This effect has been observed in the PFC and also in the parietal cortex, concretely in the precuneus and posterior cingulate and both in episodic memory tasks (Spaniol and Grady, 2012) and in working memory tasks (Reuter-Lorenz and Cappell, 2008; Mattay et al., 2006). Importantly, as regards working memory, the n-back task represents an ideal experimental condition to test this model because the cognitive load can be easily controlled by changing the number of items to be kept (Nagel et al., 2011).

The PASA model

The posterior-anterior shift with ageing (PASA) was experimentally proved by Davis et al., who used two different tasks, visuoperceptive and episodic retrieval and found that older subjects had deficits to activate regions in the posterior midline cortex accompanied with increased activity in medial frontal cortex (Davis et al., 2008).

1.4.3 Connectivity-related changes in Aging

Results from task-activation fMRI studies in aging are sometimes controversial and difficult to interpret. Therefore, more recently, studies on healthy aging have also focused in brain connectivity (Dennis and Thompson, 2014). Brain connectivity changes related to aging are thought to be also useful in order to interpret functional reorganizations in the context of the models of functional brain compensation and dedifferentiation. Whereas some of the connectivity-related findings refer to task-fMRI experiments, the majority of them have been obtained by means of resting-state fMRI.

Some evidences of task-related connectivity changes in aging are found in the working memory literature. For example, Nagel et al. (2011) found load-related increases in PFC activity (interpreted in the context of the CRUNCH model) that was accompanied with decreases in the functional coupling between PFC and premotor cortex. Also, Madden et al. (2010) used task-fMRI to study brain activity and connectivity during task switching in a group of young and a group of old subjects. They found that, besides the level of task-related brain activity was very similar between groups, older subjects showed lower functional connectivity between brain areas of the switch-related network.

Other evidences are found in episodic memory tasks, where reduced connectivity within the memory network coexists with increased connectivity in other brain regions (Daselaar et al., 2006; Dennis et al., 2008; Addis et al., 2010). Concretely, these studies reported reduced connectivity from the hippocampus and MTL to posterior and occipital regions together with increased connectivity from the same regions to frontal areas, such as the PFC. These results support the PASA model and indicate that functional connectivity changes follow similar patterns than those described with task-related activity.

Functional MRI at rest is the most widely used method for studying human brain functional connectivity. Alterations of RSFC in aging include disconnection or dysfunction within some of the large-scale networks as well as alterations in whole-brain connectivity patterns. A summary of the most important studies in aging and functional connectivity using rs-fMRI, including those that reported correlations with cognitive changes, is given in Table 1.2.

It is noteworthy that a great majority of articles have focused on the DMN. This fact can be explained because the DMN has been closely related to the functional and neurobiological changes underlying Alzheimer's Disease (AD), specially at its first stages (Buckner et al., 2009). In addition, the spatial extend of the DMN overlaps the network of intrinsic hippocampal connectivity, and therefore, all together, the DMN and the hippocampal network are believed to support episodic memory processing (Miller et al., 2008). Besides this, there are also studies reporting changes in other brain networks, as well as others using whole-brain connectivity approaches that do not specifically attempt to study any specific system.

A common finding of the studies reviewed in Table 1.2 is the decreased connectivity within the nodes of some of the main RSNs, including the DMN and the Salience and executive/attention networks. This result has been obtained with ICA (Damoiseaux et al., 2008; Jones et al., 2011; Onoda et al., 2012), and also using seed-based correlations (Andrews-Hanna et al., 2007; Wang et al., 2010) and graph-theory or whole-brain approaches (Tomasi and Volkow, 2012; Betzel et al., 2014; Geerligs et al., 2014; Song et al., 2014). Disrupted connectivity in aging persists even controlling for brain atrophy or age-related structural changes (Ferreira and Busatto, 2013). Connectivity decreases directly imply reductions in the way how information is transferred between different brain regions. In this regard, a well-reported result is the disconnection between the anterior and the posterior nodes of the DMN, which correlates with age-related cognitive decline (Andrews-Hanna et al., 2007; Damoiseaux et al., 2008), and with white-matter deficits (Andrews-Hanna et al., 2007). In addition, using task-fMRI in combination with rs-fMRI, Campbell et al. (2012) demonstrated that the disruption of antero-posterior connectivity at rest was related to deficits in the activation of task-related areas during a cognitive-control task.

The results as regards somatosensory, motor and subcortical networks are not that consistent, with some studies reporting connectivity increases (Tomasi and Volkow, 2012; Song et al., 2014), no changes (Geerligs et al., 2014) or non-linear changes (Betzel et al., 2014) within these systems.

The increased connectivity has been further explored using higher-level analysis methods. Tomasi and Volkow (2012) found that long-range FC is decreased with age whereas short-range FC is increased. These results have been interpreted under the hypothesis that some brain regions, with key roles in whole-brain connectivity, named hubs (Buckner et al., 2009), could experiment strengthening of functional connectivity with their closest regions, leading to an increase of local connectivity increases (Ferreira and Busatto, 2013). Furthermore, a recent study reported non-linear changes in the FC within some networks (Betzel et al., 2014).

In addition, some of the studies have explored connectivity between different networks at rest, mainly reporting increases between different systems (Onoda et al., 2012; Betzel et al., 2014). It should be noted that the majority of the results examining large-scale

networks are also in concordance with earlier graph-theory studies Achard and Bullmore (2007); Meunier et al. (2009), that were not focused in specific networks. These studies found reduced global efficiency by means of increased segregation and reduced integration of the whole-brain network.

Finally, few papers have reported relationships between connectivity and cognition. In some cases, connectivity changes have been related to executive and memory functions (Andrews-Hanna et al., 2007; Damoiseaux et al., 2008; Wang et al., 2010; Onoda et al., 2012), and one study reported correlations between the DMN and a mental state test (Wang et al., 2010). And, interestingly, the only study that correlated FC measures with structural connectivity found that these two measures were correlated in aging (Andrews-Hanna et al., 2007).

■ AGING & NETWORKS

- ✓ Decreased connectivity within default, salience and executive networks.
- ✓ Increased connectivity within somatosensory and subcortical networks.
- ✓ Increased connectivity between regions from different networks.
- ✓ Decreased efficiency of the whole-brain network, with higher segregation and lower integration.

In summary, connectivity changes within the common RSNs are well described in aging. However, more recent lines of research tend to focus on more complex aspects of brain connectivity. One of these aspects is the inclusion of hubness information. This idea has been motivated by studies showing that the main brain hubs are characterized by a high connection density, but also the high vulnerability (Crossley et al., 2014). In addition, another line of research refers to the study of functional connectivities within and between the main large-scale networks. In this regard, it has been described that the age-related decreases in connectivity between regions of a network can be accompanied by increases in the connectivity of these network towards regions of other RSNs, affecting the overall functional connectivity architecture (Betzel et al., 2014; Geerligs et al., 2014).

Table 1.2: Studies on Aging & Functional Connectivity

Study	Sample	Method	RSN changes	Other results	Relation to Cognition
Achard and Bullmore (2007)	17 young (18-33y) 13 old (62-76y)	Graph theory	–	↓ Global efficiency Effects on frontal & temporal regions	None
Andrews-Hanna et al. (2007)	93 (18-93y)	Seed-based	DMN ↓ DAN ↓	FC relates to white matter integrity	Executive functions, memory & processing speed.
Damoiseaux et al. (2008)	10 young (22.8 ± 2.3y) 22 old (70.73 ± 6y)	ICA	DMN ↓		Executive function & processing speed
Meunier et al. (2009)	17 young (18-33y) 13 old (62-76y)	Graph theory	–	equal modularity ↑ num. of modules ↑ segregation	
Wang et al. (2010)	17 (62-83y)	Seed based	DMN ↓	FC Hipp-PPC	Prediction of memory performance
Jones et al. (2011)	341 (64-91y)	ICA Seed-based	DMN ↓↑	↑ Anterior DMN FC ↓ Posterior DMN FC	correlation with mental state test.
Campbell et al. (2012)	12 young (18-28y) 12 old (60-78y)	Seed-based	FPN ↓ CtrN ↓	FC relates to task-activity.	None
Onoda et al. (2012)	73 (36-86y)	ICA & Seed-based	SAL ↓ DMN ↓	↓ SAL-visual ↑ SAL-auditory ↑ DMN-visual	SAL correlated with frontal & visuospatial functions.
Tomasi and Volkow (2012)	913 (13-85y)	FC density mapping. (Whole-brain)	DMN ↓ DAN ↓ SomMotor ↑ Subcortical ↑	↓ long-range FC. ↑ short-range FC	None
Betzel et al. (2014)	126 (7-85y)	Whole-brain FC Graph-theory	CtrN ↓ DMN ↓ VisPeri ↓ SAL ∩ SomMotor ∩ VisCen ∩	↑ FC between-RSN	None
Geerligs et al. (2014)	40 young (18-26y) 40 old (59-74y)	Graph-theory FPN ↓ SomMotor =	DMN ↓ CingOper ↓ ↑ FC DMN - CtrN ↑ FC Visual - CtrN Visual =	↓ Modularity ↓ Local Efficiency	None
Song et al. (2014)	26 young (24.6 ± 3y) 24 old (58 ± 6.1y)	Graph-theory	DMN ↓ SomMotor↑	↓ Modularity ↓ Local efficiency Change in hubness	None
Zhang et al. (2014)	18 young (22-33y) 22 old (60-80y)	Seed-based	DMN ↓ SAL ↓ CtrN ↓↓ DAN ↓↓ Visual =	Selective vulnerability of networks	None

FC: Functional Connectivity; RSN: Resting-State Network; CtrN: Control Network; DMN: Default Mode Network; SAL: Saliency Network; VisPeri: visual pericalcarine; VisCen: visual central network; DAN: Dorsal Attention network; CingOper: cingulo-opercular network; SomMotor: somatosensory/motor network; PPC: Precuneus/Posterior Cingulate.

1.5 Alzheimer's Disease

Alzheimer's Disease (AD) is one of the most common neurodegenerative diseases affecting elder population. Therefore, an extensive effort has been made in order to characterize brain changes that occur during the disease timecourse, especially those that appear early in the disease time course or even before the appearance of clinical symptoms. The research in fMRI and AD include studies with subjects diagnosed with AD and also subjects with Mild Cognitive Impairment (MCI), which is considered a preceding stage of AD (Petersen et al., 2009), and subjects at high-risk for AD, including those with genetic risk, carrying APOE $\epsilon 4$ gene, and those with high amyloid burden, measured by Pittsburgh Compound B (PET) imaging.

With fMRI, it has been demonstrated that AD patients have clear difficulties in the activation of some task-related areas, as well as notable disruptions in brain connectivity (Dennis and Thompson, 2014). Therefore, the utilization of task-fMRI and rs-fMRI has appeared as a good and reliable non-invasive biomarker for AD (Sperling, 2011). Its usefulness relies on its ability to find differences between healthy and diseased populations, to study brain changes in subjects with high-risk of developing AD, and also to track the evolution of changes during the disease timecourse or during treatment administration (Chhatwal and Sperling, 2012).

In this sense, the two most replicated findings in AD are the activity deficits observed in MTL during memory tasks, as well as the dysfunction of the DMN, observed both as task-related deactivations and in rs-fMRI studies.

1.5.1 Alzheimer's disease and task-fMRI

There is a general consensus that brain activity changes follow a non-linear trajectory during the timecourse of AD. Several studies have reported activity increases in MTL during memory tasks in subjects at very early phases of MCI, which has been interpreted as a compensatory mechanism to maintain memory function. However, subjects with more advanced MCI and subjects already suffering from AD have shown task-related deficits in MTL activity in comparison to healthy elders (Dickerson et al., 2005; Swindt and Black,

2009). This specific pattern of increases followed by decreases in hippocampal and parahippocampal regions differs from healthy elders, who showed a relative stability as regards hippocampal activity (Chhatwal and Sperling, 2012).

In addition to the activity decreases in MTL, AD patients have also shown increased activity regions of the prefrontal cortex during the performance of memory tasks, which has been interpreted as representing an unsuccessful effort made by AD patients to compensate for impaired memory (Chhatwal and Sperling, 2012; Schwindt and Black, 2009).

Finally, other studies have demonstrated that subjects suffering from MCI and AD have deficits in DMN deactivation (Lustig et al., 2003), suggesting an alteration in the interplay between task-positive and task-negative networks. In some cases, alterations of the DMN have been described in disease stages at which task-positive networks are still preserved (Sala-Llonch et al., 2010), or even in asymptomatic subjects with high amyloid-burden, being at high-risk for AD (Vannini et al., 2012; Pihlajamäki and Sperling, 2009; Sperling et al., 2009).

1.5.2 Alzheimer's disease and large-scale networks

The results of task-fMRI have drawn the attention towards the study of brain connectivity, suggesting that neurofunctional changes in AD might be a result of alterations within the dynamics of large-scale functional systems, and that these alterations can appear even before task-activation deficits (Matthews et al., 2013). The increasing interest in studying brain networks in the context of AD has been also supported by the 'network degeneration' hypothesis, according to which the main neurodegenerative diseases show distinguishable patterns of brain atrophy that are in concordance with patterns of intrinsic functional connectivity found in healthy subjects (Seeley et al., 2009) and with the hubs of whole-brain networks (Crossley et al., 2014). In the case of AD, the pattern of cortical atrophy matches the DMN. In addition, in an early investigation, Buckner et al. (2005) studied the convergence of cortical atrophy, metabolic changes, and functional findings (although with different samples). They found that areas within the DMN showed amyloid deposition, higher atrophy rates and metabolic abnormalities, and suggested the potential of the DMN as a biomarker for AD.

More recently, evidences of DMN disruption in AD and its preclinical stages are found in the resting-state fMRI literature (Sheline and Raichle, 2013). In this regard, some studies reported altered connectivity between DMN regions, or between regions of the DMN and task-related regions, such the MTL. These results have been reported in AD and MCI patients, and in healthy subjects at-risk for AD (Greicius et al., 2004; Hedden et al., 2009; Sheline et al., 2010; Sorg et al., 2007). Other networks, especially those involved in attention, have also found to be disrupted in these subjects (Sorg et al., 2007; Agosta et al., 2012).

In summary, the study of task-activation and resting-state studies, together with evidences from structural imaging (DTI and atrophy patterns), has lead to the idea that functional changes in AD are a result of localized activity deficits in task-related areas together with deficits in the interplaying role between the different brain networks that, in normal brain functioning, should activate and deactivate with accurate synchrony (Chhatwal and Sperling, 2012).

■ FUNCTIONAL MRI & ALZHEIMER'S DISEASE

- ✓ Altered patterns of activity during memory tasks.
- ✓ Disrupted functional connectivity measured with resting-state fMRI.
- ✓ High rates of $A\beta$ deposition in regions of the default-mode network.
- ✓ Failure to deactivate DMN regions during goal-directed tasks.
- ✓ Detection of brain functional changes at early stages of the disease time-course.

Hypotheses and Objectives

Hypotheses

1. The human brain is functionally organized as a set of networks, which could be identified during task performance and during resting-state fMRI acquisitions and that would have direct implications for cognition.
2. Connectivity signals, measured during resting-state can predict the performance of a subsequent task.
3. Healthy elders would show alterations in the functionality of the working memory system that would be related to cognitive deficits in this domain.
4. Given that aging is characterized by brain activity changes, we expected to find brain connectivity alterations in healthy elders.
5. In the genetic forms of Alzheimers disease, functional MRI can be useful to identify brain changes that occur previous to the clinical manifestations.

Objectives

MAIN OBJECTIVE:

To explore the capabilities of fMRI to identify brain networks that are present at rest and also during the performance of different goal-directed tasks in different sets of populations.

SPECIFIC OBJECTIVES:

1. To test the usefulness of resting-state connectivity to predict performance in a subsequent task.
2. To explore function-structure relationships in brain networks and how do they relate to cognitive performance.
3. To study patterns of activity and connectivity of large-scale brain networks and their relationship with successful cognitive performance in aging.
4. To characterize changes in the whole-brain connectivity in aging process and to study how these changes relate to the cognitive status.
5. To explore the power of fMRI to identify brain changes that appear in early stages of neurodegenerative processes, even before the onset of clinical symptoms.

3.1 Study Sample

3.1.1 Subjects included in each study

The results presented in this thesis have been obtained from 6 different studies. A summary of the settings and analyses for each of the studies is given in Table 3.1.

The group of subjects included in *Study 1* was composed by 16 Young Adults (YA). They were university students with no history of psychiatric or neurological alterations.

Subjects in *Study 2* were 23 YA, with no history of psychiatric or neurological disorders.

Study 3 included a group of 16 YA and a group of 29 Healthy Elders (HE). The YA group was the same than the group included in Study 1, and HEs were recruited from the *Institut Calalà de l'envelliment* and from medical centers located in Barcelona. Subjects had no history of neuropsychological or neuropsychiatric disorders and they underwent neuropsychological screening to exclude mild cognitive impairment.

The sample used in *Study 4* and *Study 5* were an extension of the HE sample from Study 3, and therefore the inclusion criteria was the same as above. Differences between the num-

Table 3.1: Sample of subjects included in each study.

Study	Sample	MRI Data	Analysis technique	Cognitive domain
1	16 YA (21.31 ± 2.41 y)	RS fMRI N-Back fMRI	ICA & dual regression Network correlation	Working Memory
2	23 YA (28.26 ± 6.76 y)	Facial N-Back fMRI Spatial N-Back fMRI Diffusion MRI	ICA DTI-Tractography	Visuospatial and visuooperative Working Memory
3	29 HE (62.55 ± 9.43 y) 16 YA (21.31 ± 2.41 y)	RS fMRI N-Back fMRI	ICA & dual regression Task-related activation	Working Memory
4	98 HE (64.87 ± 11.8 y)	RS fMRI	Whole-brain FC Graph-theory	Memory (verbal & visual)
5	73 HE (65.88 ± 10.11 y)	RS fMRI	ICA Network interactions	Memory, Executive functions
6	13 CTR 11 PSEN1-AMC 8 PSEN1-SMC	RS fMRI Encoding fMRI	ICA & dual regression Seed-based Task-related activation	Episodic memory

YA: Young Adults; HE: Healthy Elders; RS: resting-state; ICA: Independent Component Analysis; DTI: Diffusion Tensor Imaging; FC: Functional Connectivity; CTR: controls; PSEN1: Presenilin1; AMC: Asymptomatic Mutation Carriers; SMC: Symptomatic Mutation Carriers.

ber of subjects included in Study 4 (N=98) and in Study 5 (N=73) are due to the fact that the results of some neuropsychological tests were not available for all subjects.

Subjects from *Study 6* included nineteen mutation carriers from 8 families with 6 different Presenilin-1 (PSEN1) mutations, and 13 matched controls or non-carriers. PSEN1 mutations¹ cause familial Alzheimer's Disease. They affect the amyloid- β protein precursor with almost 100% penetrance and an early age of onset. Subjects were recruited from the genetic counseling program for familial dementias (PICOGEN) at the Hospital Clinic, Barcelona, Spain (Fortea et al., 2011a).

¹<http://www.molgen.ua.ac.be>

3.2 Acquisition and paradigms

3.2.1 MRI sequences

MRI data were acquired on a SIEMENS Magnetom TrioTim syngo 3-Tesla at the Diagnostic Imaging Centre of the Hospital Clinic (CDIC) in Barcelona. Images were acquired with a 32-channel coil for all the studies except from study 6 where we used a 8-channel coil. All images were obtained using the following imaging protocols:

Structural T1

High-resolution T1-weighted structural scans were obtained using an MPRAGE 3D protocol. The acquisition parameters were: repetition time (TR) = 2300 ms, echo time (TE) = 2.98 ms, 240 slices, field of view = 256 mm, matrix size = 256 x 256, slice thickness = 1mm, voxel size = 1mm x 1mm x 1mm.

Diffusion MRI

Diffusion weighted images, acquired in Study 2, were sensitized in 30 non-collinear directions with a b-value=1000 s/mm², using an echo-planar (EPI) sequence with the following parameters: TR = 9300 ms, TE = 94 ms, slice thickness = 2.0 mm, field of view = 240 mm, no gap, voxel size = 2 x 2 x 2 mm.

Functional MRI

Functional MRI scans were obtained using T2*-weighted MRI with the following acquisition parameters: TR = 2000 ms, TE = 16 ms, 40 slices per volume, slice thickness = 3mm, gap = 25% ; field of view = 240 mm, matrix size = 128 x 128, voxel size = 1.7 x 1.7 x 3.0 mm.

3.2.2 Functional Paradigms

Working memory task

The task used in Studies 1 and 3 to evaluate working memory was a verbal *n*-back paradigm using letters as stimuli and with different levels of cognitive load (*n* = 0, 1, 2, and 3 letters to

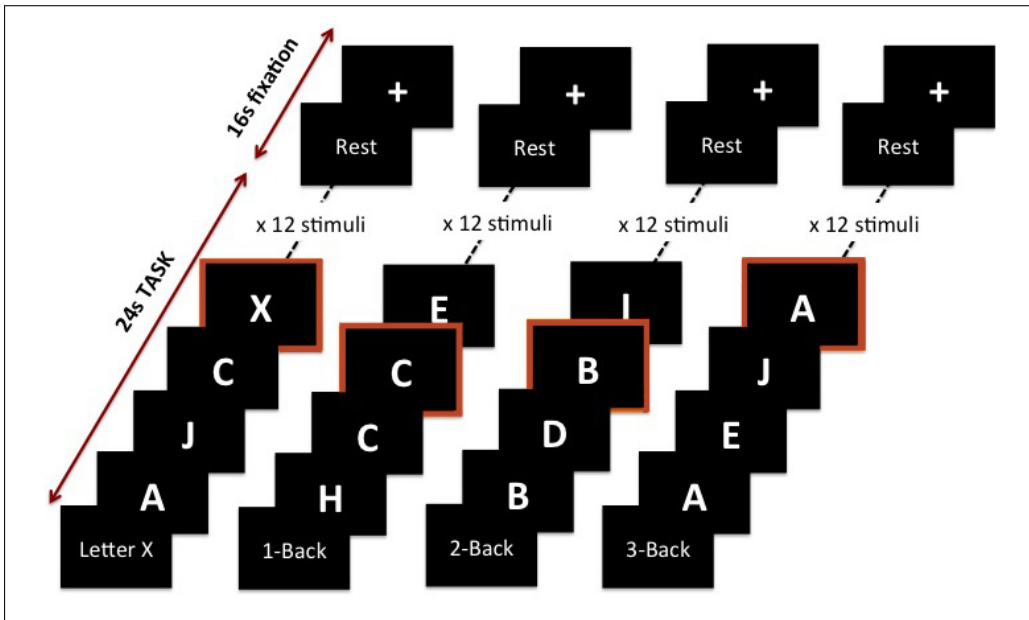


Figure 3.1: N-Back paradigm used in Study 1. Highlighted stimuli indicate the targets for each condition

be retained) (Braver et al., 1997; Owen et al., 2005). Task blocks consisted on the continuous presentation of stimuli. Stimuli were white capital letters (A-J) appearing in the middle of a black screen during 500 ms with and interstimulus interval of 1500 ms between letters. Task blocks were combined with fixation periods consisting on a white cross on a black screen. During the time course of the task, blocks of 0-, 1-, 2-, and 3-back conditions lasting 26 seconds were presented four times each in a pseudo-randomised order with inter-block fixation periods of 13 s. Before any n -back block, an instruction screen appeared for 1 s to inform the subject about the task. Within each block, a sequence of 12 letters was presented and the subject was asked to press a button when the letter on the screen was the same as the letter showed n items before. For the 0-back condition, subjects were asked to press the button when the letter 'X' appeared on the screen. The full paradigm lasted 11 min 12s (Figure 3.1).

For Study 2, we used two other versions of the n -back paradigm, one with spatial (spatial-WM) and one with facial (facial-WM) stimuli. There were two experimental conditions in each task: the 0- and the 2-back conditions. For facial-WM stimuli were faces

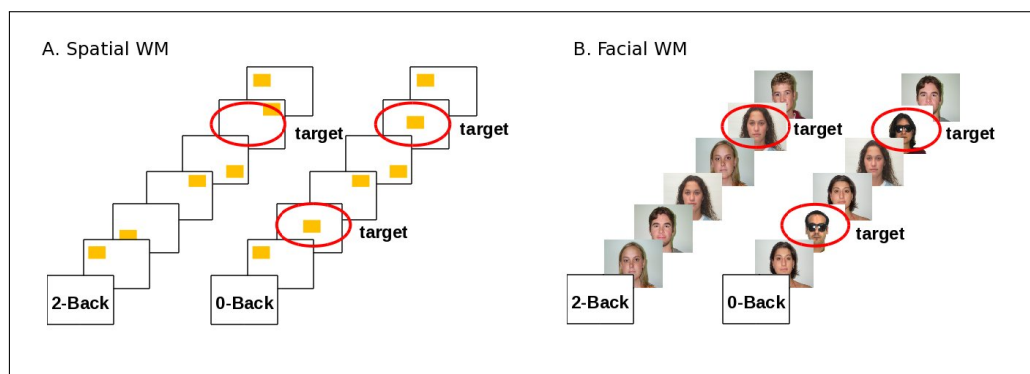


Figure 3.2: N-Back paradigm used in Study 2. (A) Spatial working memory, (B) Facial working memory

extracted from a public available database (Minear and Park, 2004) and for spatial-WM stimuli were color squares located in different parts of the screen. Subjects were asked to indicate whether the current stimulus was the same than the one presented 2 items before (2-back task) or if it matched a control stimulus (0-back task). Stimuli used for the control condition were a square in the middle of the screen for spatial-WM and any face wearing sunglasses for facial-WM (Figure 3.2). Each stimulus appeared in the screen for 1 s, with an interstimulus interval of 1 s. Each task consisted in 16 blocks of 14 stimuli, with alternating 0-back and 2-back blocks, with total task duration of 8 minutes.

In all the three studies with n -back paradigms the presentation of stimuli and the task implementation were performed using the Presentation[®] software² implemented on a computer that was synchronized with the MRI scanner. In addition, subjects' responses were collected and the performance of each condition was obtained using the d' measure, calculated as the $Z(\text{hit rate}) - Z(\text{false alarm rate})$, with higher d' scores indicating higher performance. Mean reaction time (RT) was also collected, as the time between the stimulus onset and the subject's response for each subject in each condition.

In all cases, subjects underwent a training session before entering the scanner in order to ensure that they understood the task instructions. All achieved a task accuracy of at least 80%.

²Neurobehavioral Systems, <http://www.neurobs.com/>

Episodic memory task

Episodic memory was evaluated under fMRI using a visual encoding task. The task consisted of a 15-block design that alternated 'fixation', 'repeated' and 'encoding' blocks, where each block lasted 30 s. During 'fixation' condition, a white cross was presented in the middle of a black screen. During 'encoding' and 'repeated' conditions a set of 10 images were presented as a sequence in the screen for 2 s with an interstimulus interval of 1 s. In the 'repeated' condition, the same image was shown repeatedly, whereas 'encoding' blocks consisted on the presentation of 10 novel pictures, with a total of 50 new images.

After the scanning session, subjects were tested for their memory in a two-alternative forced-choice task in which they had to decide which picture from a pair of scenes had appeared in the encoding session. A total of 50 pairs of images, matched for content, were presented. The side of presentation on the screen of the correct pictures was randomized so that the scenes appeared the same number of times on each side. In addition, the order of presentation of the pictures was randomized with respect to the encoding phase. The encoding task was also implemented with the Presentation[®] software.

3.2.3 Subjects' selection and clinical/neuropsychological assessment

To evaluate the neurocognitive status of the subjects, trained neuropsychologists administered a set of tests in order to assess a wide range of cognitive domains, including executive function, verbal and visual memory, visuoperception and processing speed.

3.3 Analysis of structural MRI

Structural MRI is commonly used to measure gray matter volume, which can be quantified using automated or manual techniques.

In order to estimate tissue volume, high-resolution MPRAGE scans are first segmented into gray matter (GM), white matter (WM) and cerebrospinal fluid (CSF) using automated tools. This can be achieved using FAST from FSL (Zhang et al., 2001), which gives an individual segmentation based on the probability of each voxel to belong to a certain brain

tissue. Whole-brain gray matter volume can be then estimated by calculating the overall density within the gray matter mask.

Furthermore, more accurate methods, such as voxel based morphometry (Ashburner and Friston, 2000) and cortical thickness (Fischl and Dale, 2000) allow examining regional differences in gray matter at the voxel-by-voxel level or by mapping the cortical gray matter on a surface-based representation of the brain.

In the studies included in this thesis, 3D structural images were used for registration purposes in functional studies, as well as to obtain measures of whole-brain gray matter. No regional or voxel-wise analyses were performed.

3.4 Analysis of Diffusion MRI

Diffusion MRI data consists on sets of 4D images containing diffusion information across several directions in the 3D space.

Prior to analysis, a preprocessing is applied to the images. It includes removal of non-brain voxels using BET (Smith, 2002), and correction for motion and for the distortion introduced by the eddy currents in the gradient coils.

3.4.1 The DTI approach

A DTI approach was used to obtain individual maps of Fractional Anisotropy (FA), Radial Diffusivity (RD) and Axial Diffusivity (AD) (Le Bihan, 2003). In DTI, the diffusion at each voxel is simplified as a 3×3 symmetric matrix. Therefore, the first eigenvector of this matrix, v_1 corresponds to the main diffusion direction, and its corresponding eigenvalue, λ_1 , is the magnitude of the diffusion in this main direction. This main direction is parallel to the direction of the fiber bundle passing by the voxel. Similarly, the other two pairs of eigenvalues and eigenvectors, v_2, λ_2 and v_3, λ_3 , correspond to the second and third diffusion directions, and they are perpendicular to the main diffusion direction (Figure 3.3).

Using the three eigenvalues, the degree of Fractional Anisotropy (FA) at each voxel can be calculated as:

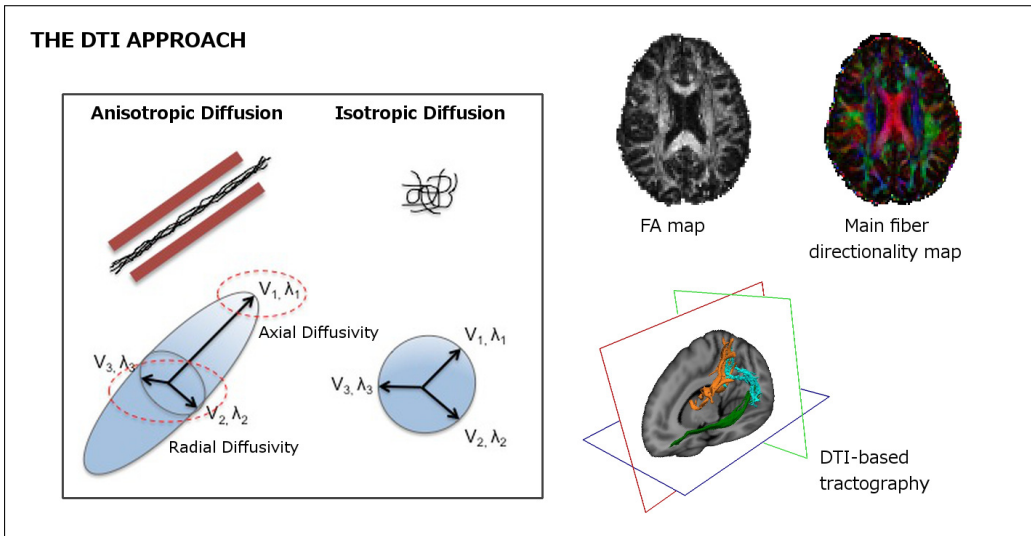


Figure 3.3: Representation of the diffusion vector in the DTI approach and examples of individual fractional anisotropy maps, directionality maps and fiber tractography.

$$FA = \sqrt{\frac{1}{2} \frac{\sqrt{(\lambda_1 - \lambda_2)^2 + (\lambda_2 - \lambda_3)^2 + (\lambda_3 - \lambda_1)^2}}{\lambda_1^2 + \lambda_2^2 + \lambda_3^2}}$$

Other DTI-related indices are the Axial Diffusivity (AxD), which is equivalent to λ_1 , the Radial Diffusivity (RD), calculated as $\frac{(\lambda_2 + \lambda_3)}{2}$, and the Mean Diffusivity (MD), calculated as $\frac{(\lambda_1 + \lambda_2 + \lambda_3)}{3}$.

3.4.2 Tract Based Spatial Statistics

The Tract Based Spatial Statistics (TBSS) approach is a tool developed in FSL to carry out voxel-wise statistics on FA maps obtained with the DTI approach. In TBSS, all subjects' FA data are aligned to a common space using nonlinear registration (Andersson et al., 2007). Next, the mean FA image is created and thinned to create a mean FA skeleton that represents the centres of all tracts common to the group. Then, the FA map of each subject is projected onto the skeleton and the resulting maps are fed into voxelwise cross-subject statistics with non-parametrical permutation methods (Nichols and Holmes, 2002).

Once the skeleton has been created with FA data, the maps of RD, AxD and MD can also

be projected to the skeleton and used for voxel-wise statistics.

After the skeleton is created with FA data, the maps of RD, AxD and MD can also be projected to the skeleton and used for voxel-wise statistics.

3.4.3 Tractography

Preprocessed diffusion MRI data is first fit into the BEDPOSTX algorithm (Behrens et al., 2003b) to perform probabilistic tractography. This method estimates the fiber directions in each voxel using probability density functions that assumes a local 3D Gaussian profile in the diffusion tensor.

Thereafter, probabilistic tractography can be estimated from a *seed* ROI to a *target* ROI. The outputs of the tractography are brain images representing the path distribution, where each voxel value is proportional to the probability of having a path passing through it.

3.5 Analysis of fMRI

3.5.1 Data preprocessing for fMRI data

The tools used for preprocessing of fMRI data were part of the FSL³ and AFNI⁴ packages. The typical preprocessing included: (1) Removal of the first scans (usually ~ 5 volumes) to allow for signal stabilization; (2) Motion correction using MCFLIRT from FSL, which uses a fully automated, robust and accurate tool based on linear or affine image registration (Jenkinson et al., 2002); (3) Skull stripping using BET, which deletes non-brain tissue from an image of the whole head (Smith, 2002); (4) Spatial smoothing using a Gaussian kernel, usually of FWHM between 5 and 8 mm; and (5) Temporal filtering, where the filter cut-off frequencies depend on the temporal design of the data. In task-fMRI, the high-pass filter is set at the Nyquist frequency of the task, and in resting-fMRI it is based on the literature, typically to remove frequencies above 0.1 Hz (Cordes et al., 2001).

³Oxford Centre for Functional Magnetic Resonance Imaging of the Brain, <http://fsl.fmrib.ox.ac.uk/fsl>

⁴<http://afni.nimh.nih.gov/afni/>

3.5.2 Image Registration

After preprocessing, fMRI data need to be registered to a common space to allow for group analyses. In general, registration is performed between functional and anatomical spaces of the same subject, as well as from individual spaces to a common standard space, where the most used standard template is the Montreal Neurological Institute (MNI)-standard space.

Registration can be achieved by using automated tools, such as FLIRT from FSL (Jenkinson et al., 2002), which performs linear affine transformations of brain images with some degrees of freedom (DOF). In FLIRT, the number of DOF is usually set to 6 when registering images from different modalities, especially where there are differences in the quality/resolution of the images, and to 12 when both images are in the same modality and of similar resolution. Then, registration parameters are computed using a cost function, which by default is based on the correlation ratio, although other more complex options can be used, such as mutual information and partial least squares.

In practice, the output of FLIRT is a 4x4 affine matrix containing the transformation-parameters needed to align the input volume to the reference image. Furthermore, there are several transformations that can be applied to the transformation matrices, without the need to calculate the registration parameters again. These transformations mainly include inversion and concatenation of multiple registration matrices. Once the registration calculations are performed, there is a subsequent image transformation, based on interpolation and a final resampling to create the output image.

In a general fMRI analysis setting, the registration algorithm includes: (1) Registration of each functional dataset to the corresponding structural MPRAGE (same subject, different modalities); (2) Registration of each individual structural MPRAGE to the standard MNI (different subjects, same modality); (3) Concatenation of the matrices obtained in previous steps in order to obtain a matrix to register individual fMRI datasets to standard MNI; and (4) inversion of all the matrices obtained before.

These steps provide a set of matrices that can be further used within FLIRT, using the *-applyxfm* option, to move any brain volume or ROI between the three different spaces.

It should be noted that recent registration algorithms are based on non-linear tools. One example is the FNIRT tool also developed within FSL (Andersson et al., 2007). However,

these methods are not used in any of the studies of the present thesis.

3.5.3 Model-driven analysis

FEAT for task-fmri

Model-driven approaches are based on fitting the fMRI data to a time-series model that depends on the experimental design. The FEAT tool from FSL is based on random-effects General Linear Model (GLM), or multiple regressions (Woolrich et al., 2001). There are two different analyses that can be performed with FEAT. One at the subject-level, called *first-level analysis* and one at the group-level, called *higher-level analysis*.

In the first-level analysis, it is necessary to introduce the experimental design of the task timeseries. Then, contrast images can be obtained, as spatial maps of the brain areas with higher activity at specific conditions. This part of the analysis is carried out with FILM (FMRIB's Improved Linear Model), which uses pre-whitening of the timeseries. First-level analyses are usually performed in each individual functional space and the results can be easily registered to either the individual anatomical or standard spaces. In addition with the results of first-level analysis it is possible to estimate the percentage of BOLD signal change between task conditions in specific brain regions.

Higher-level analyses are used to compare activation maps obtained with first-level analysis across sessions or across subjects. In this case, the resulting contrast maps indicate areas where task-related BOLD activity is similar/different between groups, or whether if activity correlates with an external variable.

In FEAT, a thresholding is performed on the Z images, or contrast maps, that result from the initial statistical test. It can be performed at the voxel or at the cluster level and it is based on Gaussian random field theory.

Seed-based correlation for resting fmri

In seed-based correlation analyses, functional datasets are regressed against the timeseries of a region that is selected 'a priori'.

The main steps are the following:

1. Define a brain area of interest to be used as a seed. This can be a single voxel or a group of voxels, and it can be defined using results from other fMRI analysis (i.e., peak areas from ICA, results from task-activations, ...) or even results from other modalities (as structural MRI or DTI). The seed needs to be registered to the same space of the preprocessed fMRI data.
2. Obtain the timeseries associated with the seed for each subject (i.e., mean temporal variation within the seed voxels across time).
3. Regression of the preprocessed fMRI data against the timeseries obtained previously. This step produces a spatial map for each subject where each voxel represents the strength of temporal correlation of that voxel's timeseries with the seed.
4. Individual maps can be used for group-level statistics using voxel-wise statistics.

3.5.4 Data-driven analysis

Unlike model-driven approaches, data-driven or exploratory approaches are used in order to obtain functional patterns that exist in the data during the time of the fMRI acquisition. Therefore, these methods can be used in task-related fMRI data but also in resting-state fMRI studies. In task-fMRI, the model can be fitted *a posteriori*, so it is possible to associate the identified patterns with the different task conditions.

Independent Component Analysis (ICA) is the most commonly used model-driven method for fMRI. In FSL, it is performed with MELODIC tool (Beckmann and Smith, 2004). ICA finds processes in the data that are statistically independent of each other. It provides a linear decomposition of the data into a set of Independent Components (ICs) consisting on spatial maps and associated time-courses.

Although the resulting components are commonly called components of spatiotemporal independence, there are several constraints about the temporal/spatial independence between components that need to be considered. First, as regards the temporal domain, complete independence between components is unrealistic, because all brain processes are somehow dependent of each other. Further, as regards the spatial domain, resulting maps

have high levels of sparsity, but can overlap between them. Between the two options, Melodic-ICA tends to impose spatial independence between components.

At the practical level, ICA pulls together all the input data to find a set of independent sources and an unmixing matrix that minimizes the dependency between them. In order to do that, it is necessary to define a cost function and an optimization technique. MELODIC uses the *FastICA* technique, which uses negative entropy and fixed-point interaction. One of the advantages of this technique, compared with others such as Jade or Infomax (used in SPM), is that it works with non-gaussian data.

One of the risks of ICA is related to the overfitting or the underfitting of the data. An unconstrained decomposition, could give an elevated number of small components that are sometimes difficult to interpret, on the contrary, too few components may not be optimal to fit the signal-to-noise ratio (SNR) of the data. For that, Probabilistic ICA (as implemented in melodic) performs an initial estimation using a Bayesian approach to determine the optimal number of components. However, it is noteworthy that in some studies, the number of components can be defined 'a priori'.

Finally, melodic performs a thresholding of the obtained spatial maps using a mixture model approach to differentiate between signal and background noise. This thresholding strategy is different from the one used in FEAT and it does not depend on the model or the contrasts.

Melodic can be used to perform ICA with single subject fMRI data, or with data from a group of subjects. Single-subject ICA is commonly used as an exploratory analysis to detect activity patterns and identify possible confounds or artifacts. For group-ICA decompositions, two approaches can be considered: The *Tensor ICA* and the *temporal concatenation ICA*.

Tensor-ICA for task-fMRI

The Tensor ICA (T-ICA) approach performs a 3D ICA of the data. In this case, the algorithm finds patterns of synchronized activity across subjects and time, and the resulting components are triplets composed of time courses, spatial maps and a subjects' mode vector. The subjects' mode vector represents the strength of the component for each subject, and it can

be used to perform post-hoc between-subject analyses.

Temporal Concatenation ICA and dual-regression for resting-fMRI

The temporal concatenation ICA (concat-ICA) approach performs a single ICA run on concatenated data of all the subjects. In this case, the ICs obtained represent connectivity patterns that commonly found in all the subjects but that do not need to have temporal coincidence across subjects. In general, it is used with rs-fMRI data.

A common limitation of concat-ICA, is that it does not give a subject modes vector, so it does not allow for post-hoc between-subject analyses. For that reason, it is necessary to perform a *dual regression* analysis to allow for between-subjects statistics (Filippini et al., 2009). The dual regression uses the group-ICA maps derived from concat-ICA and it estimates individual versions of each IC.

At the practical level, the dual regression approach includes the following steps:

1. **Concat-ICA:** This step includes the fMRI preprocessing and a concat-ICA decomposition of all the data to obtain a set of group-ICs.
2. **Spatial regression:** The set of group-spatial maps is regressed (in a multi-GLM approach) into the individual preprocessed fMRI datasets, to obtain a set of individual timecourses for each IC.
3. **Temporal regression:** The timecourses obtained previously are regressed again into the same fMRI datasets to obtain subject-specific IC maps.
4. **Between-subject analyses:** The spatial maps can be then compared across-subjects to find group differences or correlations with an external variable. This stage is performed using non-parametric testing with permutation-methods to control for multiple-comparisons, as implemented in randomise from FSL (Nichols and Holmes, 2002).

This steps are summarized in Figure 3.4.

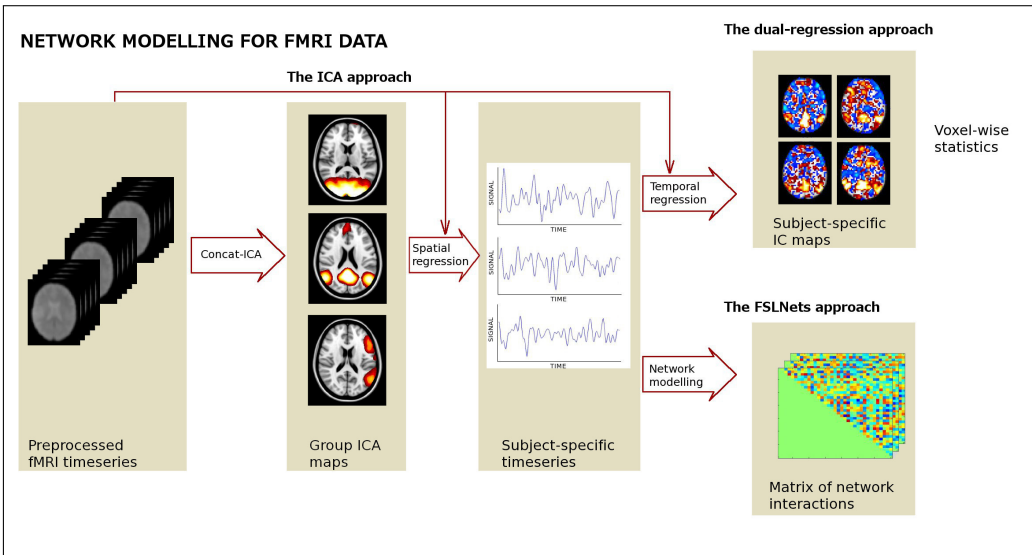


Figure 3.4: Summary of the steps performed within a dual regression and a network modelling analysis using FSLNets

3.6 Advanced fMRI analysis: whole-brain connectivity

The methods presented in this section are used with rs-fMRI and allow modeling brain functional connections at a more complex level than ICA or seed-based correlation methods that aimed to study large-scale spatial maps independently from each other.

They belong to the nascent field of *connectomics* and they attempt to study whole-brain connectivity by first identifying a number of network nodes (regions or groups of regions) and then estimating functional connections, or edges between nodes (Smith et al., 2013; Bullmore and Bassett, 2011).

3.6.1 Graph Theory

In graph theory, the brain can be represented as a big network, which is a complex system defined by a collection of nodes (or vertices) and links (or edges) between pairs of nodes. Once this network has been built, its topological⁵ and geometrical⁶ properties can be studied using tools that come from the fields of physics and mathematics (Albert and Barabási,

⁵Graph characteristics regardless of their physical or anatomical localization

⁶Graph characteristics that depend on the spatial localization of nodes

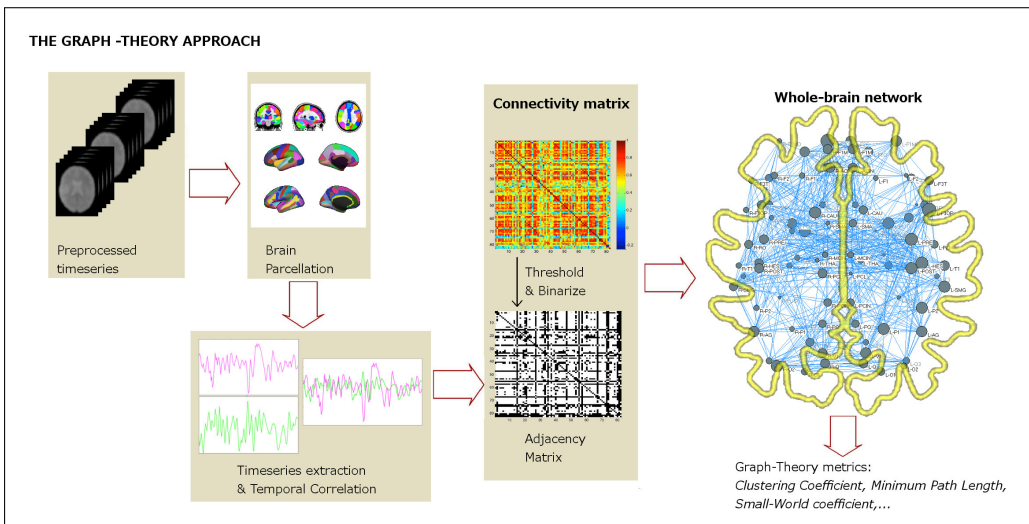


Figure 3.5: Main steps involved in the creation of whole-brain functional connectivity graphs.

2002).

Brain graphs can be constructed using data from Diffusion MRI (Hagmann et al., 2008; Gong et al., 2009), Structural MRI (He et al., 2007), and fMRI (Achard et al., 2006). In the current thesis, we only used graphs derived from fMRI.

A graph can be *weighted* or *unweighted* (also called a *binary* graph) depending on how the edges are defined. In weighted graphs, values of the edges depend on their connection strength. In unweighted graphs, edges are set to 0, when there is no connection between nodes, or to 1, when there is a connection between nodes. Furthermore, a graph can be *directed* or *undirected* depending on whether if the edges include directionality information or not. The results presented in this thesis are obtained using binary undirected graphs.

The main steps involved in the creation of binary undirected graphs from rs-fMRI data are the following (See Figure 3.5):

1. **Defining the Nodes: brain parcellation.** Several strategies have been used for parcellating the brain. The most widely used method is based on anatomical atlases or landmarks obtained from standard templates. In this context, individual fMRI images need to be coregistered with the template and the mean signal across time in each parcel is taken as the nodal timeseries at that location. Some examples of the atlases

used for parcellation are the Automated Anatomical Label (AAL) template (Tzourio-Mazoyer et al., 2002) and the atlases available in FreeSurfer ⁷ (Desikan et al., 2006; Destrieux et al., 2010).

The main advantages of using atlas-based parcellations are that they allow for direct comparison of results with other studies and that they provide meaningful interpretability of the results in relationship with more classical studies of anatomically based localization of brain functions (Bullmore and Bassett, 2011).

The two main limitations related to these methods are that the size of the parcellations is highly variable and that the anatomical subdivisions do not always coincide with regions of different functionality. In this regard, other parcellation strategies have been proposed, as the use of functionally defined regions (Smith et al., 2011) or the use of brain parcellations with equal number of voxels within each node (Zalesky et al., 2010).

It should be noted that in *Study 4* we used a parcellation based on the AAL atlas to perform all the analyses, but that we also tested brain networks obtained from a parcellation that was derived from an ICA analysis. In addition, with the same data, we also tested networks obtained with two atlases derived from FreeSurfer. The results of these latter analyses were not included in the article but they are reported in the Appendix A of the thesis.

2. **Defining the Edges: functional connectivity.** In functional MRI, the most direct measure of functional connectivity between pairs of nodes is the correlation coefficient between the nodes' timeseries (Friston, 1994). The result of this step is a symmetric matrix, called *Adjacency matrix*, and their elements, a_{ij} , denote the correlation between nodes i and j .
3. **Network thresholding:** This step allows creating a binary graph from the adjacency matrix. The threshold can be an absolute value, τ , so that matrix entries are set to 0 when $a_{ij} < \tau$ and to 1 otherwise. However, one of the main problems of using an absolute threshold is that the number of remaining edges after thresholding is highly

⁷Martinos Center for Biomedical Imaging; <http://freesurfer.net/>

variable across subjects, because some subjects can present higher overall correlations, and then, the resulting graphs may not be comparable.

An alternative strategy is the use of a relative threshold. In this case, the threshold is selected in order to ensure that all the individual graphs have the same connection density, or sparsity level, which is calculated as the ratio between the number of existing nodes and the number of all possible connections in the network. When a relative threshold is used, all the edges are ordered in terms of their connectivity strength. Then, the desired percentage of higher connected edges are set to 1, whereas the rest of edges are set to 0.

The choice of the threshold value (even using an absolute or a relative threshold) will have a clear effect on the topology of the resulting networks. For very low absolute thresholds (or high relative thresholds), the resulting networks will be very densely connected, and they may have the risk of including spurious correlations or noise. At the other end of the scale, high absolute thresholds (or low relative thresholds) will generate very sparse networks, with a small number of connections (Achard and Bullmore, 2007). These differences in network topology will have an effect on the resulting network metrics. Therefore, it is very common in graph theory studies to report the results obtained over a range of thresholds.

4. **Measures of graphs** Several measures can be obtained from the network matrix, at the regional and global levels (Rubinov and Sporns, 2010). Some of the most commonly used metrics are defined below:

The *Clustering coefficient* (C_i) of a node i is defined as the ratio of the number of existing edges to all the possible edges in the node's direct network. It corresponds to the fraction of triangles around a node and is equivalent to the fraction of a node's neighbors that are neighbors of each other:

$$C_i = \frac{2t_i}{k_i(k_i - 1)}$$

Where t_i measures the number of triangles around the node i . Clustering coefficients can be averaged across all the regions to obtain the *Global clustering coefficient*.

The *Characteristic path length* (L) is the average of the shortest path lengths (i.e., number of edges) between all pairs of nodes in the network. The shortest path length between two nodes is the lowest number of edges that must be included in the network to connect the two nodes. Lower characteristic path lengths indicate higher routing efficiency, because the information exchange involves fewer steps. This measure is representative of the brain's functional integration, that is, the ability to rapidly combine specialized information from different brain regions.

$$L_w = \frac{1}{n} \sum_{i \in N} L_i = \frac{1}{n} \sum_{i \in N} \frac{\sum_{j \in N, j \neq i} d_{ij}}{(n-1)}$$

The *Small-world coefficient* ($S-W$) measures the balance between functional segregation (i.e., the presence of functionally specialized modules) and integration (i.e., the large number of intermodular links). At the practical level, small-world networks are characterized by high clustering coefficients and relatively low path lengths (compared to random networks).

$$S - W = \frac{C/C_{rand}}{L/L_{rand}}$$

Where C_{rand} and L_{rand} are, respectively, the clustering coefficient and the average minimum path length calculated for a random network with the same number of edges (same sparsity).

5. **Group-statistics** The resulting metric values obtained with graph-theory can be fitted into any group-statistics approach. In Study 4, we evaluated correlations with age cognition. Additionally, we also performed a mediation analysis (Hayes, 2009; Preacher and Hayes, 2008; Salthouse, 2011) in order to determine the effect of age on the relationship between memory and network metrics.

3.6.2 Other approaches: FSLNets

The FSLNets approach was used in Study 5. This method was used in combination with ICA and dual-regression on rs-fMRI data.

Basically it consists on obtaining the timeseries in a set of nodes, typically estimated as ICA maps, and calculating interactions between them (Figure 3.4). These network relationships can be calculated using distinct mathematical approaches, including simple measures as correlation and covariance as well as partial correlation and regularized versions of the partial correlation (Smith et al., 2011).

Concretely, the steps carried out within Study 6 were the following:

1. **Group-ICA** Estimate group maps using concat-ICA with all the subjects. Each ICA spatial map is a node of the whole-brain network.
2. **Spatial regression** Obtain subject- and component- specific timeseries by doing the first stage of dual regression.
3. **Connectivity matrix** A connectivity matrix for each subject was calculated using partial correlation between the timeseries. In this matrix, each entry, b_{ij} represents the functional connectivity between nodes i and j after removing the effect of all the other nodes, where the nodes are the spatial maps of the different ICs.
4. **Statistics** The entries of the matrix can be used to perform statistics at the population level. In our case, the network edges were correlated with age and with the results of the cognitive tests.

CHAPTER 4

Results



Research report

Brain connectivity during resting state and subsequent working memory task predicts behavioural performance

Roser Sala-Llonch^{a,b}, Cleofé Peña-Gómez^a, Eider M. Arenaza-Urquijo^a,
 Dídac Vidal-Piñeiro^a, Nuria Bargalló^{b,c}, Carme Junqué^{a,b} and David Bartrés-Faz^{a,b,*}

^a Departament de Psiquiatria i Psicobiologia Clínica, Universitat de Barcelona, Catalonia, Spain

^b Institut d'Investigacions Biomèdiques August Pi i Sunyer (IDIBAPS), Catalonia, Spain

^c Radiology Service, Hospital Clínic de Barcelona, Catalonia, Spain

ARTICLE INFO

Article history:

Received 9 March 2011

Reviewed 26 April 2011

Revised 30 May 2011

Accepted 25 July 2011

Action editor Bradley Postle

Published online 5 August 2011

Keywords:

fMRI

Default mode network

Attention

ICA

ABSTRACT

Brain regions simultaneously activated during any cognitive process are functionally connected, forming large-scale networks. These functional networks can be examined during active conditions [i.e., task-functional magnetic resonance imaging (fMRI)] and also in passive states (resting-fMRI), where the default mode network (DMN) is the most widely investigated system. The role of the DMN remains unclear, although it is known to be responsible for the shift between resting and focused attention processing. There is also some evidence for its malleability in relation to previous experience. Here we investigated brain connectivity patterns in 16 healthy young subjects by using an *n*-back task with increasing levels of memory load within the fMRI context. Prior to this working memory (WM) task, participants were trained outside fMRI with a shortened test version. Immediately after, they underwent a resting-state fMRI acquisition followed by the full fMRI *n*-back test. We observed that the degree of intrinsic correlation within DMN and WM networks was maximal during the most demanding *n*-back condition (3-back). Furthermore, individuals showing a stronger negative correlation between the two networks under both conditions exhibited better behavioural performance. Interestingly, and despite the fact that we considered eight different resting-state fMRI networks previously identified in humans, only the connectivity within the posteromedial parts of the DMN (precuneus) prior to the fMRI *n*-back task predicted WM execution. Our results using a data-driven probabilistic approach for fMRI analysis provide the first evidence of a direct relationship between behavioural performance and the degree of negative correlation between the DMN and WM networks. They further suggest that in the context of expectancy for an imminent cognitive challenge, higher resting-state activity in the posteromedial parietal cortex may be related to increased attentional preparatory resources.

© 2011 Elsevier Srl. All rights reserved.

* Corresponding author. Departament de Psiquiatria i Psicobiologia Clínica, Facultat de Medicina, Universitat de Barcelona, Casanova 143, 08036 Barcelona, Spain.

E-mail address: dbartres@ub.edu (D. Bartrés-Faz).

0010-9452/\$ – see front matter © 2011 Elsevier Srl. All rights reserved.

<http://dx.doi.org/10.1016/j.cortex.2011.07.006>

1. Introduction

The human brain can be functionally defined as a set of networks or systems that transiently interact to perform a particular neural function. The study of the functionality and structure of such networks has become one of the most popular topics within the cognitive neuroscience community (Rykhlevskaia et al., 2008; Bassett and Bullmore, 2009; He and Evans, 2010; Van den Heuvel and Hulshoff Pol, 2010), especially since abnormalities in the interactions of network components play a critical role in common and devastating neurological and psychiatric disorders, and also because damage to specific functional connectivity networks can lead to distinct neurological syndromes (Bassett and Bullmore, 2009; Seeley et al., 2009).

During the execution of a complex cognitive process the brain networks involved can be divided into task-positive and task-negative networks (Fox et al., 2005). Task-positive networks include regions that are simultaneously activated during active cognitive processing, whereas task-negative networks (also known as resting-related networks) are those which are active during passive or stimulus-independent thought, and are subsequently deactivated during active processing. Thus, the analysis of task-functional magnetic resonance imaging (fMRI) data allows the identification of specific task-positive networks which are associated with the defined task, as well as the characterization of the task-negative networks or deactivations, which are known to be common across tasks (Shulman et al., 1997). The default mode network (DMN) is the most widely studied and characterized brain system in this passive-state context. This network comprises a set of highly functionally connected regions including the medial prefrontal cortex (MPFC), posterior cingulate cortex (PCC), lateral and medial temporal lobes and posterior inferior parietal lobule (Shulman et al., 1997; Raichle et al., 2001; Greicius et al., 2003). The DMN plays a competitive role with the majority of task-related networks. Thus, the activation of a cognitive task-related network is normally accompanied by deactivation of the DMN, whereas during rest periods the DMN presents higher levels of activity than do other networks (Fox et al., 2005; Buckner et al., 2008). Resting-fMRI studies in the healthy population have reported direct relationships between the DMN and brain functionality (Fox et al., 2005). Moreover, distinct patterns of DMN dysfunction have been related to major psychiatric and neurodegenerative diseases (Greicius, 2008; Broyd et al., 2008; Seeley et al., 2009). Regarding task-fMRI studies, it has been shown that the connectivity within DMN regions contributes to the facilitation or monitoring of cognitive performance, and that the differences in functional coupling within DMN regions can predict differences in cognitive performance (Hampson et al., 2006, 2010; Esposito et al., 2009).

The working memory (WM) system has been defined as a system for the temporary holding and manipulation of information during the performance of a range of cognitive tasks such as comprehension, learning and reasoning (Baddeley, 1986, 2010). One of the most widely used WM paradigms in the context of functional imaging studies is the *n*-back paradigm (see Owen et al., 2005 for a meta-analysis). Its application has enabled researchers to clearly identify the anatomical substrates of the WM system, including the following six

cortical regions: (1) the bilateral posterior parietal cortex (BA7, 40), (2) the bilateral premotor cortex (BA6, 8), (3) the dorsal cingulate/medial premotor cortex, including the supplementary motor area (SMA; BA32, 6), (4) the bilateral rostral prefrontal cortex or frontal pole (BA10), (5) the bilateral dorsolateral prefrontal cortex (BA9, 46) and (6) the bilateral mid-ventrolateral prefrontal cortex (BA45, 47). Moreover, the nature of the *n*-back paradigm is such that studies can be designed to examine the effects of WM load variations (Braver et al., 1997; Callicott et al., 1999).

To date, most WM studies using the *n*-back paradigm have focused on task-related changes in the brain activity of areas within the WM system, and their relationship to memory load, through the univariate analysis of fMRI data (Braver et al., 1997; Callicott et al., 1999; Volle et al., 2008). Other research has studied DMN activity during the performance of WM paradigms that include short rest periods between blocks. For example, DMN activity (BOLD signal strength) in the resting periods after an *n*-back task was found to be correlated with task performance (Hampson et al., 2006; Esposito et al., 2009), and was also increased in the context of high levels of WM load (Pyka et al., 2009). Finally, a few studies have shown how variations in WM load modulate functional connectivity between regions of the WM system, the results always showing load-dependent increases in connectivity (Honey et al., 2002; Narayanan et al., 2005; Axmacher et al., 2008).

Regarding network interactions in a WM context, Bluhm et al. (2010) found increased correlations between DMN regions and WM-related regions during 2-back performance with respect to rest scans. Newton et al. (2011) investigated functional connectivity within both the working memory network (WMN) and the DMN in the context of WM load variations, and found that functional connectivity within both networks increased as a function of load. They also studied interactions between the two networks, and found that negative correlations emerged in posterior cingulate regions at high levels of WM load.

In summary, all these studies highlight the importance of conducting functional connectivity analyses rather than a univariate analysis of functional activations when studying complex cognitive domains. In addition, results regarding both task-related networks and the DMN suggest the need for studies in which the same subjects undergo both resting-fMRI and task-fMRI acquisitions, thereby enabling brain connectivity to be investigated not only during task performance but also during a previous resting state.

Therefore, in the present study we used a load-variable WM fMRI task and a resting-fMRI acquisition to study interactions between functional networks at different levels of cognitive demands and their direct relationship with individual performance. We also aimed to investigate whether resting-state connectivity status, prior to *n*-back task execution, has any relationship with subsequent WM performance.

2. Methods

Sixteen, healthy, young university students (9 females, mean age 21.31 ± 2.41) with normal or corrected-to-normal vision and

no history of psychiatric or neurological conditions were included in the study. The cognitive paradigm was a variation of the classical letter n -back task with increasing levels of memory load (Braver et al., 1997), including 0-back, 1-back, 2-back and 3-back blocks, and with resting blocks between each task block. During n -back blocks a sequence of 12 letters (A–H) was presented on the screen. In the 0-back condition, subjects were asked to respond when the target letter 'X' appeared on the screen, whereas in the other n -back conditions a letter was a target if it was identical to the letter presented n trials before. Prior to the scan, subjects underwent a training session of sufficient length in each case to ensure that they clearly understood all the conditions of the paradigm and could perform to at least 80% accuracy in the 3-back condition. They were all informed that they would be requested to perform a longer version of the same paradigm later when inside the scanner. Immediately after the training session and before the performance of the task inside the scanner, a 5-min resting-fMRI acquisition was conducted. During this time, subjects were asked to close their eyes and not to think of any specific topic.

During the MRI n -back scanning session the task was presented using a block-design paradigm, implemented with Presentation Software®. Each n -back condition lasted 26 sec and was presented four times in a pseudo-randomized order, such that the sequence of stimuli was different between the four repetitions of the task. The number of target stimuli in each task block was between two and four (mean: 3.06, SD: .68). In addition, each n -back block was followed by an inter-block fixation period of 13 sec, during which time subjects looked at a white fixation cross in the centre of the screen. Before any n -back block was presented an instruction screen appeared to inform the subject about the task. The sequence of letters was presented in white in the centre of the screen; each letter remained visible for 500 msec, with an inter-stimulus interval of 1500 msec. Fig. 1 shows a schematic representation of the block-design task.

Task performance inside the scanner was recorded and individual scores were calculated using the d' measure, which accounts for correct responses and false alarms and is computed as: $Z(\text{hit rate}) - Z(\text{false alarm rate})$. Mean response times (RTs) in each condition were also recorded.

A one-way analysis of variance (ANOVA), followed by a post-hoc analysis, was performed in Statistical Package for

Social Sciences (SPSS, v.16, Chicago, IL, USA) to determine whether the performance scores and RT were different across distinct memory-load conditions, as well as between the four repetitions of the task, the aim being to test for fatigue or training effects.

fMRI images were acquired on a 3T MRI scanner (Magnetom Trio Tim, Siemens Medical Systems, Germany), using a 32-channel coil. During both the resting-fMRI and task-fMRI conditions a set of T2*-weighted volumes (150 and 336 volumes for resting and task-fMRI, respectively) were acquired (TR = 2000 msec, TE = 29 msec, 36 slices per volume, slice thickness = 3 mm, distance factor = 25%, FOV = 240 mm, matrix size = 128 × 128). A high-resolution 3D structural dataset using a T1-weighted magnetization prepared rapid gradient echo (MPRAGE) sequence, TR = 2300 msec, TE = 2.98 msec, 240 slices, FOV = 256 mm, matrix size = 256 × 256, slice thickness = 1 mm) was also acquired in the same scanning session for registration purposes.

Image processing and analyses were performed using both FSL (<http://www.fmrib.ox.ac.uk/fsl/>) and AFNI (<http://afni.nimh.nih.gov/>) tools. Pre-processing steps for the anatomical MPRAGE scan included removal of non-brain voxels and segmentation in white matter, grey matter and cerebro spinal fluid (CSF). For the functional data the pre-processing included motion correction, skull stripping, spatial smoothing [full width at half maximum (FWHM) = 6 mm], grand mean scaling, and filtering. Task-activation functional data were filtered using a high pass filter of 80 sec, while the resting-fMRI data were filtered in order to remove all frequencies outside the range of [0.005, .1] Hz.

All the functional images were first registered to the individual anatomical scans using linear registration, with six degrees of freedom, and further registered to the standard Montreal Neurological Institute (MNI) brain using concatenation of both registration matrices.

Nuisance regression was also applied to the fMRI datasets in order to remove the contribution of the six motion parameters, white matter, CSF and whole brain oscillations (Fox et al., 2009). Nuisance regressed data were used in the time series correlation analyses, but not in the independent components analysis (ICA) decomposition.

2.1. Analysis of the resting-fMRI data

A temporal concatenation ICA approach (Beckmann et al., 2005) followed by a dual-regression algorithm (as in Filippini et al., 2009) was used to analyse the resting-fMRI data. First, the pre-processed 4D datasets of all subjects were concatenated and decomposed using the multivariate exploratory linear optimized decomposition into independent components (MELODIC) tool from FSL. MELODIC estimated the number of independent components (ICs) using the Laplace approximation to the Bayesian evidence for a probabilistic principal components model. All the components were visually examined and compared with those reported in the resting-fMRI literature (Damoiseaux et al., 2006; Van den Heuvel and Hulshoff Pol, 2010). Resting-state networks (RSNs) of interest were then selected and introduced into a dual-regression analysis. This analysis involves two regression analysis and a voxel-wise group analysis using

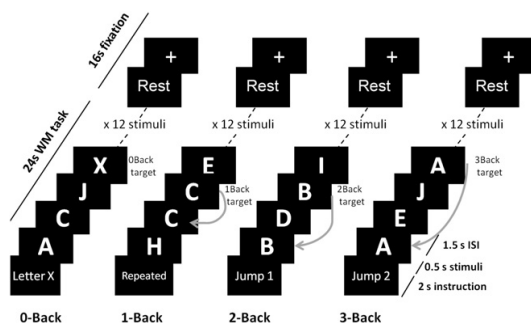


Fig. 1 – Design of the fMRI n -back task.

a permutation-based algorithm. In the first regression, group spatial maps were used as independent variables and the full pre-processed fMRI datasets were used as dependent variables in order to extract individual time series associated with each subject and each IC. Next, in a second regression, the individual time series were used as independent variables separately for each subject again with the fMRI datasets in order to obtain subject-specific maps, that were further transformed into Z-scores. These maps were then introduced into a group analysis to test their correlation with individual 3-back performance scores; this was done using general linear modelling (GLM), as implemented in the randomise tool from FSL, which corrects for family-wise error (FWE) using a permutation-based algorithm ($N = 5000$ permutations). Significance level was set at a corrected p value of $p < .05$.

Using the resting-state fMRI data we also performed an analysis based on the amplitude of low frequency fluctuations (ALFF). In the ALFF analysis (Zang et al., 2007) the pre-processed datasets are transformed to frequency domain with a fast Fourier transform (FFT) in order to calculate the power spectrum. The amplitude of the low frequency fluctuations is then computed as the square root of the power spectrum, and the ALFF is the mean amplitude within the frequencies of interest for each voxel. The standardized ALFF was obtained by dividing the ALFF map by the global mean ALFF value. As above, we obtained individual maps of ALFF and standardized ALFF that were introduced into a permutation-based group analysis using randomise from FSL ($N = 5000$ permutations, significance threshold: $p < .05$, FWE corrected), where we tested for correlations with 3-back performance scores.

2.2. Analysis of the task-activation fMRI data

A tensor-ICA decomposition of the pre-processed images was performed as implemented in MELODIC (Beckmann and Smith, 2004) version 3.10, part of the FSL software. This method extracts signal patterns that exist synchronously in all the subjects, as well as patterns associated with head motion, physiological noise, or artefacts. Thus, task time series and contrasts were also introduced into MELODIC, which performed a post-hoc regression analysis between estimated component time series and task time series in order to further identify the ICs related to WM blocks and

fixation blocks. After identifying the spatial pattern corresponding to the main networks involved in the task, two kinds of connectivity measures were calculated:

- Between-network connectivity analyses:* After identifying the main ICs their thresholded spatial maps were used to create binary masks. Individual time series for each component were obtained by computing the mean signal within each mask for the pre-processed fMRI series. Relationships between each pair of individual time series for each condition were investigated by computing Pearson's correlation coefficients. The values obtained for the between-network connectivity at each condition were introduced into SPSS and compared between conditions using two-tailed paired-samples t-tests. In order to account for Type I errors, results were corrected using Bonferroni correction for multiple comparisons. We also performed a correlation analysis to investigate the relationship between connectivity and individual performance scores on the task.
- Within-network connectivity analysis:* In order to explore the within-network connectivity the IC spatial map of each selected network was sub-divided into sets of regions of interest (ROIs) representing the main foci of activation. Time series for each of these ROIs were obtained as the mean signal within the ROI during the pre-processed fMRI series. As above, temporal correlations between pairs of time series were explored using Pearson's correlation coefficients. The intrinsic network correlation was defined as the mean of the correlation coefficients between all the possible pairs of ROIs within the network. Also as above, several paired-samples t-tests (followed by Bonferroni correction for multiple comparisons) were performed using SPSS to determine whether the intrinsic network correlation changed between conditions. A correlation analysis was also carried out to investigate relationships with performance.

3. Results

3.1. Behavioural results

Performance scores and reaction times (RTs) for all the task conditions are summarized in Fig. 2. All the subjects performed

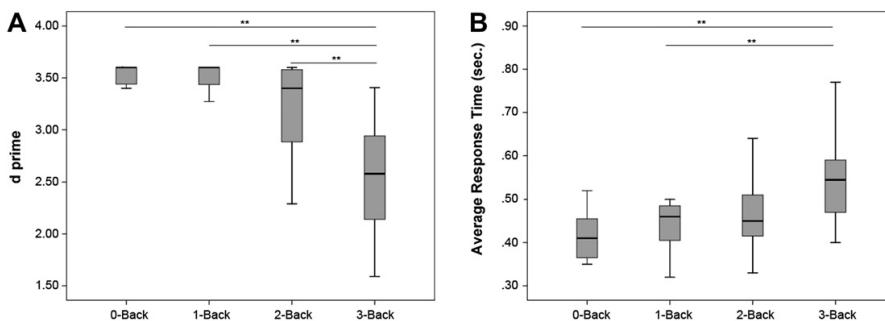


Fig. 2 – Outcomes of task performance for all the subjects. (A) Mean performance scores and (B) mean RTs. Note that for both performance (d') and RTs the condition with the highest memory load (3-back) differed from the other conditions, there being no differences between the latter (see main text for statistical differences between conditions).

well (over 80%) in all the conditions during the scanning session, but showed lower performance scores and longer RTs with increasing WM load. An ANOVA followed by a Bonferroni post-hoc analysis was then applied to the performance scores (d') and mean RT, revealing significant differences in performance scores between the 3-back condition and all the other conditions (see Fig. 2; global ANOVA results: $F = 19.625$, $p < .001$; post-hoc analysis: $p < .001$ in the 0-B vs 3-B, $p < .001$ in the 1-B vs 3-B, and $p < .001$ in the 2-B vs 3-B). However, these values did not differ between the 0-back, 1-back and 2-back conditions. Regarding mean RT the global ANOVA showed a significant effect of condition ($F = 4.08$, $p = .011$), while the post-hoc analysis revealed significant differences between the 0-B and 3-B conditions ($p = .005$) and between the 1-B and 3-B conditions ($p = .024$).

Putative practice or fatigue effects were analysed by applying a paired-samples t -test to the performance scores obtained in the first and last runs of the task. No differences were found ($t = .37$, $p = .72$).

3.2. Resting-fMRI

The ICA decomposition of the pre-task resting-fMRI data gave a set of 17 ICs, from which we selected the eight ICs that have been most commonly investigated in the resting-fMRI literature (for a review, see Van den Heuvel and Hulshoff Pol, 2010). Spatial maps and anatomical descriptions of the eight selected components can be found in Supplementary Fig. 1. All these components were introduced into the dual-regression analysis to explore whether any of them showed a relationship with subsequent individual performance during the n -back task.

These analyses revealed that among all the selected ICs, only the IC identified as the DMN (See Fig. 3A for the spatial map of the DMN) showed a relationship with WM performance, and that this was specific for the 3-back condition. In particular, subjects who performed better showed greater connectivity in the precuneus/posterior cingulate node with respect to all the other DMN nodes (MNI coordinates of the maximum value $x = -2$, $y = -54$, $z = 16$, Brodmann area 23, see Fig. 3B). Individual DMN Z-scores within this ROI were extracted and

introduced into SPSS to obtain a graphical representation and the statistical parameters of the correlation with 3-back performance ($r = .74$, $p = .001$, see Fig. 3C).

The voxel-wise analysis performed using the ALFF and standardized ALFF maps showed that there was no relationship between brain activity of low fluctuations and subsequent 3-back performance.

3.3. fMRI during n -back blocks

ICA decomposed the fMRI data of all the subjects into 77 ICs. After the selection process, two main brain components were retained (see Fig. 4). First, and as is commonly done in the ICA literature (Beckmann et al., 2005; Pyka et al., 2009), any components that were clearly related to motion artefacts or which had a mean power above .1 Hz were discarded (24 ICs). Furthermore, components that were driven by a single outlier subject were also discarded (9 ICs). The remaining ICs were then sorted according to their mean response amplitude. The selection criteria were based on the post-hoc analysis performed by MELODIC on the time series. IC1 was selected as a WM-associated component, representing the specific task-positive network for the defined task, because its time course fitted the task time series with $F = 25.02$ and $p < .000001$ and it was significant for the 1-back > 0-back contrast ($z = 3.45$, $p < .00028$), the 2-back > 0-back contrast ($z = 4.78$, $p < .000001$) and the 3-back > 0-back contrast ($z = 5.57$, $p < .000001$). IC2 was selected as a DMN-associated component since it fitted the task time series with $F = 43.22$ ($p < .000001$) and it was significant for the fixation condition ($z = 8.34$, $p < .000001$). The spatial localization of the main foci of their activations and deactivations was also used as a selection criterion, and maps were compared with those reported in the WM literature (Owen et al., 2005) and the DMN literature (Damoiseaux et al., 2006; Van den Heuvel and Hulshoff Pol, 2010). Components with no temporal association with the task, or components related to non-cognitive networks commonly found in resting analysis were not considered. Finally, components that had a temporal association with the task but which were ranked at the end of the list were also not considered because of the low percentage of variance they explained (around 1%). The supplementary

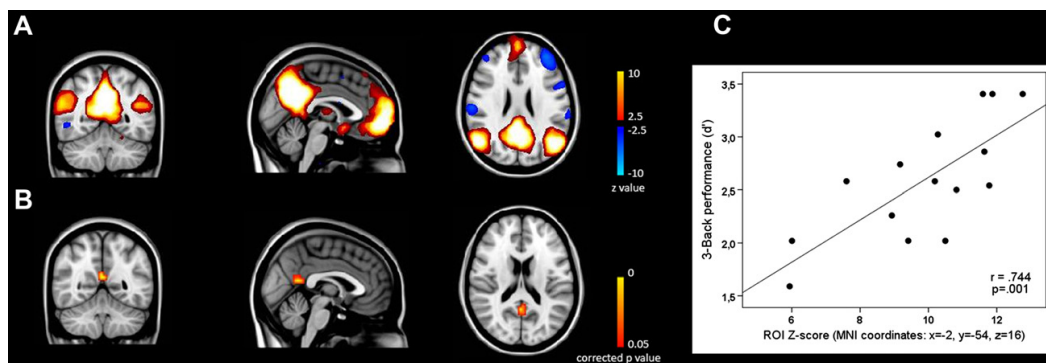


Fig. 3 – (A) Spatial pattern of the DMN for all subjects during the resting acquisition. (B) Area within the DMN whose activity correlates with subsequent 3-back performance ($p < .05$, FWE corrected). (C) Scatter plot depicting a positive correlation between the DMN Z-values of the precuneus and WM performance.

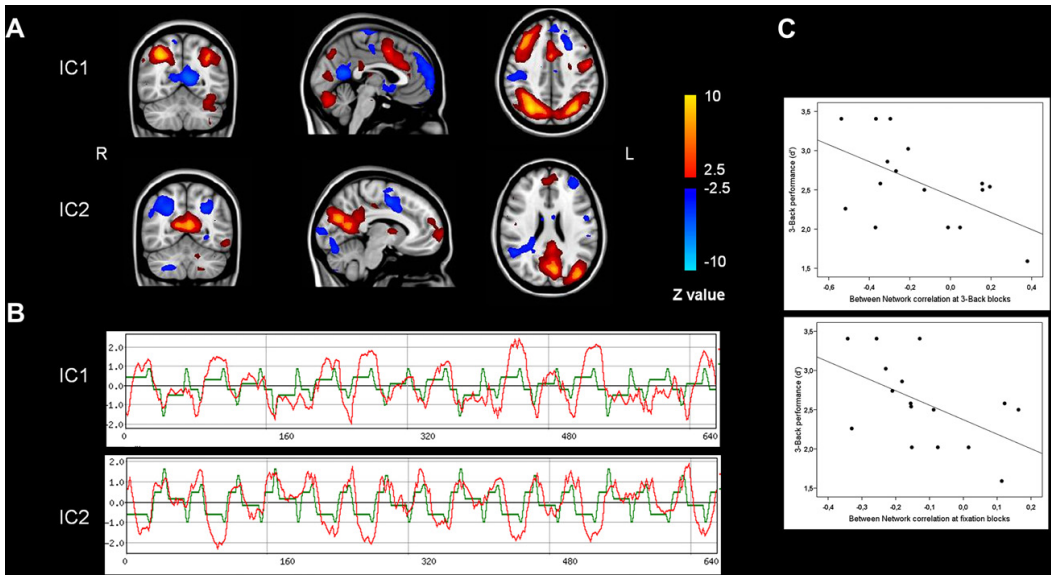


Fig. 4 – (A) Spatial maps of the two selected components: IC1 corresponds to the WMN and IC2 to the DMN. Hot colours represent brain activations and cold colours represent deactivations. (B) Time series of the two components: red lines are the component-related mean responses, while green lines show the fit with the task. (C) Scatter plots showing the relationship between the between-network correlations in the 3-back and fixation blocks and individual performance scores for the 3-back WM task.

material (supplementary Fig. 2) includes some examples of the components that were discarded, as well as the criteria used. There was a strong overlap between positive areas of the first component and negative areas of the second one, and vice-versa (see Fig. 4). Thus, only positive areas of each of them were used to define the foci of activation. Five principal foci were identified within the WM system: the anterior cingulate gyrus and supplementary motor cortex (BA32, 6, 24), the right middle frontal gyrus and frontal pole (BA9, 10), the left precentral gyrus and middle frontal area (BA6), and the lateral occipital cortex, the precuneus/parietal lobe and supra-marginal gyrus (BA7, 19, 23, 40) bilaterally. Regarding the DMN, the regions identified were the precuneus cortex and posterior cingulate (BA29, 30), the frontal pole, paracingulate and medial frontal gyrus (BA9, 10) and the left lateral occipital cortex and temporal lobe (BA19). Table 1 summarizes the main areas involved in each network, as well as their peak coordinates.

3.3.1. *Between-network correlations*

Initial evidence of the strong anti-correlation between these two networks was observed directly from their ICA spatial maps and corresponding time courses: areas that appeared activated in one component were deactivated in the other, and vice-versa (see red and blue regions for activations and deactivations, respectively, in Fig. 4A, and related time courses in Fig. 4B).

These between-network temporal correlations were further studied at an individual level and considering all the conditions of the task (fixation, 0-B, 1-B, 2-B and 3-B). In the 3-back scans the anti-correlation between the WMN and the DMN was predictive of the subject’s performance ($r = -.65, p = .012$, see Fig. 4C). This relationship was not found in any of the less-demanding *n*-back levels, although the anti-correlation during fixation periods also predicted behavioural performance during the 3-back condition ($r = -.54, p = .047$, see Fig. 4C). These two relationships are shown graphically in Fig. 4C.

Table 1 – Anatomical localization and ROI definition of the WMN and the DMN.

ROI id	Volume (mm ³)	Z max	MNI coordinates	Anatomical area
WMN_1	23,728	8.6	(39, 30, 30)	Right middle frontal gyrus and frontal pole, BA9
WMN_2	12,931	7.59	(24, -72, 57)	Right lateral occipital cortex and precuneus/parietal lobe (BA7, 19, 39)
WMN_3	5,241	6.75	(-27, -72, 45)	Left lateral occipital cortex and precuneus/parietal lobe (BA7, 19, 39)
WMN_4	2,577	5.41	(0, 6, 45)	Supplementary motor cortex, anterior cingulate (BA32, 6, 24)
WMN_5	406	4.81	(-51, -6, 39)	Left precentral gyrus and middle frontal area (BA6)
DMN_1	1,777	5.57	(-6, -57, 15)	Precuneus and PCC (BA29, 30)
DMN_2	1,000	5.44	(-9, 57, 21)	Frontal pole and medial frontal gyrus (BA9, 10)
DMN_3	258	4.97	(-45, -81, 24)	Lateral occipital cortex, temporal pole (BA19)

The paired-samples t-test also showed that the between-network correlation had higher negative values in the fixation blocks when compared to the 0-back blocks ($t = 2.25$, $p = .04$).

3.3.2. Within-network correlation

On the basis of the spatial maps of the two selected ICs we created a set of ROIs for the subsequent analysis of temporal dynamics. This set included five ROIs within the WMN and three ROIs within the DMN (see Table 1). Correlations between all these ROIs can be represented in connectivity matrices, as shown in Fig. 5. In these matrices, intrinsic connectivity of the WMN is represented in the left-upper part, while the same measure of the DMN is represented in the right-lower corner. Right-upper and left-lower corners represent the between-network connectivity (studied in the previous point). As can be seen from visual inspection of these matrices the degree of intrinsic correlation within the networks increases with task demand, as does the extent of the inverse relationship between the two competitive systems. During fixation blocks these systems also show high levels of intrinsic correlation and high levels of negative correlation between one another.

These relationships were further studied statistically. The 0-back condition was taken as the reference against which the other conditions (fixation, 1-B, 2-B and 3-B) were compared using paired t-tests. For the WMN we observed an increase of intrinsic connectivity both in the fixation blocks ($t = 2.14$; $p = .049$, uncorrected) and in the 3-back blocks ($t = 5.23$; $p < .001$, uncorrected), while for the DMN this increase was

only observed for the 3-back scans ($t = 4.14$; $p = .001$, uncorrected). When these values were corrected for Type I error using Bonferroni correction for multiple comparisons, intrinsic connectivity was only statistically greater during the 3-back blocks for both networks ($p < .004$ for both the WMN and the DMN). However, the measured intrinsic network connectivity had no relationship with the subject's subsequent performance (data not shown).

4. Discussion

The present report describes an investigation into brain connectivity and its relationship with WM performance in a set of healthy subjects. In addition to task-related regions we also studied brain regions that are active in a resting-state period prior to the full-task performance test. For the pre-task resting state, we investigated the spatio-temporal patterns of a set of well-known RSNs and found that among these the DMN predicted inter-individual behavioural differences in subsequent 3-back performance. During the n -back blocks there was an inverse temporal relationship between the WMN and the DMN, which was maximal during the highest levels of task cognitive demand (3-back blocks). Moreover, these negative correlation scores measured during 3-back blocks predicted task performance.

The resting-state analysis of a 5-min period just before task execution revealed a region within the posteromedial cortex (Brodmann area 23) whose activation correlated with the

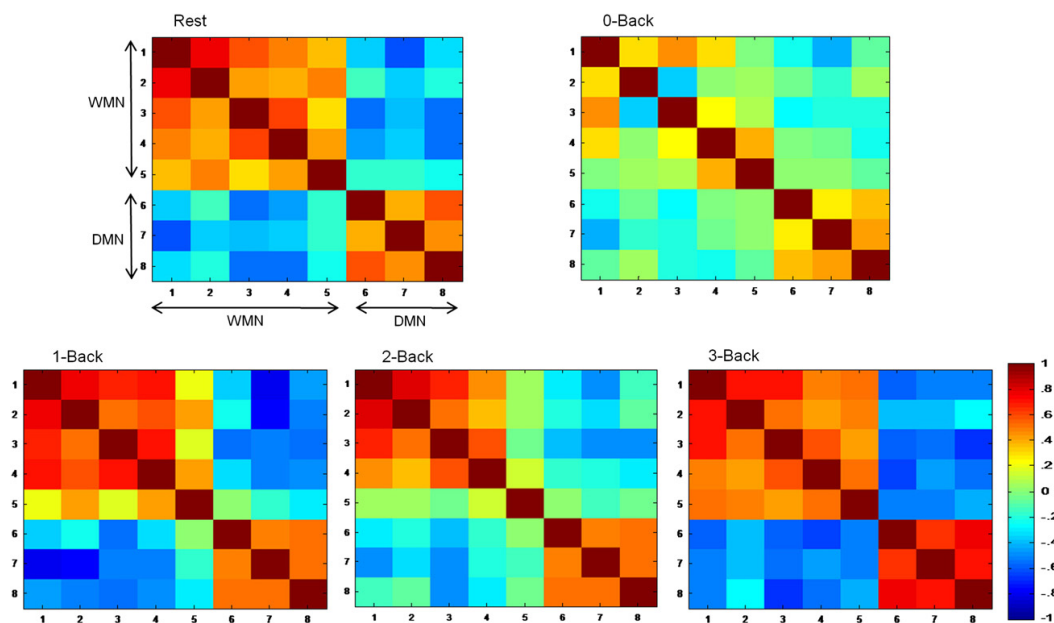


Fig. 5 – Connectivity matrices for all the conditions within the n -back task. Vertical and horizontal partitions represent the five ROIs defined within the WMN and the three ROIs defined within the DMN. Colours of the grid represent the time series correlation between each pair of ROIs; note from the legend bar that hot and cold colours represent positive and negative correlations, respectively.

subject's subsequent performance. This finding, which is the first such observation using a WM paradigm, is consistent with the report by Wang et al. (2010), who demonstrated that connectivity within the DMN measured just before the execution of an associative memory task can predict inter-individual differences in task performance. Moreover, several studies suggest that spontaneous resting-fMRI activity is dynamically associated with preceding experience (Waites et al., 2005; Lewis et al., 2009; Hasson et al., 2009).

More specifically, the connectivity–behaviour relationship found in the PCC node of the DMN may be mediated by cognitive factors such as the recruitment of attentional or motivational resources linked to the expectancy for an imminent cognitive challenge. A similar idea was suggested by Waites et al. (2005) in order to explain inter-individual differences in resting-state connectivity after a language task. Linked to this idea, one possibility is that the identified area is related to the defined attentional networks (Posner et al., 2006), whose primary purpose is to influence the operation of other brain networks. Attentional networks have been further divided into alerting, executive and orientating networks (Fan et al., 2005; Raz and Buhle, 2006), and the latter, which is involved in orienting the brain to sensory events, includes posteromedial regions. We therefore hypothesize that the probe or training phase before the resting-fMRI resulted in some sort of facilitation or *priming* effect expressed by increased connectivity in this area, which in turn led to an increased capacity for further perception and processing of complex stimuli. This interpretation linked to subject expectancies would be restricted to our specific design, where all subjects were told that after the practice and resting trials they would be required to perform the full *n*-back task. Hence, different results at the brain connectivity and behavioural level could have been obtained had this information not been provided, although this aspect was not investigated here.

Our interpretation is also in line with previous studies regarding the connectivity and functionality of the precuneus and posterior cingulate cortices (Cavanna and Trimble, 2006; Fransson and Marrelec, 2008; Cauda et al., 2010), which have described an attentional role for the same area in which we found a positive correlation with task performance (BA23). First, structural connectivity showed connections from this area with other parietal areas such as the parietal operculum and the inferior and superior parietal lobules, known to be involved in visuo-spatial information processing (Astafiev et al., 2003; Cavanna and Trimble, 2006), as well as extensive connections with the anterior cingulate, which is the core of the attentional network (Posner et al., 2006). It has therefore been concluded (Cavanna and Trimble, 2006) that the precuneus is involved in elaborating and integrating information rather than directly processing stimuli. In addition, a recent study provided a functional parcellation of the posteromedial cortex regarding its functional relationships with other brain systems (Cauda et al., 2010), concluding that the anterior portions of the posteromedial cortex, including BA23, are highly interlinked with areas involving attentional control.

In the task-activation fMRI study we obtained spatial maps that are highly consistent first with the generic task-positive network (Fox et al., 2005), and more specifically with previous

results regarding the WM system (Braver et al., 1997; Callicott et al., 1999; Owen et al., 2005; Nyberg et al., 2009; Newton et al., 2011) and the DMN (Shulman et al., 1997; Buckner et al., 2008). Furthermore, we found that the level of negative correlation between the two antagonist networks correlates with task performance at high levels of WM load. During these periods the functional connectivity within both the WMN and the DMN also revealed the highest levels, although this measure was not related to behavioural execution. These results strongly support the findings of some previous studies and extend their conclusions (Hampson et al., 2006, 2010; Newton et al., 2011). Hampson et al. (2006) found that within certain predefined nodes of the DMN, functional connectivity increased with task demand, and they also observed some positive behavioural-connectivity relationships in these regions. Newton et al. (2011) found that network connectivity within both the DMN and the WMN is modulated by WM load, although as they did not collect behavioural data they were unable to establish direct relationships between fMRI findings and behavioural outcomes. Therefore, our approach, despite being complementary, also differs from these studies in two key aspects. First, whereas these studies used either predefined ROIs or a parametrical mapping approach to fMRI data in order to obtain functional ROIs, we used a data-driven probabilistic ICA approach, which is more suitable in the context of brain network connectivity and network interactions. Secondly, the introduction of a resting-state fMRI condition between the training session and task performance was unique to our report.

In this latter regard it is also important to note that we found not only that the measure of inverse relationship between the DMN and WMN during the actual 3-back periods was correlated with behavioural performance, but also that this correlation was present during inter-block fixation scans (although this latter result did not survive correction for multiple comparisons). This observation highlights the relevance of fixation periods between cognitive tasks, which have been interpreted previously as recovery periods during which cerebral brain resources are relocated (Pyka et al., 2009). Our results not only support these previous conclusions but extend them by demonstrating a relationship between these fixation periods and individual task performance.

Although some of our results did not survive multiple comparison correction the pattern of connectivity observed during the most demanding scenario (i.e., during 3-back blocks), which was characterized by high connectivity between regions within a network and high negative correlations between the two antagonist networks (see, also, the connectivity matrices in Fig. 5), was very similar to the pattern observed during fixation scans. Hence, our results provide further evidence that the resting brain is as interconnected as the brain in a high state of cognitive functioning (Buckner et al., 2008).

Notwithstanding, it is important to note that the term functional connectivity has been used in this report both in resting-fMRI data and in task-related fMRI, and that the interpretation of the results is somehow driven by the methodology. While in the resting-fMRI analysis we could easily separate the measure of connectivity (as measured with ICA and dual-regression) and the measure of brain activity (measured with the ALFF method), in task-fMRI the measure of functional

connectivity will be somehow driven by the changes in brain activity during the performance of the task.

In summary, we have studied the functional implementation of two antagonist networks at various levels of cognitive effort, as well as during a resting-state fMRI condition between task training and its execution. Resting-state connectivity of the precuneus/posterior cingulate predicted individual performance on the task. During task execution we found a pattern characterized by high connectivity within the two networks and a high negative correlation between them, which itself was correlated with inter-individual differences in performance. Taken together the two main results of this study support the idea that the DMN plays a role in focussing attention during — and prior to — the execution of a highly demanding executive task (Greicius et al., 2003; Fox et al., 2005).

Supplementary material

Supplementary material associated with this article can be found in the online version, at doi:10.1016/j.cortex.2011.07.006.

REFERENCES

- Astafiev SV, Shulman GL, Stanley CM, Snyder AZ, Van Essen DC, and Corbetta M. Functional organization of human intraparietal and frontal cortex for attending, looking, and pointing. *The Journal of Neuroscience*, 23(11): 4689–4699, 2003.
- Axmacher N, Schmitz DP, Wagner T, Elger CE, and Fell J. Interactions between medial temporal lobe, prefrontal cortex and inferior temporal regions during visual working memory: A combined intracranial EEG and functional magnetic resonance imaging study. *The Journal of Neuroscience*, 28(29): 7304–7312, 2008.
- Baddeley A. *Working Memory*. Oxford University Press, 1986.
- Baddeley A. Working memory. *Current Biology*, 20(4): R136–140, 2010.
- Bassett DS and Bullmore ET. Human brain networks in health and disease. *Current Opinion in Neurology*, 22(4): 340–347, 2009.
- Beckmann CF and Smith SM. Probabilistic independent component analysis for functional magnetic resonance imaging. *IEEE Transactions on Medical Imaging*, 23(2): 137–152, 2004.
- Beckmann CF, De Luca M, Devlin JT, and Smith SM. Investigations into resting-state connectivity using independent component analysis. *Philosophical Transactions of the Royal Society of London. Series B, Biological Sciences*, 360(1457): 1001–1013, 2005.
- Bluhm RL, Clark CR, McFarlane AC, Moores KA, Shaw ME, and Lanius RA. Default mode connectivity during a working memory task. *Human Brain Mapping*, 32(7): 1029–1035, 2010.
- Braver TS, Cohen JD, Nystrom LE, Jonides J, Smith EE, and Noll DC. A parametric study of prefrontal cortex involvement in human working memory. *NeuroImage*, 5(1): 49–62, 1997.
- Broyd SJ, Demanuele C, Debener S, Helps SK, James CJ, and Sonuga-Barke EJS. Default-mode brain dysfunction in mental disorders: A systematic review. *Neuroscience and Biobehavioral Reviews*, 33(3): 279–296, 2008.
- Buckner RL, Andrews-Hanna JR, and Schacter DL. The brain's default network. *Anatomy, function and relevance to disease. Annals of the New York Academy of Sciences*, 1124: 1–38, 2008.
- Callicott JH, Mattay VS, Bertolino A, Finn K, Coppola R, Frank JA, et al. Physiological characteristics of capacity constraints in working memory as revealed by functional MRI. *Cerebral Cortex*, 9(1): 20–26, 1999.
- Cavanna AE and Trimble MR. The precuneus: A review of its functional anatomy and behavioural correlates. *Brain*, 129(3): 564–583, 2006.
- Cauda F, Geminiani G, D'Agata F, Sacco K, Duca S, Bagshaw AP, et al. Functional connectivity of the posteromedial cortex. *PLoS ONE*, 5(9): e13107, 2010.
- Damoiseaux JS, Rombouts SA, Barkhof F, Scheltens P, Stam CJ, Smith SM, et al. Consistent resting-state networks across healthy subjects. *Proceedings of the National Academy of Sciences of the United States of America*, 103(37): 13848–13853, 2006.
- Esposito F, Aragri A, Latorre V, Popolizio T, Scarabino T, Cirillo S, et al. Does the default-mode functional connectivity of the brain correlate with working memory performances? *Archives italiennes de biologie*, 147(1–2): 11–20, 2009.
- Fan J, McCandliss BD, Fossella J, Flombaum JI, and Posner MI. The activation of attentional networks. *NeuroImage*, 26(2): 471–479, 2005.
- Filippini N, MacIntosh BJ, Hough MG, Goodwin GM, Frisoni GB, Smith SM, et al. Distinct patterns of brain activity in young carriers of the APOE-epsilon4 allele. *Proceedings of the National Academy of Sciences of the United States of America*, 106(17): 7209–7214, 2009.
- Fox MD, Snyder AZ, Vincent JL, Corbetta M, Van Essen DC, and Raichle ME. The human brain is intrinsically organized into dynamic, anticorrelated functional networks. *Proceedings of the National Academy of Sciences of the United States of America*, 102(27): 9673–9678, 2005.
- Fox MD, Zhang D, Snyder AZ, and Raichle ME. The global signal and observed anticorrelated resting state networks. *Journal of Neurophysiology*, 101(6): 3270–3283, 2009.
- Fransson P and Marrelec G. The precuneus/posterior cingulate cortex plays a pivotal role in the default mode network: Evidence from a partial correlation network analysis. *NeuroImage*, 42(3): 1178–1184, 2008.
- Greicius MD, Krasnow B, Reiss AL, and Menon V. Functional connectivity in the resting brain: A network analysis of the default mode brain function. *Proceedings of the National Academy of Sciences of the United States of America*, 100(1): 253–258, 2003.
- Greicius M. Resting-state functional connectivity in neuropsychiatric disorders. *Current Opinion in Neurology*, 21(4): 424–430, 2008.
- Hampson M, Driesen NR, Skudlarski P, Gore JC, and Constable R. Brain connectivity related to working memory performance. *The Journal of Neuroscience*, 26(51): 13338–13343, 2006.
- Hampson M, Driesen NR, Roth JK, Gore JC, and Constable RT. Functional connectivity between task-positive and task-negative areas and its relation to working memory performance. *Magnetic Resonance Imaging*, 28(8): 1051–1057, 2010.
- Hasson U, Nusbaum HC, and Small SL. Task-dependent organization of brain regions active during rest. *Proceedings of the National Academy of Sciences of the United States of America*, 106(26): 10841–10846, 2009.
- He Y and Evans A. Graph theoretical modeling of brain connectivity. *Current Opinion in Neurology*, 23(4): 341–350, 2010.
- Honey CD, Fu CHY, Kim J, Brammer MJ, Croudance TJ, Suckling J, et al. Effects of verbal working memory load on corticocortical connectivity modeled by path analysis of functional magnetic resonance imaging data. *NeuroImage*, 17(2): 573–582, 2002.
- Lewis CM, Baldassarre A, Committeri G, Romani GL, and Corbetta M. Learning sculpt the spontaneous activity of the resting human brain. *Proceedings of the National Academy of Sciences of the United States of America*, 106(42): 17558–17563, 2009.

- Narayanan NS, Prabhakaran V, Bunge SA, Christoff K, Fine EM, and Gabrieli JD. The role of the prefrontal cortex in the maintenance of verbal working memory: An event-related fMRI analysis. *Neuropsychology*, 19(2): 223–232, 2005.
- Newton AT, Morgan VL, Rogers BP, and Gore JC. Modulation of steady state functional connectivity in the default mode and working memory networks by cognitive load. *Human Brain Mapping*, doi:10.1002/hbm.21138, 2011.
- Nyberg L, Dahlin E, Stigsdotter Nelly A, and Bäckman L. Neural correlates of variable working memory load across adult age and skill: dissociative patterns within the fronto-parietal network. *Scandinavian Journal of Psychology*, 50(1): 41–46, 2009.
- Owen AM, McMillan KM, Laird A, and Bullmore E. N-Back working memory paradigm: A meta-analysis of normative functional neuroimaging studies. *Human Brain Mapping*, 25(1): 46–59, 2005.
- Posner MI, Sheese BE, Odludas I, and Tang I. Analyzing and shaping human attentional networks. *Neural Networks*, 19(9): 1422–1429, 2006.
- Pyka M, Beckmann CF, Schöning S, Hauke S, Heider D, Kugel H, et al. Impact of working memory load on fMRI resting state pattern in subsequent resting phases. *PLoS ONE*, 4(9): e7198, 2009.
- Raichle ME, MacLeod AM, Snyder AZ, Powers WJ, Gusnard DA, and Shulman GL. A default mode of brain function. *Proceedings of the National Academy of Sciences of the United States of America*, 98(2): 676–682, 2001.
- Raz A and Buhle J. Typologies of attentional networks. *Nature Reviews Neuroscience*, 7(5): 367–379, 2006.
- Rykhlevskaia E, Gratton G, and Fabiani M. Combining structural and functional neuroimaging data for studying brain connectivity: A review. *Psychophysiology*, 45(2): 173–187, 2008.
- Seeley WW, Crawford RK, Zhou J, Miller BL, and Greicius MD. Neurodegenerative diseases target large-scale human brain networks. *Neuron*, 62(1): 42–52, 2009.
- Shulman GL, Fiez JA, Corbetta M, Buckner RL, Miezin FM, Raichle ME, et al. Searching for activations that generalize over tasks. *Human Brain Mapping*, 5(4): 317–322, 1997.
- Van den Heuvel MP and Hulshoff Pol HE. Exploring the brain network: A review on resting-state fMRI functional connectivity. *European Neuropsychopharmacology*, 20(8): 519–534, 2010.
- Volle E, Kinkingnéhun S, Pochon JB, Mondon K, Thiebaut de Schotten M, Seassau M, et al. The functional architecture of the left posterior and lateral prefrontal cortex in humans. *Cerebral Cortex*, 18(10): 2460–2469, 2008.
- Waites AB, Stanislavsky A, Abbott DF, and Jackson GD. Effect of prior cognitive state on resting state networks measured with functional connectivity. *Human Brain Mapping*, 24(1): 59–68, 2005.
- Wang L, Laviolette P, O’Keefe K, Putcha D, Bakkour A, Van Dijk KRA, et al. Intrinsic connectivity between the hippocampus and posteromedial cortex predicts performance in cognitively intact older individuals. *NeuroImage*, 51(2): 910–917, 2010.
- Zang Y-F, He Y, Zhu C-Z, Cao Q-J, Sui M-Q, Liang M, et al. Altered baseline brain activity in children with ADHD revealed by resting-state functional MRI. *Brain & Development*, 29: 83–91, 2007.



Functional and structural connectivity of visuospatial and visuo-perceptual working memory.

Roser Sala-Llloch^{1,2}, Eva M. Palacios^{1,2}, Carme Junqué^{1,2,*}, Núria Bargalló³ and Pere Vendrell^{1,2}

¹Department of Psychiatry and Clinical Psychobiology, University of Barcelona, Barcelona, Spain.

²Institute of Biomedical Research August Pi i Sunyer (IDIBAPS), Barcelona, Spain.

³Centre de Diagnòstic per la Imatge. Hospital Clínic de Barcelona (CDIC), Barcelona, Spain.

Correspondence*:

Carme Junqué

Department of Psychiatry and Clinical Psychobiology, University of Barcelona.
Casanova 143, 08036, Barcelona, Spain., cjunque@ub.edu

ABSTRACT

Neural correlates of working memory (WM) in healthy subjects have been extensively investigated using functional MRI (fMRI). However it still remains unclear how cortical areas forming part of functional WM networks are also connected by white matter fiber bundles, and whether DTI measures, used as indices of microstructural properties and bundles directionality of these connections can predict individual differences in task performance. fMRI data were obtained from 23 healthy young subjects while performing one visuospatial (square location) and one visuo-perceptual (face identification) 2-back task. Diffusion tensor imaging (DTI) data were also acquired. Independent component analysis (ICA) of fMRI data was used to identify the main functional networks involved in WM tasks. Voxel-wise DTI analyses were performed to find correlations between structural white matter and task performance measures, and probabilistic tracking of DTI data was used to identify the white matter bundles connecting the nodes of the functional networks. We found that functional recruitment of the fusiform and the inferior frontal cortex was specific for the facial working memory task, while there was a high overlap in activation of the parietal and middle frontal areas for visuospatial and visuo-perceptual tasks. Axial diffusivity, of the tracts connecting the fusiform with the inferior frontal areas showed a significant correlation with processing speed in the facial working memory task. We conclude that different functional networks, partially overlapping with the fronto-parietal attention network, differentially support perceptual and working memory tasks. Moreover, the DTI measures are predictive of the processing speed

Keywords: fMRI; DTI; tractography; fusiform; facial working memory.

1 INTRODUCTION

Working Memory (WM) refers to the capacity to maintain, manipulate and store information temporarily and involves a set of brain structures and processes to organize and integrate sensory and other information

(Baddeley, 1996). Magnetic Resonance Imaging (MRI) has been used to investigate brain networks involved in WM both at the functional and structural levels, using functional MRI (fMRI) and Diffusion Tensor Imaging (DTI).

The use of fMRI to measure blood-oxygen-level-dependent (BOLD) signal during working memory tasks evidenced consistent activation of frontal and parietal cortical regions regardless of the stimulus modality (D'Esposito et al., 1998; Wager and Smith, 2003; Owen et al., 2005). These include the bilateral posterior parietal cortex, the bilateral premotor cortex, the dorsal cingulate/medial premotor cortex, the frontal pole, and the bilateral dorsolateral-midventrolateral prefrontal cortex. However, domain-specific activation within brain structures has also been documented (Fuster, 1997; Rottschy et al., 2012). Working memory tasks activate the lateral prefrontal region and, concomitantly, a region of the posterior cortex that varies according to the sensory modality: for visual stimuli, the activation is seen in the inferior temporal and parastriate cortex, for auditory stimuli in the superior temporal cortex, and for spatial stimuli in the posterior parietal cortex (Fuster and Bressler, 2012). As regards the involvement of visual regions, it is possible to differentiate between the dorsal and ventral processing streams, both originating in the striate cortex. The ventral stream passes through the occipitotemporal cortex to its anterior temporal target and to the ventrolateral prefrontal cortex. And the dorsal stream goes from the occipitoparietal cortex to the posterior half of the inferior parietal lobule and the dorsolateral prefrontal cortex. Recently, it has been concluded that the dorsal stream gives rise to three distinct major pathways namely the parieto-prefrontal, parieto-premotor and parieto-medial temporal pathways which support spatial working memory, visually guided action, and spatial navigation respectively (Kravitz et al., 2011). In addition, studies on WM for spatial locations have reported increased activity in the right inferior parietal lobule and left insula (Passaro et al., 2013). Therefore, the simultaneous investigation of different working memory paradigms of different stimuli is necessary to identify stimulus-specific regions of activity.

Diffusion-weighted MRI allows the measurement of microstructural properties of brain white matter by means of several DTI approaches. DTI indices, such as Fractional Anisotropy (FA), Radial Diffusivity (RD) and Axial Diffusivity (AD) relate to white matter integrity, since they are thought to reflect the degree of myelination, axonal membrane thickness and axon diameter (Beaulieu, 2002; Song et al., 2002). Moreover, DTI probabilistic tractography is an effective tool that reconstructs in vivo the trajectories of white matter fasciculi connecting different cortical areas (Behrens et al., 2003; Catani and Thiebaut de Schotten, 2008). FA values have been positively correlated with working memory performance (Klingberg, 2006; Olesen et al., 2003) as well as with task-related BOLD responsivity (Burzynska et al., 2011), and the superior longitudinal fasciculus (SLF) has been identified as the main tract involved in the working memory network. The relationship between SLF integrity and working memory has also been studied in pathologies such as multiple sclerosis, schizophrenia, and traumatic brain injury (Audoin et al., 2007; Karlsgodt et al., 2008; Palacios et al., 2011). It has been reported that the integrity of major white matter tracts, including the callosal genu and splenium, the cingulum, optic radiations and the superior longitudinal fasciculus, correlates with the performance intelligence quotient, and that this relationship is mediated by genetics (Chiang et al., 2012). In children, high FA values have been linked to improved response inhibition, enhanced working memory, and faster reaction times (Madsen et al., 2011; Vestergaard et al., 2011). In adults, high FA values in parietal and frontal white matter were associated with faster performance on a lexical decision task (Gold et al., 2007) and faster reaction times for tasks involving visuospatial attention (Tuch et al., 2005).

Although many studies have aimed to describe the functional and structural properties of working memory networks, in the current study we add a novel approach to the field by using advanced neuroimaging techniques to study both functional and structural connectivity of two different tasks involving different brain networks guided by the stimuli. We aimed to: 1) identify the differences in the task-activated networks for spatial and facial working memory, and 2) describe the structural connectivity of these networks.

Whereas brain functional connectivity can be studied as the temporal correlation between spatially remote neuropsychological events during the performance of a cognitive task (Biswal et al., 1995),

structural connectivity refers to the presence of fiber tracts directly connecting regions (Rykhlevskaia et al., 2008). Our aim was to combine data-driven fMRI analysis with probabilistic tractography and DTI maps to determine the functionality and connectivity between brain regions involved in visual working memory tasks and their relationship with cognitive performance. For this purpose, we independent component analysis of fMRI data and a whole-brain analysis of DTI-derived maps. In the WM tasks, different stimuli were used to determine the possible domain-specificity of the neural basis of working memory: one n-back task involving visuospatial processing (squares), and a second n-back task using visuo-perceptual stimuli (faces). We hypothesized that the functional networks extracted from either task would have some overlapping areas, as well as some specific areas that would be stimuli-dependent. Moreover, we expected that these functional networks would have their structural circuitry substrate in the fiber bundles that connect the different cortical regions involved simultaneously in the task.

2 MATERIAL & METHODS

2.1 SUBJECTS AND ACQUISITION

Twenty-three healthy young subjects (mean age: 28.26, SD: 6.76, 12 males, 11 females) with no history of psychiatric or neurological pathologies were included in the study. The study was approved by the research ethics committees of the University of Barcelona. All participants gave written informed consent. Subjects were scanned on a 3T MRI scanner (Magnetom Trio Tim, Siemens Medical Systems, Germany) during the performance of the working memory tasks, using a single shot gradient-echo EPI sequence (TR=2000 ms; TE=16 ms; FOV = 220 x 220 mm²; voxel size = 1.7 x 1.7 x 3.0 mm). High resolution T1-weighted images were acquired with the MPRAGE 3D protocol (TR=2300 ms; TE= 3 ms; TI=900 ms; FOV=244 mm²; 1mm isotropic voxel) and diffusion-weighted images were sensitized in 30 non-collinear directions with a b-value=1000 s/mm², using an echo-planar (EPI) sequence (TR=9300 ms, TE= 94 ms, slice thickness=2 mm, voxel size=2 x 2 x 2 mm, FOV=240 mm², no gap).

The cognitive tasks presented during the MRI scanning consisted of a 2-back paradigm, in which a sequence of stimuli was presented on the screen and the subject was asked to indicate whether the stimulus was identical to the one shown 2 trials before. For the assessment of visuo-perceptual working memory, facial images from an available database were used as stimuli (Minear and Park, 2004). For the visuospatial working memory task, the stimuli were color squares located in different positions on a black screen. In both tasks, a 0-back task was used as a control condition, and subjects were asked to indicate whether the current trial matched a specific stimuli. For the facial control task, subjects were asked to press the button when the person that appeared in the screen was wearing glasses, and for the spatial control task, subjects were asked to indicate if the color square shown was placed in the middle of the screen. Stimuli sizes were 55% and 74% of the screen width for the squares and faces respectively. Tasks were presented and synchronized with functional acquisition using the Presentation[®] software (NeuroBehavioral Systems, NBS). During fMRI acquisition, the task was projected in a big screen outside the scanner, and shown to the subject using a mirror system placed in front of subject's eyes. The subject was provided with a response button, also synchronized with the stimuli presentation, and responses were recorded in a computer outside the scanner.

During the scanning session, 12 subjects underwent first the facial 2-back task and then the spatial 2-back task, while the remaining subjects performed the tasks in the opposite order.

For each task, the sequence of stimuli was presented using a block-design paradigm, where 2-back blocks were alternated with 0-back blocks. Within each block, a total number of 14 stimuli were presented. Each image appeared on the screen for 1 second, with an interstimulus interval (black screen) of 1 second. An instruction screen was presented at the beginning of each block for 2 sec. The total number of blocks presented for each task was 16 alternating between conditions, presented in the course of the 8-minute

experiment. Individual responses were collected, and performance scores were computed using the d-prime measure [$Z(\text{hits rate}) - Z(\text{false alarm rate})$](Macmillan and Creelman, 1991). In addition, mean reaction times (RT) separately for each task and condition were collected, where RT was measured as the time between the stimulus onset and the subject's response.

2.2 ANALYSIS OF FMRI DATA

Functional MRI data were analyzed using Multivariate Exploratory Linear Optimized Decomposition into Independent Components (MELODIC) (Beckmann and Smith, 2004), as implemented in FSL (<http://www.fmrib.ox.ac.uk/fsl>). Before the ICA decomposition, the preprocessing of fMRI data included motion correction using MCFLIRT (Jenkinson and Smith, 2001), removal of non-brain regions with BET (Smith, 2002), spatial smoothing using a Gaussian kernel of FWHM 5 mm, grand-mean intensity normalization and high-pass temporal filtering (of FWHM=160s).

Then, three different ICA decompositions were carried out. First, facial and spatial tasks were analyzed separately, and a third analysis was performed with data from the two tasks. In each case, ICA decomposed functional data into a set of spatio-temporal Independent Components (ICs). Each IC was composed by a spatial map, an associated time-course and a subjects mode vector, indicating the strength of the component for each subject.

For each task-separated analysis, we identified the components related with the 2-back>0-back contrast and we selected the IC with the best fit to the task time-series. This procedure allowed the identification of the main functional network associated with spatial WM processing (spatial IC), and facial WM processing (facial IC). In addition, with the ICA analysis performed with data from the two tasks, we could identify components of higher activity in one on the two tasks with respect to the other.

2.3 PREPROCESSING OF DIFFUSION MRI DATA

Diffusion MRI Images were analyzed using FDT (FMRIB's Diffusion Toolbox), from FSL (Behrens et al., 2007). Firstly, data were corrected for distortions caused by the eddy currents in the gradient coils and for simple head motion, using the B0 non-diffusion data as a reference volume. Then, Fractional Anisotropy (FA) maps from each subject were obtained using a diffusion tensor image (DTI) model fit. With DTI, we also obtained individual maps for axial diffusivity (AD) and radial diffusivity (RD). Maps were registered and projected to a common skeleton map using the TBSS algorithm (Smith et al., 2006). Further, we performed voxel-wise statistics between subjects using these maps.

In addition, a probabilistic tractography algorithm was applied to the diffusion images (Behrens et al., 2007). This analysis is described in supplementary material.

2.4 STATISTICAL ANALYSES

Statistical comparison between activation maps were performed using the subjects' vector from the whole-group (facial and spatial) ICA decomposition. These vectors had a score for each subject and task that indicates the activation of a given component. They were introduced into PASW (Statistical Package for Social Sciences, Chicago, IL, USA) and we evaluated differences between tasks using paired t-test analysis. As regards the measures derived from the DTI analysis. First, spatial maps of FA, AD and RD were introduced in voxel-wise statistics to find regions that correlate with the results of the tasks. These maps were corrected for multiple comparisons using a permutation testing (Nichols and Holmes, 2002).

In addition, scores of mean FA, AD, and RD were obtained within the tracts of interest derived from the DTI-tractography analysis. We used Pearson's correlation in PASW to investigate correlations between the measures of FA, AD, and RD within the tracts and cognitive performance (see Supplementary material).

Table 1. Behavioral results of the two working memory tasks for both conditions.

FMRI Task	d prime mean(SD)	Response Time mean(SD)
Spatial 0-Back	4.03 (0.31)	0.416(0.08) s
Spatial 2-Back	3.49 (0.40)	0.47(0.09) s
Facial 0-Back	4.08 (0.28)	0.495(0.07) s
Facial 2-Back	3.33 (0.65)	0.546 (0.09) s

3 RESULTS

3.1 TASK PERFORMANCE

All subjects showed high task performance measured by d prime. A summary of behavioral measures for each task and condition is shown in Table 1. We found significant differences between 0-back and 2-back tasks for both RT and d prime measures and for both spatial and facial tasks. Subjects were slower in respond and performed worse in the 2-back conditions compared with 0-back conditions ($p < 0.001$ in paired T-Tests).

3.2 IDENTIFICATION OF FUNCTIONAL NETWORKS INVOLVED IN SPATIAL AND FACIAL WORKING MEMORY

Using T-ICA for the whole group of 23 subjects and separately for each task, we identified the functional pattern for spatial and facial working memory processes (spatial IC and facial IC, Figure 1). Spatial IC covered regions of the frontal and parietal cortices, with the main foci of activation in Middle Frontal and Parietal regions. The Facial IC, shared the middle frontal and parietal regions of activity, but showed additional activity in areas of the Fusiform and in a region of the Inferior Frontal. Additionally, we identified foci of activation in the Insula and in a region of the temporal cortex. The coordinates of all the foci are reported in Table 1.

With the ICA analysis of the facial and the spatial task together, we identified a component, associated with the 2-Back > 0-Back contrast, with higher activity during facial WM than during spatial WM ($p = 0.01$ in a paired-samples t-test analysis). Its spatial map included the left inferior frontal frontal gyrus, a small region in the right middle frontal gyrus, part of the paracingulate gyrus, and a cluster located in the occipital pole, occipital fusiform, the lingual and fusiform gyrii and the inferior division of the lateral occipital cortex.

3.3 WHOLE-BRAIN DTI ANALYSIS

In the voxel-wise analysis of maps derived from DTI analysis, we identified a cluster where AD correlated negatively with RT of the facial WM task ($p < 0.05$, corrected). This cluster was located in the left inferior fronto-occipital fasciculus and left uncinate fasciculus.

3.4 DTI TRACTOGRAPHY

We used the spatial pattern of the structural connection between the fusiform and the inferior frontal to demonstrate that it overlapped the region where AD correlated with response time of the facial WM task (Figure 2). This connection included the inferior fronto-occipital fasciculus, inferior longitudinal fasciculus, part of the uncinate fasciculus and part of the anterior thalamic radiation. Spatial maps of the rest of connections and their descriptions are given in Supplementary Material.

In addition, DTI measures of some of the showed correlations at the uncorrected level with results of the task (see Supplementary Material). In summary, FA and AD of the tracts from the fusiform to the inferior frontal regions correlated with reaction time of the facial task, and RD of the tracts from the insula to the middle frontal correlated with d prime of the spatial task.

4 DISCUSSION

By using Independent Component Analysis of fMRI data, we found two different patterns of brain activity in two working memory tasks: one involving working memory for spatial locations (visuospatial) and another involving working memory for facial stimuli (visuoperceptual). Both tasks recruited areas of the frontal and parietal lobes, while the fusiform gyrus was only recruited in working-memory for facial stimuli. We found statistical differences in brain activation between tasks, consisting on higher involvement of occipital pole, fusiform gyrus and inferior frontal gyrus during the performance of the facial WM task. We used DTI data to investigate whether the stimuli-specificity found in functional data was also present in the properties measured in the structural connections. By doing a whole-brain analysis, we identified a region in the left inferior fronto-occipital fasciculus and the left uncinate where AD correlated with the response time in the facial WM task. We then used tractography to identify structural connections related to the functional patterns observed with fMRI and we identified the main tracts connecting the main areas involved in each task.

Results from fMRI data showed that both visuoperceptual and visuospatial tasks activated regions described as forming part of the core working memory network. We observed bilateral activation of the superior parietal lobule, frontal pole, dorsolateral-midventrolateral prefrontal cortex, and the anterior insula. These activated regions coincide with those described in several meta-analyses of the n-back task (**Fuster**, 1997; **Owen et al.**, 2005; **Rottschy et al.**, 2012). We also found brain activity involving the ventral and lateral intraparietal region and the mid-temporal area, which receives strong input from visual processing regions. For the facial working memory task, in addition to the fronto-parietal and mid-temporal pattern of activity, we observed increased activity in the fusiform region and in the inferior parietal gyrus. This is in agreement with previous works showing the involvement of the fusiform area in face processing, including the detection and discrimination of faces (**McCarthy et al.**, 1997; **Haxby et al.**, 2001; **Kanwisher**, 2010). It should be noted that the design of the task could not differentiate the specific processes of face identification and facial memory, because the control task did not specifically require face identification, and therefore, the involvement of the fusiform could also be explained by differences in perceptual processing. In the spatial task, the shape processing, which could be considered a visuoperceptive process, was controlled by the task design, as the control task involved the same shape and color figure as the target task; therefore, we did not identify the participation of any region of the ventral stream. As expected due to the nature of the task, the superior parietal region of the dorsal stream was involved (**Rottschy et al.**, 2012).

The rest of the ROI pairs resulted in tractography maps that included several tracts, and that were in accordance with reported structural brain connections (**Catani et al.**, 2002).

In the whole-brain DTI analysis, we found a cluster in the left inferior fronto-occipital fasciculus and the uncinate where AD correlated with RT for the facial WM task. In addition, by doing probabilistic tractography, we identified the main tracts involved in the functional networks and we found that mean FA and mean AD scores within the pathway connecting the fusiform and the inferior frontal ROIs also correlated with facial RT. In all cases, subjects with higher AD or FA scores had faster reaction times. Although these last results were not corrected for multiple comparisons and they are reported in supplementary material, we believe that they support and extend the results obtained with the whole-brain DTI analysis. Previous studies have reported positive correlations between reaction time and DTI indices. In adult subjects, **Gold et al.** (2007) found that the speed of visual word recognition correlated with tract integrity, measured with FA in parietal regions; and **Tuch et al.** (2005) found that reaction time of visuospatial learning also correlated with FA values in the parietal region. In our results, the

whole-brain analysis showed a negative correlation between AD and response time in the left hemisphere, which differs from other studies showing right hemispheric preference in the correlation between DTI and performance in facial recognition (Tavor et al., 2014). It has been suggested that AD is a more putative measure of axonal integrity, providing information about the status of the axons (Di Paola et al., 2010) and that it could be more directly related with the capacity of the brain white matter to conduct information between different brain regions (Lazar et al., 2014). Furthermore, studies using animal models with inflammatory and demyelinating lesions have concluded that AD reflects axonal transport properties (Budde et al., 2009; DeBoy et al., 2007). Although we could not find a specific explanation for the fact that the correlations with AD were found mainly in the left hemisphere, we suggest that, considering that AD is more directly associated with processing speed, its correlations would be found more generally in areas reflecting bilateral antero-posterior communication. In conclusion, our results suggest that AD could be measuring axonal properties that are directly related to the capacity to conduct information between brain regions (Lazar et al., 2014), whereas RD is related to myelination and measures properties of brain maturation with a more direct impact on task performance.

As regards the rest of results of tractography analyses, which are reported in Supplementary material because they did not survive correction for multiple comparisons, we found a correlation in the tract connecting the insula and the middle frontal ROIs in the left hemisphere. That is, the RD of this tract correlated with the d prime score in the spatial 2-Back task. Regions in the left hemisphere, and specially the left insula have been previously associated with the maintenance of information for object location in fMRI studies (Passaro et al., 2013). In this case, as opposite to the facial task, the correlation was found only with RD index. It has been suggested that RD is a measure of the degree of myelination and reflects processes of brain maturation or degeneration (Song et al., 2002), and it has been related to task performance in several studies (Tamnes et al., 2010; Østby et al., 2011; Tavor et al., 2014).

It should be noted that apart from this correlation, we did not find strong evidence of a structure-performance relationship in the spatial WM task. We suggest several explanations for this lack of correlation. One possibility is that task-performance may be the result of more complex network interactions between structure and function in both positive and negative task-networks, as suggested in other reports (Burzynska et al., 2013). In addition, this lack of relationships may also be attributable to divergences between structure and function, and the fact that the tracts identified in the structural network are shared by different functional networks (Park and Friston, 2013). In this case, some of the fasciculi, like the SLF, would not be specific for the spatial WM task.

In summary, simultaneous use of two MRI techniques enabled us to characterize the function and structure of working memory networks for spatial and facial stimuli. We studied the relationship between brain structure and cognitive function and we conclude that networks underlying the working memory function with spatial and visual stimuli share the fronto-parietal connections, and that facial working memory involves additional recruitment of the fusiform gyri. Furthermore, the DTI results highlighted the involvement of the inferior fronto-occipital fasciculus, as part of the fusiform-frontal connection during working memory for faces. The study of brain networks, beyond the study of isolated brain regions, is of increasing interest in the neuroscience community. The present study underlines the importance of studying both the function and the structure of brain networks. Our results corroborate the idea that functional networks are supported by structural connections of white matter pathways, but also partially support the concept of divergence, introduced by Park and Friston (Park and Friston, 2013) according to which the same structural connectivity can support many functions.

This study has several limitations. The first is the small sample size, especially for the DTI analysis. Other limitations are related to the design of the study itself. In this regard, the first one is that we could not control for eye movements, because we did not include a fixation condition in the task design. In addition, the control conditions used for spatial and facial WM were not exactly equivalent, so part of the observed activity in the fusiform cortex could be related to facial-processing rather than to face-memory processes.

We have studied the main tracts derived from the different ROI-related activations of the task; however, the use of the fMRI analysis as the basis for describing the working memory networks may have missed certain brain regions. Finally, another limitation is the fact that the results from tractography analyses did not survive correction for multiple comparisons and they should be interpreted with caution.

DISCLOSURE/CONFLICT-OF-INTEREST STATEMENT

The authors declare that the research was conducted in the absence of any commercial or financial relationships that could be construed as a potential conflict of interest.

ACKNOWLEDGEMENT

The authors thank Cesar Garrido from the Centre de Diagnostic per la Image of the Hospital Clinic (CDIC) for assistance with data collection.

REFERENCES

- Audoin, B., Guye, M., Reuter, F., Au Duong, M.-V., Confort-Gouny, S., Malikova, I., et al. (2007), Structure of WM bundles constituting the working memory system in early multiple sclerosis: a quantitative DTI tractography study., *NeuroImage*, 36, 4, 1324–30
- Baddeley (1996), Working Memory (Oxford University Press)
- Beaulieu, C. (2002), The basis of anisotropic water diffusion in the nervous system - a technical review., *NMR in biomedicine*, 15, 7-8, 435–55
- Beckmann, C. F. and Smith, S. M. (2004), Probabilistic independent component analysis for functional magnetic resonance imaging., *IEEE transactions on medical imaging*, 23, 2, 137–52
- Behrens, T. E. J., Berg, H. J., Jbabdi, S., Rushworth, M. F. S., and Woolrich, M. W. (2007), Probabilistic diffusion tractography with multiple fibre orientations: What can we gain?, *NeuroImage*, 34, 1, 144–55
- Behrens, T. E. J., Johansen-Berg, H., Woolrich, M. W., Smith, S. M., Wheeler-Kingshott, C. A. M., Boulby, P. A., et al. (2003), Non-invasive mapping of connections between human thalamus and cortex using diffusion imaging., *Nature neuroscience*, 6, 7, 750–7
- Biswal, B., Yetkin, F. Z., Haughton, V. M., and Hyde, J. S. (1995), Functional connectivity in the motor cortex of resting human brain using echo-planar MRI., *Magnetic resonance in medicine*, 34, 4, 537–41
- Budde, M. D., Xie, M., Cross, A. H., and Song, S.-K. (2009), Axial diffusivity is the primary correlate of axonal injury in the experimental autoimmune encephalomyelitis spinal cord: a quantitative pixelwise analysis., *The Journal of neuroscience : the official journal of the Society for Neuroscience*, 29, 9, 2805–13
- Burzynska, A. Z., Garrett, D. D., Preuschhof, C., Nagel, I. E., Li, S.-C., Bäckman, L., et al. (2013), A scaffold for efficiency in the human brain., *The Journal of neuroscience : the official journal of the Society for Neuroscience*, 33, 43, 17150–9
- Burzynska, A. Z., Nagel, I. E., Preuschhof, C., Li, S.-C., Lindenberger, U., Bäckman, L., et al. (2011), Microstructure of frontoparietal connections predicts cortical responsivity and working memory performance., *Cerebral cortex (New York, N.Y. : 1991)*, 21, 10, 2261–71
- Catani, M., Howard, R. J., Pajevic, S., and Jones, D. K. (2002), Virtual in vivo interactive dissection of white matter fasciculi in the human brain., *NeuroImage*, 17, 1, 77–94
- Catani, M. and Thiebaut de Schotten, M. (2008), A diffusion tensor imaging tractography atlas for virtual in vivo dissections., *Cortex; a journal devoted to the study of the nervous system and behavior*, 44, 8, 1105–32
- Chiang, M.-C., Barysheva, M., McMahon, K. L., de Zubicaray, G. I., Johnson, K., Montgomery, G. W., et al. (2012), Gene network effects on brain microstructure and intellectual performance identified in

- 472 twins., *The Journal of neuroscience : the official journal of the Society for Neuroscience*, 32, 25, 8732–45
- DeBoy, C. A., Zhang, J., Dike, S., Shats, I., Jones, M., Reich, D. S., et al. (2007), High resolution diffusion tensor imaging of axonal damage in focal inflammatory and demyelinating lesions in rat spinal cord., *Brain : a journal of neurology*, 130, Pt 8, 2199–210
- D'Esposito, M., Aguirre, G. K., Zarahn, E., Ballard, D., Shin, R. K., and Lease, J. (1998), Functional MRI studies of spatial and nonspatial working memory., *Brain research. Cognitive brain research*, 7, 1, 1–13
- Di Paola, M., Spalletta, G., and Caltagirone, C. (2010), In vivo structural neuroanatomy of corpus callosum in Alzheimer's disease and mild cognitive impairment using different MRI techniques: a review., *Journal of Alzheimer's disease : JAD*, 20, 1, 67–95
- Fuster, J. M. (1997), Network memory., *Trends in neurosciences*, 20, 10, 451–9
- Fuster, J. M. and Bressler, S. L. (2012), Cognit activation: a mechanism enabling temporal integration in working memory., *Trends in cognitive sciences*, 16, 4, 207–18
- Gold, B. T., Powell, D. K., Xuan, L., Jiang, Y., and Hardy, P. A. (2007), Speed of lexical decision correlates with diffusion anisotropy in left parietal and frontal white matter: evidence from diffusion tensor imaging., *Neuropsychologia*, 45, 11, 2439–46
- Haxby, J. V., Gobbini, M. I., Furey, M. L., Ishai, A., Schouten, J. L., and Pietrini, P. (2001), Distributed and overlapping representations of faces and objects in ventral temporal cortex., *Science (New York, N.Y.)*, 293, 5539, 2425–30
- Jenkinson, M. and Smith, S. (2001), A global optimisation method for robust affine registration of brain images., *Medical image analysis*, 5, 2, 143–56
- Kanwisher, N. (2010), Functional specificity in the human brain: a window into the functional architecture of the mind., *Proceedings of the National Academy of Sciences of the United States of America*, 107, 25, 11163–70
- Karlsgodt, K. H., van Erp, T. G. M., Poldrack, R. A., Bearden, C. E., Nuechterlein, K. H., and Cannon, T. D. (2008), Diffusion tensor imaging of the superior longitudinal fasciculus and working memory in recent-onset schizophrenia., *Biological psychiatry*, 63, 5, 512–8
- Klingberg, T. (2006), Development of a superior frontal-intraparietal network for visuo-spatial working memory., *Neuropsychologia*, 44, 11, 2171–7
- Kravitz, D. J., Saleem, K. S., Baker, C. I., and Mishkin, M. (2011), A new neural framework for visuospatial processing., *Nature reviews. Neuroscience*, 12, 4, 217–30
- Lazar, M., Miles, L. M., Babb, J. S., and Donaldson, J. B. (2014), Axonal deficits in young adults with High Functioning Autism and their impact on processing speed., *NeuroImage. Clinical*, 4, 417–25
- Macmillan, N. and Creelman, C. (1991), *Detection Theory: A User's Guide* (Cambridge University Press)
- Madsen, K. S., Baaré, W. F. C., Skimminge, A., Vestergaard, M., Siebner, H. R., and Jernigan, T. L. (2011), Brain microstructural correlates of visuospatial choice reaction time in children., *NeuroImage*, 58, 4, 1090–100
- McCarthy, G., Puce, A., Gore, J. C., and Allison, T. (1997), Face-specific processing in the human fusiform gyrus., *Journal of cognitive neuroscience*, 9, 5, 605–10
- Minear, M. and Park, D. C. (2004), A lifespan database of adult facial stimuli., *Behavior research methods, instruments, & computers : a journal of the Psychonomic Society, Inc*, 36, 4, 630–3
- Nichols, T. E. and Holmes, A. P. (2002), Nonparametric permutation tests for functional neuroimaging: a primer with examples., *Human brain mapping*, 15, 1, 1–25
- Østby, Y., Tamnes, C. K., Fjell, A. M., and Walhovd, K. B. (2011), Morphometry and connectivity of the fronto-parietal verbal working memory network in development., *Neuropsychologia*, 49, 14, 3854–62
- Olesen, P. J., Nagy, Z., Westerberg, H., and Klingberg, T. (2003), Combined analysis of DTI and fMRI data reveals a joint maturation of white and grey matter in a fronto-parietal network., *Brain research. Cognitive brain research*, 18, 1, 48–57
- Owen, A. M., McMillan, K. M., Laird, A. R., and Bullmore, E. (2005), N-back working memory paradigm: a meta-analysis of normative functional neuroimaging studies., *Human brain mapping*, 25, 1, 46–59

- Palacios, E. M., Fernandez-Espejo, D., Junque, C., Sanchez-Carrion, R., Roig, T., Tormos, J. M., et al. (2011), Diffusion tensor imaging differences relate to memory deficits in diffuse traumatic brain injury., *BMC neurology*, 11, 24
- Park, H.-J. and Friston, K. (2013), Structural and functional brain networks: from connections to cognition., *Science*, 342, 6158, 1238411
- Passaro, A. D., Elmore, L. C., Ellmore, T. M., Leising, K. J., Papanicolaou, A. C., and Wright, A. A. (2013), Explorations of object and location memory using fMRI., *Frontiers in behavioral neuroscience*, 7, 105
- Rottschy, C., Langner, R., Dogan, I., Reetz, K., Laird, A. R., Schulz, J. B., et al. (2012), Modelling neural correlates of working memory: a coordinate-based meta-analysis., *NeuroImage*, 60, 1, 830–46
- Rykhlevskaia, E., Gratton, G., and Fabiani, M. (2008), Combining structural and functional neuroimaging data for studying brain connectivity: a review., *Psychophysiology*, 45, 2, 173–87
- Smith, S. M. (2002), Fast robust automated brain extraction., *Human brain mapping*, 17, 3, 143–55
- Smith, S. M., Jenkinson, M., Johansen-Berg, H., Rueckert, D., Nichols, T. E., Mackay, C. E., et al. (2006), Tract-based spatial statistics: voxelwise analysis of multi-subject diffusion data., *NeuroImage*, 31, 4, 1487–505
- Song, S.-K., Sun, S.-W., Ramsbottom, M. J., Chang, C., Russell, J., and Cross, A. H. (2002), Demyelination revealed through MRI as increased radial (but unchanged axial) diffusion of water., *NeuroImage*, 17, 3, 1429–36
- Tamnes, C. K., Østby, Y., Walhovd, K. B., Westlye, L. T., Due-Tønnessen, P., and Fjell, A. M. (2010), Intellectual abilities and white matter microstructure in development: a diffusion tensor imaging study., *Human brain mapping*, 31, 10, 1609–25
- Tavor, I., Yablonski, M., Mezer, A., Rom, S., Assaf, Y., and Yovel, G. (2014), Separate parts of occipito-temporal white matter fibers are associated with recognition of faces and places., *NeuroImage*, 86, 123–30
- Tuch, D. S., Salat, D. H., Wisco, J. J., Zaleta, A. K., Hevelone, N. D., and Rosas, H. D. (2005), Choice reaction time performance correlates with diffusion anisotropy in white matter pathways supporting visuospatial attention., *Proceedings of the National Academy of Sciences of the United States of America*, 102, 34, 12212–7
- Vestergaard, M., Madsen, K. S., Baaré, W. F. C., Skimminge, A., Ejersbo, L. R., Ramsø y, T. Z., et al. (2011), White matter microstructure in superior longitudinal fasciculus associated with spatial working memory performance in children., *Journal of cognitive neuroscience*, 23, 9, 2135–46
- Wager, T. D. and Smith, E. E. (2003), Neuroimaging studies of working memory: a meta-analysis., *Cognitive, affective & behavioral neuroscience*, 3, 4, 255–74

FIGURES

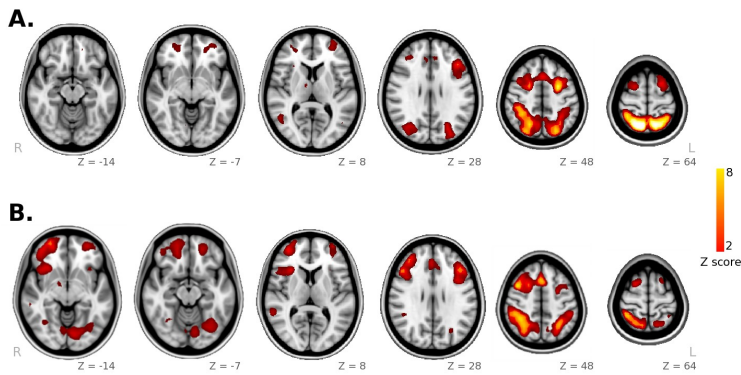


Figure 1. Spatial maps obtained from ICA decomposition of functional data. (A) Main component for the spatial WM task; (B) main component for the facial WM task.

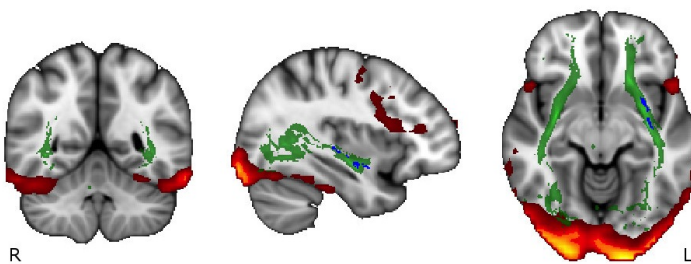


Figure 2. Overlapping map of the ICA, the whole-brain DTI and the tractography analyses.

SUPPLEMENTARY MATERIAL

Supplementary Methods:

Definition of ROIs from functional data

We used the maps obtained in the two task-specific separate ICA analyses to create a set of ROIs for the facial and the spatial task. For each task, we selected the component having the best fit with the task timeseries and we thresholded its spatial map ($Z > 2.3$) to obtain the clusters of higher activity. Each cluster was assigned to a region using the Harvard-Oxford atlas available in FSL. Overall, 5 ROIs were created in each hemisphere (Table S.1): the Fusiform ROI (Fus ROI), the Inferior Frontal ROI (IF ROI), the Insular ROI (Ins ROI), the Middle Frontal ROI (MF ROI) and the Parietal ROI (Par ROI). The Fus ROI was specific for the facial task, whereas the other ROIs were common for spatial and facial tasks.

ROI id	Hemisphere	IC	Atlas region	MNI coordinates
Fus ROI	L/R	facial	Fusiform	(-33, -70, -12)
IF ROI	L/R	spatial/facial	Inferior frontal	(-34, 58, 8)
Ins ROI	L/R	spatial/facial	Insular cortex	(-30, 22, 4)
MF ROI	L/R	spatial/facial	Middle frontal	(-42, 26, 28)
Par ROI	L/R	spatial/facial	Parietal cortex	(-29, -58, 52)
Temp ROI	R	spatial/facial	Temporal cortex	(55, -37, 1)

Table S.1. Definition and localization of ROIs from functional data.

Tractography analysis

Tractography was used to estimate the connectivity between pairs of ROIs (seed ROI and end ROI) individually for each subject, resulting in maps indicating the probability of each voxel to have a tract connecting both ROIs. The entire probabilistic tracking procedure was carried out in each subject's anatomical space. Using the probabilistic tractography algorithm, we obtained individual maps for each pair of ROIs, where each voxel value indicated the probability of having fibers connecting the two regions.

These maps were thresholded (at 2% of their maximum) in order to remove very-low probability fiber paths.

Individual FA scores inside each pathway were calculated as the mean FA of all voxels in the tract and they were then used to quantify and compare the integrity of the identified paths. Tract-averaged scores for axial diffusivity (AD) and radial diffusivity (RD) were also obtained for the main tracts of interest.

Supplementary Results:

Seed-to-seed fiber tracking

Using probabilistic tractography, we obtained the main tracts involved in the functional tasks. In total, 15 ROI-to-ROI pathways were identified in each hemisphere (Figure S.1). Although all possible pairs of ROIs were explored, we aimed to characterize stimulus-dependent tracts. For this purpose, we focused on the pathways from the fusiform ROI to the parietal and inferior frontal regions (facial/visuoperceptive WM), and the pathway from the mid-frontal to parietal regions (spatial/visuospatial WM).

Correlation between DTI measures and task performance

We evaluated correlations between task measures and DTI parameters of the tracts identified previously (i.e. all the ROI-to-ROI paths shown in Figure S.1).

The mean FA values of the tracts connecting the Fus ROI and the IF ROI correlated with RT scores during the facial-WM 2-Back task ($r=-0.639$, $p=0.001$ for the right hemisphere, $r=-0.464$, $p=0.030$ for the left hemisphere). Axial Diffusivity (AD) of the same pathway (Fus to IF ROIs) also correlated with RT scores of the facial WM 2-back task ($r=-0.449$, $p=0.036$ in the right hemisphere and $r=-0.603$, $p=0.003$ in the left hemisphere).

In addition, we observed a significant correlation between d prime measures and RD indices in the tracts connecting the Ins ROI and the MF ROI of the left hemisphere ($r=-0.447$, $p=0.037$).

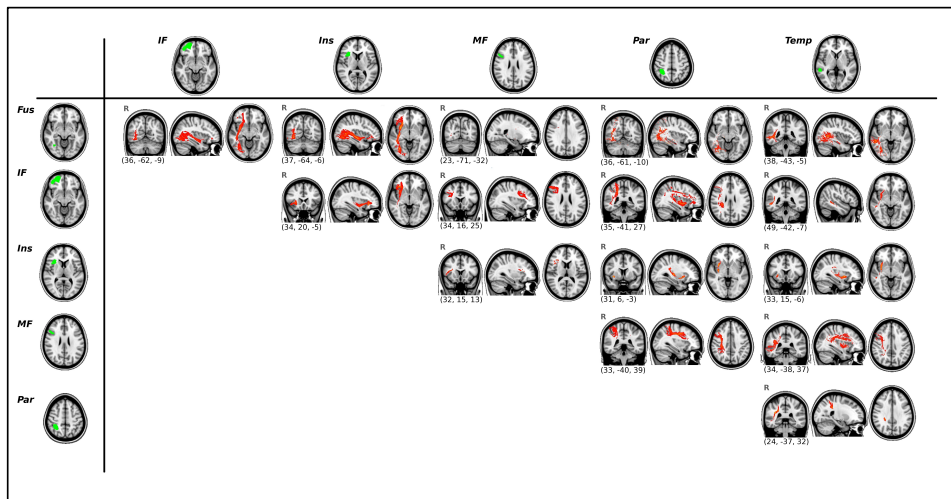


Figure S.1. Results of the ROI-to-ROI tractography. Functional ROIs are shown in green (left column and upper row) and their corresponding white matter connections are displayed in red. All tracts are thresholded at their 2% and averaged across all subjects.



Dynamic functional reorganizations and relationship with working memory performance in healthy aging

Roser Sala-Llloch¹, Eider M. Arenaza-Urquijo¹, Cinta Valls-Pedret², Dídac Vidal-Piñero¹, Nuria Bargalló³, Carme Junqué^{1,4} and David Bartrés-Faz^{1,4}*

¹ Departament de Psiquiatria i Psicobiologia Clínica, Facultat de Medicina, Universitat de Barcelona, Barcelona, Spain

² Unitat de lípids, Servei Endocrinologia i Nutrició, Hospital Clínic de Barcelona, Barcelona, Spain

³ Radiology Service, Hospital Clínic de Barcelona, Barcelona, Spain

⁴ Institut d'Investigacions Biomèdiques August Pi i Sunyer, Barcelona, Spain

Edited by:

Simone Rossi, Azienda Ospedalira
Universitaria Senese, Italy

Reviewed by:

Stefano F. Cappa, Vita-Salute San
Raffaele University, Italy
Massimiliano Oliveri, University of
Palermo, Italy

*Correspondence:

David Bartrés-Faz, Departament de
Psiquiatria i Psicobiologia Clínica,
Facultat de Medicina, Universitat de
Barcelona, Casanova 143, 08036
Barcelona, Spain.
e-mail: dbartrés@ub.edu

In recent years, several theories have been proposed in attempts to identify the neural mechanisms underlying successful cognitive aging. Old subjects show increased neural activity during the performance of tasks, mainly in prefrontal areas, which is interpreted as a compensatory mechanism linked to functional brain efficiency. Moreover, resting-state studies have concluded that elders show disconnection or disruption of large-scale functional networks. We used functional MRI during resting-state and a verbal *n*-back task with different levels of memory load in a cohort of young and old healthy adults to identify patterns of networks associated with working memory and brain default mode. We found that the disruption of resting-state networks in the elderly coexists with task-related overactivations of certain brain areas and with reorganizations within these functional networks. Moreover, elders who were able to activate additional areas and to recruit a more bilateral frontal pattern within the task-related network achieved successful performance on the task. We concluded that the balanced and plastic reorganization of brain networks underlies successful cognitive aging. This observation allows the integration of several theories that have been proposed to date regarding the aging brain.

Keywords: fMRI, aging, working memory, compensation, plasticity, frontal cortex, default-mode network

INTRODUCTION

Cognitive aging affects a wide range of functions including working memory, processing speed, and inhibitory function (Park et al., 2002; Reuter-Lorenz and Park, 2010). Despite the gradual decline described in aging, some seniors are able to keep their cognitive functions with minimal differences in performance compared to healthy young subjects. Several theories have been proposed in attempts to identify the neural correlates of what is known as “successful cognitive aging” (Cabeza et al., 2002a; Park and Reuter-Lorenz, 2009).

Functional imaging is well suited to the study of changes in brain functionality in advanced age (for a review, see Eyler et al., 2011). Across various cognitive domains, age-related functional reorganizations have been described as changes in brain responsivity in several brain regions when subjects are scanned during the performance of cognitively demanding tasks (see Spreng et al., 2010; Turner and Spreng, 2012 for recent meta-analyses). Hence, both reductions and increases in activity have been described in different brain regions. Reductions in activity are commonly located in the left prefrontal cortex (PFC) and temporo-occipital areas and are normally associated with less efficient processing in aging (Cabeza et al., 1997), but the interpretation of increases is less straightforward. However, when associated with better or preserved performance they have been commonly interpreted as evidence of functional compensatory mechanisms (Grady, 2000; Cabeza et al., 2002b; Grady et al., 2006; Mattay et al., 2006; Berlinger et al., 2010).

Moreover, recent advances in neuroimaging techniques have made possible the study of functional brain networks that can be observed even during resting-state periods, revealing an intrinsic network-based organization of the brain (Smith et al., 2009). In this context, cognitive aging has been associated with disruptions/reorganizations within certain brain functional networks (Grady et al., 2010; Littow et al., 2010; Tomasi and Volkow, 2012). Particularly, areas forming part of the default-mode network (DMN), including the posterior cingulate cortex and middle frontal gyrus, are characterized by patterns of age-related decreases in functional connectivity (Damoiseaux et al., 2008; Hafkemeijer et al., 2012). These functional correlation reductions have been associated with cognitive decline across multiple domains in healthy old individuals (Andrews-Hanna et al., 2007).

Despite this evidence of changes in both brain activity and brain connectivity, very few studies have simultaneously investigated the DMN and a task-related brain network in aging in terms of their BOLD responsivity and functional connectivity, and during both resting and cognitive performance. Hence, the objective of our study was to investigate the brain connectivity/activity characteristics of the DMN and a working memory network in a sample of healthy elders (HE) and young adults (YA). In the present report, we placed special emphasis on investigating how these patterns differ between elders who are able to keep their working memory abilities at a level comparable to young subjects during the most demanding conditions, and those who show a decline in this function.

MATERIAL AND METHODS

SUBJECTS AND SCANNING

Twenty-nine HE (mean age: 62.55, SD: 9.43, 20 women) and 16 YA (mean age: 21.31, SD: 2.41, 9 women) were included in the study. Old subjects underwent neuropsychological testing, including memory, language, attention, and visuosperceptive/visuospatial functions. The neuropsychological battery was similar to the one used recently in other reports by our group (e.g., Arenaza-Urquijo et al., 2011). All reported scores were within normal range on the domains tested, and all subjects had scores on the mini-mental state examination ≥ 24 (mean: 28.83, SD: 1.64). All participants in the study were scanned using functional MRI (fMRI) in the resting-state and during the performance of a working memory task, an n -back task including different levels of working memory load ($n = 0, 1, 2$, and 3 letters to be retained; see Braver et al., 1997; Sala-Llonch et al., 2011). Basically, during the task, blocks of 0-, 1-, 2-, 3-back conditions lasting 26 s were presented four times each in a pseudo-randomized order with inter-block fixation periods (white cross on a black screen) of 13 s. Before any n -back block was presented, an instruction screen appeared to inform the subject about the task. Within each block, a sequence of 12 letters was presented in white in the center of the screen; each letter remained visible for 500 ms, with an inter-stimulus interval of 1500 ms. The subject was asked to press a button when the stimulus on the screen was the same as the one showed n items before. For the 0-back task, subjects were asked to press the button when the letter “X” appeared. All subjects underwent a training session before entering the scanner in order to ensure that they understood the task instructions. All achieved a task accuracy of at least 80%.

Subjects' responses were collected and the performance of each n -back condition was calculated using the d' measure (Z hit rate $- Z$ false alarm rate), with higher d' scores indicating higher performance. Mean reaction time (RT) was also collected for each subject within each load condition.

The HE group was further subdivided into low performers (low-HE) and high-performers (high-HE) according to the score obtained during the performance of the 3-back task (percentile 50 of the distribution). Between-group differences in d' measures and RT measures were assessed with one-way ANOVA implemented in PASW vs. 17 (Statistical Package for Social Sciences, Chicago, IL, USA).

Functional MRI images were acquired on a 3T MRI scanner (Magnetom Trio Tim, Siemens Medical Systems, Germany), using a 32-channel coil. During both the resting-fMRI and task-fMRI conditions, a set of T2*-weighted volumes (150 and 336 volumes for resting and task fMRI, respectively) were acquired (TR = 2000 ms, TE = 29 ms, 36 slices per volume, slice thickness = 3 mm, distance factor = 25%, FOV = 240 mm, matrix size = 128 × 128). A high-resolution 3D structural dataset (T1-weighted MPRAGE, TR = 2300 ms, TE = 2.98 ms, 240 slices, FOV = 256 mm; matrix size = 256 × 256; slice thickness = 1 mm) was also acquired in the same scanning session for registration purposes.

ANALYSIS OF RESTING-fMRI DATA

Resting-state fMRI images were analyzed with independent component analysis (ICA) and a dual-regression approach. Image

preprocessing was carried out in FSL¹ and AFNI² softwares. This step included the removal of the first five scans, motion correction, skull stripping, spatial smoothing using a Gaussian kernel of FWHM = 6 mm, grand mean scaling, temporal filtering (low-pass and high-pass filters). Functional scans were then registered to their corresponding individual MPRAGE structural scans using linear registration with 6 df (Jenkinson and Smith, 2001) and further registered to the standard MNI template by concatenation of both registration matrices. Resampling resolution was set to 3 mm.

We used ICA, as implemented in MELODIC (Beckmann et al., 2005) from FSL, in order to decompose resting-state data into 25 independent components (ICs) which described common spatio-temporal independent patterns of correlated brain activity across the whole group of subjects in the study. Within the 25 ICs obtained, we identified the common resting-state functional networks (Damoiseaux et al., 2008; Smith et al., 2009; van den Heuvel and Hulshoff Pol, 2010), and selected the DMN, and two components corresponding to the right-lateralized and the left-lateralized fronto-parietal networks (right-FPN, and left-FPN). The selection procedure was performed by visual inspection together with template matching with online available data (Smith et al., 2009; Biswal et al., 2010) and with average task-related activation maps obtained from the data-driven analysis (see Figure 1 for a summary of the methods used in the study).

Then, we used the spatial patterns of the three selected networks in a dual-regression approach (as described in Filippini et al., 2009; Leech et al., 2011) in order to explore between-group differences. In the dual-regression analysis, we first regressed each subject's resting-state functional data against the spatial IC maps and obtained individual time-series associated to each network (DMN, right-FPN, and left-FPN). These time-courses were then used to regress again the individual preprocessed fMRI data and to obtain individual spatial maps that were also specific for networks. Spatial maps were finally tested for voxel-wise differences between groups using non-parametric testing with 5000 random permutations.

ANALYSIS OF TASK-fMRI DATA

Task-fMRI images were analyzed with a model-driven protocol to explore ROI-based BOLD signal change across task conditions. We also used a dual-regression analysis of task-fMRI data to investigate differences in network integration.

First, data preprocessing was performed in FSL and AFNI. It included motion correction, skull stripping, spatial smoothing using a Gaussian kernel of FWHM = 6 mm, grand mean scaling, temporal filtering (high-pass filter of sigma = 80 s), and registration to individual anatomical scans and to MNI standard space (Jenkinson and Smith, 2001). As in resting-fMRI, resampling resolution was set to 3 mm.

Task-fMRI data were analyzed using standard random-effects general linear model. We used the procedure as implemented in FMRI Analysis Tool (FEAT, Woolrich et al., 2001) from FSL. Five

¹<http://www.fmrib.ox.ac.uk/fsl/>

²<http://afni.nimh.nih.gov/afni>

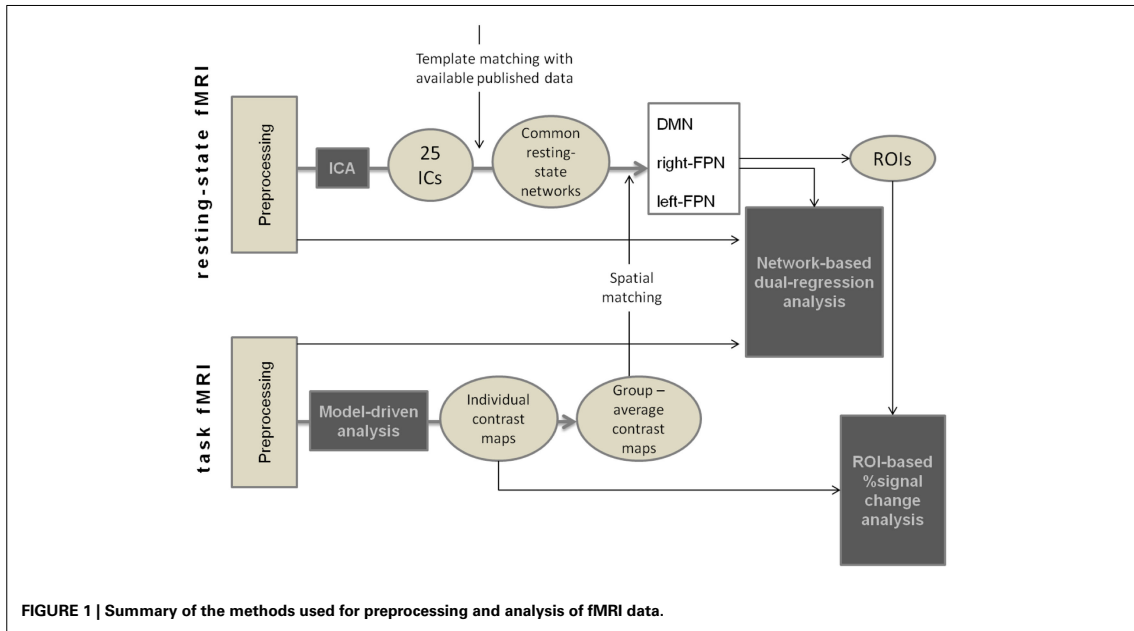


FIGURE 1 | Summary of the methods used for preprocessing and analysis of fMRI data.

regressors were used to model the different blocks (0, 1-, 2-, 3-back, and fixation), and five additional regressors, modeling their first derivatives were introduced as nuisance variables. Contrast images were computed from the preprocessed functional data as follows: for the different levels of cognitive load, each condition was evaluated against the 0-back (1-, 2-, and 3-back >0-back), and for the fixation blocks, the signal was compared against the average of the other blocks. Average maps were created including all the subjects in the study. To investigate the load-dependent differences in brain activity especially within the networks of interest, we used peak coordinates of the selected IC spatial maps in order to create a set of spherical ROIs of 6 mm radius and extracted the percentage signal change for each contrast.

Between-group differences on all the quantitative measures of percentage signal change were assessed using one-way ANOVA implemented in PASW. The significance level was set at $p < 0.05$ (two-tailed).

As with resting-fMRI data, a dual-regression approach was applied to the preprocessed task-fMRI data. The spatial maps of the DMN and the right- and left-frontoparietal networks were used to regress task-fMRI data and to obtain individual patterns of these networks during task-performance. These maps were introduced in a voxel-wise group comparison with 5000 permutations.

RESULTS

Low-HE and high-HE groups differed in task-performance, but there were no significant differences in the performance of the 3-back task between YA and high-HE subjects. Mean RT was higher in elders than in young subjects for all the conditions, but there were no differences between high-HE and low-HE. Across the

two groups of elders, age, gender, and MMSE were comparable, but high-HE had significantly higher education levels (Table 1; Figure 2).

The main findings, which are reported in the following sections, are summarized in Table 2.

RESTING-STATE fMRI ANALYSIS

Spatial maps derived from the whole-sample ICA decomposition of resting-state fMRI data corresponding to the DMN, the right-FPN, and the left-FPN are shown in Figure 3. The component identified as the DMN (Figure 3A) comprised areas in the frontal pole, middle frontal gyrus, and paracingulate gyrus (BA9, 10), the precuneus and posterior cingulate gyrus (BA7, 18, 23, 30, 31), and bilaterally in the superior occipital and posterior parietal cortices (BA19, 39). The right- and left-lateralized FPN (Figures 3B,C) involved areas in the middle and inferior frontal cortices (BA8, 9, 10, and 46), the paracingulate and anterior cingulate (BA6, BA8, BA32) and right and left parietal lobes, including the supramarginal and angular gyri. Although the lateralized pattern differed between right- and left-FPN, there was a broad overlap between these two networks.

With the dual-regression approach, we found differences in these three networks during the resting-state. As regards the DMN, low-HE exhibited decreased connectivity during the resting-state in frontal areas compared with YA and high-HE groups (Figure 4A). In the right-FPN (Figure 4B), the high-HE group had lower resting-state connectivity than both YA and low-HE groups. Finally, in the left-FPN (Figure 4C), low-HE, and high-HE had decreased resting-state connectivity in frontal areas. In the low-HE group, this decreased connectivity was observed in the left inferior and middle frontal gyri, left pars opercularis and left

frontal pole (BA10, 44, 45, and 46). High-HE subjects showed the same pattern of decreased connectivity, but it was bilateral and extended to the anterior part of the superior temporal gyri, also including the anterior cingulate (BA6) and the insular cortex.

ANALYSIS OF TASK-RELATED BRAIN ACTIVITY

We focused the analysis of task-fMRI data on a set of spherical ROIs that were selected from the networks identified in the resting-fMRI analysis (Figure 5). Three ROIs were created from the right-FPN: one in the right inferior frontal gyrus: *right-IFG ROI* (MNI coordinates: $x = 42, y = 54, z = -4$), one in the right middle frontal gyrus: *right-MFG ROI* (MNI coordinates: $x = 46, y = 34, z = 32$) and one in the right superior parietal gyrus: *right-PAR ROI* (MNI coordinates: $x = 42, y = -58, z = 52$). Three were created from the left-FPN: one in the left inferior frontal gyrus: *left-IFG ROI* (MNI coordinates: $x = -46, y = 50, z = 0$), one in the left middle frontal gyrus: *left-MFG ROI* (MNI coordinates: $x = -46, y = 34, z = 20$), and one in the left superior parietal gyrus: *left-PAR ROI* ($x = -46, y = -50, z = 31$). We also selected a region in the anterior cingulate cortex that was common for the right-FPN and the left-FPN: *ACC ROI* (MNI coordinates: $x = -2, y = 26, z = 44$). As regards the DMN, we defined four ROIs, one in the precuneus and posterior cingulate cortex: *PCC ROI* (MNI coordinates: $x = 2, y = -66, z = 40$), two in the left and right lateral occipital cortices: *LLO ROI* (MNI coordinates: $x = -38, y = -82, z = 32$), and *RLO ROI* (MNI coordinates: $x = 42, y = -74, z = 36$) and one in the middle frontal cortex: *MFC ROI* (MNI coordinates: $x = 2, y = 58, z = -8$).

As shown in Figure 5, ROIs inside the task-positive networks showed, in general, a positive percentage of signal change during cognitively demanding blocks and negative values during fixation blocks, and ROIs within the DMN had the opposite behavior.

BOLD responsivity scores for the high-HE group were significantly higher ($p < 0.05$) than those for the YA group in the *ACC*, *left-IFG*, and *right-IFG* ROIs, for the 1-back and the 2-back conditions, and only in the *right-IFG* for the 3-back condition. No differences were observed in these regions between the low-HE and the YA groups. Moreover, in the *right-IFG* ROI, responsivity was also greater in the high-HE group than in the low-HE during 2-back blocks. During fixation, the high-HE group also showed greater deactivation of the *right-IFG* compared to YA.

No significant group-effects were found in task-related BOLD response in *left-MFG*, *right-MFG*, *left-PAR*, and *right-PAR* ROIs, during any of the cognitive blocks. During fixation, both high-HE and low-HE groups showed increased deactivation of the *right-PAR* ROI compared to YA.

Within the *MFC* ROI, only the YA group showed a clear pattern of deactivation (negative percentage signal change) during cognitive blocks that was not observable in the other two groups. High-HE had significant differences in BOLD response of this region with respect to YA in 2-back condition. Overall, in the *MFC* ROI we observed positive percentage signal changes associated with cognitive demands in high-HE whereas these values were always negative for the YA group.

In the *PCC* ROI, high-HE also showed increased task-related activation during cognitive blocks than YA. Although the described effect could be seen at all the load levels of the task, this difference was statistically significant only in 1-back blocks. In Figure 4, we see that the *PCC* was moderately activated in the YA group when performing the levels of the task with the highest demand.

Finally, no group differences were found regarding BOLD response in left and right lateral occipital ROIs within the DMN.

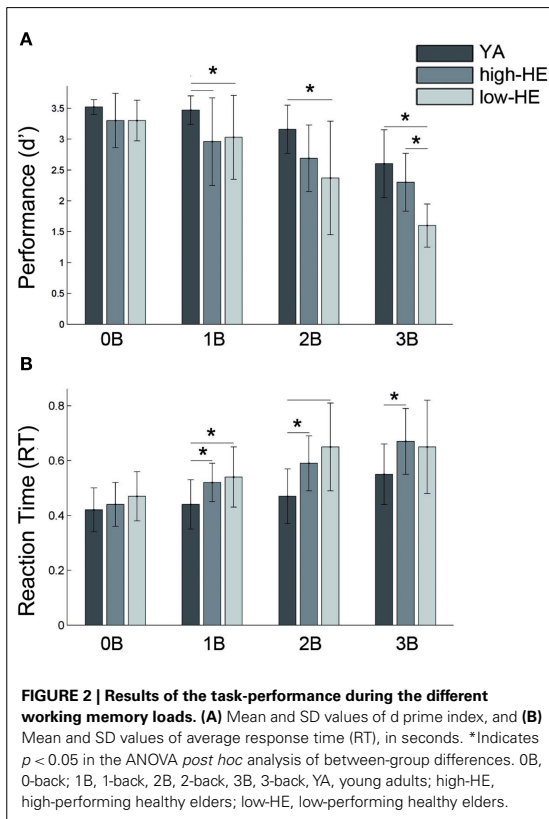
Table 1 | Group demographics and behavioral results on the *n*-back task.

	YA	High-HE	Low-HE	High-HE vs. low-HE comparison				
Age (years)	21.31 (2.41)	60.67 (10.35)	64.5 (8.23)	$t = 1.12, p = 0.27$				
Gender (men/women)	9/7	10/5	10/4					
MMSE		28.83 (1.64)	28.82 (1.72)	$t = 0.02, p = 0.98$				
Education		3.42 (0.67)	2.67 (0.68)	$t = 2.53, p = 0.02$				
ANOVA								
				F	Sig.	YA vs. high-HE	YA vs. low-HE	High-HE vs. low-HE
0-Back – d'	3.52 (0.12)	3.30 (0.44)	3.30 (0.33)	2.37	0.106	0.064	0.070	0.992
0-Back – RT (sec.)	0.42 (0.08)	0.44 (0.08)	0.47 (0.09)	1.13	0.334	0.658	0.150	0.310
1-Back – d'	3.47 (0.23)	2.96 (0.71)	3.03 (0.68)	3.53	0.038	0.018	0.045	0.722
1-Back – RT (sec.)	0.44 (0.09)	0.52 (0.07)	0.54 (0.11)	4.61	0.016	0.025	0.007	0.585
2-Back – d'	3.16 (0.39)	2.69 (0.54)	2.37 (0.92)	5.47	0.008	0.054	0.002	0.190
2-Back – RT (sec.)	0.47 (0.10)	0.59 (0.10)	0.65 (0.16)	8.15	0.001	0.009	<0.001	0.222
3-Back – d'	2.60 (0.55)	2.30 (0.47)	1.60 (0.35)	17.42	< 0.001	0.09	<0.001	<0.001
3-Back – RT (sec.)	0.55 (0.11)	0.67 (0.12)	0.65 (0.17)	3.25	0.05	0.022	0.057	0.704

MMSE, mini-mental state examination; d' , sensitivity index for task-performance; F, result of the analysis of variance (ANOVA) between the three groups; Sig., significance; RT, reaction time; YA, young adults; High-HE, high-performing healthy elders; Low-HE, low-performing healthy elders. Education levels were quantified in a scale from 1 to 4, with: 1, no education; 2, primary school; 3, secondary school, and 4, university studies. All scores are given as mean(SD). Significance levels are given in *p* values and considered significant when $p < 0.05$.

NETWORK ANALYSIS ON TASK-fMRI DATA

We used the dual-regression approach to explore differences in the selected networks during task-fMRI. High-HE showed decreased connectivity of the DMN with respect to YA (Figure 6A). However, in the right-FPN the same subjects had increased connectivity with respect to YA in several regions (Figure 6B), including the frontal pole, precentral gyrus, supplementary motor areas, anterior cingulate and paracingulate, insular cortex, and frontal orbital areas (BA6, 9, and 10). Finally, we found no differences in the connectivity of the left-FPN during task-fMRI.



DISCUSSION

Using ICA we identified intrinsic functional connectivity networks that are in operation during resting-state fMRI and during task fMRI, supporting the idea that brain connectivity has a network-based functional substrate that is not limited to the fact that the brain is functionally active (Smith et al., 2009). Although the ICA decomposition allowed the identification of other common resting-state brain networks, we only studied the DMN and the networks in the frontoparietal system due to their involvement in the working memory task that we used (similar to the approach considered in Leech et al., 2011). The three networks were identified in both resting- and task-fMRI, and functional reorganizations were found in both conditions, but in different directions. During the resting-state, elders with lower task-performance showed the largest differences with respect to YA within DMN connectivity, and those with higher task-performance showed reduced connectivity of the frontoparietal system. However, during task-fMRI, high-HE showed decreased connectivity of the DMN and increased connectivity of the FPN, but no differences were found between low-HE and young individuals. The analysis of task-related brain activity helped the interpretation of the results obtained by the ICA and the dual-regression approach, revealing task-related overactivations in frontal areas of the FPN, and the involvement of some DMN areas during task-performance in high-HE. Overall, our data show an age-by-performance modulation of brain networks that depends on external task demands.

COMPENSATORY ROLE OF DMN AREAS

Our data suggest evidence of reorganizations in the DMN connectivity in elders when compared to the group of YA. The pattern of functional reorganizations varied according to whether subjects are performing a cognitively demanding task. We found decreases in DMN connectivity that are in agreement with previously published work reporting age-related reduced DMN connectivity at rest (Damoiseaux et al., 2008; Littow et al., 2010; Wu et al., 2011; Tomasi and Volkow, 2012), and during task-fMRI (Sambataro et al., 2010, see Hafkemeijer et al., 2012 for a review of DMN and aging). Interestingly, we observed that disruptions in DMN connectivity, when studied at rest, were related with poor cognitive performance in the working memory domain. Studying the DMN connectivity in a group of aged subjects, Andrews-Hanna et al. (2007) also found a relationship

Table 2 | Summary of findings.

	Resting-state fMRI		Task-fMRI
	Dual-regression analysis	ROI analysis	Dual-regression analysis
DMN	Low-HE: decreased connectivity in frontal areas	High-HE: activation of MFC during task. Increased activation of PCC with task	High-HE: decreased connectivity
Right-FPN	High-HE: overall decreased connectivity	High-HE: increased activation in ACC, right-IFG High-HE and Low-HE: increased deactivation of PAR during fixation	High-HE: increased connectivity of frontal and prefrontal areas
Left-FPN	High-HE and Low-HE: decreased connectivity	High-HE: increased activation in ACC and left-IFG	n.d.

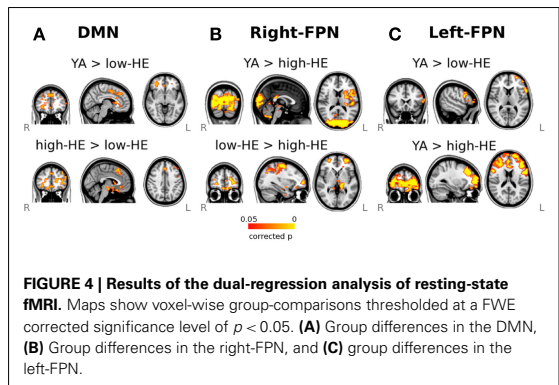
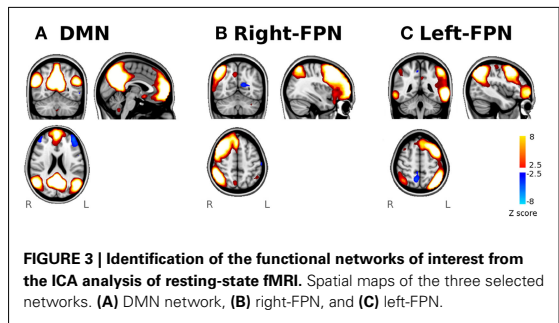
between anterior-posterior connectivity and cognitive performance in several cognitive domains. Moreover, during task-fMRI, only the high-HE group showed a reduction in DMN connectivity compared to YA. This latter result suggests dynamic modulations/interactions within networks during the performance of a task: old adults who performed the task successfully needed to recruit/engage additional brain resources which are typically not related to the WM task. Other studies using task-fMRI (Grady et al., 2006, 2010; Filippini et al., 2012) reported age-related increases in activity within DMN regions, such as the mPFC, which are not traditionally implicated in task-performance. They also found that these activity increases were accompanied with decreases in task-related functional connectivity in the same areas (Grady et al., 2010).

The results we obtained with ICA and dual-regression were supported and extended by those of brain responsivity in DMN regions. We found differences in brain activity (measured as percent signal change) in two core regions of the DMN, the PCC, and the MFC. High-HE subjects recruited these areas during task-performance, but YA and low-HE groups did not. The recruitment of the anterior/frontal node of the DMN was specific for the high-HE group (Figure 5), a finding that supports the utilization of non-task-related resources as a compensation mechanism in the aged brain (Cabeza et al., 1997; Mattay et al., 2006). The fact that this area is located in the frontal node may support the notion of the Posterior-anterior shift in aging (PASA model, see Davis et al., 2008). As regards the recruitment of the PCC node, this effect was also observable in the YA cohort at high levels of working memory load, in agreement with other studies showing involvement of the precuneus in cognitive control (Leech et al., 2011). High-performing elders recruited this area at the lowest memory load. This result can be interpreted in the light of the compensation-related utilization of neural circuits hypothesis (CRUNCH) which posits that older adults need to recruit additional neural resources at lower loads than younger adults (Reuter-Lorenz and Cappell, 2008; Schneider-Garces et al., 2009).

In summary, age-related DMN disruptions have been discussed either as a compensatory mechanism (Grady et al., 2010; Filippini et al., 2012) or as a functional marker of deficits in cognitive control that lead to poorer performance in elder subjects (Persson et al., 2007; Sambataro et al., 2010; Hedden et al., 2012). Our results clearly support the first idea. However it is also plausible that both mechanisms of compensation and dysfunction associated with cognition coexist in the aging brain. Finally, as our elder groups differed in educational attainment, the present results may also be interpreted within the context of neural compensation, as posited by Stern (2009).

CHANGES IN FRONTOPARIETAL NETWORKS

Focusing on the brain networks responsible for the working memory system, we found functional reorganizations in terms of altered connectivity and greater BOLD response in the high-performing elders. During the resting-state, high-HE showed decreased connectivity of the frontoparietal system. To date, few studies have reported age-related changes in resting-state networks other than the DMN. Filippini et al. (2012) found age-related increases in the executive network at rest but they did not consider the cognitive



performance of the subjects. However, Littow et al. (2010) found age-related decreases in some resting-state networks related to executive control.

During task-fMRI, the ROI-based analysis of responsivity showed increased activity in frontal regions, mainly in the inferior frontal gyrus bilaterally and in the anterior cingulate cortex. The same behavior was observed in the left middle frontal gyrus, but did not reach the level of significance established. Although the greater effects were observed in areas of the right-FPN, we interpreted this result as a reduction of asymmetry in task-related networks. The results of the dual-regression on task-fMRI also showed that the spatial pattern of the right-FPN becomes almost bilateral in high-HE subjects when compared to YA. Grady et al. (2010) also found that a greater expression of a network comprising right dorsolateral prefrontal areas predicted better performance in old adults. In some studies, the contralateral PFC activation was interpreted as a result of the difficulty of recruiting specialized neural mechanisms (the dedifferentiation hypothesis, see Persson et al., 2006; Eyler et al., 2011); however, our results add evidence for the compensation hypothesis, and more specifically for the hemispheric asymmetry reduction in older adults (HAROLD, Cabeza et al., 2002a) pattern, since this effect was specific to the elders who performed well on the task. In addition, studies with other techniques such as TMS have also supported the HAROLD model and its relationship with successful aging in episodic memory performance (Solé-Padullés et al., 2006; Manenti et al., 2011).

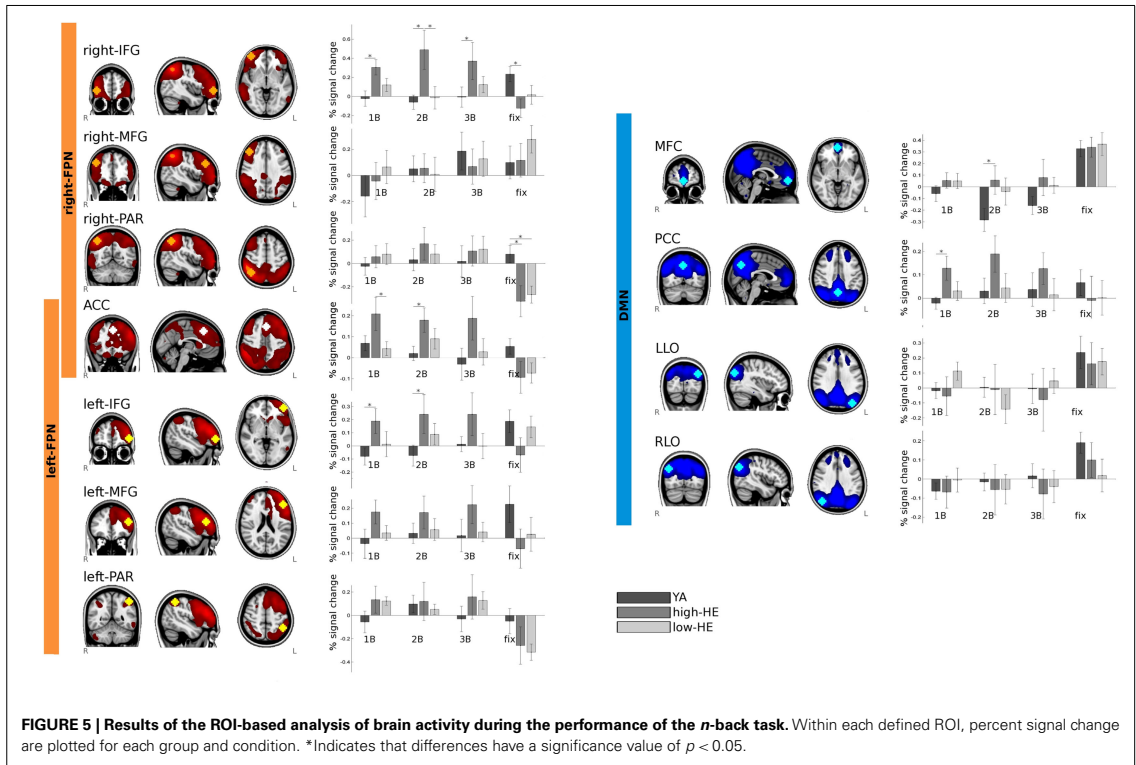


FIGURE 5 | Results of the ROI-based analysis of brain activity during the performance of the *n*-back task. Within each defined ROI, percent signal change are plotted for each group and condition. *Indicates that differences have a significance value of $p < 0.05$.

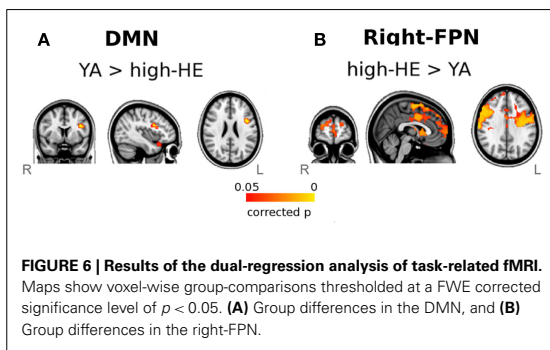


FIGURE 6 | Results of the dual-regression analysis of task-related fMRI. Maps show voxel-wise group-comparisons thresholded at a FWE corrected significance level of $p < 0.05$. (A) Group differences in the DMN, and (B) Group differences in the right-FPN.

Compensation mechanisms in terms of increased task-related BOLD activity have also been described in the pathologic brain in Alzheimer’s disease and mild cognitive impairment (Bokde et al., 2010). However, these patterns usually reflect activation of additional brain areas due to inefficient functioning of a network that might be compromised by disease; what is more, they have been studied in the context of keeping the same performance level as their age-matched controls, rather than in the context of increased performance as we found in healthy adults.

The interpretation of our results as the specialization of a task-related network also provides an insight into the study of

intervention methods that include cognitive training in healthy aging. Although the neural mechanisms of training effects are still unknown, it has been commonly reported that higher BOLD activity is associated with better performance or higher improvement in task-performance (for a review see Klingberg, 2010). Thus, the study of inter-individual differences in the relationship between brain activity and behavioral outcome may be a key point in the design of effective training programs for patients whose limited cognitive capacities are restricting their daily lives. Moreover, further studies should determine whether these brain-behavior associations are limited to the cognitive task that is being performed in the scanner or whether they can be extrapolated to other cognitive domains. The latter question can be partially answered by examining our results of the resting-state analysis, since we already found brain reorganizations in the resting-state networks in high-performing old subjects.

CONCLUSION

Using analysis of functional data during resting-state and during the performance of an *n*-back task, we provide evidence that the precepts of the principal neurocognitive theories of aging can be accommodated. First, functional compensation mechanisms were found: older people with successful working memory performance utilize different brain regions during cognitive activity than young people, and some of these regions are recruited from the DMN, a brain network that is typically deactivated during

working memory performance. The recruitment of the frontal DMN regions was specific to elders with high-performance levels; however, recruitment of the precuneus was also observed in young subjects at high levels of working memory load (supporting the CRUNCH hypothesis, Reuter-Lorenz and Cappell, 2008). Moreover, within task-related networks, high-performing elders showed both increased connectivity and increased BOLD response bilaterally in frontal regions, supporting the HAROLD model (Cabeza et al., 2002a) as well as the PASA model (Davis et al., 2008). Moreover, these dynamic network reorganizations were different at rest, when high-performing elders had less disruption of the DMN

but greater disruption within the frontoparietal system than low-performing elders. We therefore suggest that successful aging is characterized by a level of brain plasticity that may mediate the efficient recruitment of functional resources in task-relevant areas when the subject is exposed to a task with a high cognitive demand even though this recruitment is not observable at rest. It has been proposed that there is an optimal level of brain plasticity during the age span that varies across subjects and allows this adaptation to a changing environment. Thus, both hypo- and hyperplastic mechanisms may set the stage for dementia or age-related declines in cognitive abilities (Pascual-Leone et al., 2011).

REFERENCES

- Andrews-Hanna, J. R., Snyder, A. Z., Vincent, J. L., Lustig, C., Head, D., Raichle, M. E., and Buckner, R. L. (2007). Disruption of large-scale brain systems in advanced aging. *Neuron* 56, 924–935.
- Arenaza-Urquijo, E. M., Bosch, B., Sala-Llonch, R., Solé-Padullés, C., Junqué, C., Fernández-Espejo, D., Bargalló, N., Rami, L., Molinuevo, J. L., and Barrés-Faz, D. (2011). Specific anatomic associations between White matter integrity and cognitive reserve in normal and cognitively impaired elders. *Am. J. Geriatr. Psychiatry* 19, 33–42.
- Beckmann, C. F., De Luca, M., Devlin, J. T., and Smith, S. M. (2005). Investigations into resting-state connectivity using independent component analysis. *Philos. Trans. R. Soc. Lond. B Biol. Sci.* 360, 1001–1013.
- Berlinger, M., Bottini, G., Danelli, L., Ferri, F., Traficante, D., Sacheli, L., Colombo, N., Sberna, M., Sterzi, R., Scialfa, G., and Paulesu, E. (2010). With time on our side? Task-dependent compensatory processes in graceful aging. *Exp. Brain Res.* 205, 307–324.
- Biswal, B. B., Mennes, M., Zuo, X. N., Gohel, S., Kelly, C., Smith, S. M., Beckmann, C. F., Adelstein, J. S., Buckner, R. L., Colcombe, S., Dogonowski, A. M., Ernst, M., Fair, D., Hampson, M., Hoptman, M. J., Hyde, J. S., Kiviniemi, V. J., Kötter, R., Li, S. J., Lin, C. P., Lowe, M. J., Mackay, C., Madden, D. J., Madsen, K. H., Margulies, D. S., Mayberg, H. S., McMahon, K., Monk, C. S., Mostofsky, S. H., Nagel, B. J., Pekar, J. J., Peltier, S. J., Petersen, S. E., Riedl, V., Rombouts, S. A., Rypma, B., Schlaggar, B. L., Schmidt, S., Seidler, R. D., Siegle, G. J., Sorg, C., Teng, G. J., Vejjola, J., Villringer, A., Walter, M., Wang, L., Weng, X. C., Whitfield-Gabrieli, S., Williamson, P., Windischberger, C., Zang, Y. F., Zhang, H. Y., Castellanos, F. X., and Milham, M. P. (2010). Toward discovery science of human brain function. *Proc. Natl. Acad. Sci. U.S.A.* 107, 4734–4739.
- Bokde, A. L. W., Karmann, M., Born, C., Teipel, S. J., Omerovic, M., Ewers, M., Frodl, T., Meisenzahl, E., Reiser, M., Möller, H. J., and Hampel, H. (2010). Altered brain activation during a verbal working memory task in subjects with amnesic mild cognitive impairment. *J. Alzheimers Dis.* 21, 103–118.
- Braver, T. S., Cohen, J. D., Nystrom, L. E., Jonides, J., Smith, E. E., and Noll, D. C. (1997). A parametric study of prefrontal cortex involvement in human working memory. *Neuroimage* 5, 49–62.
- Cabeza, R., Anderson, N. D., Locantore, J. K., and McIntosh, R. (2002a). Aging gracefully: compensatory brain activity in high-performing older adults. *Neuroimage* 17, 1394–1402.
- Cabeza, R., Dolcos, F., Graham, R., and Nyberg, L. (2002b). Similarities and differences in the neural correlates of episodic memory retrieval and working memory. *Neuroimage* 16, 317–330.
- Cabeza, R., Grady, C. L., Nyberg, L., McIntosh, A. R., Tulving, E., Kapur, S., Jennings, J. M., Houle, S., and Craik, F. I. M. (1997). Age-related differences in neural activity during memory and retrieval: a positron emission tomography study. *J. Neurosci.* 17, 391–400.
- Damoiseaux, S., Beckmann, C. F., Arigita, E. J., Barkhof, F., Scheltens, P., Stam, C. J., Smith, S. M., and Rombouts, S. A. (2008). Reduced resting-state brain activity in the “default network” in normal aging. *Cereb. Cortex* 18, 1856–1864.
- Davis, S. W., Dennis, N. A., Daselaar, S. M., Fleck, M. S., and Cabeza, R. (2008). Que PASA? The posterior-anterior shift in aging. *Cereb. Cortex* 18, 1201–1209.
- Eyler, L. T., Sherzai, A., Kaup, A. R., and Jeste, D. V. (2011). A review of functional brain imaging correlates of successful cognitive aging. *Biol. Psychiatry* 70, 115–122.
- Filippini, N., MacIntosh, B. J., Hough, M. G., Goodwin, G. M., Frisoni, G. B., Smith, S. M., Matthews, P. M., Beckmann, C. F., and Mackay, C. E. (2009). Distinct patterns of brain activity in young carriers of the APOE-epsilon4 allele. *Proc. Natl. Acad. Sci. U.S.A.* 29, 1021–1026.
- Filippini, N., Nickerson, L. D., Beckmann, C. F., Ebmeier, K. P., Frisoni, G. B., Mathews, P. M., Smith, S. M., and Mackay, C. E. (2012). Age-related adaptations of brain function during a memory task are also present at rest. *Neuroimage* 59, 565–572.
- Grady, C. L. (2000). Functional brain imaging and age-related changes in cognition. *Biol. Psychol.* 54, 259–281.
- Grady, C. L., Protzner, A. B., Kovacevic, N., Strother, S. C., Afshin-Pour, B., Wojtowicz, M., Anderson, J. A. E., Churchill, N., and McIntosh, A. R. (2010). A multivariate analysis of age-related differences in default mode and task-positive networks across multiple cognitive domains. *Cereb. Cortex* 20, 1432–1447.
- Grady, C. L., Springer, M. V., Hongwanishkul, D., McIntosh, A. R., and Winocur, G. (2006). Age-related changes in brain activity across the adult lifespan. *J. Cogn. Neurosci.* 18, 227–241.
- Hafkemeijer, A., Van der Grond, J., and Rombouts, S. A. (2012). Imaging the default mode network in aging and dementia. *Biochim. Biophys. Acta.* 1822, 431–441.
- Hedden, T., Van Dijk, K. R., Shire, E. R., Sperling, R. A., Johnson, K. A., and Buckner, R. L. (2012). Failure to modulate attentional control in white matter pathology. *Cereb. Cortex* 22, 1038–1051.
- Jenkinson, M., and Smith, S. M. (2001). A global optimization method for robust affine registration of brain images. *Med. Image Anal.* 5, 143–156.
- Klingberg, T. (2010). Training and plasticity of working memory. *Trends Cogn. Sci. (Regul. Ed.)* 14, 317–324.
- Leech, R., Kamouriech, S., Beckmann, C. F., and Sharp, D. J. (2011). Fractionating the default mode network: distinct contributions of the ventral and dorsal posterior cingulate cortex to cognitive control. *J. Neurosci.* 31, 3217–3224.
- Littow, H., Elseoud, A. A., Haapea, M., Isohanni, M., Moilanen, I., Mankinen, K., Nikkinen, J., Rahko, J., Rantala, H., Remes, J., Starck, T., Tervonen, O., Veijola, J., Beckmann, C., and Kiviniemi, V. J. (2010). Age-related differences in functional nodes of the brain cortex – a high model order group ICA study. *Front. Syst. Neurosci.* 4:32. doi:10.3389/fnsys.2010.00032
- Manenti, R., Cotelli, M., and Miniussi, C. (2011). Successful physiological aging and episodic memory: a brain stimulation study. *Behav. Brain Res.* 216, 153–158.
- Mattay, V. S., Fera, F., Tessitore, A., Hariri, A. R., Berman, K. F., Das, S., Meyer-Lindenberg, A., Goldberg, T. E., Callicott, J. H., and Weinberger, D. R. (2006). Neurophysiological correlates of age-related changes in working memory capacity. *Neurosci. Lett.* 392, 32–37.
- Park, D. C., Lautenschlager, G., Hedden, T., Davidson, N. S., Smith, A. D., and Smith, P. K. (2002). Models of visuospatial and verbal memory across the adult life span. *Psychol. Aging* 17, 229–320.
- Park, D. C., and Reuter-Lorenz, P. (2009). The adaptive brain: aging and neurocognitive scaffolding. *Annu. Rev. Psychol.* 60, 173–196.
- Pascual-Leone, A., Freitas, C., Oberman, L., Horvath, J. C., Halko, M., Eldaief, M., Bashir, S., Vernet, M., Shafi, M., Westover, B., Vahabzadeh-Hagh, A. M., and Rottenberg, A. (2011). Characterizing brain cortical plasticity and network dynamics across the age-span in health and disease with TMS-EEG and TMS-fMRI. *Brain Topogr.* 24, 302–315.

- Persson, J., Lustig, C., Nelson, J. K., and Reuter-Lorenz, P. A. (2007). Age differences in deactivation: a link to cognitive control? *J. Cogn. Neurosci.* 19, 1021–1032.
- Persson, J., Nyberg, L., Lind, J., Larsson, A., Nilsson, L. G., Ingvar, M., and Buckner, R. L. (2006). Structure-function correlates of cognitive decline in aging. *Cereb. Cortex* 16, 907–915.
- Reuter-Lorenz, P. A., and Cappell, K. A. (2008). Neurocognitive aging and the compensation hypothesis. *Curr. Dir. Psychol. Sci.* 17, 177–182.
- Reuter-Lorenz, P. A., and Park, D. C. (2010). Human neuroscience and the aging mind: a new look at old problems. *J. Gerontol. B Psychol. Sci. Soc. Sci.* 65B, 405–415.
- Sala-Llonch, R., Peña-Gómez, C., Arenaza-Urquijo, E. M., Vidal-Piñeiro, D., Bargalló, N., Junqué, C., and Bartrés-Faz, D. (2011). Brain connectivity during resting state and subsequent working memory task predicts behavioural performance. *Cortex*. (in press).
- Sambataro, F., Murty, V. P., Callicott, J. H., Tan, H. Y., Das, S., Weinberger, D. R., and Mattay, V. S. (2010). Age-related alterations in default mode network: impact on working memory performance. *Neurobiol. Aging* 31, 839–852.
- Schneider-Garces, N. J., Gordon, B. A., Brumback-Peltz, C. R., Shin, E., Lee, Y., Sutton, B. P., Maclin, E. L., Gratton, G., and Fabiani, M. (2009). Span, CRUNCH, and beyond: working memory capacity and the aging brain. *J. Cogn. Neurosci.* 22, 655–669.
- Smith, S. M., Fox, P. T., Miller, K. L., Glahn, D. C., Fox, P. M., Mackay, C. E., Filippini, N., Watkins, K. E., Toro, R., Laird, A. R., and Beckmann, C. F. (2009). Correspondence of the brain's functional architecture during activation and rest. *Proc. Natl. Acad. Sci. U.S.A.* 106, 13040–13045.
- Solé-Padullés, C., Bartrés-Faz, D., Junqué, C., Clemente, I. C., Molinuevo, J. L., Bargalló, N., Sánchez-Aldeguer, J., Bosch, B., Falcón, C., and Valls-Solé, J. (2006). Repetitive transcranial magnetic stimulation effects on brain function and cognition among elders with memory dysfunction. A randomized sham-controlled study. *Cereb. Cortex* 16, 1487–1493.
- Spreng, R. N., Wojtowicz, M., and Grady, C. L. (2010). Reliable differences in brain activity between young and old adults: a quantitative meta-analysis across multiple domains. *Neurosci. Biobehav. Rev.* 34, 1178–1194.
- Stern, Y. (2009). Cognitive reserve. *Neuropsychologia* 47, 2015–2028.
- Tomasi, D., and Volkow, N. D. (2012). Aging and functional brain networks. *Mol. Psychiatry* 17, 549–558.
- Turner, G. R., and Spreng, R. N. (2012). Executive functions and neurocognitive aging: dissociable patterns of brain activity. *Neurobiol. Aging* 33, 826.e1–826.e13.
- van den Heuvel, M. P., and Hulshoff Pol, H. E. (2010). Exploring the brain network: a review on resting-state fMRI functional connectivity. *Eur. Neuropsychopharmacol.* 20, 519–534.
- Woolrich, M. W., Ripley, B. D., Brady, J. M., and Smith, S. M. (2001). Temporal autocorrelation in univariate linear modelling of fMRI data. *Neuroimage* 14, 1370–1386.
- Wu, J. T., Wu, H. Z., Yan, C. G., Chen, W. X., Zhang, H. Y., He, Y., and Yang, H. S. (2011). Aging-related changes in the default mode network and its anti-correlated networks: a resting-state fMRI study. *Neurosci. Lett.* 504, 62–67.

Conflict of Interest Statement: The authors declare that the research was conducted in the absence of any commercial or financial relationships that could be construed as a potential conflict of interest.

Received: 15 January 2012; accepted: 15 May 2012; published online: 07 June 2012.

Citation: Sala-Llonch R, Arenaza-Urquijo EM, Valls-Pedret C, Vidal-Piñeiro D, Bargalló N, Junqué C and Bartrés-Faz D (2012) Dynamic functional reorganizations and relationship with working memory performance in healthy aging. *Front. Hum. Neurosci.* 6:152. doi: 10.3389/fnhum.2012.00152
Copyright © 2012 Sala-Llonch, Arenaza-Urquijo, Valls-Pedret, Vidal-Piñeiro, Bargalló, Junqué and Bartrés-Faz. This is an open-access article distributed under the terms of the Creative Commons Attribution Non Commercial License, which permits non-commercial use, distribution, and reproduction in other forums, provided the original authors and source are credited.



Changes in whole-brain functional networks and memory performance in aging



Roser Sala-Llloch^{a,b}, Carme Junqué^{a,b}, Eider M. Arenaza-Urquijo^a, Dídac Vidal-Piñeiro^a, Cinta Valls-Pedret^c, Eva M. Palacios^a, Sara Domènech^d, Antoni Salvà^d, Nuria Bargalló^e, David Bartrés-Faz^{a,b,*}

^a Departament de Psiquiatria i Psicobiologia Clínica, Universitat de Barcelona, Barcelona, Catalonia, Spain

^b Institut d'Investigacions Biomèdiques Agustí Pi i Sunyer (IDIBAPS), Barcelona, Catalonia, Spain

^c Unitat de Lípids, Servei Endocrinologia i Nutrició, Hospital Clínic de Barcelona, Barcelona, Catalonia, Spain

^d Institut Català de l'Envel·liment, Universitat Autònoma de Barcelona, Barcelona, Catalonia, Spain

^e Radiology Service, Hospital Clínic de Barcelona, Barcelona, Catalonia, Spain

ARTICLE INFO

Article history:

Received 30 May 2013

Received in revised form 27 March 2014

Accepted 11 April 2014

Available online 19 April 2014

Keywords:

Graph theory

Resting-state fMRI

Aging

Frontal lobe

Memory

ABSTRACT

We used resting-functional magnetic resonance imaging data from 98 healthy older adults to analyze how local and global measures of functional brain connectivity are affected by age, and whether they are related to differences in memory performance. Whole-brain networks were created individually by parcellating the brain into 90 cerebral regions and obtaining pairwise connectivity. First, we studied age-associations in interregional connectivity and their relationship with the length of the connections. Aging was associated with less connectivity in the long-range connections of fronto-parietal and fronto-occipital systems and with higher connectivity of the short-range connections within frontal, parietal, and occipital lobes. We also used the graph theory to measure functional integration and segregation. The pattern of the overall age-related correlations presented positive correlations of average minimum path length ($r = 0.380$, $p = 0.008$) and of global clustering coefficients ($r = 0.454$, $p < 0.001$), leading to less integrated and more segregated global networks. Main correlations in clustering coefficients were located in the frontal and parietal lobes. Higher clustering coefficients of some areas were related to lower performance in verbal and visual memory functions. In conclusion, we found that older participants showed lower connectivity of long-range connections together with higher functional segregation of these same connections, which appeared to indicate a more local clustering of information processing. Higher local clustering in older participants was negatively related to memory performance.

© 2014 Elsevier Inc. All rights reserved.

1. Introduction

Cognitive aging is characterized by notable interindividual variability. Some persons show few changes with advancing age, whereas others present a typical “age-associated cognitive decline”. A subpopulation of older adults exhibit marked cognitive deficits, which may be indicative of incipient neurodegenerative processes (Yaffe et al., 2009). Despite this heterogeneity, most studies comparing old and young populations highlight a cognitive profile commonly characterized by decreased performance in tests of executive functions, processing speed, and memory (Hedden and

Gabrieli, 2004). Of these cognitive domains, age-related memory changes are particularly relevant because memory dysfunctions are the first cognitive symptoms in Alzheimer's disease (AD) (McKhann et al., 2011) and in its prodromal stage, mild cognitive impairment (MCI) (Albert et al., 2011). Furthermore, longitudinal population-based studies have shown that, even in normal older adults, low scores on memory tests are reliable predictors of future dementia (Rabin et al., 2012). Classically, memory impairment in the aged and in dementia has been attributed to hippocampal dysfunctions, but newer methodologies allowing analyses of the whole-brain dynamics from neuroimaging data indicate that memory dysfunctions may result from a disruption of complex large-scale brain networks (Seeley et al., 2009). The characterization of changes in brain connectivity related to normal aging and their relationship with differences in memory function may help to identify preclinical stages of degenerative illness.

* Corresponding author at: Departament de Psiquiatria i Psicobiologia Clínica, Facultat de Medicina, University of Barcelona, Casanova, 143, 08036 Barcelona, Catalonia, Spain. Tel.: +34934039295; fax: +34934035294.

E-mail address: dbartres@ub.edu (D. Bartrés-Faz).

Functional magnetic resonance imaging (fMRI) has been widely used to study the brain functional changes associated with aging and their relation to cognitive decline (Grady, 2012). When acquired during task performance, fMRI has revealed a complex pattern characterized by decreases, increases, or no differences in brain activity between old and young participants, depending on variables such as the type of the cognitive test and the level of difficulty (Grady, 2005). Nonetheless, there is a relative consensus that the increase in the activity of the prefrontal cortex is a common characteristic of cognitive studies of aging (Turner and Spreng, 2012). It has been hypothesized that this increased demand on frontal lobe processing reflects the progressive inefficiency of neural circuits that occurs during the aging process (Park and Reuter-Lorenz, 2009). Other common (but not contrasting) hypotheses support less lateralized functional processing (Cabeza et al., 2002), or anterior-posterior (i.e., more frontal than occipital activity) shifts in brain activity (Davis et al., 2008) associated with more optimal cognitive processing in older adults. Besides task activation studies, fMRI acquired during resting-state allows investigation of the functional connectivity of spontaneous brain fluctuations when individuals are not engaged in a specific task (Biswal et al., 1995). One advantage of resting-state data over task-based data is that they are much easier to record and they are not influenced by task difficulty. In resting-state fMRI, the findings regarding age-related changes include both increased and decreased connectivity between brain regions (Ferreira and Busatto, 2013). It has been suggested that these increases and decreases in brain activation and connectivity are promoted by a differential effect which depends on the nature of the connections, and that long-range connections are more affected than short-range connections (Alexander-Bloch et al., 2012; Tomasi and Volkow, 2012). Graph theory has emerged as an effective tool for investigating the effects of localized connectivity changes on whole-brain functioning (Bullmore and Bassett, 2011; Rubinov and Sporns, 2010; Stam and van Straaten, 2012). Graph theory measures allow quantification of topological changes in whole-brain connectivity (Filippi et al., 2013). Measures of segregation and integrity of brain networks provide insight into the changes occurring at the global level. These measures relate to the dynamic interactions of the networks elements and how they are embedded in the whole-brain connectivity structure, providing information that cannot be obtained from properties of the elements. In graph theory, whole brain networks are drawn as a set of nodes defined by anatomic or functional regions, and a set of edges that are calculated as the connectivity between each pair of nodes. Paths can then be described as sequences of edges linking pairs of nodes, and they are considered to be the basis for inter-neural communication and information flow (Sporns, 2011). Thus, for any network, the minimum path length measures its integrity, whereas the clustering coefficient measures the functional segregation. Small-world networks have the specific characteristic of showing a balance between integration and segregation, with some densely interconnected groups of nodes and some long-range connections that allow fast information transferability (Watts and Strogatz, 1998). Graph theory approaches have been used to explore the organization of the healthy brain as well as functional alterations in neurologic or psychiatric pathologies (Guye et al., 2010; Wang et al., 2010a). Some studies have reported disrupted small-world properties from resting-fMRI in AD (Sanz-Arigita et al., 2010; Supekar et al., 2008), in preclinical AD (Brier et al., 2014), and in normal old individuals carrying the APOE-4 allele, a genetic risk for AD (Brown et al., 2011).

Only a few studies have used graph theory methodologies to examine whole-brain resting-state networks in healthy aging. Comparing groups of young and old participants, Achard and Bullmore (2007) found healthy aging to be associated with a less efficient global network, whereas Meunier et al. (2009) reported the restructuring of the overall modular organization of the aged brain. At the regional level, the 2 studies found that the main age

effects were located in the frontal and temporal regions. Moreover, the effects of these local changes on whole-brain functioning and their relationship with differences in memory function as age progresses have not yet been investigated in large samples. In the present study we used resting-state fMRI and graph theory measures to: (1) depict and characterize subtle age-related brain functional changes in region-to-region connectivity; and (2) determine the effect of these functional connectivity changes on whole-brain complex network measures and memory functions.

We hypothesized that older participants would show alterations in the functional connectivity between several brain regions and that altered region-to-region connectivity would impact the measures of functional segregation and integrity. We also hypothesized that network measures would explain individual differences in memory performance in the context of healthy aging.

2. Methods

2.1. Participants, neuropsychological assessment, and scanning

One hundred and four healthy older adults (mean age: 64.87 years, standard deviation [SD]: 11.8; 56 females, 48 males) were included in the study. Six individuals were excluded a posteriori because of vascular subcortical lesions or abnormal cognitive performance, leaving a final sample of $n = 98$. Participants were recruited from the Institut Català de l'Envel·liment (Catalan Institute for the Study of Aging) and from medical centers in Barcelona. The study was approved by the University of Barcelona ethics committee and all participants gave written consent. They underwent neuropsychological screening to rule out MCI, and all those included in the analysis presented scores within the normal range on all tests (attention, memory, language, and visuo-perceptual and executive functions).

Auditory memory learning and visual memory scores were obtained by the Rey Auditory Verbal Learning Test (RAVLT) and the Rey-Osterrieth Complex Figure (ROCF), respectively. In the RAVLT, participants were asked to recall as many words as possible from an initial oral 15-word list, in any order. This procedure was repeated 5 times consecutively (acquisition trials 1–5); the score for each trial was the number of words correctly recalled, and the memory score was obtained as the sum of the words recalled in each trial. In this study, the mean (SD) of this test was 44.15 (10.7). The measure that we selected from the ROCF was the 30-minute delayed recall of the complex figure. The mean (SD) of our sample was 18.72 (5.06).

All participants were scanned with a 3T MRI scanner (Magnetom Trio Tim, Siemens Medical Systems, Germany), using a 32-channel coil. The scanning protocol included functional MRI acquisition during a 5-minute resting-state (150 T2*-weighted volumes, repetition time = 2000 ms, echo time = 16 ms, 40 slices per volume, slice thickness = 3 mm, distance factor = 25%, field of view = 240 mm, matrix size = 128 × 128) and a high-resolution 3D structural dataset (T1-weighted MP-RAGE, repetition time = 2300 ms, echo time = 2.98 ms, 240 slices, field of view = 256 mm; matrix size = 256 × 256; slice thickness = 1 mm). For the resting-state fMRI, participants were asked to close their eyes, not to fall asleep, and not to think about anything special.

2.2. Gray matter volume

Gray matter (GM) volume of each participant was measured using the high-resolution MPRAGE acquisition. We used FMRIB's Automated Segmentation Tool (FAST), (Zhang et al., 2001) from FSL to obtain whole-brain tissue masks corresponding to gray matter, white matter, and cerebrospinal fluid (CSF). Whole-brain GM volumes were calculated as the number of voxels in the GM mask

multiplied by the GM density (average voxel intensity within the GM mask).

2.3. Processing of resting-state fMRI data

Functional data sets from resting fMRI were preprocessed individually. Preprocessing was carried out using tools available in FSL (version 5, <http://www.fmrib.ox.ac.uk/fsl>) and AFNI (<http://afni.nimh.nih.gov/afni>) software. Briefly, it included the removal of the first 5 scans, motion correction, skull stripping, grand mean scaling, and temporal filtering (bandpass filtering of 0.01–0.1 Hz). Then, nuisance variables were regressed out from data; these included the 6 motion parameters, as well as CSF and white matter oscillations. To define the CSF and white matter regressors, we used the CSF and WM masks obtained from the segmentation of MPRAGE image with the FAST tool and we obtained mean fMRI signal oscillations within the 2 masks.

Finally, registration matrices from each individual functional space to MNI spaces were calculated using a 2-step procedure that included: (1) registration from functional space to each individual MPRAGE anatomic scan, and (2) registration from the anatomic scan to the standard MNI template. Both steps were performed using linear registration algorithms (Jenkinson and Smith, 2001). The number of degrees of freedom was set at 6 for the functional scans and 12 for the anatomic images.

2.4. Atlas-based definition of nodes

We used the automated anatomical labeling (AAL) atlas (Tzourio-Mazoyer et al., 2002) to parcellate the whole brain into a set of regions of interest (ROIs). The AAL atlas includes 45 ROIs in each hemisphere and is based on anatomic landmarks on the standard MNI surface (Table 1). AAL regions were registered to each individual functional space using previously obtained transformation matrices (Jenkinson and Smith, 2001) to extract ROI-associated time series and to construct networks of functional connectivity.

2.5. Network computation and parameters

Connectivity matrices were created using all the AAL-ROIs as network nodes and using Pearson correlation of pairs of time series to calculate the edges. These matrices were then converted into binary undirected networks by thresholding and binarizing the connections. We used a relative threshold for the correlations to keep the 15% strongest connections of all the possible connections for each individual (called the sparsity threshold). However, since it has been demonstrated that the choice of the threshold may have a strong effect on the estimation of the network parameters (Bullmore and Bassett, 2011), we performed additional analyses using a range of thresholds (see description of additional analysis in the following and Supplementary Material). The networks obtained were analyzed in terms of their node-to-node connectivity and their local and global network characteristics. We used the MATLAB toolbox provided by Rubinov and Sporns (2010) to obtain graph theory measures.

2.5.1. Inter-regional connectivity

The measures of connectivity between each pair of nodes were obtained from the individual correlation matrices. To classify the nature of the connections we calculated the length of each connection as the physical distance between their 2 nodes (Euclidean distance between the centroid's coordinates of the nodes in the standard MNI space).

2.5.2. Clustering coefficient (C_i)

The clustering coefficient (C_i) of a node i is the ratio of the number of existing edges to all the possible edges in the node's

Table 1
AAL regions

ROI	Lobe	Name
Central region		
1	Precentral gyrus	PRE
2	Postcentral gyrus	POST
3	Rolandic operculum	RO
Frontal lobe		
4	Superior frontal gyrus, dorsolateral	F1
5	Middle frontal gyrus	F2
6	Inferior frontal gyrus, opercular part	F3OP
7	Inferior frontal gyrus, triangular part	F3T
8	Superior frontal gyrus, medial	F1M
9	Supplementary motor area	SMA
10	Paracentral lobule	PCL
11	Superior frontal gyrus, orbital part	F1O
12	Superior frontal gyrus, medial orbital	F1MO
13	Middle frontal gyrus, orbital part	F2O
14	Inferior frontal gyrus, orbital part	F3O
15	Gyrus rectus	GR
16	Olfactory cortex	OC
Temporal lobe		
17	Superior temporal gyrus	T1
18	Heschl gyrus	HES
19	Middle temporal gyrus	T2
20	Inferior temporal gyrus	T3
Parietal lobe		
21	Superior parietal gyrus	P1
22	Inferior parietal	P2
23	Angular gyrus	AG
24	Supramarginal gyrus	SMG
25	Precuneus	PQ
Occipital lobe		
26	Superior occipital gyrus	O1
27	Middle occipital gyrus	O2
28	Inferior occipital gyrus	O3
29	Cuneus	Q
30	Calcarine fissure	V1
31	Lingual gyrus	LING
32	Fusiform gyrus	FUSI
Limbic lobe		
33	Temporal pole: superior temporal gyrus	T1P
34	Temporal pole: middle temporal gyrus	T2P
35	Anterior cingulate and paracingulate gyri	ACIN
36	Median cingulate and paracingulate gyri	MCIN
37	Posterior cingulate gyrus	PCIN
38	Hippocampus	HIP
39	Parahippocampal gyrus	PHIP
40	Insula	INS
Subcortical		
41	Amygdala	AMYG
42	Caudate nuclei	CAU
43	Lenticular nucleus, putamen	PUT
44	Lenticular nucleus, pallidum	PAL
45	Thalamus	THAL

Key: AAL, automated anatomical labeling; ROI, region of interest.

direct network. It corresponds to the fraction of triangles around a node and is equivalent to the fraction of a node's neighbors that are neighbors of each other:

$$C_i = \frac{2t_i}{k(k_i - 1)} \quad (1)$$

where t_i measures the number of triangles around the node i . Clustering coefficients can be averaged across all the regions to obtain the global clustering coefficient.

2.5.3. Characteristic path length (L)

The characteristic path length is the average of the shortest path lengths (i.e., number of edges) between all pairs of nodes in the network. The shortest path length between 2 nodes is the lowest number of edges that must be included in the network to connect the 2 nodes. Lower characteristic path lengths indicate higher

routing efficiency, because the information exchange involves fewer steps. This measure is representative of the brain's functional integration, that is, the ability to rapidly combine specialized information from different brain regions.

$$L_w = \frac{1}{n} \sum_{i \in N} L_i = \frac{1}{n} \sum_{i \in N} \frac{\sum_{j \in N, j \neq i} d_{ij}}{(n-1)} \quad (2)$$

2.5.4. Small-world coefficient

Finally, the small-world coefficient measures the balance between functional segregation (i.e., the presence of functionally specialized modules) and integration (i.e., the large number of intermodular links). At the practical level, small-world networks are characterized by high clustering coefficients and relatively low path lengths (compared with random networks).

$$S - W = \frac{C/C_{rand}}{L/L_{rand}} \quad (3)$$

Where C_{rand} and L_{rand} are, respectively, the clustering coefficient and the average minimum path length calculated for a random network with the same number of edges (same sparsity).

2.6. Statistical analyses

Age-related changes in the global and local measures described previously were tested using SPSS software (v21 SPSS Inc, Chicago, IL, USA). We first performed linear regressions with age for the region-to-region connectivity and considered them to be significant at $p < 0.001$. This value accounts for only 4 false positives within all the possible pairs of regions. All the parameters from graph theory (regional and global clustering coefficient, characteristic path length, global efficiency, and small-world coefficient) were also regressed against age using linear correlation. Further, all the global parameters were included in a multiple-regression analysis to predict age.

GM volumes were also correlated with age and with global graph theory metrics.

Finally, regional clustering coefficients were correlated with individual scores of memory tests. We explored simple correlations as well as age-corrected partial correlations to identify brain regions involved in verbal and visual memory. Further, to determine whether age has a causal role between clustering and memory or if, on the contrary, clustering coefficients mediate the relationship between age and memory, we performed a mediation analysis using the methods described in Preacher and Hayes 2008. In the mediation models, we included age, the average clustering within areas that correlated with memory, and the individual memory scores for verbal and visual memory, separately. Two different models were tested in each case: in the first model, clustering coefficients were considered as a mediator in the correlation between age and memory; and in the second model, age was considered as a mediator between clustering coefficients and memory. These 2 mediation models were tested using bootstrapping with 5000 iterations and a confidence interval (CI) level of 95% (Hayes, 2009).

2.7. Methodological issues

We evaluated certain methodological issues related to the definition of networks that may have influenced the results:

2.7.1. Effect of the connectivity threshold

Although the main results are extracted from the matrices using a relative threshold of 15%, we also created networks using a range

of thresholds from 5% to 40%, and repeated the age-correlation analyses with them.

2.7.2. Effect of negative correlations

To account for pairs of nodes showing negative functional connectivity, we converted negative connections into positive connections by using the squared value of connectivity r^2 and repeated all the analyses.

2.7.3. Effect of the brain parcellation strategy

For the main analysis, we used the AAL template to define the brain regions, a widely used approach in graph theory investigations. However, we wanted to evaluate the consistency of the results over different parcellations. We also evaluated graph theory measures on a parcellation derived from a high-order independent component analysis (ICA) using MELODIC tool from FSL (Beckmann et al., 2005; Ray et al., 2013).

2.7.4. Differences in ROI size

Because AAL ROIs can vary significantly in size, we sought to determine whether there was a correlation between the size of the ROIs and the age of the participants.

3. Results

3.1. Inter-regional functional connectivity

Connectivity matrices of 90x90 regions were used to study the effects of age on inter-regional connectivity. We also evaluated the relationship between these differences in connectivity and the physical length of the edges. The edges with significant correlations ($p < 0.001$) with age are represented in Fig. 1. Significant edges are presented in a node-to-node matrix (Fig. 1A), in a scatter plot as a function of edge length (Fig. 1B), and in a brain-graph representation (Fig. 1C). We found within-lobe age-related increases in frontal, parietal, and occipital regions, and decreases in the connections mainly from frontal to parietal and occipital regions. As can be observed in Fig. 1C and in Supplementary Tables 1.1 to 1.3, inter-hemispheric connections exhibiting increases with advancing age were in general of shorter range (i.e., frontal-frontal, or occipital-occipital, parietal-parietal), whereas those showing age-related decreases involved edges of greater length, mostly affecting fronto-parietal connectivity. Table 2 shows the number of nodes and connections that correlated significantly with age (see Supplementary Material for complete information).

3.2. Global network metrics

Age was positively correlated with average clustering coefficients ($r = 0.454$, $p < 0.001$) and minimum path length ($r = 0.380$, $p = 0.008$), and negatively correlated with global efficiency ($r = -0.395$, $p = 0.001$). However, the small-world coefficient was not correlated with age at the threshold of 15% ($r = 0.03$, $p = 0.76$). The plots of these correlations are represented in Fig. 2. The results of the multiple regression analysis show that the clustering coefficient was the best predictor of age among the 3 variables. Minimum path length and small-world coefficient showed collinearity with clustering coefficients (with tolerances of 0.42 and 0.98, respectively).

3.3. Regional clustering coefficients and age

Several regions showed positive correlations of the clustering coefficient with age ($p < 0.05$). The affected regions are mainly located in frontal and parietal lobes (Fig. 3).

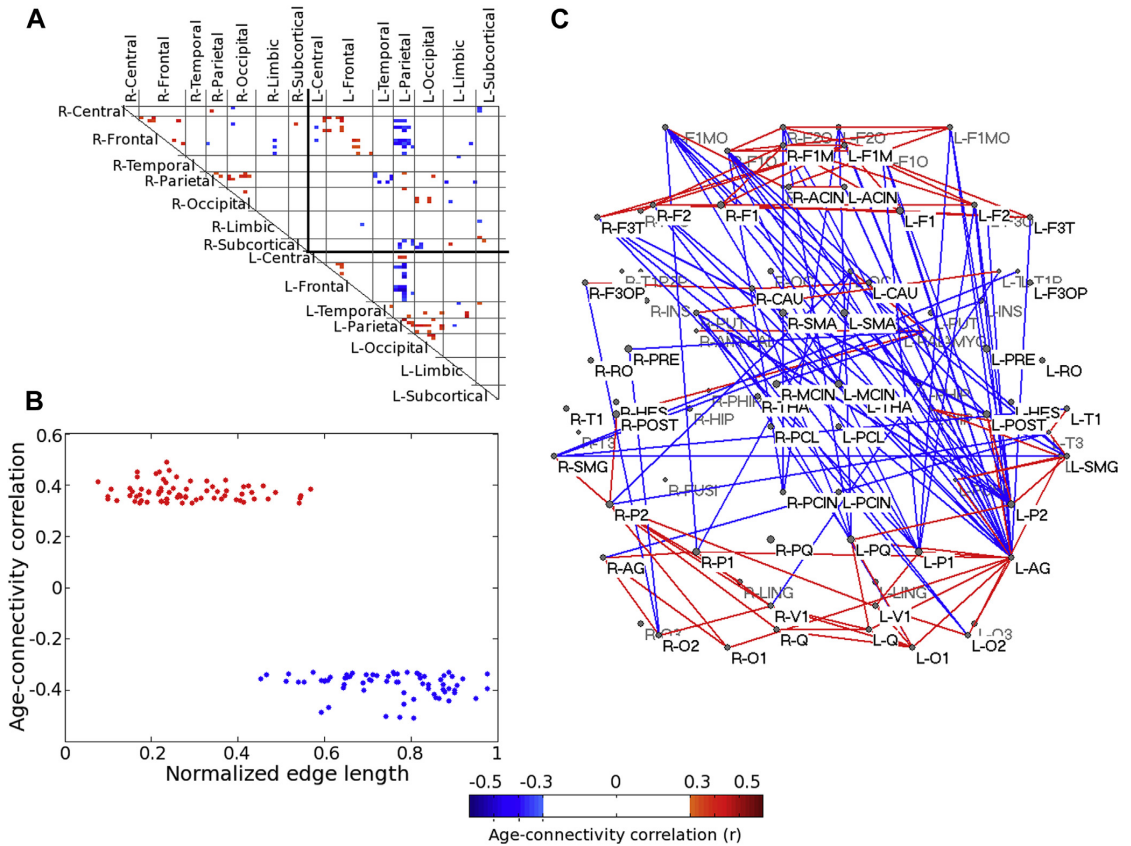


Fig. 1. Analysis of ROI-to-ROI connectivity. Node pairs showing positive (red) and negative (blue) correlations with age ($p < 0.001$). (A) Matrix representation of the edges, ordered by lobes and hemispheres. (B) Scatter plot showing the connections as a function of their normalized length (i.e., distance between their 2 nodes), and (C) graph representation of the connections. Spheres represent the nodes (see Table 1 for codification of the areas). Only connections with a significant age effect are shown. Abbreviation: ROI, region of interest. (For color reproduction, please refer to online article at neurobiologyofaging.org.)

3.4. Regional clustering coefficients and memory performance

We found a negative correlation between age of the participants and performance in verbal and visual memory tests ($r = -0.56, p < 0.001$ for verbal learning and $r = -0.255, p = 0.016$ for visual recall). Several nodes showed a negative correlation between their regional clustering coefficients and scores on verbal and visual memory tests. Correlations with verbal memory were found in: angular gyrus (right/left), posterior cingulate (left), cuneus (left), precuneus (right/left), hippocampus (right) occipital superior (left/right), postcentral (left), and superior temporal (left) (Fig. 4A). Correlations with visual memory were found in: angular gyrus (left/right), caudate (left), frontal middle orbital (left), frontal superior medial (right), hippocampus (right), superior parietal (left), and precuneus (left) (Fig. 4C). To assess whether these changes were mediated by

age, we performed partial correlations between the average clustering coefficients of all the brain regions. For verbal memory, we found positive correlations in areas of the frontal lobe and a negative correlation in the precuneus (Fig. 4B) For visual memory, we also observed a trend (though not significant) toward positive correlations in frontal areas. The negative correlations in precuneus and angular gyrus remained significant after removing the age effects, and the correlation in the right parietal lobe was not maintained (Fig. 4B and D).

In the mediation analysis we found different results for the 2 domains tested. For verbal memory, the correlation between regional clustering coefficients and verbal learning scores was strongly mediated by age, with a 95% CI of the effect of (-39.95 to -12.54), whereas the other model tested (clustering coefficients mediating the correlation between age and memory) had a much

Table 2
Summary of the number of nodes and edges affected by age

	Right hemisphere	Left hemisphere	Inter-hemispheric	Total
Nodes with connectivity increases	22	27		49
Nodes with connectivity decreases	23	24		47
Connections with increases (positive/negative)	16 (16/0)	27 (27/0)	25 (25/0)	68 (68/0)
Connections with decreases (positive/negative)	13 (12/1)	9 (5/4)	23 (11/12)	45 (28/17)

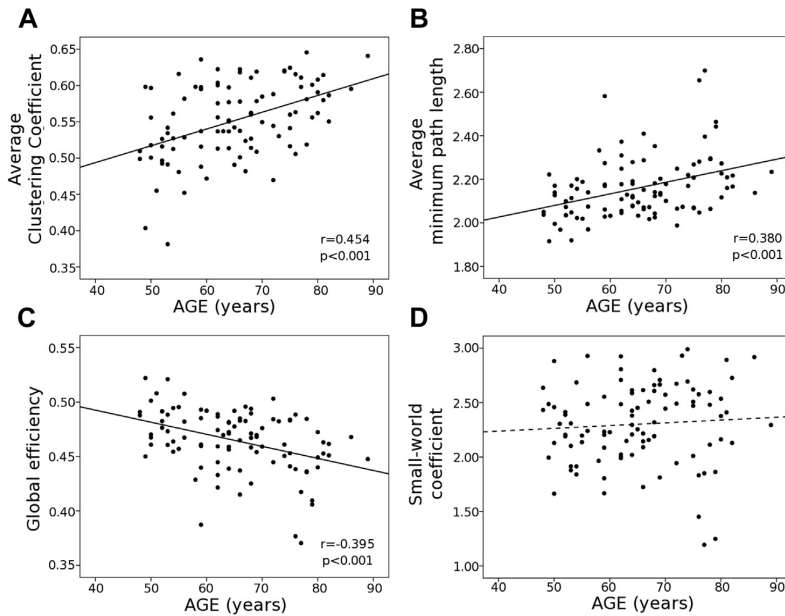


Fig. 2. Scatter-plots of the correlations between global network measures and age for healthy older adults. (A) Average network clustering coefficients, (B) average network minimum path length, (C) global efficiency, and (D) small-world coefficient.

lower effect. On the contrary, for the visual memory recall, we found that clustering coefficients mediated the correlation between age and memory scores, with a 95% CI of $(-0.14$ to $-0.03)$, and that the other model tested was no statistically significant.

3.5. GM volume

Whole-brain GM volumes correlated negatively with participants' age ($r = -0.44$, $p < 0.001$), but there was no relationship between GM volume and graph theory metrics ($r = -0.079$, $p = 0.44$ for average clustering coefficient, $r = -0.125$, $p = 0.219$ for average minimum path length, and $r = 0.020$, $p = 0.84$ for small-world coefficient).

3.6. Methodological issues

As regards the choice of the threshold, the correlations with age and global measures were observed at almost the whole range of

sparsity thresholds evaluated (i.e., from 5% to 40%). That is, the clustering coefficient (in thresholds from 10%) and average path length (in all thresholds) correlated positively with age and global efficiency correlated negatively with age ($p < 0.001$, in all cases). The small-world coefficient was positively correlated with age in dense network configurations (in thresholds greater than 20%). See [Supplementary Material](#) for a full description of these results.

The analysis of r^2 network matrices to account for the negative correlations also confirmed the correlations between age and the global clustering coefficient ($r = 0.37$, $p < 0.001$) and the average minimum path length ($r = 0.23$, $p = 0.026$). The small-world coefficient did not correlate with age ($r = -0.01$, $p = 0.93$).

Networks derived from the ICA data-driven approach showed a positive correlation between age and the average clustering coefficient ($r = 0.202$, $p = 0.04$) but no correlation with the average minimum path length or the small-world coefficient.

Finally, there were no significant correlations between participants age and the size of any AAL ROIs (data not shown).

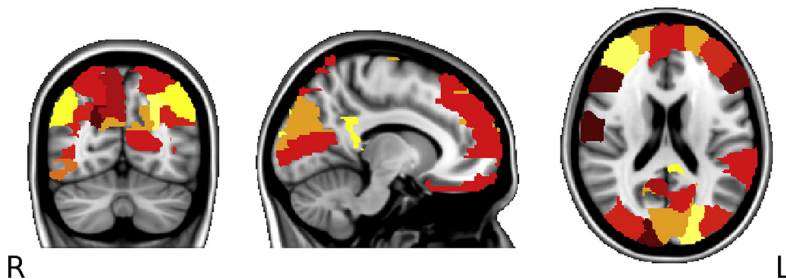


Fig. 3. Age effects on regional clustering coefficients. AAL regions that have a significant correlation with age are represented on the standard MNI brain. In all the ROIs, correlations are positive and $p < 0.05$. Abbreviations: AAL, automated anatomical labeling; ROIs, regions of interest.

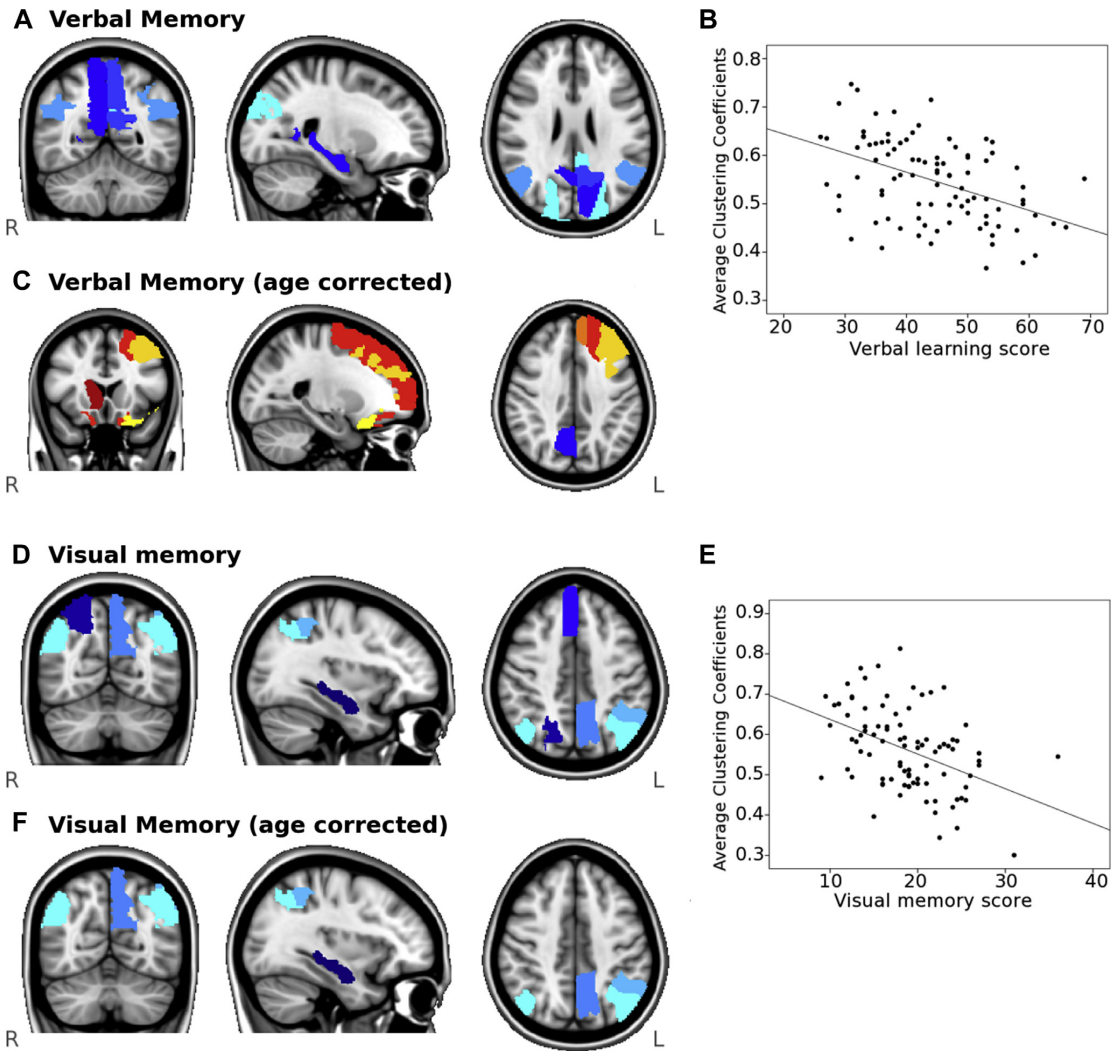


Fig. 4. Correlation between regional clustering coefficients and memory ($p < 0.05$). (A) Regions that correlate with verbal learning scores (data available for $n = 94$ participants), (B) scatter plot of the average clustering coefficient in all the regions highlighted in (A) and the scores on verbal memory. (C) Regions that correlate with verbal learning scores, after removing the effect of age. (D) regions that correlate with visual memory (data available for $n = 89$ participants), (E) scatter plot of the previous correlation, and (F) regions that correlate with visual memory after removing the effect of age.

4. Discussion

This study analyzed whole-brain functional networks and their reorganization during healthy aging measured with resting-state fMRI. In summary, by doing a cross-sectional analysis, we found that increased age is related to less functional connectivity of long-range brain connections and higher connectivity of short-range connections. Furthermore, age of the participants correlated with global clustering coefficients (higher segregation) and with averaged minimum path length (lower integration), being global clustering coefficients the best predictor of age among all the network variables evaluated. We also explored network properties at the local level and we found that correlations between age and clustering coefficients were located mainly in frontal and parietal regions. Finally, we studied how network measures were related to

the performance of verbal learning and visual recall tests, which showed significant age-related decline. Higher local clustering correlated negatively with interindividual differences in both tests. For verbal memory, age had a mediating role in the correlation between local clustering coefficients and learning scores, but for visual memory, clustering coefficients mediated the correlation between age and memory.

With the analysis of inter-regional connectivity, we found that older participants had higher functional connectivity in connections within the frontal, parietal, and temporal regions and weaker functional connectivity between the frontal and parietal lobes. Furthermore, regarding the physical length of the connections, we found that shorter connections showed positive correlations with age, and that longer connections showed negative age-connectivity correlations. Differential effects between long-range and short-range

connections with aging have previously been reported using fMRI (Alexander-Bloch et al., 2012; Tomasi and Volkow, 2012), and also with other modalities such as electroencephalography and magnetoencephalography (McIntosh et al., 2013). It has also been demonstrated that long-distance connections play an important role in large-scale communication and integration of information (Markov et al., 2013). In our study, around half of the connections showing age-related reduced connectivity were inter-hemispheric connections and a considerable number of these reduced connections were the ones affecting long-range interlobular (mainly frontoparietal) communication. In contrast, higher connectivity in older adults was found in connections with shorter lengths, mainly located within the occipital, parietal, and frontal lobes. These results lend support to the theory of a disruption in the communication between hemispheres and between the anterior and the posterior parts of the brain proposed by Cabeza 2002 and expressed in the hemispheric asymmetry reduction in old adults (HAROLD) and posterior-anterior shift in aging (PASA), (Davis et al., 2008) models. Both models are based on observations derived from task-fMRI studies reflecting interhemispheric and anterior-posterior reorganizations of brain activity. Our study was performed during resting-state and we cannot determine whether a less lateralized or a more frontalized task-related processing is taking place. However, intrinsic brain activity measured with resting-fMRI has been shown to provide reliable information on the network structure underlying brain functioning (Fox and Raichle, 2007; Smith et al., 2009; van den Heuvel et al., 2009).

As regards global measures derived from graph theory, the average minimum path length correlated positively with age, and global efficiency correlated negatively with age. A general interpretation of this result is that there is an overall age-related decrease in the ease of communication between brain areas. Achard and Bullmore (2007) also found increased path length and reduced global efficiency of the functional network in old compared with young participants, which they interpreted as evidence of the topological marginalization of some brain areas because of the aging process. In the present study we found a strong effect of larger global clustering coefficients, indicating a greater propensity for connections to occur in clusters surrounding each node rather than in the form of long-distance connections (Watts and Strogatz, 1998). As evidenced here, graph theory-based approaches provide integrative measures reflecting global efficiency (such as path length) and segregated processing (such as clustering coefficients) which may represent useful complementary information to the “more classical” resting-state measures. Interestingly, in a multiple-regression analysis one of these integrative measures, the increase in clustering, was the best predictor of age.

The small-world coefficient did not correlate with age at the threshold of 15%, indicating a balance between mean clustering coefficient and average minimum path length. However, when exploring higher thresholds (including a higher number of connections), we found the small-world coefficient to be positively correlated with age, also supporting the idea that the age-differences in clustering coefficients are greater than those in average minimum path length. From this result, we conclude that the stronger coupling in short-distance functional connectivity contribute to noneffective increases in local processing.

Studying the localization of changes in local clustering, we found a pattern of age-related correlations mainly in the frontal and parietal regions, including the precuneus, posterior cingulate, and angular gyrus. We hypothesize that this clustered connectivity is a consequence of a progressive disconnection of these regions from the whole network and a hyperconnection with their spatially closest regions (i.e., increased segregation), leading to more local information processing. Although our results for regional metrics

are reported at the uncorrected level of $p < 0.05$, the pattern of changes corresponds to areas typically affected by age (Turner and Spreng, 2012).

We also found that local clustering coefficients correlated negatively with the scores on verbal and visual memory tests. Importantly, both verbal and visual memory scores showed an age-related decline. Significant correlations with local clustering were found mainly in associative areas, as well as in areas of the default-mode network such as angular gyri, which are regions typically involved in memory functions (Buckner et al., 2008). Participants with greater age-related alterations in these areas also present worse performance. Furthermore, poorer scores in visual memory recall were associated with higher clustering in frontal and temporal regions, including the hippocampus and the precuneus. These regions have previously been identified as part of the memory network, which is altered in aging and may indicate the involvement of these areas in age-related differences in performance (Vannini et al., 2013; Wang et al., 2010b).

The pattern of correlations between clustering and memory differed significantly when the effect of age was removed. In particular, areas in the frontal lobes and the interconnected striatum (caudate) showed significant positive correlations for the verbal memory task (a trend for the visual memory scores in the same direction was also observed). These findings suggest that, taking older adults as a group (i.e., without taking age variability into account), higher local clustering in these areas is related to more effective memory processing. However, as local clustering increases with age, this association is attenuated and negative correlations appear in other brain areas. A possible interpretation of these observations is that the neural circuits exhibit a progressive inefficiency during the aging process (Park and Reuter-Lorenz, 2009), which is not equally distributed in the brain with the frontostriatal systems being the most affected (Hedden and Gabrieli, 2004). Furthermore, we found that age strongly mediated the relationship between clustering coefficients and verbal memory, indicating that clustering and scores in the verbal learning test are differentially influenced by age. Similar results have been consistently found in studies examining the role of aging in the relationship between brain structure and cognition (Salthouse, 2011). On the contrary, for visual memory, we found that local clustering coefficients mediated the relationship between age and memory. Previous findings indicate that this latter model is less commonly found (Salthouse, 2011). We suggest that the differences in the mediation models can be attributed to the different functions involved in each test. The RAVLT test, in addition to verbal learning that is age-dependent, involves vocabulary abilities, which are known to be preserved until the last decades of life (Park and Reuter-Lorenz, 2009). Then, the correlation between clustering coefficients and the performance of the verbal memory test seems to be strongly driven by the direct effect of age in learning and memory. However, visual memory, measured with the ROCF-recall test, involves a broader range of cognitive abilities, such as visuo-spatial, visuo-perceptive, and visuo-constructive functions, depending on the integrity of posterior parietal, medial temporal, and prefrontal regions, which have an earlier age-related disruption (Park and Reuter-Lorenz, 2009). Thus, it is expectable that performance of the visual recall test is highly influenced by more complex measures of integration and/or segregation of brain networks.

It is also possible that effective memory performance in aging is not simply maintained through an intensification of functional measures but is instead mediated by other variables, such as structural integrity (Daselaar et al., 2013). In our study, global clustering did not correlate with whole-brain gray matter volumes, but further studies are required to determine whether more localized measures of gray matter atrophy or even white matter

integrity can explain the associations between memory performance and the more segregated processing observed (increased clustering).

Another interesting observation is that, in contrast to frontal regions, posterior midline structures, particularly the precuneus, exhibited a negative correlation between their clustering coefficient and memory scores even when adjusting for the effect of age. These findings may reveal a more direct association between the functional integrity of this region and memory performance, which remains independent of age variability in old healthy adults. This result is also evidenced in the mediation analysis, where we found that local clustering of these regions was mediating the relationship between age and decline in visual memory. This posterior midline structure is a core area of the DMN, critically related to memory processing and one of the main functional hubs identified in previous connectivity studies (Cole et al., 2010). The impact of its dysfunction on cognitive processing is thought to be related to neurodegenerative processes, particularly AD (Buckner et al., 2009). In this regard a recent study conducted in participants in the prodromal stage of AD (MCI) reported that the metabolism of the precuneus (measured with FDG-PET) was associated with scores on the same verbal learning test (RAVLT) in the memory-impaired group, irrespective of age and education (Brugnolo et al., 2014).

In conclusion, we present evidence that graph theory, together with an understanding of the age-related differences in inter-regional functional connectivity, can provide additional biomarkers for identifying functional variability occurring in the aging brain. We used graph theory to quantify large-scale network cross-sectional differences in a group of healthy older adults in whom we first described alterations in the long-range connections and found that the measures of integrity were also altered. Moreover, we found that the mean clustering coefficient was predictive of participants' age. This result is important considering that it would be difficult to define an "overall connectivity" measure of all the possible pairs of nodes in the brain, due to the fact that some connections show positive associations and others show negative associations with age (and the global results might be canceled out). We believe that measures extracted from graph theory have a special interest in the study of brain dynamics in scenarios with functional differences that can include regions of both higher and lower connectivity. We have shown that these measures can provide a better understanding of the functional architecture underlying cognitive functions, characterized by an age-related decline, such as memory.

Our study has some limitations. First, we only explored correlations with the memory domain. Further studies are needed to determine whether similar correlations exist in other domains such as perception or attention. Furthermore, our study design is cross-sectional, and the main conclusions are made from correlational analyses, that show patterns of shared variance rather than representing a causal effect between variables. Longitudinal studies would be useful to determine the causal (direct) effects between the variables. Another limitation is that the parcellation used (AAL atlas) is based on anatomic landmarks and it may not fully represent the functional diversity of the cortical architecture (Sporns, 2011). Although we acknowledge this limitation, the use of this specific parcellation method in our study allowed us to calculate the length of all the pairwise connections as the physical distance between nodes and this would not have been possible without the anatomic support of the atlas. Interestingly, we obtained graph theory metrics using a different parcellation strategy, an ICA-based segmentation which is derived from the variance of our functional data, and found that clustering coefficients correlated with age in all these network configurations.

Disclosure statement

All authors report no biomedical financial interests or potential conflicts of interest related to this work. The authors declare no competing financial interests.

Acknowledgements

This work was supported by the Spanish Ministerio de Ciencia e Innovación (SAF20090748) and an Instituto de Mayores y Servicios Sociales (IMSERSO 2011/200) research grants to D.B-F and BES-2011-047053 to RS-LL. The authors report no conflict of interest.

Appendix A. Supplementary data

Supplementary data associated with this article can be found, in the online version, at <http://dx.doi.org/10.1016/j.neurobiolaging.2014.04.007>.

References

- Achard, S., Bullmore, E., 2007. Efficiency and cost of economic brain functional networks. *PLoS Comput. Biol.* 3, e17.
- Albert, M.S., DeKosky, S.T., Dickson, D., Dubois, B., Feldman, H.H., Fox, N.C., Gamst, A., Holtzman, D.M., Jagy, W.J., Petersen, R.C., Snyder, P.J., Carrillo, M.C., Thies, B., Phelps, C.H., 2011. The diagnosis of mild cognitive impairment due to Alzheimer's disease: recommendations from the National Institute on Aging-Alzheimer's Association workgroups on diagnostic guidelines for Alzheimer's disease. *Alzheimers Dement.* 7, 270–279.
- Alexander-Bloch, A.F., Vértes, P.E., Stidd, R., Lalonde, F., Clasen, L., Rapoport, J., Giedd, J., Bullmore, E.T., Gogtay, N., 2012. The anatomical distance of functional connections predicts brain network topology in health and schizophrenia. *Cereb. Cortex* 23, 127–138.
- Beckmann, C.F., DeLuca, M., Devlin, J.T., Smith, S.M., 2005. Investigations into resting-state connectivity using independent component analysis. *Philos. Trans. R. Soc. B Biol. Sci.* 360, 1001–1013.
- Biswal, B., Zerrin Yetkin, F., Haughton, V.M., Hyde, J.S., 1995. Functional connectivity in the motor cortex of resting human brain using echo-planar MRI. *Magn. Reson. Med.* 34, 537–541.
- Brier, M.R., Thomas, J.B., Fagan, A.M., Hassenstab, J., Holtzman, D.M., Benzinger, T.L., Morris, J.C., Ances, B.M., 2014. Functional connectivity and graph theory in preclinical Alzheimer's disease. *Neurobiol. Aging* 35, 757–768.
- Brown, J.A., Terashima, K.H., Burggren, A.C., Ercoli, L.M., Miller, K.J., Small, G.W., Bookheimer, S.Y., 2011. Brain network local interconnectivity loss in aging APOE-4 allele carriers. *Proc. Natl. Acad. Sci. USA* 108, 20760–20765.
- Brugnolo, A., Morbelli, S., Arnaldi, D., De Carli, F., Accardo, J., Bossert, I., Dessi, B., Famà, F., Ferrara, M., Girtler, N., Picco, A., Rodriguez, G., Sambucetti, G., Nobili, F., 2014. Metabolic correlates of Rey auditory verbal learning test in elderly subjects with memory complaints. *J. Alzheimer's Dis.* 39, 103–113.
- Buckner, R.L., Andrews-Hanna, J.R., Schacter, D.L., 2008. The brain's default network: anatomy, function, and relevance to disease. *Ann. N.Y. Acad. Sci.* 1124, 1–38.
- Buckner, R.L., Sepulcre, J., Talukdar, T., Krienen, F.M., Liu, H., Hedden, T., Andrews-Hanna, J.R., Sperling, R.A., Johnson, K.A., 2009. Cortical hubs revealed by intrinsic functional connectivity: mapping, assessment of stability, and relation to Alzheimer's disease. *J. Neurosci.* 29, 1860–1873.
- Bullmore, E.T., Bassett, D.S., 2011. Brain graphs: graphical models of the human brain connectome. *Annu. Rev. Clin. Psychol.* 7, 113–140.
- Cabeza, R., 2002. Hemispheric asymmetry reduction in older adults: the HAROLD model. *Psychol. Aging* 17, 85–100.
- Cabeza, R., Anderson, N.D., Locantore, J.K., McIntosh, A.R., 2002. Aging gracefully: compensatory brain activity in high-performing older adults. *Neuroimage* 17, 1394–1402.
- Cole, M.W., Pathak, S., Schneider, W., 2010. Identifying the brain's most globally connected regions. *Neuroimage* 49, 3132–3148.
- Daselaar, S.M., Iyengar, V., Davis, S.W., Eklund, K., Hayes, S.M., Cabeza, R.E., 2013. Less wiring, more firing: low-performing older adults compensate for impaired white matter with greater neural activity. *Cereb. Cortex. PubMed PMID:* 24152545.
- Davis, S.W., Dennis, N.A., Daselaar, S.M., Fleck, M.S., Cabeza, R., 2008. Que PASA? the posterior-anterior shift in aging. *Cereb. Cortex* 18, 1201–1209.
- Ferreira, L.K., Busatto, G.F., 2013. Resting-state functional connectivity in normal brain aging. *Neurosci. Biobehav. Rev.* 37, 384–400.
- Filippi, M., van den Heuvel, M.P., Fornito, A., He, Y., Hulshoff Pol, H.E., Agosta, F., Comi, G., Rocca, M.A., 2013. Assessment of system dysfunction in the brain through MRI-based connectomics. *Lancet Neurol.* 12, 1189–1199.
- Fox, M.D., Raichle, M.E., 2007. Spontaneous fluctuations in brain activity observed with functional magnetic resonance imaging. *Nat. Rev. Neurosci.* 8, 700–711.

Whole-brain network interactions and aging. Relationship with cognition.

Roser Sala-Llloch^{a,b}, Carme Junqué^{a,1}, Eider M. Arenaza-Urquijo^a, Dídac Vidal-Piñeiro^a, Cinta Valls-Pedret^c, Nuria Bargallo^d, David Bartrés-Faz^{a,b,*}

^a*Departament de Psiquiatria i Psicobiologia Clínica, Universitat de Barcelona. 08036, Barcelona, Catalonia, Spain.*

^b*Institut d'Investigacions Biomèdiques Agustí Pi i Sunyer (IDIBAPS). 08036, Barcelona, Catalonia, Spain.*

^c*Unitat de Lípids. Servei Endocrinologia i Nutrició. Hospital Clínic de Barcelona. 08036, Barcelona, Catalonia, Spain.*

^d*Radiology Service, Hospital Clínic de Barcelona, 08036, Barcelona, Catalonia, Spain.*

Abstract

Healthy aging is characterized by changes in brain functional connectivity that have an impact in the organization of resting state networks (RSN). Advanced neuroimaging methods allow characterizing these large scale networks at different levels, including their spatial patterns, their amplitudes and the interactions between networks. We used resting-state fMRI data from a cohort of 73 healthy elders to investigate whole-brain connectivity patterns and their relationship with the cognitive state of the subjects. We found that subjects' age correlated with increased connectivity of areas surrounding the main nodes of the RSNs. Further, RSN interactions revealed whole-brain reorganizations characterized by decreased connectivity between the different components of the same system, such as the anterior and the posterior parts of the default mode network and increased connectivity between different networks. This pattern of alterations in the between-RSN connectivity correlated with the results of memory and executive tests.

Keywords: independent component analysis, resting-state fMRI, aging, memory, executive functions.

1. Introduction

Functional MRI (fMRI) has emerged as a powerful tool to study brain functional changes during the aging process. Task-activation fMRI studies have given controversial results, reporting decreases, increases, or no changes in brain activity (Grady, 2012). The age-related increases in brain activity have been often interpreted as compensatory mechanisms (Cabeza et al., 2002).

When acquired during resting-state, rs-fMRI can be used to identify a set of Resting State Networks (RSNs) that provide a strong characterization of

the brain architecture and that have high correspondence with task-related networks (Smith et al., 2009). In healthy aging, connectivity disruptions within some of the RSNs have been consistently described. The most common and well-reported finding is the disruption of the Default Mode Network (DMN) (Damoiseaux et al., 2008). However, other systems have shown age-related alterations, including the salience network and networks supporting executive functions (Onoda et al., 2012). In some cases, these disruptions have been related to reductions in cognitive functioning (Andrews-Hanna et al., 2007). In addition, other studies, mainly those that focused on whole-brain connectivity approaches found evidences of age-related connectivity increase involving short-range connections (Tomasi and Volkow, 2012).

Our objective was to characterize the whole-brain functional connectivity structure during

*Corresponding Author

Departament de Psiquiatria i Psicobiologia Clínica, Facultat de Medicina

Casanova, 143. 08036 Barcelona, Catalonia (Spain)

Email address: dbartres@ub.edu

Tel.: +34934039295, Fax: +34934035294

healthy aging and its relationship with cognitive performance by looking first at the main RSNs taken individually, identified with Independent Component Analysis (ICA) of rs-fMRI data, and then looking at the interactions between these RSNs. We used a novel methodology to calculate interactions between RSNs that is based on the use of partial correlation to identify key connectivity features (Smith et al., 2011; Tian et al., 2011). We correlated our results with the scores obtained in visual and verbal memory tests, as well as scores of executive functions.

Despite age-related changes in brain function have been widely described in the literature and they have shown correlations with cognition, the novelty of the present work relies on the use of complex network modeling to study interactions between networks. We believe that this approach could help understanding the functional changes usually found in aging, that are often characterized by the coexistence of increases and decreases of functional activity/connectivity, and therefore difficult to interpret.

2. Materials and Methods

2.1. Subjects and scanning

Seventy-three healthy elders were included in the study (mean age: 65.88, SD: 9.95 years). Participants were recruited from the *Institut Català de l' Envelliment* (Catalan Institute for the Study of Aging) and from medical centers in Barcelona. The study was approved by the University of Barcelona ethics committee and all participants gave written consent. They underwent neuropsychological testing including memory, language, attention, visuo-perceptual and executive functions. All reported scores were within normal range on the domains tested and all subjects had scores on the mini-mental state examination (MMSE) $>=24$. The tests used to evaluate correlations with imaging findings were:

1. Visual memory skills, evaluated with the 30 minute recall ReysOsterrich Complex Figure (ROCF-30min).

2. Verbal memory capability, measured with the Rey Auditory Verbal Learning Tests recall at 30 minutes (RAVLT-30min).
3. Cognitive flexibility was evaluated with the Trail Making Test (TMT), using the TMTB-TMTA.
4. Cognitive control/inhibition was measured with the Stroop test (interference).
5. Working Memory function was evaluated with the Digit test from WAISIII.

Subjects were scanned in a Siemens 3T MRI scanner (Magnetom Trio Tim, Siemens Medical Systems, Germany), using a 32-channel coil, during a 5-minute resting-state fMRI session (repetition time=2s, echo time=16ms, 40 slices per volume, voxel size=1.7x1.7x3.75 mm, field of view=240 mm). During resting-state, participants were asked to close their eyes, not to fall asleep and not to think about anything in particular.

2.2. fMRI Analysis

Resting-state fMRI data were analyzed using Independent Component Analysis (ICA) followed by a dual regression approach and a network modeling analysis. All procedures were performed with tools from FSL (<http://fsl.fmrib.ox.ac.uk/fsl/fslwiki/FSL>). Data timeseries were first preprocessed using FSL's FEAT. Basically, preprocessing included: motion correction, brain extraction, spatial smoothing with a gaussian kernel of 5mm, temporal filtering using a high-pass filter of 150s and registration to the MNI standard space using linear (affine) transformations (Jenkinson et al., 2002). Thereafter, group-ICA was performed with MELODIC from FSL using data concatenated from all the subjects (Beckmann et al., 2005), in order to define a set of Independent Components (ICs), representing common spatiotemporal patterns of brain activity. The number of ICs was set to 20 from those we selected the 10 maps of the main RSNs. The dual regression approach was then used to obtain subject-specific maps of the ICs (Filippini et al., 2009). This approach included a spatial regression of the IC maps into each individual

preprocessed data to obtain subject specific IC timeseries followed by a temporal regression of the timeseries to the same individual data to obtain the subject-specific IC maps.

Network spatial maps

The subject-specific maps from dual-regression were introduced in a voxel-wise analysis, using both age and cognitive scores as regressors (in separate analyses) to depict areas where the spatial extent of the networks correlate with age or cognition. These results were evaluated with a permutation-based method that corrects for multiple comparisons (Nichols and Holmes, 2002). It should be noted that the fact that we did not performed partial (or covariated) analysis between maps and cognition is because we were interested in finding correlations that are associated with the age-related decline in cognition and this effect is removed when introducing age as covariate.

Network amplitudes

A measure of network amplitude was obtained by calculating the standard deviation of each subjects specific IC timeseries.

Network interactions

Whole-brain connectivity matrices were created using the FSLNets tool (Smith et al., 2011). First, subject specific timeseries were obtained by projecting each IC map to the preprocessed fMRI data, and then, matrices were created for each subject using partial correlation between all the ICs timeseries (Duff et al., n.d.). In these matrices, each edge represents the connectivity between pairs of ICs by regressing out the effect of all the other interactions.

We explored correlations between network amplitudes and interactions with age and with the results of the cognitive tests.

Measure	Mean (SD)
Age	65.88 (10.11)
RAVLT-30 min	18.75 (4.86)
Stroop (Interference)	25 (16.81)
TMT (B-A)	66.86 (46.85)
Digits	8.97 (2.03)

3. Results

3.1. Subjects demographics and behavioral results

3.2. Resting-state networks

We identified the common 10 RSNs from the group-ICA decomposition. Maps were selected using template matching with available data from the resting-state literature (Smith et al., 2009).

3.3. Correlations with network spatial maps

We found positive correlations in the spatial extent of the networks (corrected $p < 0.05$) with age in the spatial maps of all the networks except the posterior DMN (Figure 1). In that cases, increased connectivity was found in areas surrounding the main peaks of the group-IC maps. Furthermore, we found negative correlations with age in the spatial maps of the left frontoparietal network (L-FPN, IC7) and the right dorsolateral-prefrontal network (R-DLPFC, IC8). In these two networks, decreased connectivity was found in areas that are spatially distant from the main foci of the network, indicating a decrease of inter-hemispheric connectivity (in the case of the L-FPN) and anterior-posterior connectivity (in the case of the R-DLPFC). As regards the cognitive scores, only few components showed correlation with these measures and (Figure 1). Visual memory scores were negatively correlated with increased regional connectivity in the L-FPN. Verbal memory was negatively correlated with connectivity from the anterior DMN to the visual cortex (i.e., increased connectivity, worse memory performance), as well as with connectivity from the bilateral-FPN to similar visual areas. Finally, the performance of the TMT was positively correlated (i.e., increased connectivity associated

with reduced time) with the connectivity from the R-DLPFC to areas in the left temporal lobe. We did not find any correlations for the digits or the stroop tests.

3.4. Correlations with amplitude of the networks

Some of the networks showed correlation between their amplitudes and age. The posterior node of the DMN (IC5) and the salience network (IC8) correlated negatively with age ($r=-0.2345$, $p=0.045$). Furthermore, we observed a trend towards significance in the anterior DMN (IC1) being positively correlated with age ($r=0.21$, $p=0.07$). As regards the correlations with cognition, we found that the amplitudes of bilateral-FPN (IC2) and posterior DMN (IC5) were positively correlated with the results of the Stroop test ($r=0.22$, $p=0.05$ and $r=0.23$, $p=0.05$ respectively). However, these results did not survive correction for multiple comparisons. There were no any other correlations between network amplitudes and cognition.

3.5. Network interactions

Age was significantly correlated with the interactions between some pairs of RSNs. These results are shown in Figure 2. Interestingly, there were both positive and negative correlations between age and connectivity. Only three edges survived bonferroni correction for multiple comparisons: the positive correlations with the IC1-IC2 edge (DMN-FPN) and the IC2-IC3 edge (FPN-visual), and the negative correlation with the IC1-IC5 (anterior-DMN - posterior-DMN) edge.

We also found some correlations between network interactions and cognition (Figure 3). These correlations were also both positive and negative. When correcting for the number of tests evaluated ($N=5$), only the three negative correlations with the digits test, and one of the correlations with the TMT remained significant.

4. Discussion

By using network analysis and network modeling we described changes in the main RSNs dur-

ing the aging process and their relation to cognition. We explored the characteristics of the RSN from three perspectives, including their spatial extend, network amplitudes, and network interactions. Overall, we found that age was associated with increased connectivity in areas surrounding the main foci of the RSNs and decreased connectivity in widespread connections, suggesting increased local connectivity of short-range connections and disruption of antero-posterior and inter-hemispheric connectivities. Age was also correlated with decreased overall amplitudes of the default and salience networks and with a more complex pattern of changes as regards whole-brain network interactions, which consisted in decreased connectivity between pairs of networks within the same or similar system and increased connectivity between pairs of networks from different systems. The observed age-related connectivity changes also correlated with the performance of the subjects on memory and executive functioning domains.

As regards the results obtained with dual-regression spatial maps, we described age-related increases in connectivity that can be interpreted as a result of increased short-range FC, in accordance with what we already reported in a previous study using whole-brain connectivity (Sala-Llonch et al., 2014), and also in accordance with results reported by other groups (Tomasi and Volkow, 2012). This pattern of increased FC was found in all the RSNs studied except the cerebellum and the posterior-DMN, which differs from our previous findings, where we described increased clustered connectivity in the precuneus, as one of the main cores of the posterior-DMN (Sala-Llonch et al., 2014). These differences might be caused by the fact that in the present work we studied functional connectivity using a network-based parcellation of the brain, instead of a parcellation based on an anatomical atlas.

In addition, we found connectivity decreases in two networks within the fronto-parietal system. First, the left-lateralized FPN showed reductions in connectivity with regions in the right hemisphere, which is in accordance with other studies that

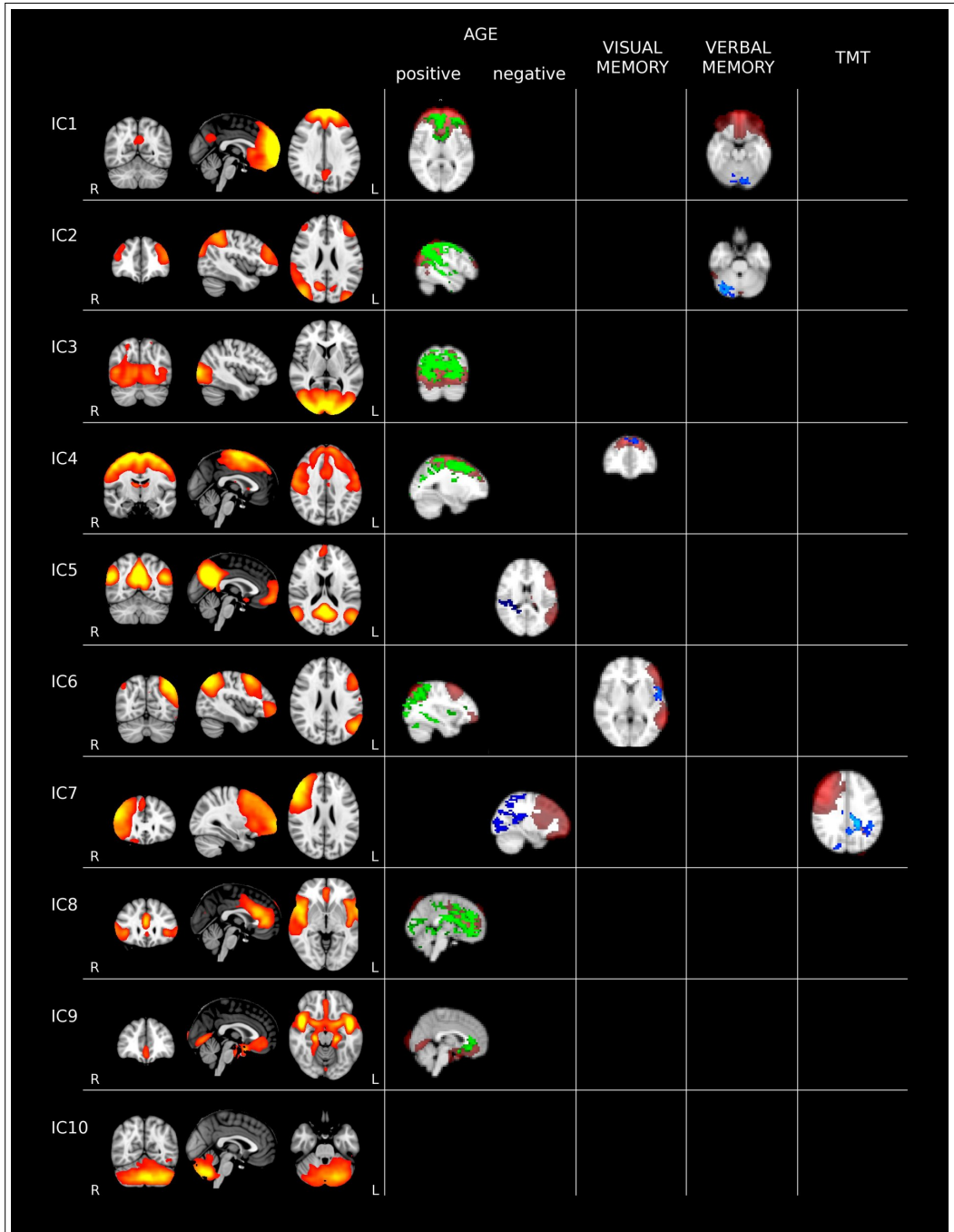


Figure 1: results of the dual-regression analysis on ICA maps. ICA group-maps (red-yellow). Positive (green) and negative (blue) correlations with age. And correlations with cognitive tests (blue).

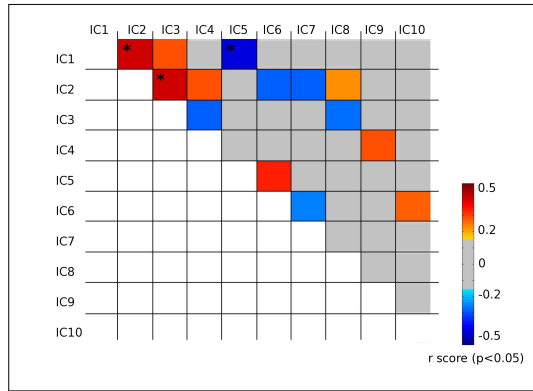


Figure 2: Network interactions and their correlation with age (uncorrected $p < 0.05$). * Indicates significant after Bonferroni correction ($p < 0.05$)

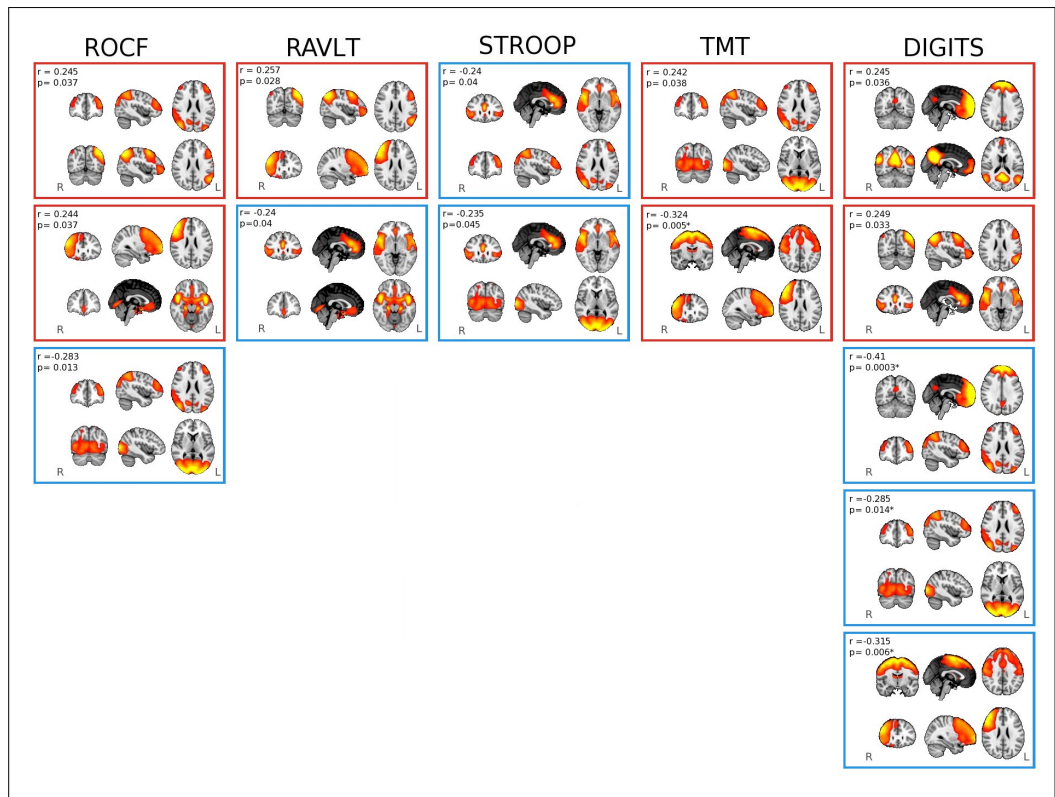


Figure 3: Correlations between network interactions and cognition. Each pair of networks is represented in a red/blue box (for positive/negative correlations with cognition). The values given as r and p represent the correlation of the connectivity between networks and the results of the tests. * indicates significant after correction for multiple comparisons.

demonstrated reduced connectivity in the FPN in aging (Campbell et al., 2012; Geerligs et al., 2014). Similarly, we found decreases in the connectivity from the R-DLPFC towards parietal/dorsal areas, which could be interpreted as a result of disrupted connectivity between anterior and posterior brain areas, also in accordance with the more classical models in aging describing posterior-to-anterior alterations in brain function (Davis et al., 2008).

ICA-spatial maps showed only few correlations with cognitive scores. Verbal and visual memory scores correlated negatively with the increased local connectivity of some RSNs, including the motor system, the FPN and the DMN, indicating that this increased local connectivity is not compensatory, and on the contrary, it is disadvantageous. On the other hand, the connectivity from the R-DLPFC network with distant contralateral regions correlated positively with the results of the Train Making Test, indicating that the described age-related connectivity disruption between these areas is directly affecting executive functioning, as other authors already suggested (Andrews-Hanna et al., 2007).

As regards the amplitude of the networks, both the DMN and the salience network showed decreases with age. Importantly, this is a measure of the overall amplitude of the oscillations, and thus, it provides additional information to the measure of the spatial extension of ICA maps. The fact that only these two networks showed age-related decreases coincides with other studies reporting alterations of these systems (Damoiseaux et al., 2008).

When considering the cognitive status of the subjects, only the results of the Stroop test correlated with network amplitudes, and these correlations were found in bilateral-FPN and posterior-DMN. The Stroop test was used as a measure of the cognitive control and inhibition. The FPN has been associated with action-inhibition and with general executive functioning using evidences obtained from both resting-state fMRI and task-fMRI analyses (Smith et al., 2009) and in the context of healthy aging. Furthermore, the correlation between Stroop performance and the posterior-DMN

could be interpreted considering that (1) this same network was also strongly affected by age, and (2) the DMN is known to modulate focused attention, cognitive control, and action inhibition (Buckner et al., 2008).

Finally, the most interesting findings from our study were those regarding network interactions: some of the edges correlated positively with age and they mainly represented connections between pairs of RSNs from different brain systems, for example, the connection between the anterior-DMN and the visual network or the FPN, or the connection of the FPN with the motor or the salience networks. Increased between-network connectivity with age has been described using ICA and seed-based connectivity (Onoda et al., 2012) and also using other approaches using graph-theory (Betzel et al., 2014; Song et al., 2014). On the contrary, other RSN pairs showed age-related decreases in connectivity, and these were mainly those representing the connectivity of sub-networks of the same well-known large-scale systems. These negative correlations included, for example, the anterior-posterior connectivity of the DMN (IC1 and IC5), the connection between different RSNs of the FPN (IC2, IC6 and IC7). Disconnection within large-scale networks, and especially within the DMN and the FPN, is also a common finding in aging.

We found that network interactions correlated with the cognitive status of the subjects. Importantly, the relationship between network interactions and the results of the cognitive tests were stronger and more meaningful than those reported when the networks were evaluated individually, indicating that successful cognitive performance in aging may be rather a result of a more complex pattern of network interactions than the status of individual brain networks.

Despite the fact that not all of the abovementioned results survived correction for multiple comparisons, we believe that they are of meaningful interest. For example, visual and verbal memory correlated positively with connections from the right dorsolateral prefrontal cortex, supporting the

role of this region as regards age-related decline in memory (Rossi et al., 2004). The results of the Stroop test correlated negatively with connections from the salience to visual and frontoparietal networks, meaning that old subjects having the salience network more disconnected/isolated from the others are able to perform better. This network includes areas of the anterior cingulate, paracingulate and the insula, and has been associated with cognitive-control and inhibition (Smith et al., 2009; Seeley et al., 2007). In addition, this network has a monitoring role in the sense that it gives signals to the other brain networks, to indicate whether they need to be active or unactive depending on cognitive demands (Jilka et al., 2014). Furthermore, the TMT scores correlated with the connectivity of executive networks (FPN and R-DLPFC) with visual and motor networks, which are two systems directly involved in the task. And finally, the correlations with the digits test also indicated that increased connectivity within similar networks, as the two parts of the DMN and salience-executive was beneficial for cognition, whereas increased connectivity between different networks was disadvantageous.

5. Acknowledgments

This work was supported by the Spanish Ministerio de Ciencia e Innovación (SAF20090748) and an Instituto de Mayores y Servicios Sociales (IM-SERSO 2011/200) research grants to D.B-F and BES-2011-047053 to RS-LL.

References

- Andrews-Hanna, J.R., Snyder, A.Z., Vincent, J.L., Lustig, C., Head, D., Raichle, M.E., Buckner, R.L., 2007. Disruption of large-scale brain systems in advanced aging. *Neuron* 56, 924–35.
- Beckmann, C.F., DeLuca, M., Devlin, J.T., Smith, S.M., 2005. Investigations into resting-state connectivity using independent component analysis. *Philosophical transactions of the Royal Society of London. Series B, Biological sciences* 360, 1001–13.
- Betzel, R.F., Byrge, L., He, Y., Goñi, J., Zuo, X.N., Sporns, O., 2014. Changes in structural and functional connectivity among resting-state networks across the human lifespan. *NeuroImage*.
- Buckner, R.L., Andrews-Hanna, J.R., Schacter, D.L., 2008. The brain's default network: anatomy, function, and relevance to disease. *Annals of the New York Academy of Sciences* 1124, 1–38.
- Cabeza, R., Anderson, N.D., Locantore, J.K., McIntosh, A.R., 2002. Aging gracefully: compensatory brain activity in high-performing older adults. *NeuroImage* 17, 1394–402.
- Campbell, K.L., Grady, C.L., Ng, C., Hasher, L., 2012. Age differences in the frontoparietal cognitive control network: implications for distractibility. *Neuropsychologia* 50, 2212–23.
- Damoiseaux, J.S., Beckmann, C.F., Arigita, E.J.S., Barkhof, F., Scheltens, P., Stam, C.J., Smith, S.M., Rombouts, S.A.R.B., 2008. Reduced resting-state brain activity in the "default network" in normal aging. *Cerebral cortex* 18, 1856–64.
- Davis, S.W., Dennis, N.a., Daselaar, S.M., Fleck, M.S., Cabeza, R., 2008. Que PASA? The posterior-anterior shift in aging. *Cerebral Cortex* 18, 1201–9.
- Filippini, N., MacIntosh, B.J., Hough, M.G., Goodwin, G.M., Frisoni, G.B., Smith, S.M., Matthews, P.M., Beckmann, C.F., Mackay, C.E., 2009. Distinct patterns of brain activity in young carriers of the APOE-epsilon4 allele. *Proceedings of the National Academy of Sciences of the United States of America* 106, 7209–14.
- Geerligs, L., Renken, R.J., Saliassi, E., Maurits, N.M., Lorist, M.M., 2014. A Brain-Wide Study of Age-Related Changes in Functional Connectivity. *Cerebral cortex* 2, 1–13.
- Grady, C., 2012. The cognitive neuroscience of ageing. *Nature reviews. Neuroscience* 13, 491–505.
- Jenkinson, M., Bannister, P., Brady, M., Smith, S., 2002. Improved optimization for the robust and accurate linear registration and motion correction of brain images. *NeuroImage* 17, 825–41.
- Jilka, S.R., Scott, G., Ham, T., Pickering, A., Bonnelle, V., Braga, R.M., Leech, R., Sharp, D.J., 2014. Damage to the Salience Network and Interactions with the Default Mode Network. *The Journal of neuroscience* 34, 10798–10807.
- Nichols, T.E., Holmes, A.P., 2002. Nonparametric permutation tests for functional neuroimaging: a primer with examples. *Human brain mapping* 15, 1–25.
- Onoda, K., Ishihara, M., Yamaguchi, S., 2012. Decreased functional connectivity by aging is associated with cognitive decline. *Journal of cognitive neuroscience* 24, 2186–98.
- Rossi, S., Miniussi, C., Pasqualetti, P., Babiloni, C., Rossini, P.M., Cappa, S.F., 2004. Age-related functional changes of prefrontal cortex in long-term memory: a repetitive transcranial magnetic stimulation study. *The Journal of neuroscience* 24, 7939–44.
- Sala-Llonch, R., Junqué, C., Arenaza-Urquijo, E.M., Vidal-Piñero, D., Valls-Pedret, C., Palacios, E.M., Domènech, S., Salvà, A., Bargalló, N., Bartrés-Faz, D., 2014. Changes in whole-brain functional networks and memory performance in aging. *Neurobiology of aging* 35, 2193–202.
- Seeley, W.W., Menon, V., Schatzberg, A.F., Keller, J., Glover,

- G.H., Kenna, H., Reiss, A.L., Greicius, M.D., 2007. Dissociable intrinsic connectivity networks for salience processing and executive control. *The Journal of neuroscience* 27, 2349–56.
- Smith, S.M., Fox, P.T., Miller, K.L., Glahn, D.C., Fox, P.M., Mackay, C.E., Filippini, N., Watkins, K.E., Toro, R., Laird, A.R., Beckmann, C.F., 2009. Correspondence of the brain's functional architecture during activation aSmith, S. M., Fox, P. T., Miller, K. L., Glahn, D. C., Fox, P. M., Mackay, C. E., ... Beckmann, C. F. (2009). Correspondence of the brain's functional architecture during activation an. *Proceedings of the National Academy of Sciences of the United States of America* 106, 13040–5.
- Smith, S.M., Miller, K.L., Salimi-Khorshidi, G., Webster, M., Beckmann, C.F., Nichols, T.E., Ramsey, J.D., Woolrich, M.W., 2011. Network modelling methods for FMRI. *NeuroImage* 54, 875–91.
- Song, J., Birn, R., Boly, M., Meier, T.B., Nair, V.A., Meyerand, M.E., Prabhakaran, V., 2014. Age-related Re-organizational Changes in Modularity and Functional Connectivity of Human Brain Networks. *Brain connectivity* .
- Tian, L., Wang, J., Yan, C., He, Y., 2011. Hemisphere- and gender-related differences in small-world brain networks: a resting-state functional MRI study. *NeuroImage* 54, 191–202.
- Tomasi, D., Volkow, N.D., 2012. Aging and functional brain networks. *Molecular psychiatry* 17, 471, 549–58.

Evolving Brain Functional Abnormalities in PSEN1 Mutation Carriers: A Resting and Visual Encoding fMRI Study

Roser Sala-Llloch^{a,b}, Juan Fortea^{c,d}, David Bartrés-Faz^{a,b}, Beatriz Bosch^{b,c}, Albert Lladó^{b,c}, Cleofé Peña-Gómez^a, Anna Antonell^{b,c}, Fernando Castellanos-Pinedo^e, Nuria Bargalló^{b,f}, José Luis Molinuevo^{b,c} and Raquel Sánchez-Valle^{b,c,*}

^aDepartment of Psychiatry and Clinical Psychobiology, Universitat de Barcelona, Barcelona, Spain

^bInstitut d'Investigació Biomèdica August Pi i Sunyer (IDIBAPS), Barcelona, Spain

^cAlzheimer's Disease and Other Cognitive Disorders Unit, Department of Neurology, Hospital Clínic, Barcelona, Spain

^dMemory Unit, Department of Neurology, Hospital de Sant Pau, Barcelona, Spain

^eDepartment of Neurology, Hospital Virgen del Puerto, Plasencia, Spain

^fDepartment of Radiology, Hospital Clínic, Barcelona, Spain

Accepted 11 March 2013

Abstract. PSEN1 mutations are the most frequent cause of familial Alzheimer's disease and show nearly full penetrance. Here we studied alterations in brain function in a cohort of 19 PSEN1 mutation carriers: 8 symptomatic (SMC) and 11 asymptomatic (AMC). Asymptomatic carriers were, on average, 12 years younger than the predicted age of disease onset. Thirteen healthy subjects were used as a control group (CTR). Subjects underwent a 10-min resting-state functional magnetic resonance imaging (fMRI) scan and also performed a visual encoding task. The analysis of resting-state fMRI data revealed alterations in the default mode network, with increased frontal connectivity and reduced posterior connectivity in AMC and decreased frontal and increased posterior connectivity in SMC. During task-related fMRI, SMC showed reduced activity in regions of the left occipital and left prefrontal cortices, while both AMC and SMC showed increased activity in a region within the precuneus/posterior cingulate, all as compared to CTR. Our findings suggest that fMRI can detect evolving changes in brain mechanisms in PSEN1 mutation carriers and support the use of this technique as a biomarker in Alzheimer's disease, even before the appearance of clinical symptoms.

Keywords: Alzheimer's disease, default mode network, functional magnetic resonance imaging, presenilin1, visual memory

INTRODUCTION

A minority of Alzheimer's disease (AD) cases is inherited with an autosomal dominant pattern of inheritance [1] and is caused by a genetic mutation. The mutations identified so far (<http://www.molgen.ua.ac.be>) affect the amyloid- β protein precursor,

presenilin-1 (PSEN1), and presenilin-2. These forms, also called familial AD, show almost 100% penetrance and have an early age of onset, which is also relatively predictable in a given family [2]. They are a good model that allows us to look into the early pathogenic mechanisms of the disease [3].

Altered synaptic function is characteristic of AD and there is consistent evidence that it is present very early in the disease process, possibly long before the development of clinical symptoms or even of significant neuropathology [4]. Functional magnetic

*Correspondence to: Raquel Sánchez-Valle, Alzheimer's Disease and Other Cognitive Disorders Unit, Department of Neurology, Hospital Clínic, Villarroel 170, 08036 Barcelona, Spain. Tel.: +34 932275785; Fax: +34 932275783; E-mail: rsanchez@clinic.ub.es.

resonance imaging (fMRI) is based on the strength of the blood-oxygen-level-dependent (BOLD) signal and it is thought to provide an *in vivo* correlate of neural activity. Thus, it is particularly useful for detecting alterations in brain function that may be present very early in the course of AD [5]. When examined at rest, fMRI can be used to study patterns of intrinsic brain connectivity or functional networks [6]. The most widely studied of these patterns is the default mode network (DMN), which involves the precuneus and posterior cingulate cortex, parietal and temporal cortices bilaterally, and the medial prefrontal cortex, as well as some regions within the hippocampal memory system [7, 8]. DMN regions are typically co-activated during rest and deactivated during the processing of external stimuli, and they are among the earliest and most consistently affected regions in AD [9]. DMN functioning and connectivity have been widely assessed along the AD continuum, with functional connectivity abnormalities being reported in both AD [10–14] and mild cognitive impairment [15–17]. Furthermore, studies with cognitively-preserved populations at risk for AD have shown abnormal connectivity in elderly subjects with evidence of amyloid deposition [18–21], as well as in apolipoprotein (APOE) $\epsilon 4$ carriers [22–26]. However, to the best of our knowledge, there are no published studies assessing the effect of the presence of a pathogenic PSEN1 mutation on the DMN.

Another fMRI strategy, known as task-related fMRI, can be used to study brain activity when the subject is engaged in a given task. By using memory encoding paradigms, fMRI studies have revealed task-associated brain activity during encoding in a specific set of brain regions that include the medial temporal lobe, prefrontal cortex, and ventral temporal cortex [5]. During the encoding of new information, patients with AD have shown decreased fMRI activation in the hippocampus and related structures within the medial temporal lobe when compared to their matched control subjects [27]. However, it has been suggested that there may be a phase of paradoxically increased activation earlier in the course of the disease, that is, in prodromal AD or in individuals at genetic risk for AD [28, 29].

Few encoding-based fMRI studies have been conducted in PSEN1 mutation carriers. Encoding-related activity was found to be altered in one asymptomatic mutation carrier (AMC) subject 30 years prior to the mean familial age of onset [30]. In other studies, PSEN1 AMC exhibited increased activation in the right hippocampus and parahippocampus during memory encoding [31]. Increased fMRI activity was also

reported in the fusiform and middle temporal gyri as mutation carriers approached the mean familial age of disease diagnosis [32].

Based on previous work, we hypothesized that PSEN1 mutation carriers would demonstrate functional connectivity changes in the DMN along disease progression. We further hypothesized that during visual memory fMRI, symptomatic mutation carriers (SMC) would present a pattern of reduced brain activity similar to what is reported in sporadic AD, and also that task-related activity within memory networks would already be altered in AMC compared to normal controls. In order to test these hypotheses, we examined brain functioning in a sample of PSEN1 mutation carriers, including both asymptomatic and symptomatic subjects. Specifically, this was done by analyzing the DMN during resting fMRI and memory networks during encoding-based task fMRI.

MATERIALS AND METHODS

Subjects

Nineteen mutation carriers from 8 families with 6 different PSEN1 mutations (M139T, K239N, L235R, L282R, L286P, I439S) and 13 normal controls, asymptomatic non-carriers, were recruited from the genetic counseling program for familial dementias (PICOGEN) at the Hospital Clinic, Barcelona, Spain [33]. Subjects were made aware of their at-risk status for genetic AD in a session of genetic counseling and were given the option of knowing their genetic status through the genetic counseling protocol. The study was approved by the Hospital Clinic ethics committee and all subjects gave written informed consent.

Genetic analysis

Genomic DNA was extracted from peripheral blood using the QIAamp DNA Blood Mini Kit (Qiagen). Mutation screening was performed as previously described [34].

Clinical and neuropsychological characterization

Subjects underwent clinical and cognitive assessments, and a comprehensive neuropsychological battery was also administered, as described previously [35]. Subjects were classified clinically as asymptomatic (AMC) if they had no memory complaints,

a normal cognitive assessment, and a score of 0 on the Clinical Dementia Rating (CDR) scale. They were classified as symptomatic (SMC) if their cognitive performance was more than 1.5 SD below the mean with respect to their age and educational level on any cognitive test and/or if their CDR score was >0 .

The current sample included 8 families with 6 different mutations and different median ages of onset (range 40–54 years). In order to compare subjects from different families, we therefore defined and calculated for each mutation carrier the *adjusted age* as the subject's age relative to the median familial age of onset.

MRI scanning

All subjects were scanned in a 3T machine (Siemens Trio Tim, Siemens, Germany) during both a 10-min resting fMRI protocol and while performing a visual encoding task. During scanning, a set of T2*-weighted volumes were acquired (voxel size = $1.7 \times 1.7 \times 3.0$ mm, TR = 2000 ms, TE = 29 ms, 36 slices per volume, slice thickness = 3 mm, distance factor = 25%, FOV = 240 mm, matrix size = 128×128). A high-resolution 3D structural dataset (T1-weighted MP-RAGE, voxel size = $1.0 \times 1.0 \times 1.0$ mm, TR = 2300 ms, TE = 2.98 ms, 240 slices, FOV = 256 mm, matrix size = 256×256 , slice thickness = 1 mm) was acquired in the same session.

During resting-state, subjects were asked to lie down in the machine, to not think of anything in particular, and to avoid falling asleep. For encoding-fMRI, we employed a visual encoding task used previously by our group [36]. Briefly, this consisted of a 15-block design paradigm with alternating “fixation”, “repeated”, and “encoding” conditions. During “fixation”, a white cross on a black screen was presented to the subject; during the “repeated” condition, a sample image was presented repeatedly to the subject; while during “encoding”, a set of new colored images was shown to the subject for each block. The whole session lasted 7 minutes and 30 seconds and subjects were tested for their memory performance outside the scanner in a two-alternative forced-choice task (maximum score of 50).

Preprocessing and analysis of resting-state fMRI data

Resting-fMRI data were preprocessed using tools implemented in both FSL (<http://www.fmrib.ox.ac.uk/fsl/>) and AFNI (<http://afni.nimh.nih.gov/afni>)

softwares. The procedures for data preprocessing included: removing the first 5 scans, motion correction [37], skull stripping/removal of non-brain voxels [38], spatial smoothing (using a Gaussian kernel of FWHM = 6.0 mm), grand mean scaling of the whole 4D series, temporal filtering (with a bandpass filter, 0.01–0.1 Hz), and removal of linear and quadratic trends. Nuisance variables were regressed out from preprocessed resting-fMRI data. These included the 6 motion parameters, global whole-brain BOLD signal, and white matter and cerebrospinal fluid oscillations. In order to perform group analyses, we registered each individual functional acquisition to Montreal Neurological Institute (MNI) standard space by using a two-step registration with FMRIB's Linear Image Registration Tool (FLIRT; [39]), involving the registration of each individual fMRI set to its anatomical high-resolution scan and the registration from anatomical space to the standard MNI template.

Resting-fMRI data were further analyzed using seed-based connectivity. A region of interest (ROI) placed in the precuneus/posterior cingulate (spherical ROI of 6 mm radius centered at MNI coordinates $x = 2$, $y = -54$, $z = 24$; [40]) was used to assess whole-brain resting-state functional connectivity. The procedure for seed-based connectivity was performed on preprocessed resting data as follows: 1) average time-series were extracted for each subject within the ROI; 2) these time-series were then used to calculate the temporal correlation against all the voxels in the brain; and 3) individual correlation maps were transformed into Z-scores using Fisher's r to Z transformation, and then moved to MNI standard space. All Z maps were concatenated and introduced into a voxel-wise group statistical analysis using General Linear Modeling. Group analysis included average connectivity maps for each group (one-sample t -test) and group differences (two-sample t -test). Results were corrected for multiple comparisons using a permutation-based method with 5000 iterations [41].

Preprocessing and analysis of encoding-fMRI data

Task-fMRI data were analyzed using a model-driven approach, as implemented in the FMRI Analysis Tool (FEAT) from FSL. Data preprocessing included motion correction [37], non-brain removal [38], spatial smoothing with a Gaussian kernel of FWHM 6 mm, grand-mean intensity normalization, and high-pass temporal filtering ($\sigma = 50.0$ s). Time-series statistical analysis was carried out for each piece of

individual functional data using FMRIB's Improved Linear Model (FILM) with local autocorrelation correction [42]. Three regressors were used to model the different task blocks (encoding, repeated, and fixation), and three additional regressors, modeling their first derivatives, were introduced as nuisance variables. Individual activation maps were computed from the preprocessed functional data using the "encoding" > "repeated" images contrast.

In order to assess group-activation maps and group differences, we performed higher-level analyses using the General Linear Model and FLAME (FMRIB's Local Analysis of Mixed Effects) stage 1 and stage 2 [43–45]. This included averaged maps for the three groups (CTR, AMC, and SMC) and group comparisons (CTR versus AMC and CTR versus SMC). Performance scores, measured as the number of correctly recognized images, were introduced as covariates for the group comparisons.

Two additional correlation analyses were performed using encoding-fMRI data. First, and in order to assess brain activity associated with correct coding of new images, we created a General Linear Model design in which whole-brain activity maps were regressed against individual performance scores for the three groups separately. Then, and based on the results reported by Braskie et al. [32], who found increased functional activity as their subjects approached the age of onset, we evaluated the relationship between brain activation maps and adjusted age in the AMC subgroup.

Statistical analysis

Group analyses were conducted using PASW (Predictive Analytics SoftWare, IBM Corp.) v.18. Comparisons between groups were performed using the two-tailed Student's *t* test or ANOVA for continuous variables, and a chi square test for categorical variables.

RESULTS

Demographics, cognitive testing and genetic status

Demographic and clinical data of the participants are summarized in Table 1. Eight mutation carriers were SMC, with a mean age of 48.91 years (SD = 7.53). The remaining 11 mutation carriers were AMC, with a mean age of 39.09 years (SD = 10.74) and a mean adjusted age of -11.92 years (SD = 8.96). There were 13 controls (36.27 years \pm 7.45). Age and Mini-Mental State Examination (MMSE) scores did not differ between controls and AMC (Table 1). As expected, SMC were older than both controls and AMC, and they presented significantly different MMSE scores.

Resting-state connectivity

Average default mode network maps

The seed-based connectivity analysis of resting-state fMRI data from the precuneus/posterior cingulate ROI (ROI placement is shown in Fig. 1A) identified a pattern of connectivity that corresponded to the DMN in each group separately (Fig. 1B–D). The DMN maps included areas in bilateral parietal regions and both angular gyri (for the three groups), as well as areas in the medial prefrontal cortex (only in the control and AMC groups).

Group differences

Figures 1E–H show the results of voxel-wise group comparisons of the precuneus/posterior cingulate connectivity maps. When compared to the control group, AMC showed reduced resting-state connectivity in areas of the hippocampus, parahippocampal, lingual and fusiform gyri, the middle temporal cortex and parts of the precuneus/posterior cingulate, and the lateral occipital cortex. Conversely, AMC presented increased connectivity in the paracingulate and anterior cingulate, parts of the superior, middle and inferior frontal cortices, and in the frontal pole.

Table 1
Demographic and clinical data in the different groups. **p* < 0.05 compared to controls

	Healthy controls (non-carriers) (<i>n</i> = 13)	Asymptomatic mutation carriers (<i>n</i> = 11)	Symptomatic mutation carriers (<i>n</i> = 8)
Age (years)	36.27 (7.45)	39.09 (10.74)	48.91 (7.53)*
Relative age (years)	NA	-11.92 (8.96)	3.35 (2.94)
Education (years)	14 (3.91)	12.45 (2.54)	10.88 (3.09)
Gender (%Female)	53.84 %	63.63 %	62.50%
MMSE	29.54 (0.50)	29.09 (1.04)	19.63 (6.21)*
CDR-total	0	0	1.25 (0.65)*

MMSE, Mini-Mental State Examination; CDR, Clinical Dementia Rating.

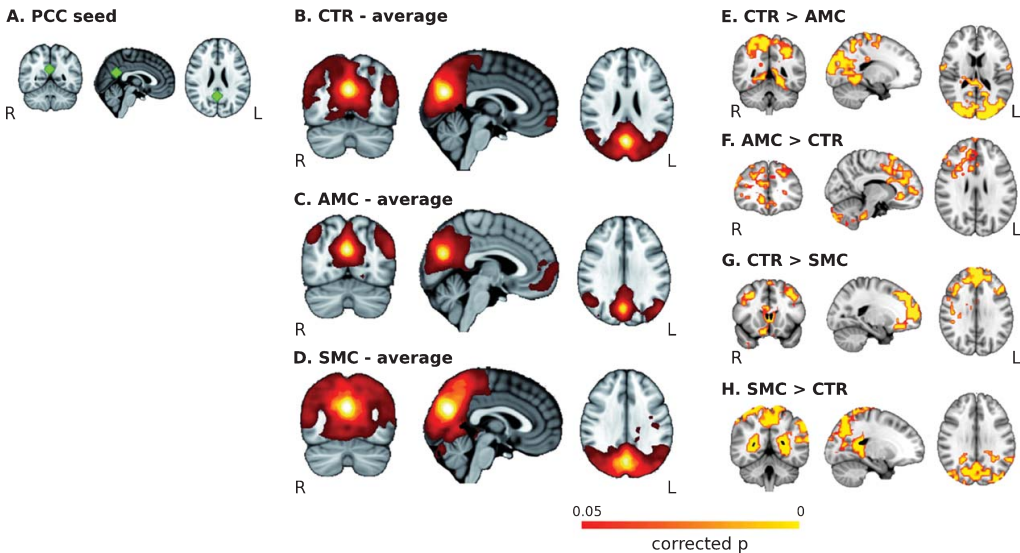


Fig. 1. Seed-based connectivity analysis of resting-state fMRI data. A) Location of the posterior cingulate cortex (PCC) seed in MNI standard space (spherical ROI of 6 mm radius; MNI coordinates $x=2, y=-54, z=24$). B) Average connectivity maps for healthy controls (CTR). C) Average connectivity map for asymptomatic mutation carriers (AMC). D) Average connectivity map for symptomatic mutation carriers (SMC). E-H) Group difference maps corrected for multiple comparisons. All difference maps are thresholded at a corrected family-wise $p < 0.05$ level. Maps (G) and (H) include age as a covariate.

The SMC group showed reduced connectivity with respect to controls in the anterior cingulate and paracingulate, the frontal pole, the medial frontal cortex, and the superior frontal gyrus. However, SMC had increased connectivity in supramarginal areas, the angular gyrus, parietal cortex, precuneus cortex, supracalcarine cortex, and lingual/fusiform areas. These results remain significant when age was included as covariate.

Encoding-fMRI activity

fMRI data during encoding were available for a subsample of 23 subjects (12 controls, 6 AMC, and 5 SMC subjects). This sample size difference was due to timing limitations during the scanning session, to excessive movement and MRI-related artifacts, and to extremely poor task performance.

Task performance outside the scanner

Memory performance outside the scanner did not differ significantly between AMC and control subjects. However, there was a trend for AMC subjects to perform worse than controls [mean (SD) values were 47.54 (2.21) for controls versus 40.84 (7.94) for AMC;

$t=2.14, p=0.08$]. SMC had a poorer performance outside the scanner (mean: 23.0, SD: 16.32) than both controls ($t=3.35, p=0.028$) and AMC ($t=2.4, p=0.039$).

Average maps

All group-average maps revealed the main pattern of brain regions involved in encoding for novel images (“encoding” > “repeated” condition). For the control and AMC groups (Fig. 2A and B, respectively), activity patterns included the lateral occipital cortex (left and right), the temporal occipital fusiform cortex, the middle and inferior temporal gyrus, the lingual gyrus, and the parahippocampal gyrus. Moreover, in the control group we also observed activity in the middle and inferior frontal gyrus bilaterally (although more pronounced in the left hemisphere), as well as in the frontal medial cortex and paracingulate gyrus (Fig. 2A). The group-average maps for the SMC group revealed areas of activity in the lateral occipital cortex, middle temporal gyrus, lingual gyrus, angular gyrus, and fusiform (Fig. 2C), although to a lesser extent than in controls and AMC. There was no activity in frontal areas in SMC.

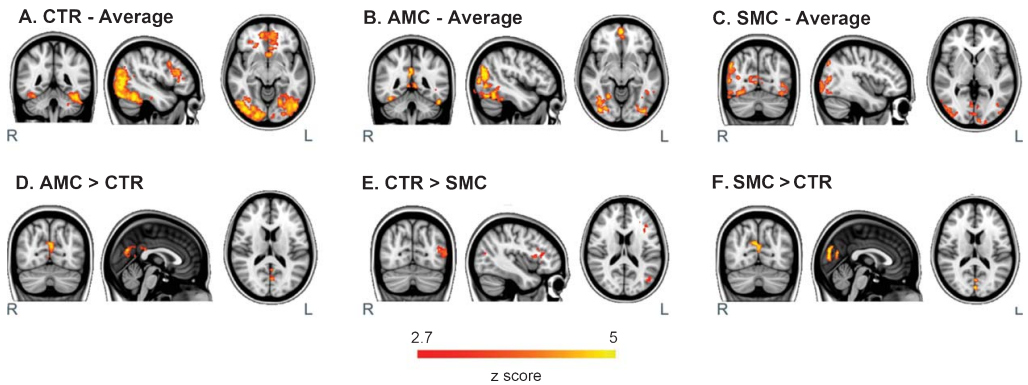


Fig. 2. Results of the analysis of task-related fMRI activity in the “encoding > repeated” images condition. A) Average map for the healthy control (CTR) group. B) Average map for the asymptomatic mutation carrier (AMC) group. C) Average map for the symptomatic mutation carrier (SMC) group. D) Areas where AMC had greater task-associated BOLD response than did CTR. E) Areas where SMC showed less task-associated BOLD response than did CTR. F) Areas where SMC had greater task-associated BOLD response with respect to CTR. Maps (E) and (F) include age as a covariate.

Table 2
Group differences in brain activity during memory encoding. Summary of significant clusters in the “encoding > repeated” images contrast

Cluster	Size (mm ²)	Cluster p	Z max	Peak coordinates (MNI)		
				x	y	z
<i>Asymptomatic Mutation Carriers > Controls</i>						
1	1952	0.000253	4.96	2	-68	24
<i>Symptomatic Mutation Carriers > Controls</i>						
1	1276	0.0171	4.05	0	-84	28
<i>Controls > Symptomatic Mutation Carriers</i>						
1	1160	0.015	4.33	-38	16	12
2	1220	0.0109	4.89	-54	-74	8

Group comparisons

In the “encoding > repeated” images contrast, AMC showed increased BOLD activity in comparison with the control group in regions of the precuneus/posterior cingulate cortex (Fig. 2D). There were no regions of increased BOLD activity in the control group with respect to AMC. SMC showed decreased BOLD activity with respect to controls in a region within the left middle and inferior frontal gyri and left frontal operculum, as well as in the left lateral occipital cortex (Fig. 2E). Conversely, SMC showed areas of increased BOLD activity in comparison with controls in the precuneus cortex, the intracalcarine cortex, and in part of the lingual gyrus (Fig. 2F). The results of all these comparisons are also summarized in Table 2.

Correlations with task performance

Brain activity was positively correlated with performance outside the scanner in the AMC group. This positive association involved areas of the right

parahippocampal gyrus, right hippocampus, and right temporal fusiform and lingual gyrus (Fig. 3A). We extracted average signal change between repeated and encoding conditions for each individual within these regions (Fig. 3A, right panel). Task performance correlated with activity scores in AMC ($r=0.98$, $p<0.001$) but not in the control group ($r=0.27$, $p=0.42$).

Correlations with adjusted age

In AMC, BOLD activity during encoding was positively correlated with the adjusted age of subjects in regions within the angular gyrus ($r=0.94$, $p=0.005$; Fig. 3B). In other words, subjects who were closer to their familial age of onset showed greater activation in these areas.

DISCUSSION

We performed an fMRI study to assess resting-state and encoding-task activity in a cohort of symptomatic

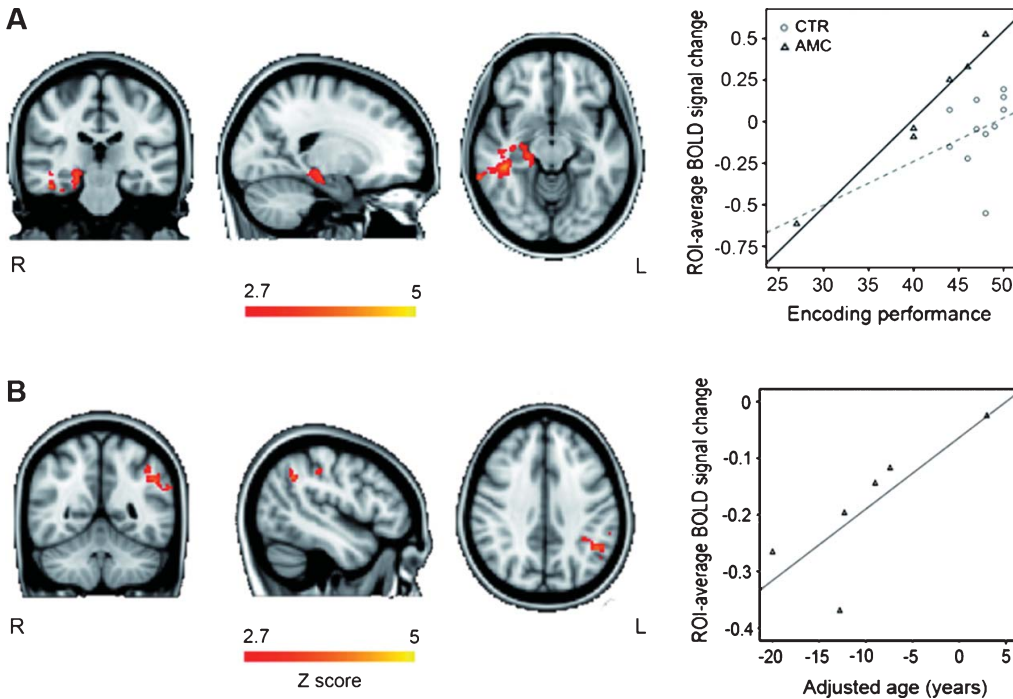


Fig. 3. Correlations found with encoding-related brain activity in the asymptomatic mutation carrier (AMC) group. A) Correlations with task performance. Spatial map of brain regions with significant correlation (left panel) and scatter plot of performance scores and mean BOLD signal change within significant areas in AMC subjects and healthy controls (CTR) (right panel). B) Correlations with adjusted age within AMC subjects. Spatial map of brain regions showing significant correlation (left panel) and scatter plot of adjusted age and mean BOLD signal change in these regions (right panel). All maps are thresholded at a corrected level of $p < 0.05$.

and asymptomatic PSEN1 mutation carriers and a group of matched healthy controls. To the best of our knowledge, this is the first study to examine intrinsic functional connectivity by means of resting-state fMRI in PSEN1 subjects. The asymptomatic and symptomatic subjects showed divergent changes in connectivity between the anterior and posterior components of the DMN, with connectivity being increased in AMC and reduced in SMC. Conversely, short distance connections in posterior regions of the DMN were increased in SMC and decreased in AMC. The analysis of task fMRI revealed common encoding-related BOLD activity in areas within the memory network. Compared to controls, SMC showed reduced activity in left prefrontal and left occipital cortices. However, both SMC and AMC presented increased activity during encoding compared to controls in areas of the precuneus/posterior cingulate.

The reduced connectivity from the precuneus/posterior cingulate to frontal areas in SMC is consis-

tent with previous studies that have assessed the DMN in sporadic AD and mild cognitive impairment [10, 12, 15]. Moreover, the increased within-lobe functional connectivity in the same subjects is also in line with previously published research on sporadic AD [11, 46] and mild cognitive impairment [15]. However, other studies on AD have also showed opposite changes with decreases in functional connectivity of posterior regions and increases in frontal regions (reviewed in [47]). These discrepancies may rely on differences in the methodology used to isolate the DMN together with differences in subjects' atrophy between studies.

More interesting, we also found altered connectivity in mutation carriers prior to the appearance of clinical symptoms. Specifically, AMC subjects showed reduced resting-state connectivity from the precuneus/posterior cingulate to other posterior brain regions, including part of the hippocampus, the fusiform and parahippocampal gyri, and the lingual gyrus. These regions are known to be structurally

affected very early in AD and this reduction in connectivity is in accordance with seed-based studies that have demonstrated decreased connectivity in AD between the hippocampus and DMN regions [48]. We also found an increase in precuneus/posterior cingulate functional connectivity within frontal regions. We suggest two explanations for the increased connectivity between the posterior and anterior core components of the DMN in AMC. First, the increased functional connectivity in the frontal cortex might reflect reorganization mechanisms within the network that serve to maintain function despite the reduced connectivity with medial temporal and hippocampal regions of the DMN found in AMC. These increases in frontal areas agree with studies identifying the frontal lobe as a key region for functional compensation mechanisms in AD [49]. On the other hand, the increased functional connectivity might also reflect aberrant excitatory responses to early amyloid- β deposition that could trigger a variety of inhibitory compensatory responses in memory circuits and would, thus, explain the divergent network connectivity changes in the medial temporal lobe and prefrontal regions [4, 29, 50]. Our results are congruent with the findings in APOE $\epsilon 4$ carriers [51, 52] with increased connectivity in frontal regions of the DMN.

During visual encoding, SMC showed reduced activity in encoding-associated areas such as the left occipital and left prefrontal cortex. The results in SMC confirm the decreased brain activity engaged by the visual memory task that has been widely reported in the literature on sporadic AD [27]. AMC showed increased encoding-related BOLD activity in precuneus/posterior cingulate with respect to controls. These results are in agreement with studies of preclinical AD by our group [36] and others [19, 29] and have been interpreted as a compensatory mechanism, as the precuneus/posterior cingulate plays an important role in memory functions. In healthy young controls, precuneus/posterior cingulate deactivates during encoding and is activated in retrieval, a phenomenon known as the encoding/retrieval flip. Impaired ability to modulate activity in the precuneus/posterior cingulate has been associated with increasing age, greater amyloid burden, and worse memory performance [53] and has also been described in healthy APOE $\epsilon 4$ carriers [54–57], and in a previous study in another sample of PSEN1 asymptomatic carriers [58]. The hyperactivity (or lack of deactivation) in the precuneus/posterior cingulate could be a consequence of amyloid deposition, that would produce a decrease in synaptic inhibition and modify the functional properties of the

neurons themselves, rendering them hyperactive [59] or a compensatory mechanism, in the sense that additional cognitive resources are required to achieve and maintain a performance level similar to that of non-carriers. In the same sense, a previous study of PSEN1 mutation carriers showed that fMRI activity in the fusiform and middle temporal gyri increased as subjects approached the age of symptom onset, suggesting that during novelty encoding, increased fMRI activity may relate to incipient AD processes [32, 60].

Of note, we also found a significant correlation both between brain activity and performance outside the scanner and between brain activity and adjusted age in the AMC group. First, activity in areas in the right middle temporal and right hippocampus correlated with task performance, indicating that the system might be already compromised prior to the appearance of symptoms. In the same sense, positive correlations between hippocampus activity and encoding performance have previously been reported in PSEN1 mutation carriers [30, 31]. The positive correlation between adjusted age and brain activity in a region within the left angular gyrus is in agreement with the study published by the group of Braskie et al. also based on a visual encoding task [61]. These results, together with the previously discussed hyperactivity in the precuneus/posterior cingulate, suggest that the activity of other regions such as the hippocampus or the angular gyrus would compensate in PSEN1 mutation carriers a precocious alteration in the encoding/retrieval flip.

Thus, taken together, our results would support the possibility of a phase of paradoxically increased activation early in the course of the disease that evolves over the course of the AD disease process [5, 28]. The present study therefore provides evidence to support that fMRI may be a suitable biomarker in familial AD to track longitudinally disease progression. In contrast, the distinct and evolving changes in the DMN in PSEN1, with increases followed by decreases in functional connectivity in some areas, might complicate the interpretation of cross-sectional results.

The main limitation of our study is the relatively small sample size. However, previous investigations in familial AD neuroimaging all have similar sample sizes and the main results survived a correction for multiple comparisons.

In summary, PSEN1 mutation carriers present disruption of normal connections in large-scale networks over a decade before symptoms onset. However, the trajectory of changes during the AD disease process may be complex, with increases and decreases in functional connectivity in different areas of the memory

systems and the DMN. These changes might reflect aberrant excitatory responses to amyloid- β and subsequent inhibitory responses or functional network reorganization mechanisms that evolve with disease progression.

ACKNOWLEDGMENTS

This work was supported by research grants from the Instituto Carlos III (FIS080036 and FIS1200013 to RSV) and from the Spanish Ministerio de Ciencia e Innovación (SAF200907489 to DB and BES-2011-047053 to RSL). Juan Fortea was a receptor of a Josep Font grant from Hospital Clinic.

We thank all the volunteers for their participation in this study.

Authors' disclosures available online (<http://www.jalz.com/disclosures/view.php?id=1710>).

REFERENCES

- [1] Lleo A, Blesa R, Queralt R, Ezquerra M, Molinuevo JL, Pena-Casanova J, Rojo A, Oliva R (2002) Frequency of mutations in the presenilin and amyloid precursor protein genes in early-onset Alzheimer disease in Spain. *Arch Neurol* **59**, 1759-1763.
- [2] Fox NC, Kennedy AM, Harvey RJ, Lantos PL, Roques PK, Collinge J, Hardy J, Hutton M, Stevens JM, Warrington EK, Rossor MN (1997) Clinicopathological features of familial Alzheimer's disease associated with the M139V mutation in the presenilin 1 gene. Pedigree but not mutation specific age at onset provides evidence for a further genetic factor. *Brain* **120**, 491-501.
- [3] Bateman RJ, Xiong C, Benzinger TL, Fagan AM, Goate A, Fox NC, Marcus DS, Cairns NJ, Xie X, Blazey TM, Holtzman DM, Santacruz A, Buckles V, Oliver A, Moulder K, Aisen PS, Ghetti B, Klunk WE, McDade E, Martins RN, Masters CL, Mayeux R, Ringman JM, Rossor MN, Schofield PR, Sperling RA, Salloway S, Morris JC (2012) Dominantly Inherited Alzheimer Network. Clinical and biomarker changes in dominantly inherited Alzheimer's disease. *N Engl J Med* **367**, 795-804.
- [4] Selkoe DJ (2002) Alzheimer's disease is a synaptic failure. *Science* **298**, 789-791.
- [5] Dickerson BC, Sperling RA (2009) Large-scale functional brain network abnormalities in Alzheimer's disease: Insights from functional neuroimaging. *Behav Neurol* **21**, 63-75.
- [6] Smith SM, Fox PT, Miller KL, Glahn DC, Fox PM, Mackay CE, Filippini N, Watkins KE, Toro R, Laird AR, Beckmann CF (2009) Correspondence of the brain's functional architecture during activation and rest. *Proc Natl Acad Sci U S A* **106**, 13040-13045.
- [7] Raichle ME, MacLeod AM, Snyder AZ, Powers WJ, Gusnard DA, Shulman GL (2001) A default mode of brain function. *Proc Natl Acad Sci U S A* **98**, 676-682.
- [8] Buckner RL, Andrews-Hanna JR, Schacter DL (2008) The brain's default network: Anatomy, function, and relevance to disease. *Ann N Y Acad Sci* **1124**, 1-38.
- [9] Buckner RL, Snyder AZ, Shannon BJ, LaRossa G, Sachs R, Fotenos AF, Sheline YI, Klunk WE, Mathis CA, Morris JC, Mintun MA (2005) Molecular, structural, and functional characterization of Alzheimer's disease: Evidence for a relationship between default activity, amyloid, and memory. *J Neurosci* **25**, 7709-7717.
- [10] Greicius MD, Srivastava G, Reiss AL, Menon V (2004) Default-mode network activity distinguishes Alzheimer's disease from healthy aging: Evidence from functional MRI. *Proc Natl Acad Sci U S A* **101**, 4637-4642.
- [11] Wang K, Liang M, Wang L, Tian L, Zhang X, Li K, Jiang T (2007) Altered functional connectivity in early Alzheimer's disease: A resting-state fMRI study. *Hum Brain Mapp* **28**, 967-978.
- [12] Zhang HY, Wang SJ, Xing J, Liu B, Ma ZL, Yang M, Zhang ZJ, Teng GJ (2009) Detection of PCC functional connectivity characteristics in resting-state fMRI in mild Alzheimer's disease. *Behav Brain Res* **197**, 103-108.
- [13] Zhang HY, Wang SJ, Liu B, Ma ZL, Yang M, Zhang ZJ, Teng GJ (2010) Resting brain connectivity: Changes during the progress of Alzheimer disease. *Radiology* **256**, 598-606.
- [14] Damoiseaux JS, Prater KE, Miller BL, Greicius MD (2012) Functional connectivity tracks clinical deterioration in Alzheimer's disease. *Neurobiol Aging* **33**, 828.e19-e30.
- [15] Sorg C, Riedl V, Muhlau M, Calhoun VD, Eichele T, Laer L, Drzezga A, Forstl H, Kurz A, Zimmer C, Wohlschlagel AM (2007) Selective changes of resting-state networks in individuals at risk for Alzheimer's disease. *Proc Natl Acad Sci U S A* **104**, 18760-18765.
- [16] Bai F, Watson DR, Yu H, Shi Y, Yuan Y, Zhang Z (2009) Abnormal resting-state functional connectivity of posterior cingulate cortex in amnesic type mild cognitive impairment. *Brain Res* **1302**, 167-174.
- [17] Qi Z, Wu X, Wang Z, Zhang N, Dong H, Yao L, Li K (2010) Impairment and compensation coexist in amnesic MCI default mode network. *Neuroimage* **50**, 48-55.
- [18] Hedden T, Van Dijk KR, Becker JA, Mehta A, Sperling RA, Johnson KA, Buckner RL (2009) Disruption of functional connectivity in clinically normal older adults harboring amyloid burden. *J Neurosci* **29**, 12686-12694.
- [19] Sperling RA, Laviolette PS, O'Keefe K, O'Brien J, Rentz DM, Pihlajamaki M, Marshall G, Hyman BT, Selkoe DJ, Hedden T, Buckner RL, Becker JA, Johnson KA (2009) Amyloid deposition is associated with impaired default network function in older persons without dementia. *Neuron* **63**, 178-188.
- [20] Sheline YI, Raichle ME, Snyder AZ, Morris JC, Head D, Wang S, Mintun MA (2010) Amyloid plaques disrupt resting state default mode network connectivity in cognitively normal elderly. *Biol Psychiatry* **67**, 584-587.
- [21] Mormino EC, Smiljic A, Hayenga AO, Onami SH, Greicius MD, Rabinovici GD, Janabi M, Baker SL, Yen IV, Madison CM, Miller BL, Jagust WJ (2011) Relationships between beta-amyloid and functional connectivity in different components of the default mode network in aging. *Cereb Cortex* **21**, 2399-2407.
- [22] Persson J, Lind J, Larsson A, Ingvar M, Slegers K, Van Broeckhoven C, Adolfsson R, Nilsson LG, Nyberg L (2008) Altered deactivation in individuals with genetic risk for Alzheimer's disease. *Neuropsychologia* **46**, 1679-1687.
- [23] Fleisher AS, Sherzai A, Taylor C, Langbaum JB, Chen K, Buxton RB (2009) Resting-state BOLD networks versus task-associated functional MRI for distinguishing Alzheimer's disease risk groups. *Neuroimage* **47**, 1678-1690.
- [24] Machulda MM, Jones DT, Vemuri P, McDade E, Avula R, Przybelski S, Boeve BF, Knopman DS, Petersen RC, Jack

- CR Jr. (2011) Effect of APOE epsilon4 status on intrinsic network connectivity in cognitively normal elderly subjects. *Arch Neurol* **68**, 1131-1136.
- [25] Drzezga A, Becker JA, Van Dijk KR, Sreenivasan A, Talukdar T, Sullivan C, Schultz AP, Sepulcre J, Putcha D, Greve D, Johnson KA, Sperling RA (2011) Neuronal dysfunction and disconnection of cortical hubs in non-demented subjects with elevated amyloid burden. *Brain* **134**, 1635-1646.
- [26] Trachtenberg AJ, Filippini N, Ebmeier KP, Smith SM, Karpe F, Mackay CE (2012) The effects of APOE on the functional architecture of the resting brain. *Neuroimage* **59**, 565-572.
- [27] Schwindt GC, Black SE (2009) Functional imaging studies of episodic memory in Alzheimer's disease: A quantitative meta-analysis. *Neuroimage* **45**, 181-190.
- [28] Sperling R (2007) Functional MRI studies of associative encoding in normal aging, mild cognitive impairment, and Alzheimer's disease. *Ann N Y Acad Sci* **1097**, 146-155.
- [29] Mormino EC, Brandel MG, Madison CM, Marks S, Baker SL, Jagust WJ (2012) AB deposition in aging is associated with increases in brain activation during successful memory encoding. *Cereb Cortex* **22**, 1813-1823.
- [30] Mondadori CR, Buchmann A, Mustovic H, Schmidt CF, Boesiger P, Nitsch RM, Hock C, Streffer J, Henke K (2006) Enhanced brain activity may precede the diagnosis of Alzheimer's disease by 30 years. *Brain* **129**, 2908-2922.
- [31] Quiroz YT, Budson AE, Celone K, Ruiz A, Newmark R, Castrillon G, Lopera F, Stern CE (2010) Hippocampal hyperactivation in presymptomatic familial Alzheimer's disease. *Ann Neurol* **68**, 865-875.
- [32] Braskie MN, Medina LD, Rodriguez-Agudelo Y, Geschwind DH, Macias-Islas MA, Cummings JL, Bookheimer SY, Ringman JM (2012) Increased fMRI signal with age in familial Alzheimer's disease mutation carriers. *Neurobiol Aging* **33**, 424.e411-421.
- [33] Fortea J, Llado A, Clarimon J, Lleo A, Oliva R, Peri J, Pintor L, Yague J, Blesa R, Molinuevo JL, Sanchez-Valle R (2011) PICOGEN: Five years experience with a genetic counselling program for dementia. *Neurologia* **26**, 143-149.
- [34] Sanchez-Valle R, Llado A, Ezquerro M, Rey MJ, Rami L, Molinuevo JL (2007) A novel mutation in the PSEN1 gene (L286P) associated with familial early-onset dementia of Alzheimer type and lobar haematomas. *Eur J Neurol* **14**, 1409-1412.
- [35] Fortea J, Sala-Llloch R, Bartres-Faz D, Bosch B, Llado A, Bargallo N, Molinuevo JL, Sanchez-Valle R (2010) Increased cortical thickness and caudate volume precede atrophy in PSEN1 mutation carriers. *J Alzheimers Dis* **22**, 909-922.
- [36] Rami L, Sala-Llloch R, Sole-Padullés C, Fortea J, Olives J, Llado A, Pena-Gomez C, Balasa M, Bosch B, Antonell A, Sanchez-Valle R, Bartres-Faz D, Molinuevo JL (2012) Distinct functional activity of the precuneus and posterior cingulate cortex during encoding in the preclinical stage of Alzheimer's disease. *J Alzheimers Dis* **31**, 517-526.
- [37] Jenkinson M, Bannister PR, Brady JM, Smith SM (2002) Improved optimisation for the robust and accurate linear registration and motion correction of brain images. *NeuroImage* **17**, 825-841.
- [38] Smith SM (2002) Fast robust automated brain extraction. *Hum Brain Mapp* **17**, 143-155.
- [39] Jenkinson, Smith SM (2001) A global optimisation method for robust affine registration of brain images. *Medi Image Anal* **5**, 143-156.
- [40] Andrews-Hanna JR, Snyder AZ, Vincent JL, Lustig C, Head D, Raichle ME, Buckner RL (2007) Disruption of large-scale brain systems in advanced aging. *Neuron* **56**, 924-935.
- [41] Nichols TE, Holmes AP (2002) Nonparametric permutation tests for functional neuroimaging: A primer with examples. *Hum Brain Mapp* **15**, 1-25.
- [42] Woolrich MW, Ripley BD, Brady JM, Smith SM (2001) Temporal autocorrelation in univariate linear modelling of FMRI data. *Neuroimage* **14**, 1370-1386.
- [43] Beckmann CF, Jenkinson M, Smith SM (2003) General multi-level linear modelling for group analysis in FMRI. *Neuroimage* **20**, 1052-1063.
- [44] Woolrich MW, Behrens TEJ, Beckmann CF, Jenkinson M, Smith SM (2004) Multi-level linear modelling for FMRI group analysis using Bayesian inference. *Neuroimage* **21**, 1732-1747.
- [45] Woolrich M (2008) Robust group analysis using outlier inference. *Neuroimage* **41**, 286-301.
- [46] Wang Z, Yan C, Zhao C, Qi Z, Zhou W, Lu J, He Y, Li K (2011) Spatial patterns of intrinsic brain activity in mild cognitive impairment and Alzheimer's disease: A resting-state functional MRI study. *Hum Brain Mapp* **32**, 1720-1740.
- [47] Hafkemeijer A, van der Grond J, Rombouts SA (2012) Imaging the default mode network in aging and dementia. *Biochim Biophys Acta* **1822**, 431-441.
- [48] Allen G, Barnard H, McColl R, Hester AL, Fields JA, Weiner MF, Ringe WK, Lipton AM, Brooker M, McDonald E, Rubin CD, Cullum CM (2007) Reduced hippocampal functional connectivity in Alzheimer disease. *Arch Neurol* **64**, 1482-1487.
- [49] Prvulovic D, Bokde AL, Faltraco F, Hampel H (2011) Functional magnetic resonance imaging as a dynamic candidate biomarker for Alzheimer's disease. *Prog Neurobiol* **95**, 557-569.
- [50] Palop JJ, Chin J, Mucke L (2006) A network dysfunction perspective on neurodegenerative diseases. *Nature* **443**, 768-773.
- [51] Filippini N, MacIntosh BJ, Hough MG, Goodwin GM, Frisoni GB, Smith SM, Matthews PM, Beckmann CF, Mackay CE (2009) Distinct patterns of brain activity in young carriers of the APOE-epsilon4 allele. *Proc Natl Acad Sci U S A* **106**, 7209-7214.
- [52] Damoiseaux JS, Seeley WW, Zhou J, Shirer WR, Coppola G, Karydas A, Rosen HJ, Miller BL, Kramer JH, Greicius MD: Alzheimer's Disease Neuroimaging Initiative (2012) Gender modulates the APOE ε4 effect in healthy older adults: Convergent evidence from functional brain connectivity and spinal fluid tau levels. *J Neurosci* **32**, 8254-8262.
- [53] Vannini P, Hedden T, Huijbers W, Ward A, Johnson KA, Sperling RA (2012) The ups and downs of the posteromedial cortex: Age- and amyloid-related functional alterations of the encoding/retrieval flip in cognitively normal older adults. *Cereb Cortex*. doi: 10.1093/cercor/bhs108
- [54] Bartres-Faz D, Serra-Grabulosa JM, Sun FT, Sole-Padullés C, Rami L, Molinuevo JL, Bosch B, Mercader JM, Bargallo N, Falcon C, Vendrell P, Junque C, D'Esposito M (2008) Functional connectivity of the hippocampus in elderly with mild memory dysfunction carrying the APOE epsilon4 allele. *Neurobiol Aging* **29**, 1644-1653.
- [55] Bondi MW, Houston WS, Eyler LT, Brown GG (2005) fMRI evidence of compensatory mechanisms in older adults at genetic risk for Alzheimer disease. *Neurology* **64**, 501-508.
- [56] Bookheimer SY, Strojwas MH, Cohen MS, Saunders AM, Pericak-Vance MA, Mazziotta JC, Small GW (2000) Patterns of brain activation in people at risk for Alzheimer's disease. *N Engl J Med* **343**, 450-456.
- [57] Han SD, Houston WS, Jak AJ, Eyler LT, Nagel BJ, Fleisher AS, Brown GG, Corey-Bloom J, Salmon DP, Thal LJ, Bondi

- MW (2007) Verbal paired-associate learning by APOE genotype in non-demented older adults: fMRI evidence of a right hemispheric compensatory response. *Neurobiol Aging* **28**, 238-247.
- [58] Reiman EM, Quiroz YT, Fleisher AS, Chen K, Velez-Pardo C, Jimenez-Del-Rio M, Fagan AM, Shah AR, Alvarez S, Arbelaez A, Giraldo M, Acosta-Baena N, Sperling RA, Dickerson B, Stern CE, Tirado V, Munoz C, Reiman RA, Huentelman MJ, Alexander GE, Langbaum JB, Kosik KS, Tariot PN, Lopera F (2012) Brain imaging and fluid biomarker analysis in young adults at genetic risk for autosomal dominant Alzheimer's disease in the presenilin 1 E280A kindred: A case-control study. *Lancet Neurol* **11**, 1048-1056.
- [59] Harris JA, Devidze N, Verret L, Ho K, Halabisky B, Thwin MT, Kim D, Hamto P, Lo I, Yu G-Q, Palop JJ, Masliah E, Mucke L (2010) Transsynaptic progression of amyloid- β -induced neuronal dysfunction within the entorhinal-hippocampal network. *Neuron* **68**, 428-441.
- [60] Ringman JM, Medina LD, Braskie M, Rodriguez-Agudelo Y, Geschwind DH, Macias-Islas MA, Cummings JL, Bookheimer S (2011) Effects of risk genes on BOLD activation in presymptomatic carriers of familial Alzheimer's disease mutations during a novelty encoding task. *Cereb Cortex* **21**, 877-883.
- [61] Braskie MN, Medina LD, Rodriguez-Agudelo Y, Geschwind DH, Macias-Islas MA, Thompson PM, Cummings JL, Bookheimer SY, Ringman JM (2012) Memory performance and fMRI signal in presymptomatic familial Alzheimer's disease. *Hum Brain Mapp*, doi: 10.1002/hbm.22141

CHAPTER 5

General Discussion

In the present thesis, which includes 6 research articles, we have used advanced neuroimaging approaches and techniques to investigate brain structure, brain activity, and brain connectivity. From different MRI modalities, we have described changes in large-scale functional brain networks and changes in whole-brain connectomics by identifying functionally associated brain regions. We also have used DTI-tractography to characterize the brain structural connectivity and its relationship with the functional connectivity findings. In addition, we have found that functional and structural properties of brain networks are related memory functions in healthy young subjects and in the context of healthy aging and Alzheimer's disease.

Advantages of Resting-state fMRI

In 5 of the 6 studies presented in this thesis, resting-state fMRI has been used to investigate the functional brain organization of cognitive functions in samples of young and old subjects, as well as in subjects with familiar Alzheimer's disease. One of the main advantages of rs-fMRI is that it is easy to acquire and that it can be equally obtained from different

sets of populations without being affected by task difficulty (Barkhof et al., 2014). Overall, our research adds evidence to the utility of this technique to describe a common functional brain architecture (Smith et al., 2013).

The utility of rs-fMRI in health and disease has raised several questions. One of these questions refers to its ability to perform predictions about subjects cognitive performance. In this regard, in our first study, we aimed to explore the relationship between connectivity at rest and the execution of a subsequent working memory task in a sample of healthy young subjects. We found that the connectivity of the precuneus, the posterior node of the default mode network, measured prior to the task, explained the better execution of the task. This finding was interpreted as a preparatory mechanism of the attentional brain system to respond to a high-demanding cognitive task. Our results are in accordance with other studies regarding the involvement of the precuneus in attentional systems, suggesting a pivotal role of the DMN to predict the efficacy of cognitive functioning (Wang et al., 2010; Cauda et al., 2010; Cavanna and Trimble, 2006; Lee et al., 2013).

Continuing with the study of functional connectivity at rest, in our third study we explored rs-fMRI measures and its relation with task performance in healthy aging. We found that disruptions in some specific rs-fMRI networks were related to worse working memory performance in healthy elders. This result was further supported and extended with the findings of our fourth and fifth studies. In these two studies, we found correlations between rs-fMRI networks and other cognitive functions in aging, including visual memory, verbal memory, and executive functions.

Finally, in the last study of this thesis (study 6) we reported an altered functional connectivity at rest in subjects that were in early stages of familial Alzheimer's disease, even before the emergence of clinical symptoms. All these findings, support the applicability of this technique in the clinical context of neurodegenerative diseases (Matthews et al., 2013; Sheline and Raichle, 2013; Dennis and Thompson, 2014).

Convergences of rs-fMRI findings across studies

Along this thesis, we have explored different methodologies related to the analysis of resting-state fMRI data. We have used Independent Component Analysis (ICA), which is

currently the most widely used method in rs-fMRI studies (Damoiseaux et al., 2006). ICA is a fully exploratory method that can be used to define large-scale networks from a set of resting-state data (Beckmann et al., 2005) and it presents several advantages such as the fact of being data-driven, with no hypotheses or design required a priori. In our studies, ICA was always followed by a dual-regression analysis, which allowed performing voxel-wise group statistics on network spatial maps (Filippini et al., 2009). Besides ICA, we also used the seed-based connectivity approach. This method was used to define the DMN pattern as the set of regions that correlate temporally with a given region defined a priori, which was the precuneus. Although it is strongly dependent on the definition of the seed, seed-based connectivity is the best method to answer specific questions when there is a strong hypothesis as regards some specific connection (Cole et al., 2010). In addition, we have also used more complex methods to analyze rs-fMRI from a whole-brain perspective, such as graph-theory (Rubinov and Sporns, 2010) in study 4, and the FSLNets approach (Smith et al., 2011) in study 5.

In the rs-fMRI literature it is common to find different methodologies that sometimes give similar results but that can also produce discrepancies between studies. In our case, we believe that the different analyses performed are complementary, and that some of the questions that could not be answered by one of the methods, were further solved using other approaches. As an example, in study 2 we used ICA and dual-regression of rs-fMRI data and we found reduced connectivity in aging within the fronto-parietal and the default mode systems. However, a clear relationship with cognition could not be established using these approaches. Therefore, in the next study, we analyzed patterns of whole-brain connectivity. In agreement with other studies (Tomasi and Volkow, 2012), we found age-related reductions in long-range functional connections. Considering our previous results, we hypothesized that this long-range functional disruption, would be directly affecting the brain networks that involve fronto-parietal or antero-posterior connectivity. In addition, in the same study, we used global measures derived from graph-theory and we found that these measures captured the trajectory of connectivity changes in aging, defined as increased segregation and decreased integration of brain systems. We found that graph theory measures such as regional clustering correlated with memory alterations in aging.

Another methodological approach to analyze whole-brain connectivity patterns focuses on the interactions between sets of networks, and it was used in study number 5. We believe that this approach solves some of the issues raised by graph theory, concretely because the nodes are patterns of functionally independent areas defined by ICA, as opposite to anatomical-based parcellations, and also because interactions are modeled using partial correlations and thus, the effect of the other networks is removed (Smith et al., 2011). Using this methodology, we found that rs-fMRI data can be successfully used to find increases and decreases in the functional coupling between networks that are strongly affected by age. This is in agreement with the theoretical concepts of functional segregation and functional integration used in graph analysis approaches. In this study, we also found that network interactions correlated with cognitive performance, even when the individual networks were not related to performance per se.

Working memory networks

Three of the studies presented in this thesis include fMRI acquisitions during n-back paradigms in order to assess working memory functions. In study 1 and study 3 we used a version of the paradigm with letters as stimuli and with different levels of cognitive load ($n=0,1,2,3$ items to be retained). This version of the task was acquired in young and healthy elders. In study 2, we studied only young subjects and we used two different versions of the paradigm with visual stimuli, which were spatial locations and faces. Therefore, we studied the working memory system from different points of view.

First, as regards the task activity-patterns, in the three studies we found consistent patterns of brain activation in accordance with what has been described in the previous working memory fMRI research, more specifically, with n-back paradigms (Fuster, 1997; Braver et al., 1997; Owen et al., 2005; Rottschy et al., 2012). These patterns of activation include: the superior parietal lobule, the frontal pole, the dorsal cingulate and the dorsolateral-midventrolateral prefrontal cortex. Furthermore, in study 2, we found additional activation of the fusiform region and the inferior frontal area during working memory for faces, which is in accordance with previous studies showing the specificity of the fusiform area in face processing tasks (Haxby et al., 2001; Kanwisher, 2010).

When looking at the connectivity networks, in the first study we used ICA to define two main brain networks: one that was related to the task itself and the other related to rest periods or task-deactivations. These networks were identified as the fronto-parietal network and the DMN respectively. In the same study, we also found that the functional coupling of within-network regions, and the functional decoupling between the two networks were modeled by the task difficulty. In a situation that requires a high cognitive demand, the nodes within each network became positively correlated whereas the correlation between the two networks was strongly negative. At the same time, this pattern of functional switching between networks correlated with the task performance. This result highlights the importance of a correct synchrony between the activation and deactivation of brain networks during the timecourse of a task (Fox et al., 2005). Interestingly, when we studied the same task in a group of healthy elders, we found functional alterations during task performance that were related with lack of deactivation of the DMN regions.

Function-structure relationships in brain networks

In the present thesis we have also aimed to assess the structural characteristics underlying the working memory networks. The results of such research are included in study 2. Whereas the functional specificity of different networks depending on the stimulus used has been widely explored in the neuroimaging literature (Kanwisher, 2010), there are only few studies focusing on the specificity of the structural networks in brain function and cognitive performance (Tavor et al., 2014).

In study 2, we first described the functional networks implicated in working memory for faces and for locations. Afterwards, we studied DTI parameters of the anatomical connections derived from these functional networks. The whole-brain analyses of the measures derived from DTI analyses, revealed that the axial diffusivity of the inferior fronto-occipital fasciculus correlated with reaction time in the facial working memory task. Moreover, we also carried out a DTI-tractography analysis where we identified the fronto-occipital fasciculus as the main tract connecting the fusiform and the inferior frontal gyrus, which were two of the main regions involved in facial working memory. These findings are in agreement with previous DTI studies demonstrating that function specificity might affect the

microstructural composition of white matter (Tavor et al., 2014).

In this thesis, we did not include DTI data in any of the other studies, but some of the results obtained could be interpreted on the basis of known structural connectivity findings. For example, in study 4 we showed changes in the functional correlation between nodes and how these changes were related to the physical distance. Although results were obtained from functional data, measures related to physical distances pointed that long-range connectivity might be affected due to alteration of white matter pathways, which is a commonly reported finding in aging (Madden et al., 2012).

Aging & fMRI

Along this thesis, we have used different techniques to describe functional changes that occur in the aging brain, which were studied in the context of functional activity and functional connectivity. Although some of the results as regards these findings have been already mentioned in this discussion, we will now give a more comprehensive interpretation in the context of different aging functional models.

In the third study, we focused in brain activity patterns during working memory performance. We associated the successful task performance in aging to a higher level of brain activity in some parts of the fronto-parietal network in comparison with young subjects: the inferior frontal gyrus bilaterally, left middle frontal gyrus, and in the anterior cingulate. On the contrary, elder subjects with worse task performance, showed those task-activity patterns more similar to the young subjects. These results support the HAROLD model, which states that older adults activate regions more bilaterally as a compensation mechanism during a cognitive task (Cabeza et al., 2002). Moreover, our results also agree with the PASA model, which relates to reductions in activity of posterior areas and higher activation in frontal areas (Davis et al., 2008).

In addition, in the same study, high performance levels were associated with abnormal activity in the DMN. We found positive task-related activity in the precuneus/posterior cingulate, and in the medial frontal cortex, which are two core regions of the DMN and therefore should deactivate during task. This result also falls into the functional compensation hypothesis and it can be interpreted within the CRUNCH model (Reuter-Lorenz and

Cappell, 2008). As it can be seen in Figure 5 of study 3, these two regions also show positive levels of activity in young subjects when they are exposed to high cognitive demands (i.e., during the 3-back blocks). We hypothesized that old subjects with reduced brain resources need to activate these additional resources at lower cognitive demands than young subjects in order to achieve good performance. In the same study, the results from task-related activity were supported by the results of the connectivity patterns of the default and fronto-parietal networks, supporting the idea that functional connectivity changes can be accompanied by functional activity changes in aging.

Thereafter, in the fourth study, we extended the sample of healthy elders and we focused on the analysis of rs-fMRI data. We found that older subjects had higher clustering (increased segregation) and increased average minimum path length (decreased integrity) of the global functional network, also in accordance with the literature on rs-fMRI and aging (Achard and Bullmore, 2007; Meunier et al., 2009). Furthermore, the localization of such changes indicated that frontal and parietal regions become more clustered with age, but that the connectivity between these two regions is highly reduced. This finding is in agreement with the disruptions of the fronto-parietal network reported in the previous study.

Finally, we also studied changes in the status and interactions of large-scale networks, which are reported in study 5. We found that the majority of networks showed local increases in connectivity of areas surrounding the main network nodes. However, when we looked at the effect of age in the interactions between networks we observed both increases and decreases in its connectivity. Connectivity decreases were found between networks that belong to the same brain system, such as the posterior and anterior parts of the DMN or different parts of the FPN, whereas connectivity increases were found between components representing distinct RSNs. The results of this study also indicate a loss of functional specialization and integration of networks, specially the DMN and FPN systems. Further, they are in agreement with the findings of study 3, where we found that the interplaying roles of the DMN and FPN systems were affected by age and with study 4, where we described that the whole brain network was more segregated and less integrated with aging. Alterations in the connectivity between networks have been also recently reported in the literature (Betzel et al., 2014; Geerligs et al., 2014).

fMRI & Alzheimers disease

In one of the studies presented in this thesis, we studied functional changes in carriers of the PSEN1 mutation, which causes familiar Alzheimers disease with 100% of penetrance (Fortea et al., 2011a). Some of the subjects included were at the dementia stages of the disease, but other were asymptomatic, scanned in average 12 years prior to the predicted age of onset. We described functional alterations in areas within the episodic memory network during the encoding of novel images, as well as alterations in the connectivity of the default mode network measured during resting-fMRI. With our results, we first evidenced that the pattern of functional alterations in the clinical stages of familial AD is in accordance with what has been described in sporadic AD (Schwindt and Black, 2009; Greicius et al., 2004), adding evidence to the potential use of fMRI as a biomarker for AD. Furthermore, the results obtained with the asymptomatic cohort support previous studies suggesting that functional alterations may appear in the preclinical stages of the disease (Sheline and Raichle, 2013; Dennis and Thompson, 2014). Finally, it should be noted that in this study we reported a non-linear trajectory of the changes in the connectivity of the default mode network, being that symptomatic subjects showed decreased connectivity between the anterior and the posterior nodes of this network, but asymptomatic subjects showed increased connectivity. Similar results have been reported with APOE e4 carriers (Filippini et al., 2009; Damoiseaux et al., 2012) and they have been interpreted as aberrant excitatory responses to early amyloid-b deposition triggering compensatory mechanism.

The default mode network

The default mode network has appeared in several parts of the thesis, therefore in the following section we aimed to put together all our findings as regards this system and their relationship with what has been described in the literature.

In the first study, the DMN appeared as a system that deactivates during the performance of a task, showing negative temporal correlation with task-positive networks, supporting previous findings (Fox et al., 2005). We found that this continuous switching between networks was more clearly marked in higher cognitive loads and that it correlated with task performance. Later on, in study 3, we found that the DMN functioning was al-

tered in healthy aging, in the sense that some of its parts remained active during task and were not completely separated from task-positive networks. In this case, the engagement of DMN regions during task was associated with better task performance, indicating compensation.

A common finding as regards DMN changes in aging is the disconnection between its anterior and posterior nodes (Andrews-Hanna et al., 2007; Damoiseaux et al., 2008; Vidal-Piñero et al., 2014b). We replicated this finding in several parts of this thesis. For example, in study 4, we explored correlations between all regions in the parcellated brain, and we found that the connectivity between frontal nodes and precuneus/posterior cingulate regions correlated negatively with age. In addition, in the same study, increased clustering in regions coinciding with anterior and posterior DMN nodes correlated with the age of the subjects and negatively with the results of memory tests. This disconnection of the DMN sub-modules with age was also observed in study 5, where it also correlated with results of the executive functions. Our findings add evidence to the implication of the DMN in memory processes (Buckner et al., 2008) and in general cognitive functioning.

CHAPTER 6

Conclusions

1. Functional networks can be estimated from functional MRI during task and at rest and they provide information about cognitive states and task performance.
2. The connectivity of the default mode network, measured during a resting-state acquisition before the performance of a task, indicates preparatory, attentional mechanisms that predict task performance.
3. Large-scale networks involved in working memory have functional specificity depending on the kind of stimuli used, which can be observed in their functional activity patterns as well as in the DTI measures reflecting microstructural white matter properties.
4. Healthy aging is associated with reorganizations of functional networks that we observed using functional MRI at rest and during the performance of a working memory task, that have a compensatory role and contribute to successful performance in the task.
5. Analysis of whole-brain functional connectivity revealed a loss of long-range func-

tional connectivity and an increase in short-range connectivity, resulting in topological changes of the whole network, which can be summarized as decreased network integration and increased segregation.

6. In addition to patterns of age-related changes affecting isolated networks, we also evidenced changes in the interactions between large-scale networks.
7. Resting-state functional connectivity and task-related brain activity are altered in Alzheimers disease, even many years before the emergence of clinical symptomatology.
8. The Default Mode Network appears as a highly compromised system in both healthy aging and in Alzheimer disease, in the sense that its connectivity is disrupted and its normal activation-deactivation behavior is altered with some of its nodes being abnormally recruited during working memory or episodic memory tasks as compensatory mechanisms.

Methodological issues in Graph Theory

A.1 Introduction and motivation of the study

In this appendix, we evaluate some of the issues that raised during the graph-theory analyses presented in *Study 4*. Therefore, the study sample, the preprocessing of rs-fMRI data and the main analysis settings are the same as reported there (and described in the Methods section of the present thesis).

The main motivation for these additional analyses was to study and to quantify the impact of some methodological choices that needed to be taken during the process of data analysis. In addition, some of the points presented here were derived from the comments made by the experts during the revision and publication processes of the study.

Table A.1: Regions in FS-82 atlas

Frontal lobe	Occipital lobe
1 Superior frontal	26 Lateral occipital
2 Rostral middle frontal	27 Lingual
3 Caudal middle frontal	28 Cuneus
4 Pars opercularis	29 Pericalcarine
5 Pars triangularis	Cingulate
6 Pars orbitalis	30 Rostral anterior
7 Lateral Orbitofrontal	31 Caudal anterior
8 Medial orbitofrontal	32 Posterior
9 Precentral	33 Isthmus
10 Paracentral	Other
11 Frontal Pole	34 Insula
Parietal Lobe	35 Cerebellum
12 Superior parietal	Subcortical
13 Inferior Parietal	36 Thalamus
14 Supramarginal	37 Caudate
15 Postcentral	38 Putamen
16 Precuneus	39 Pallidum
Temporal lobe	40 Hippocampus
17 Superior temporal	41 Amygdala
18 Middle temporal	
19 Inferior temporal	
20 Banks of the superior temporal sulcus (bankssts)	
21 Fusiform	
22 Transverse temporal	
23 Entorhinal	
24 Temporal pole	
25 Parahippocampal	

A.2 Methods

A.2.1 Evaluation of different brain parcellations strategies

Brain parcellation is one of the first stages performed in graph theory studies. However, its implications can not be observed until the whole study has been done. Therefore, we repeated the network creation and the evaluation of network metrics. We evaluated parcellations derived from the AAL atlas (Tzourio-Mazoyer et al., 2002) and from two atlases available in Freesurfer (Desikan et al., 2006; Destrieux et al., 2010) (Figure A.1 and Tables A.1 and A.2). Subsequently, we repeated the main analyses of *Study 4* in the three atlases.

Table A.2: Regions in FS-164 atlas

1	Fronto-marginal gyrus (Wernike) and sulcus	42	Medial wall
2	Inferior occipital gyrus (O3) and sulcus	43	Occipital pole
3	Paracentral lobule and sulcus	44	Temporal pole
4	Subcentral gyrus (operculum) and sulci	45	Calcarine sulcus
5	Transverse frontopolar gyri and sulci	46	Central sulcus
6	Anterior cingulate gyrus and sulcus	47	Marginal branch of cingulate gyrus
7	Middle-anterior cingulate gyrus and sulcus	48	Anterior circular sulcus of the insula
8	Middle-posterior cingulate gyrus and sulcus	49	Inferior circular sulcus of the insula
9	Posterior-dorsal cingulate	50	Superior of the circular sulcus of the insula
10	Posterior-ventral cingulate	51	Anterior transverse collateral sulcus
11	Cuneus (O6)	52	Posterior transverse collateral sulcus
12	Opercular Inferior frontal gyrus	53	Inferior frontal sulcus
13	Orbital Inferior frontal gyrus	54	Midle frontal sulcus
14	Triangular inferior frontal gyrus	55	Superior frontal sulcus
15	Middle frontal gyrus (F2)	56	Sulcus intermedius primus (of Jensen)
16	Superior frontal gyrus (F1)	57	Intraparietal sulcus and transverse parietal
17	Long insular gyrus and central insula	58	Middle occipital sulcus and lunatus sulcus
18	Short insular gyri	59	Superior occipital sulcus and preoccipital notch
19	Middle occipital gyrus (O2)	60	Anterior occipital sulcus and preoccipital notch
20	Superior occipital gyrus (O1)	61	Lateral occipito-temporal sulcus
21	Lateral occipito-temporal gyrus (fusiform, O4-T4)	62	Medial occipito-temporal sulcus and lingual
22	Lingual gyrus (O5)	63	Lateral orbital sulcus
23	Parahippocampal gyrus (T5)	64	Medial orbital sulcus (olfactory sulcus)
24	Orbital gyri	65	Orbital sulci (H-shaped sulci)
25	Angular gyrus	66	Parieto-occipital sulcus (or fissure)
26	Supramarginal gyrus	67	Pericallosal sulcus (S of corpus callosum)
27	Superior parietal lobule (lateral P1)	68	Postcentral sulcus
28	Postcentral gyrus	69	Inferior part of the precentral sulcus
29	Precentral gyrus	70	Superior part of the precentral sulcus
30	Precuneus (medial P1)	71	Suborbital sulcus (sulcus rostrales, supraorbital sulcus)
31	Straight gyrus, gyrus rectus	72	Subparietal sulcus
32	Subcallosal area, subcallosal gyrus	73	Inferior temporal sulcus
33	Anterior transverse temporal gyrus (Heschl)	74	Superior temporal sulcus (parallel sulcus)
34	Lateral aspect of the superior temporal gyrus	75	Transverse temporal sulcus
35	Planum polare of the superior temporal gyrus	76	Cerebellum
36	Planum temporale of the superior temporal gyrus	77	Thalamus
37	Inferior temporal gyrus (T3)	78	Caudate
38	Middle temporal gyrus	79	Putamen
39	Horizontal ramus of the anterior lateral sulcus	80	Pallidum
40	Vertical ramus of the anterior lateral sulcus	81	Hippocampus
41	Posterior ramus of the lateral sulcus	82	Amygdala

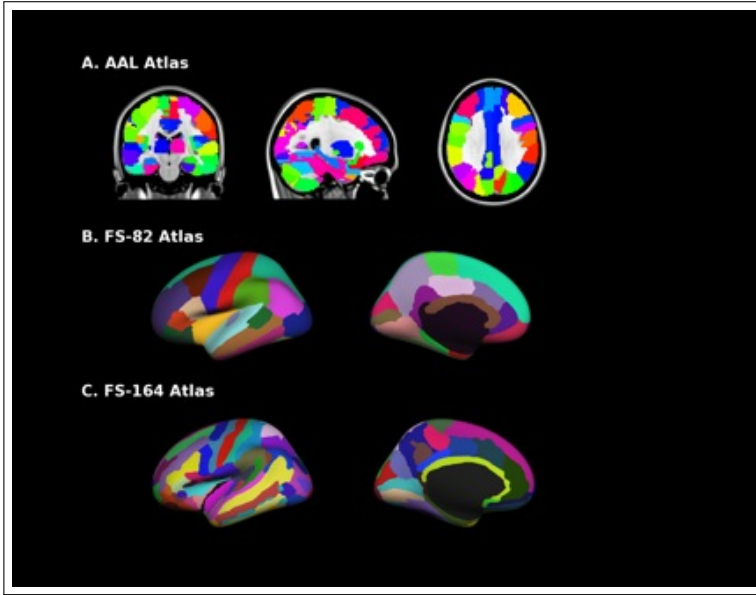


Figure A.1: Three different atlas-based parcellation strategies evaluated. Parcellations are shown on the standard brain template

A.2.2 Evaluation of networks at different threshold levels

For each of the different parcellations, we evaluated the resulting networks across a set of thresholds. We used a relative threshold and we evaluated network sparsities from 5% to 40%.

A.3 Results

We first examined the topological structure of the obtained networks, in the three atlases, that is, in three parcellation dimensionalities, and covering a wide range of sparsity levels. These analyses were done in order to evaluate at the same time the effect of increasing the number of nodes and the number of edges and connections. Examples of network obtained at each configuration are shown in Figure A.2.

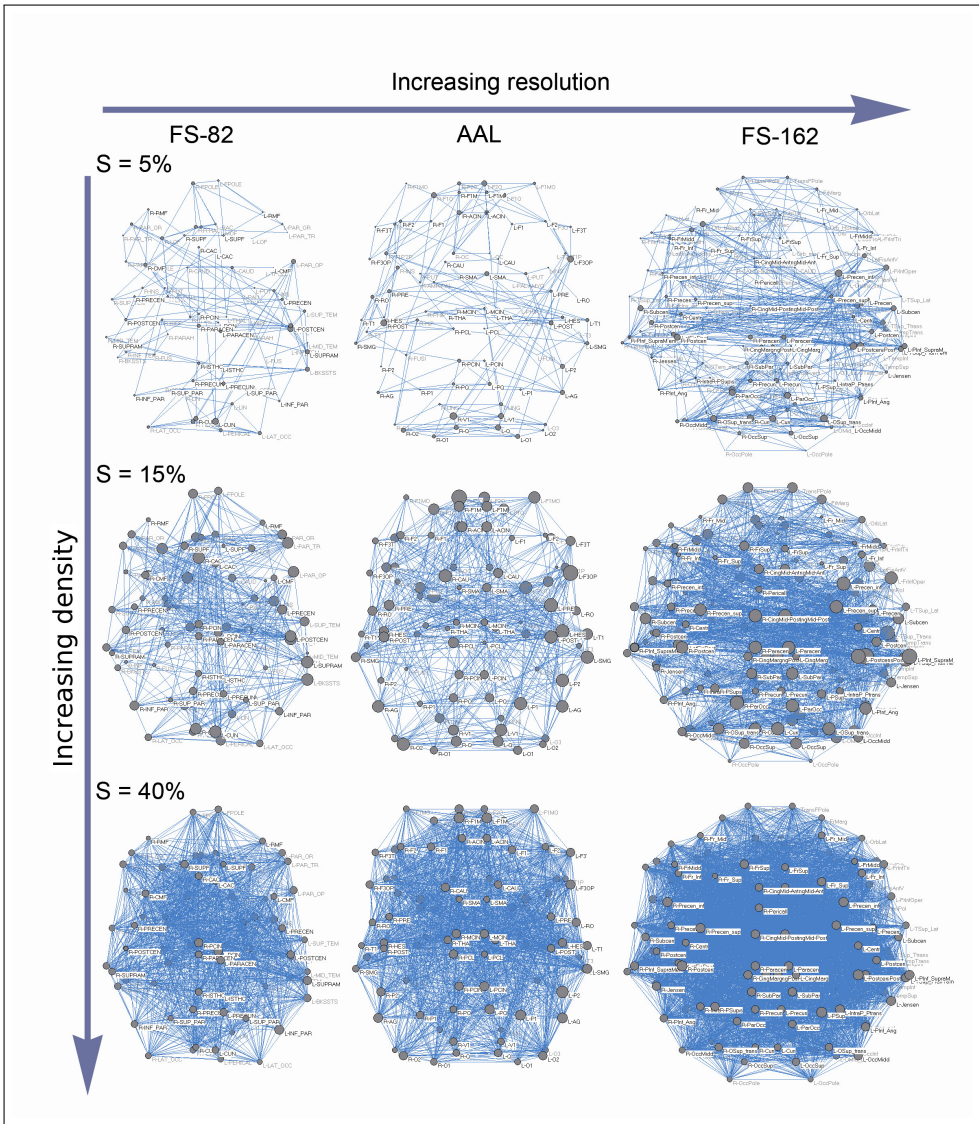


Figure A.2: Examples of networks obtained with different atlases and at different levels of sparsity.

A.3.1 Network metrics

We evaluated the correlation between measures obtained at the different network configurations.

A.3.2 Correlations with age

Table A.3: Age-correlations of graph theory metrics using different atlases and threshold levels

Threshold	Atlas	Correlation with age <i>Clustering Coefficient</i> r (p)	Correlation with age <i>Minimum Path Length</i> r (p)	Correlation with age <i>Small-World</i> r (p)
5%				
	AAL	.122 (.235)	.242 (.017)	-.183 (.073)
	FS-82	-.041 (.680)	.17 (.095)	-.098 (.339)
	FS-162	.173 (.092)	.283 (.005)	-.200 (.05)
10%				
	AAL	.428 (<.001)	.321 (.001)	-.027 (.79)
	FS-82	.226 (.026)	.313 (.002)	-.111 (.28)
	FS-162	.354 (<.001)	.344 (.001)	-.071 (.491)
15%				
	AAL	.454 (<.001)	.380 (<.001)	.030 (.768)
	FS-82	.373 (<.001)	.294 (<.001)	-.011 (.91)
	FS-162	.424 (<.001)	.357 (<.001)	.088 (.392)
20%				
	AAL	.480 (<.001)	.409 (<.001)	.223 (.028)
	FS-82	.352 (<.001)	.306 (.002)	.247 (.015)
	FS-162	.404 (<.001)	.359 (<.001)	.287 (.005)
25%				
	AAL	.469 (<.001)	.389 (<.001)	.276 (<.001)
	FS-82	.352 (<.001)	.306 (.002)	.247 (.015)
	FS-162	.404 (<.001)	.359 (<.001)	.287 (.005)
30%				
	AAL	.443 (<.001)	.358 (<.001)	.413 (<.001)
	FS-82	.355 (<.001)	.303 (.003)	.245 (.016)
	FS-162	.398 (<.001)	.323 (.001)	.335 (.001)
35%				
	AAL	.425 (<.001)	.326 (.001)	.424 (<.001)
	FS-82	.352 (<.001)	.288 (.004)	.293 (.004)
	FS-162	.392 (<.001)	.292 (.004)	.362 (<.001)
40%				
	AAL	.401 (<.001)	.263 (.009)	.442 (<.001)
	FS-82	.347 (<.001)	.251 (.013)	.302 (.003)
	FS-162	.374 (<.001)	.247 (.015)	.361 (<.001)

Resum en català

Antecedents i plantejament de la investigació

Aquesta tesi s'ha elaborat en el format de compendi de sis estudis en els quals s'han utilitzat diversos mètodes de ressonància magnètica amb la finalitat de caracteritzar la connectivitat cerebral i la seva relació amb l'estat cognitiu en diverses etapes de la vida: joves sans, persones amb alt risc de demència i pacients amb malaltia d'Alzheimer.

El concepte de connectivitat cerebral engloba l'estudi de les interaccions entre diferents regions cerebrals. Aquestes interaccions es poden observar tant a nivell estructural com funcional. Les tècniques avançades d'Imatge per Ressonància Magnètica (IRM) ens permeten estudiar ambdós aspectes de la connectivitat (Behrens and Sporns, 2012). Per l'estudi de la connectivitat estructural s'usa bàsicament la IRM de difusió que es basa en l'adquisició d'una sèrie de volums de IRM en diferents direccions i s'analitza a partir de les imatges de Tensor de Difusió, o *Diffusion Tensor Imaging* (DTI), amb les quals es poden calcular mapes de direccionalitat a nivell de vòxel, i que també permeten realitzar tractografia entre dues regions d'interès (Basser et al., 1994). La connectivitat funcional es pot estudiar mitjançant

la IRM funcional (IRMf). Aquesta tècnica consisteix en l'adquisició seqüencial d'imatges durant un període de temps i està basada en la mesura del senyal dependent del nivell d'oxigen a la sang (*Blood-Oxygen Level Dependent*, BOLD). La IRMf ens permet veure canvis regionals en el nivell d'activitat cerebral, quan s'adquireix durant l'execució d'una tasca, i també ens permet mesurar la connectivitat funcional a partir de les correlacions entre les oscil·lacions temporals de diferents regions cerebrals. La connectivitat funcional es pot mesurar durant l'execució d'una tasca, però també durant l'estat de repòs, o *resting-state*. En el darrer cas, es mesuren les correlacions entre les oscil·lacions derivades de l'activitat espontània de baixa freqüència (Biswal et al., 1995).

Les tècniques derivades de la IRMf han permès caracteritzar un conjunt de xarxes o patrons que són comuns a tots els subjectes i que defineixen una arquitectura funcional del cervell (Smith et al., 2009). Dintre d'aquest grup de xarxes, trobem xarxes associades a aspectes simples sensorials o motors, com per exemple les xarxes visuals o somatosensorials/motors, i altres associades a funcions cognitives complexes com per exemple la xarxa fronto-parietal que es relaciona amb les funcions executives i amb la memòria de treball. Aquestes xarxes es poden identificar amb adquisicions de IRMf concomitants a una tasca en les que s'observa un increment d'activitat BOLD durant la seva execució i també durant l'estat de repòs. En l'activitat de repòs els nodes de les xarxes correlacionen en les seves oscil·lacions espontànies de baixa freqüència.

Dintre del grup de les principals xarxes funcionals, destaca la xarxa neuronal per defecte, o *Default Mode Network* (DMN). La DMN té un comportament diferent a les altres xarxes perquè es mostra activa durant el repòs i es desactiva durant l'execució d'una tasca que impliqui una alta demanda cognitiva. La DMN comprèn regions frontals, regions del cingulat posterior i precuneus i regions parietals. Es considera que participa en modes interns de cognició tals com la memòria autobiogràfica o la introspecció (Buckner et al., 2008). La DMN també s'ha relacionat amb els processos de la memòria declarativa degut a la seva connexió amb l'hipocamp. Ha demostrat ser una xarxa de gran interès en el curs de la malaltia d'Alzheimer, incloent les fases inicials o pre-clíniques, ja que es troba alterada tant en pacients amb simptomatologia clínica com en subjectes en risc de desenvolupar-la.

El concepte d'envelliment sà fa referència a persones d'edat avançada que són capaces

de mantenir les seves funcions cognitives dintre de la normalitat malgrat els processos degeneratius associats al propi envelliment. Cal destacar que, tot i mantenir-se dintre de la normalitat, els subjectes d'edat avançada poden mostrar declivis cognitius, en especial en la memòria episòdica i la memòria de treball. Així doncs, un dels principals objectius dintre del camp de la neurociència cognitiva en l'envelliment és poder entendre quins són els canvis cerebrals que són l'origen de les diferències individuals en el grau de declivi cognitiu associat a l'edat (Park and Reuter-Lorenz, 2009).

Els estudis previs han demostrat que mitjançant la IRMf es poden detectar canvis en l'activitat cerebral en subjectes que no tenen cap diagnòstic clínic de demència o de deteriorament cognitiu lleu (Grady, 2012). Una de les troballes més comunes és que els subjectes d'edat avançada mostren nivells més alts d'activació cerebral en comparació amb els subjectes joves durant l'execució de tasques cognitives. Aquesta activació addicional es localitza principalment a regions frontals i sembla reflectir processos de compensació funcional ja que una major activació s'ha vist relacionada amb un millor rendiment (Cabeza et al., 2002). A més dels canvis en l'activació cerebral, durant l'envelliment també s'han trobat canvis en la connectivitat cerebral, que afecten a l'estructura i funció de les principals xarxes (Dennis and Thompson, 2014). Així, s'ha vist que hi ha una reducció de la connectivitat entre regions dins de la DMN i en la xarxa fronto-parietal.

La malaltia d'Alzheimer és la forma de demència més comuna en la societat actual. En pacients en estats avançats de la malaltia, s'han descrit alteracions cerebrals tant a nivell estructural com funcional que inclouen pèrdues de volum, alteracions en la substància blanca i alteracions en l'activitat i la connectivitat funcional (Chhatwal and Sperling, 2012). Actualment, un dels principals objectius de la investigació en neuroimatge és definir marcadors per detectar aquells canvis que apareixen en els estats previs a l'aparició de la simptomatologia clínic dels subjectes. Amb aquesta finalitat, s'han estudiat subjectes sans que tenen un risc elevat de desenvolupar la malaltia, que inclouen portadors del gen APOE- ϵ 4 o subjectes d'edat avançada amb valors positius en els biomarcadors de β -Amiloide.

Hipòtesis i Objectius

Hipòtesis

1. El cervell humà està organitzat funcionalment com a un grup de xarxes que es poden identificar amb ressonància magnètica funcional durant l'execució d'una tasca o en estat de repòs i que tindran una implicació directe en la cognició.
2. La connectivitat cerebral, mesurada durant el repòs, pot predir l'execució d'una tasca realitzada immediatament després.
3. El sistema de la memòria de treball es trobarà alterat en els subjectes sans d'edat avançada, i aquesta alteració tindrà una implicació en els dèficits cognitius en aquest domini.
4. Donat que l'envelliment està relacionat amb canvis en els patrons d'activitat cerebral, esperem trobar també alteracions en les mesures de connectivitat funcional cerebral en l'envelliment.
5. En les formes genètiques de la malaltia d'Alzheimer, la Ressonància Magnètica funcional pot ser d'utilitat per identificar canvis cerebrals que apareixen en estats previs a la manifestació dels símptomes clínics.

Objectius

OBJECTIU PRINCIPAL:

Estudiar el potencial de la Ressonància Magnètica per identificar i estudiar les xarxes cerebrals que es troben presents en l'estat de repòs i durant l'execució d'una tasca en diferents grups de subjectes.

OBJECTIUS ESPECÍFICS:

1. Estudiar la utilitat de les mesures de connectivitat funcional en repòs per predir els resultats en l'execució d'una tasca.

2. Investigar les relacions entre la funcionalitat i l'estructura de les xarxes cerebrals, i com aquestes es relacionen amb el rendiment cognitiu.
3. Estudiar els patrons d'activitat i connectivitat de les xarxes funcionals de gran escala en el context de l'envelliment sà, i com aquests poden donar lloc a diferències en l'execució.
4. Caracteritzar els patrons de connectivitat funcional cerebral a nivell global en l'envelliment i estudiar correlacions amb l'estat cognitiu dels subjectes.
5. Investigar el potencial de la IRMf per identificar els canvis cerebrals que apareixen en les etapes inicials de les malalties neurodegeneratives, fins i tot abans de l'aparició de símptomes clínics.

Resultats

En el primer dels treballs de la tesi, es va estudiar un grup de 16 subjectes joves sans mitjançant IRM funcional, durant l'estat de repòs i durant una tasca de memòria de treball. La tasca que es va utilitzar va ser un paradigma n-back amb diversos nivells de dificultat. Durant la tasca, els subjectes veien una seqüència d'estímuls, dels quals n'havien de memoritzar n ítems successivament (amb $n = 0, 1, 2$ o 3 , segons el nivell de dificultat). Primerament, a partir de l'estudi de la IRMf en repòs, es va trobar que el grau de connectivitat de la xarxa neuronal per defecte correlacionava amb la bona execució de la tasca, la qual cosa indicava el paper dels mecanismes de preparació dels sistemes atencionals cerebrals per a resoldre exitosament la tasca. Després, a partir de la IRMf durant la tasca, es varen identificar les dues xarxes principals implicades en l'execució d'aquesta. La primera, la xarxa fronto-parietal, es mostrà activa durant els blocs de demanda cognitiva, mentre que una segona xarxa, la xarxa neuronal per defecte, o default mode network es mostrà activa durant els blocs de repòs i es desactivà durant la tasca. Vàrem observar que ambdues xarxes presentaven una forta correlació negativa, això és que quan una es mostrava activa l'altra es desactivava i viceversa. Aquesta sincronia negativa, s'observà de forma més evident en els blocs de més dificultat, i alhora correlacionà amb la bona execució.

En el segent estudi, vàrem voler aprofundir en la identificació dels patrons cerebrals de les xarxes implicades en la memòria de treball en joves sans. En aquest cas també vàrem estudiar l'especialització funcional d'aquestes en funció del tipus d'estímul. Així, es van utilitzar dues tasques de memòria de treball en un grup de 23 subjectes joves sans, una amb estímuls visuo-perceptius (cares) i l'altra amb estímuls visuo-espacials (localització de quadrats). Els resultats d'aquest estudi indicaren que les xarxes de la memòria de treball tenen un patró comú que és independent del tipus d'estímul i que inclou regions parietals i frontals, però que hi ha algunes regions addicionals que s'activen en funció de l'estímul. En el nostre cas, vàrem trobar activitat en el gir fusiforme i en una regió del còrtex inferior frontal associada a la tasca amb estímuls facials. En aquest treball també es va fer un estudi de IRM de Difusió mitjançant DTI i es va veure que les propietats microestructurals de la substància blanca dels tractes que unien el gir fusiforme i el còrtex inferior frontal facilitaven la velocitat de processament en retenció temporal de cares.

En el tercer treball es van incloure 29 subjectes sans d'edat avançada, juntament amb un grup de 16 subjectes joves, que varen ser estudiats amb la IRMf en repòs i durant una tasca de memòria de treball, amb l'objectiu d'estudiar els canvis en la connectivitat i activitat cerebrals relacionats amb la memòria de treball en l'envelliment. Es va utilitzar la mateixa tasca que en el primer estudi, que permetia controlar el nivell de càrrega cognitiva. Primerament, es varen identificar els patrons d'activitat associats a la tasca a nivell de grup, que correspongueren a les xarxes fronto-parietals i a la xarxa neuronal per defecte, i que coincidiren amb les xarxes identificades al primer estudi, així com amb altres estudis de la literatura. El grup de subjectes d'edat avançada es va dividir en dos subgrups en funció dels resultats obtinguts en la tasca. El subgrup amb alta execució mostrà un patró d'activitat cerebral significativament diferent al patró dels subjectes amb baixa execució i al patró del grup de joves. Es va observar una activació addicional que principalment implicava regions frontals bilaterals. A més, també s'observà una activació cerebral associada a la tasca en algunes de les regions que pertanyen a la xarxa neuronal per defecte. Els resultats d'aquest estudi indicaren mecanismes compensatoris dintre de les xarxes fronto-parietals, així com l'activació de regions d'altres xarxes, en aquest cas de la xarxa neuronal per defecte, en situacions d'alta

demanda cognitiva. Els subjectes d'edat avançada que no van activar aquests mecanismes, i que per tant tenien un patró similar al dels joves, tenien una execució més baixa en la tasca.

En el quart i cinquè treballs es va ampliar la mostra de subjectes amb envelliment i es van estudiar els patrons de connectivitat a nivell global i la seva relació amb l'estat cognitiu dels subjectes. En el primer d'aquests estudis, en el qual es van incloure 98 subjectes, es va utilitzar la teoria de grafs, o *Graph Theory*, per analitzar les connexions entre regions obtingudes d'una parcel·lació del cervell derivada de l'atles AAL (Automated Anatomical Labeling, (Tzourio-Mazoyer et al., 2002)). Es va trobar que els subjectes de més edat mostraven menys connectivitat funcional en les connexions de llarga distància, sobretot en les connexions entre regions frontals i parietals, però que pel contrari, hi havia un increment relacionat amb l'edat en la connectivitat funcional en les connexions curtes. També es van obtenir mesures de connectivitat derivades de la teoria de grafs, que van permetre estudiar la integració i la segregació de les xarxes cerebrals, tant a nivell global com a nivell regional. A nivell global, els subjectes de més edat presentaren un increment de la segregació i un increment de la integració, que donà com a resultat xarxes menys eficients. A nivell regional, es va estudiar el coeficient de *Clustering*, que mesura l'agrupament funcional de regions properes i que es relaciona amb la segregació regional. Es va trobar que l'agrupament funcional d'algunes regions, sobretot de regions frontals i parietals, augmentava amb l'edat i correlacionava negativament amb l'execució en els tests de memòria visual i verbal.

En el segent estudi, el cinquè de la tesi, es van voler ampliar els resultats pel que fa al comportament global de la connectivitat funcional en l'envelliment, per això es van utilitzar també les imatges de IRMf en repòs en un grup de 76 subjectes d'edat avançada. En aquest estudi, s'identificaren les principals xarxes funcionals i s'estudiaren les seves interaccions funcionals. En consonància amb l'estudi anterior, es va observar que algunes de les xarxes estaven més interconnectades en els subjectes de més edat mentre que d'altres disminuen la seva connectivitat. Aquests patrons de connectivitat entre xarxes també es van relacionar amb el rendiment cognitiu en memòria i funcions executives. Es va concloure que la correcta sincronia entre les parts de la mateixa xarxa funcional té una implicació positiva en

l'estatus cognitiu en l'envelliment, mentre que el fet de que els elements d'una xarxa concreta incrementin la correlació amb regions d'un altre sistema pot tenir efectes negatius.

Finalment, en el sisè treball de la tesi, es van investigar els patrons d'activitat i connectivitat funcional en un grup de subjectes amb una mutació en el gen *Presenilin-1* (PSEN-1). Aquesta mutació és causant de la malaltia d'Alzheimer familiar. En l'estudi es van incloure portadors de la mutació que es trobaven ja en fases simptomàtiques de la malaltia, però també es van poder estudiar subjectes portadors de la mutació que es trobaven lluny de l'edat estimada d'inici de la malaltia i que per tant, no mostraven cap símptoma clínic. A tots els subjectes se'ls va realitzar una IRMf durant el repòs i durant una tasca de memòria episòdica. Es van trobar alteracions de la connectivitat funcional dintre de la xarxa neuronal per defecte durant el repòs, així com alteracions de l'activitat funcional en la xarxa de la memòria episòdica durant la tasca. Aquestes alteracions es varen poder identificar tant en subjectes simptomàtics com en aquells que estaven lluny de l'edat estimada d'inici de la malaltia, el que indica que la IRMf pot ser un bon biomarcador per detectar canvis cerebrals funcionals abans de que aquests es facin clínicament evidents. En el cas específic de la xarxa neuronal per defecte, es va veure que els subjectes pre-simptomàtics tenien increments de la connectivitat mentre que els simptomàtics en tenien decrements, troballes que indicaven que els canvis neurodegeneratius en la malaltia d'Alzheimer no segueixen un recorregut lineal.

Conclusions

1. Els patrons de les xarxes cerebrals funcionals es poden obtenir a partir de la Resonància Magnètica Funcional tant durant l'execució d'una tasca com en l'estat de repòs. L'estat d'aquestes xarxes aporta informació sobre l'estat cognitiu dels subjectes.
2. La connectivitat de la xarxa neuronal per defecte, mesurada durant l'estat de repòs previ a l'execució d'una tasca, indica que hi ha mecanismes d'atenció que preparen per la resposta i que faciliten l'execució correcta de la tasca.

3. Les xarxes neuronals implicades en la memòria de treball tenen especificitat funcional que depèn dels tipus d'estímuls utilitzats. Aquesta especificitat es pot observar en els patrons d'activació funcional i també en els índexs de DTI que mesuren les propietats micro-estructurals de la substància blanca.
4. L'envelliment està associat a les reorganitzacions en les xarxes funcionals, que hem pogut observar utilitzant IRMf en repòs i durant l'execució d'una tasca de memòria de treball. Aquestes reorganitzacions donen lloc a processos compensatoris ja que es relacionen amb la correcta execució de les tasques cognitives.
5. L'anàlisi de la connectivitat funcional a nivell global de tot el cervell en l'envelliment indicà una pèrdua de connectivitat funcional en les connexions de llarga distància i un increment de connectivitat en les de curta distància. Aquests canvis associats a l'envelliment es van veure reflectits en un decrement de la integració funcional i un increment de la segregació.
6. A part dels canvis allats observats en les diferents xarxes durant l'envelliment, també es van observar canvis en la seva interacció funcional.
7. En subjectes amb malaltia d'Alzheimer, trobarem alteracions en la connectivitat funcional mesurada durant l'estat de repòs, així com en l'activitat funcional mesurada durant l'execució d'una tasca de memòria. Aquestes alteracions es detectaren prèviament a l'aparició dels símptomes clínics.
8. La xarxa neuronal per defecte es mostrà com un sistema altament compromès tant en l'envelliment normal com en la malaltia d'Alzheimer. Trobarem alteracions en la seva connectivitat funcional, i també alteracions en el seu comportament normal d'activació i desactivació en els estats de repòs i de tasca, respectivament. Algunes de les seves regions mostraren evidències de formar part dels mecanismes compensatoris per la pèrdua de memòria episòdica i de treball.

ACKNOWLEDGEMENTS

I am immensely grateful to my supervisors, Dr. David Bartrés Faz and Dr. Carme Junqué, for guiding me during the development of this thesis, and for giving me the opportunity to participate in the research carried out in their teams. I would also like to thank Dr. Pere Vendrell, for his wise advices and for how much I have learned from him, but also for helping me to be an active part of the team. Thanks to all of them, I have had the opportunity to participate in a wide range of projects, which have provided me a great professional and personal enrichment. They have given me unconditional support and encouragement.

I have to thank all the institutions that have given financial support to the research included in this thesis. They have provided the resources needed to carry out the research included in this thesis. I would also like to thank the Neurology Unit of the Hospital Clínic in Barcelona and all the volunteers, patients and relatives that have participated in the studies included in the thesis.

Thanks to the FMRIB Center, at the University of Oxford, especially to Dr. Eugene Duff and Dr. Stephen Smith for allowing me to collaborate in their research. All the things that I've learned during my internship have been extremely useful.

I would like to give my heartfelt gratitude to all my colleagues in the Department and in the Hospital Clinic, with whom I've worked hand by hand during the last years. This thesis contains all that I've learned from them. Thanks for

sharing their scientific knowledge with me, but also thanks for your friendship, for the good times that we've spent together, and for giving me their support and confidence.

Finally, I would like to give my warmest thanks to my family. They have always encouraged me and they have given me the strength to achieve all my goals. My deep thanks to all my friends, for the support and the confidence, but specially for being always there, for making me laugh, and for the great moments that I've spent with them.

AGRAÏMENTS

El meu incondicional agraïment als directors de tesi, el Dr. David Bartrés Faz i la Dra. Carme Junqué, per guiar-me durant el desenvolupament de la tesi, i per donar-me la oportunitat de formar part dels seus equips d'investigació. També haig de donar un especial agraïment al Dr. Pere Vendrell, director del Departament durant el temps que he fet la tesi, per tot el que he après d'ell aquests anys i per permetre'm formar part activa de l'equip. Gràcies a tots ells, he tingut la possibilitat de participar en un ampli ventall de projectes, que m'han aportat una gran riquesa tant a nivell professional com personal. Així, els dono les gràcies per la confiança dipositada en mi, per ensenyar-me a entendre i estimar la ciència des de diverses perspectives i per transmetre'm una infinitat de capacitats, incloent el respecte, l'esforç i la perseverança.

Haig d'agrair a les institucions que han finançat la recerca que forma part d'aquesta tesi, que han facilitat els recursos necessaris per dur a terme els estudis. Gràcies als membres de la Unitat de Neurologia de l'Hospital Clínic, que m'han permès realitzar recerca des d'un punt de vista clínic. També a tots els pacients i familiars, i als voluntaris que han participat en els estudis i en les proves pilot que he hagut de fer durant la tesi.

Gràcies al centre FMRIB de la Universitat d'Oxford, particularment al Dr. Eugene Duff i al Dr. Stephen M. Smith, per acollir-me al grup i donar-me la oportunitat de formar part del seu equip. Per compartir amb mi la seva professionalitat, i per tot el que he après durant la meva estada a Oxford.

M'agradaria donar les gràcies de forma especial a tots aquells amb els qui he treballat 'braç a braç' durant aquests anys, a tots els companys del Departament i del Hospital. Aquesta tesi conté part de tot el què he pogut aprendre d'ells. Ho dic pensant en el coneixement que m'han transmés i en les seves in comptables aportacions científiques, però també pels in comptables bons moments que hem compartit, per la seva amistat, i pel suport personal que m'han donat al llarg de la tesi.

Finalment, un agraïment immens a la família, a uns pares i germans que m'han donat la força per seguir endavant i creure en els meus objectius. Gràcies també a tots els amics, per estar al meu costat, per escoltar-me i per saber arrencar-me les rialles quan ha calgut.

ABSTRACT

INTRODUCTION: This thesis has been elaborated as a compendium of 6 research studies. We have used a variety of methods related with Magnetic Resonance Imaging (MRI) with the objective to characterize brain connectivity and its relationship with cognition in young and aged healthy subjects and in preclinical Alzheimers Disease (AD).

Brain Connectivity refers to any pattern of links connecting different brain areas. It can be studied at its *functional* level, by using functional MRI (fMRI), which measures the statistical dependence between brain activity at different regions, or at its *structural* level, with Diffusion Tensor Imaging (DTI), which estimates the directionality of white matter fiber tracts.

fMRI can be acquired during a task (task-fMRI) or during resting state (rs-fMRI). With task-fMRI, it is possible to obtain patterns of brain co-activations, measured by the Blood-Oxygen Level Dependent (BOLD) signal. On the other hand, rs-fMRI allows measuring patterns of brain connectivity, known as Resting State Networks (RSNs), as correlations between spontaneous oscillations. Functional connectivity has been used to describe a set of networks in the brain, including the Default Mode Network (DMN), which is deactivated during task and shows high activity levels at rest.

RESULTS: In the first study, we included 16 healthy young subjects, under rs-fMRI and during a Working Memory (WM) task-fMRI. The connectivity of the DMN at rest correlated with the performance in the subsequent task. During task-fMRI, we described the DMN and the WM network. The connectivity between these networks was highly negative in the most demanding blocks and during fixation, which also correlated with performance. In addition, within-network connectivity increased with cognitive demands.

In the second study, we analyzed the networks involved in two different WM

tasks, with visuoperceptive (faces) and visuospatial (squares) stimuli. We used task-fMRI and DTI. We found that the fusiform and the inferior frontal gyrus were selectively activated for faces, and that the DTI measures of the tracts connecting these regions correlated with task performance for the facial-WM.

In the third study, we analyzed a sample of young and old subjects during a WM task. We found patterns of increased activity in the WM networks in aging that were related to successful performance, indicating compensatory mechanisms. The results of this study supported and extended previous research on fMRI and aging.

In study 4, we included a sample of 98 healthy elders, during rs-fMRI. We used graph-theory to analyze whole-brain patterns of connectivity. Age correlated with a loss of functional connectivity in long-range connections and an increase in functional connectivity in short-range connections. These changes resulted in increases in clustering coefficient and larger average minimum path-length of the global network, indicating higher functional segregation and less integration. Increases in clustering were located in frontal and parietal regions and they correlated negatively with visual and verbal memory functions.

In study 5, we used a sample of 76 healthy elders during rs-fMRI and we analyzed functional interactions between the components of the main RSNs. The anterior and posterior components of the DMN were less connected in older subjects, and the connectivity between different networks increased with age, indicating alterations in the global architecture of functional networks. RSN-interactions correlated with the results in memory and executive functions.

Finally, in the last study, we included a sample of asymptomatic and symptomatic carriers of the PSEN1 mutation, which causes Familial AD. We found altered functional connectivity and brain activity at rest and during memory encoding that appear even before the onset of AD.

CONCLUSIONS: Overall, we proved the usefulness of fMRI to study brain con-

nectivity networks and we concluded that connectivity signals correlate with cognitive status and with task performance. In addition, we described alterations in connectivity during the healthy aging process and in AD, even before the disease onset. Finally, we identified the DMN as the system showing the highest correlations in healthy subjects but also as a core target for aging and AD.

References

- Achard, S. and Bullmore, E. (2007). Efficiency and cost of economical brain functional networks. *PLoS computational biology*, 3(2):e17.
- Achard, S., Salvador, R., Whitcher, B., Suckling, J., and Bullmore, E. (2006). A resilient, low-frequency, small-world human brain functional network with highly connected association cortical hubs. *The Journal of neuroscience*, 26(1):63–72.
- Adachi, Y., Osada, T., Sporns, O., Watanabe, T., Matsui, T., Miyamoto, K., and Miyashita, Y. (2012). Functional connectivity between anatomically unconnected areas is shaped by collective network-level effects in the macaque cortex. *Cerebral cortex*, 22(7):1586–92.
- Addis, D. R., Leclerc, C. M., Muscatell, K. A., and Kensinger, E. A. (2010). There are age-related changes in neural connectivity during the encoding of positive, but not negative, information. *Cortex*, 46(4):425–33.
- Agosta, F., Pievani, M., Geroldi, C., Copetti, M., Frisoni, G. B., and Filippi, M. (2012). Resting state fMRI in Alzheimer’s disease: beyond the default mode network. *Neurobiology of aging*, 33(8):1564–78.
- Albert, R. and Barabási, A.-L. (2002). Statistical mechanics of complex networks. *Rev. Mod. Phys.*, 74(1):47–97.
- Andersson, J., Jenkinson, M., and Smith, S. M. (2007). Non-linear registration, aka Spatial normalisation FMRIB technical report TR07JA2. Technical report, FMRIB, Oxford.
- Andrews-Hanna, J. R., Snyder, A. Z., Vincent, J. L., Lustig, C., Head, D., Raichle, M. E., and Buckner, R. L. (2007). Disruption of large-scale brain systems in advanced aging. *Neuron*, 56(5):924–35.
- Arenaza-Urquijo, E. M., Bosch, B., Sala-Llloch, R., Solé-Padullés, C., Junqué, C., Fernández-Espejo, D., Bargalló, N., Rami, L., Molinuevo, J. L., and Bartrés-Faz, D. (2011). Specific anatomic associations between white matter integrity and cognitive reserve in normal and cognitively impaired elders. *The American journal of geriatric psychiatry*, 19(1):33–42.
- Arenaza-Urquijo, E. M., Molinuevo, J.-L., Sala-Llloch, R., Solé-Padullés, C., Balasa, M., Bosch, B., Olives, J., Antonell, A., Lladó, A., Sánchez-Valle, R., Rami, L., and Bartrés-Faz, D. (2013). Cognitive reserve proxies relate to gray matter loss in cognitively healthy elderly with abnormal cerebrospinal fluid amyloid- β levels. *Journal of Alzheimer’s disease : JAD*, 35(4):715–26.
- Ashburner, J. and Friston, K. J. (2000). Voxel-based morphometry—the methods. *NeuroImage*, 11(6 Pt 1):805–21.
- Baddeley, A. D. (1986). *Working Memory*. Oxford: Clarendon Press.
- Baggio, H.-C., Sala-Llloch, R., Segura, B., Martí, M.-J., Valldeoriola, F., Compta, Y., Tolosa, E., and Junqué, C. (2014a). Functional brain networks and cognitive deficits in Parkinson’s disease. *Human brain mapping*, 35(9):4620–34.
- Baggio, H.-C., Segura, B., Sala-Llloch, R., Martí, M.-J., Valldeoriola, F., Compta, Y., Tolosa, E., and Junqué, C. (2014b). Cognitive impairment and resting-state network connectivity in Parkinson’s disease. *Human brain mapping*.
- Barkhof, F., Haller, S., and Rombouts, S. A. R. B. (2014). Resting-state functional MR imaging: a new window to the brain. *Radiology*, 272(1):29–49.
- Basser, P. J., Mattiello, J., and LeBihan, D. (1994). Estimation of the effective self-diffusion tensor from the NMR spin echo. *Journal of magnetic resonance. Series B*, 103(3):247–54.
- Basser, P. J. and Pierpaoli, C. (1996). Microstructural and physiological features of tissues elucidated by quantitative-diffusion-tensor MRI. *Journal of magnetic resonance. Series B*, 111(3):209–19.

- Beckmann, C. F., DeLuca, M., Devlin, J. T., and Smith, S. M. (2005). Investigations into resting-state connectivity using independent component analysis. *Philosophical transactions of the Royal Society of London. Series B, Biological sciences*, 360(1457):1001–13.
- Beckmann, C. F. and Smith, S. M. (2004). Probabilistic independent component analysis for functional magnetic resonance imaging. *IEEE transactions on medical imaging*, 23(2):137–52.
- Behrens, T. E. J., Johansen-Berg, H., Woolrich, M. W., Smith, S. M., Wheeler-Kingshott, C. A. M., Boulby, P. A., Barker, G. J., Sillery, E. L., Sheehan, K., Ciccarelli, O., Thompson, A. J., Brady, J. M., and Matthews, P. M. (2003a). Non-invasive mapping of connections between human thalamus and cortex using diffusion imaging. *Nature neuroscience*, 6(7):750–7.
- Behrens, T. E. J. and Sporns, O. (2012). Human connectomics. *Current opinion in neurobiology*, 22(1):144–53.
- Behrens, T. E. J., Woolrich, M. W., Jenkinson, M., Johansen-Berg, H., Nunes, R. G., Clare, S., Matthews, P. M., Brady, J. M., and Smith, S. M. (2003b). Characterization and propagation of uncertainty in diffusion-weighted MR imaging. *Magnetic resonance in medicine*, 50(5):1077–88.
- Betzal, R. F., Byrge, L., He, Y., Goñi, J., Zuo, X.-N., and Sporns, O. (2014). Changes in structural and functional connectivity among resting-state networks across the human lifespan. *NeuroImage*.
- Biswal, B., Yetkin, F. Z., Haughton, V. M., and Hyde, J. S. (1995). Functional connectivity in the motor cortex of resting human brain using echo-planar MRI. *Magnetic resonance in medicine*, 34(4):537–41.
- Bosch, B., Arenaza-Urquijo, E. M., Rami, L., Sala-Llonch, R., Junqué, C., Solé-Padullés, C., Peña Gómez, C., Bargalló, N., Molinuevo, J. L., and Bartrés-Faz, D. (2012). Multiple DTI index analysis in normal aging, amnesic MCI and AD. Relationship with neuropsychological performance. *Neurobiology of aging*, 33(1):61–74.
- Braver, T. S., Cohen, J. D., Nystrom, L. E., Jonides, J., Smith, E. E., and Noll, D. C. (1997). A parametric study of prefrontal cortex involvement in human working memory. *NeuroImage*, 5(1):49–62.
- Buckner, R. L., Andrews-Hanna, J. R., and Schacter, D. L. (2008). The brain’s default network: anatomy, function, and relevance to disease. *Annals of the New York Academy of Sciences*, 1124:1–38.
- Buckner, R. L., Sepulcre, J., Talukdar, T., Krienen, F. M., Liu, H., Hedden, T., Andrews-Hanna, J. R., Sperling, R. A., and Johnson, K. A. (2009). Cortical hubs revealed by intrinsic functional connectivity: mapping, assessment of stability, and relation to Alzheimer’s disease. *The Journal of neuroscience*, 29(6):1860–73.
- Buckner, R. L., Snyder, A. Z., Shannon, B. J., LaRossa, G., Sachs, R., Fotenos, A. F., Sheline, Y. I., Klunk, W. E., Mathis, C. A., Morris, J. C., and Mintun, M. A. (2005). Molecular, structural, and functional characterization of Alzheimer’s disease: evidence for a relationship between default activity, amyloid, and memory. *The Journal of neuroscience*, 25(34):7709–17.
- Bullmore, E. and Sporns, O. (2009). Complex brain networks: graph theoretical analysis of structural and functional systems. *Nature reviews. Neuroscience*, 10(3):186–98.
- Bullmore, E. T. and Bassett, D. S. (2011). Brain graphs: graphical models of the human brain connectome. *Annual review of clinical psychology*, 7(November 2010):113–40.
- Cabeza, R. (2002). Hemispheric asymmetry reduction in older adults: The HAROLD model. *Psychology and Aging*, 17(1):85–100.
- Cabeza, R. (2004). Task-independent and Task-specific Age Effects on Brain Activity during Working Memory, Visual Attention and Episodic Retrieval. *Cerebral Cortex*, 14(4):364–375.
- Cabeza, R., Anderson, N. D., Locantore, J. K., and McIntosh, A. R. (2002). Aging gracefully: compensatory brain activity in high-performing older adults. *NeuroImage*, 17(3):1394–402.
- Cabeza, R. and Dennis, N. a. (2013). Principles of frontal lobe function (eds. Donald T. Stuss, Robert T. Knight). Oxford University Press.

- Cabeza, R., Grady, C. L., Nyberg, L., McIntosh, a. R., Tulving, E., Kapur, S., Jennings, J. M., Houle, S., and Craik, F. I. (1997). Age-related differences in neural activity during memory encoding and retrieval: a positron emission tomography study. *The Journal of neuroscience*, 17(1):391–400.
- Campbell, K. L., Grady, C. L., Ng, C., and Hasher, L. (2012). Age differences in the frontoparietal cognitive control network: implications for distractibility. *Neuropsychologia*, 50(9):2212–23.
- Catani, M., Thiebaut de Schotten, M., Slater, D., and Dell’Acqua, F. (2013). Connectomic approaches before the connectome. *NeuroImage*, 80:2–13.
- Cauda, F., Geminiani, G., D’Agata, F., Sacco, K., Duca, S., Bagshaw, A. P., and Cavanna, A. E. (2010). Functional connectivity of the postero-medial cortex. *PLoS one*, 5(9).
- Cavanna, A. E. and Trimble, M. R. (2006). The precuneus: a review of its functional anatomy and behavioural correlates. *Brain*, 129(Pt 3):564–83.
- Chhatwal, J. P. and Sperling, R. A. (2012). Functional MRI of mnemonic networks across the spectrum of normal aging, mild cognitive impairment, and Alzheimer’s disease. *Journal of Alzheimer’s disease : JAD*, 31 Suppl 3:S155–67.
- Cole, D. M., Smith, S. M., and Beckmann, C. F. (2010). Advances and pitfalls in the analysis and interpretation of resting-state fMRI data. *Frontiers in systems neuroscience*, 4:8.
- Cole, M. W., Bassett, D. S., Power, J. D., Braver, T. S., and Petersen, S. E. (2014). Intrinsic and task-evoked network architectures of the human brain. *Neuron*, 83(1):238–51.
- Cordes, D., Haughton, V. M., Arfanakis, K., Carew, J. D., Turski, P. a., Moritz, C. H., Quigley, M. a., and Meyerand, M. E. (2001). Frequencies contributing to functional connectivity in the cerebral cortex in “resting-state” data. *AJNR. American journal of neuroradiology*, 22(7):1326–33.
- Crossley, N. A., Mechelli, A., Scott, J., Carletti, F., Fox, P. T., McGuire, P., and Bullmore, E. T. (2014). The hubs of the human connectome are generally implicated in the anatomy of brain disorders. *Brain*, 137(Pt 8):2382–95.
- Crossley, N. A., Mechelli, A., Vértes, P. E., Winton-Brown, T. T., Patel, A. X., Ginestet, C. E., McGuire, P., and Bullmore, E. T. (2013). Cognitive relevance of the community structure of the human brain functional coactivation network. *Proceedings of the National Academy of Sciences of the United States of America*, 110(28):11583–8.
- Damoiseaux, J. S., Beckmann, C. F., Arigita, E. J. S., Barkhof, F., Scheltens, P., Stam, C. J., Smith, S. M., and Rombouts, S. a. R. B. (2008). Reduced resting-state brain activity in the “default network” in normal aging. *Cerebral cortex*, 18(8):1856–64.
- Damoiseaux, J. S., Rombouts, S. A. R. B., Barkhof, F., Scheltens, P., Stam, C. J., Smith, S. M., and Beckmann, C. F. (2006). Consistent resting-state networks across healthy subjects. *Proceedings of the National Academy of Sciences of the United States of America*, 103(37):13848–53.
- Damoiseaux, J. S., Seeley, W. W., Zhou, J., Shirer, W. R., Coppola, G., Karydas, A., Rosen, H. J., Miller, B. L., Kramer, J. H., and Greicius, M. D. (2012). Gender modulates the APOE ϵ 4 effect in healthy older adults: convergent evidence from functional brain connectivity and spinal fluid tau levels. *The Journal of neuroscience*, 32(24):8254–62.
- Daselaar, S. M., Fleck, M. S., Dobbins, I. G., Madden, D. J., and Cabeza, R. (2006). Effects of healthy aging on hippocampal and rhinal memory functions: an event-related fMRI study. *Cerebral cortex*, 16(12):1771–82.
- Daselaar, S. M., Prince, S. E., and Cabeza, R. (2004). When less means more: deactivations during encoding that predict subsequent memory. *NeuroImage*, 23(3):921–7.
- Davis, S. W., Dennis, N. a., Daselaar, S. M., Fleck, M. S., and Cabeza, R. (2008). Que PASA? The posterior-anterior shift in aging. *Cerebral Cortex*, 18(5):1201–9.
- de Chastelaine, M., Wang, T. H., Minton, B., Mufftler, L. T., and Rugg, M. D. (2011). The effects of age, memory performance, and callosal integrity on the neural correlates of successful associative encoding. *Cerebral cortex*, 21(9):2166–76.
- Dennis, E. L. and Thompson, P. M. (2014). Functional brain connectivity using fMRI in aging

- and Alzheimer's disease. *Neuropsychology review*, 24(1):49–62.
- Dennis, N. A., Hayes, S. M., Prince, S. E., Madden, D. J., Huettel, S. A., and Cabeza, R. (2008). Effects of aging on the neural correlates of successful item and source memory encoding. *Journal of experimental psychology. Learning, memory, and cognition*, 34(4):791–808.
- Desikan, R. S., Ségonne, F., Fischl, B., Quinn, B. T., Dickerson, B. C., Blacker, D., Buckner, R. L., Dale, A. M., Maguire, R. P., Hyman, B. T., Albert, M. S., and Killiany, R. J. (2006). An automated labeling system for subdividing the human cerebral cortex on MRI scans into gyral based regions of interest. *NeuroImage*, 31(3):968–80.
- D'Esposito, M., Aguirre, G. K., Zarahn, E., Ballard, D., Shin, R. K., and Lease, J. (1998). Functional MRI studies of spatial and nonspatial working memory. *Brain research. Cognitive brain research*, 7(1):1–13.
- Destrieux, C., Fischl, B., Dale, A., and Halgren, E. (2010). Automatic parcellation of human cortical gyri and sulci using standard anatomical nomenclature. *NeuroImage*, 53(1):1–15.
- Dickerson, B. C., Salat, D. H., Greve, D. N., Chua, E. F., Rand-Giovannetti, E., Rentz, D. M., Bertram, L., Mullin, K., Tanzi, R. E., Blacker, D., Albert, M. S., and Sperling, R. A. (2005). Increased hippocampal activation in mild cognitive impairment compared to normal aging and AD. *Neurology*, 65(3):404–11.
- Ferreira, L. K. and Busatto, G. F. (2013). Resting-state functional connectivity in normal brain aging. *Neuroscience and biobehavioral reviews*, 37(3):384–400.
- Filippini, N., MacIntosh, B. J., Hough, M. G., Goodwin, G. M., Frisoni, G. B., Smith, S. M., Matthews, P. M., Beckmann, C. F., and Mackay, C. E. (2009). Distinct patterns of brain activity in young carriers of the APOE-epsilon4 allele. *Proceedings of the National Academy of Sciences of the United States of America*, 106(17):7209–14.
- Fischl, B. and Dale, A. M. (2000). Measuring the thickness of the human cerebral cortex from magnetic resonance images. *Proceedings of the National Academy of Sciences of the United States of America*, 97(20):11050–5.
- Fortea, J., Lladó, A., Clarimón, J., Lleó, A., Oliva, R., Peri, J., Pintor, L., Yagüe, J., Blesa, R., Molinuevo, J. L., and Sánchez-Valle, R. (2011a). PICOGEN: five years experience with a genetic counselling program for dementia. *Neurología*, 26(3):143–9.
- Fortea, J., Sala-Llonch, R., Bartrés-Faz, D., Bosch, B., Lladó, A., Bargalló, N., Molinuevo, J. L., and Sánchez-Valle, R. (2010). Increased cortical thickness and caudate volume precede atrophy in PSEN1 mutation carriers. *Journal of Alzheimer's disease : JAD*, 22(3):909–22.
- Fortea, J., Sala-Llonch, R., Bartrés-Faz, D., Lladó, A., Solé-Padullés, C., Bosch, B., Antonell, A., Olives, J., Sanchez-Valle, R., Molinuevo, J. L., and Rami, L. (2011b). Cognitively preserved subjects with transitional cerebrospinal fluid β -amyloid 1-42 values have thicker cortex in Alzheimer's disease vulnerable areas. *Biological psychiatry*, 70(2):183–90.
- Fox, M. D., Snyder, A. Z., Vincent, J. L., Corbetta, M., Van Essen, D. C., and Raichle, M. E. (2005). The human brain is intrinsically organized into dynamic, anticorrelated functional networks. *Proceedings of the National Academy of Sciences of the United States of America*, 102(27):9673–8.
- Fox, M. D., Snyder, A. Z., Vincent, J. L., and Raichle, M. E. (2007). Intrinsic fluctuations within cortical systems account for inter-trial variability in human behavior. *Neuron*, 56(1):171–84.
- Fransson, P. (2005). Spontaneous low-frequency BOLD signal fluctuations: an fMRI investigation of the resting-state default mode of brain function hypothesis. *Human brain mapping*, 26(1):15–29.
- Friston, K. J. (1994). Functional and effective connectivity in neuroimaging: A synthesis. *Human Brain Mapping*, 2(1-2):56–78.
- Fuster, J. M. (1997). Network memory. *Trends in neurosciences*, 20(10):451–9.
- García-García, I., Jurado, M. A., Garolera, M., Segura, B., Marqués-Iturria, I., Pueyo, R., Vernet-Vernet, M., Sender-Palacios, M. J., Sala-Llonch, R., Ariza, M., Narberhaus, A., and Junqué, C. (2012). Functional connectivity in obesity during reward processing. *NeuroImage*, 66C:232–239.

- García-García, I., Jurado, M. A., Garolera, M., Segura, B., Sala-Llonch, R., Marqués-Iturria, I., Pueyo, R., Sender-Palacios, M. J., Vernet-Vernet, M., Narberhaus, A., Ariza, M., and Junqué, C. (2013). Alterations of the salience network in obesity: a resting-state fMRI study. *Human brain mapping*, 34(11):2786–97.
- Geerligs, L., Renken, R. J., Saliassi, E., Maurits, N. M., and Lorist, M. M. (2014). A Brain-Wide Study of Age-Related Changes in Functional Connectivity. *Cerebral cortex*, 2:1–13.
- Gong, G., He, Y., Concha, L., Lebel, C., Gross, D. W., Evans, A. C., and Beaulieu, C. (2009). Mapping anatomical connectivity patterns of human cerebral cortex using in vivo diffusion tensor imaging tractography. *Cerebral cortex*, 19(3):524–36.
- Grady, C. (2012). The cognitive neuroscience of ageing. *Nature reviews. Neuroscience*, 13(7):491–505.
- Grady, C. L., Maisog, J. M., Horwitz, B., Ungerleider, L. G., Mentis, M. J., Salerno, J. A., Pietrini, P., Wagner, E., and Haxby, J. V. (1994). Age-related changes in cortical blood flow activation during visual processing of faces and location. *The Journal of neuroscience*, 14(3 Pt 2):1450–62.
- Grady, C. L., Springer, M. V., Hongwanishkul, D., McIntosh, A. R., and Winocur, G. (2006). Age-related changes in brain activity across the adult lifespan. *Journal of cognitive neuroscience*, 18(2):227–41.
- Greicius, M. D., Krasnow, B., Reiss, A. L., and Menon, V. (2003). Functional connectivity in the resting brain: a network analysis of the default mode hypothesis. *Proceedings of the National Academy of Sciences of the United States of America*, 100(1):253–8.
- Greicius, M. D., Srivastava, G., Reiss, A. L., and Menon, V. (2004). Default-mode network activity distinguishes Alzheimer’s disease from healthy aging: evidence from functional MRI. *Proceedings of the National Academy of Sciences of the United States of America*, 101(13):4637–42.
- Griffanti, L., Salimi-Khorshidi, G., Beckmann, C. F., Auerbach, E. J., Douaud, G., Sexton, C. E., Zsoldos, E., Ebmeier, K. P., Filippini, N., Mackay, C. E., Moeller, S., Xu, J., Yacoub, E., Baselli, G., Ugurbil, K., Miller, K. L., and Smith, S. M. (2014). ICA-based artefact removal and accelerated fMRI acquisition for improved resting state network imaging. *NeuroImage*, 95:232–47.
- Guo, C. C., Kurth, F., Zhou, J., Mayer, E. A., Eickhoff, S. B., Kramer, J. H., and Seeley, W. W. (2012). One-year test-retest reliability of intrinsic connectivity network fMRI in older adults. *NeuroImage*, 61(4):1471–83.
- Gusnard, D. A. and Raichle, M. E. (2001). Searching for a baseline: functional imaging and the resting human brain. *Nature reviews. Neuroscience*, 2(10):685–94.
- Hagmann, P., Cammoun, L., Gigandet, X., Meuli, R., Honey, C. J., Wedeen, V. J., and Sporns, O. (2008). Mapping the structural core of human cerebral cortex. *PLoS biology*, 6(7):e159.
- Haxby, J. V., Gobbini, M. I., Furey, M. L., Ishai, A., Schouten, J. L., and Pietrini, P. (2001). Distributed and overlapping representations of faces and objects in ventral temporal cortex. *Science*, 293(5539):2425–30.
- Hayes, A. F. (2009). Beyond Baron and Kenny: Statistical Mediation Analysis in the New Millennium. *Communication Monographs*, 76(4).
- He, Y., Chen, Z. J., and Evans, A. C. (2007). Small-world anatomical networks in the human brain revealed by cortical thickness from MRI. *Cerebral cortex*, 17(10):2407–19.
- Hedden, T., Van Dijk, K. R. a., Becker, J. A., Mehta, A., Sperling, R. a., Johnson, K. a., and Buckner, R. L. (2009). Disruption of functional connectivity in clinically normal older adults harboring amyloid burden. *The Journal of neuroscience*, 29(40):12686–94.
- Honey, C. J., Sporns, O., Cammoun, L., Gigandet, X., Thiran, J. P., Meuli, R., and Hagmann, P. (2009). Predicting human resting-state functional connectivity from structural connectivity. *Proceedings of the National Academy of Sciences of the United States of America*, 106(6):2035–40.
- Huijbers, W., Vannini, P., Sperling, R. A., C M, P., Cabeza, R., and Daselaar, S. M. (2012). Explaining the encoding/retrieval flip: memory-related deactivations and activations in the posteromedial cortex. *Neuropsychologia*, 50(14):3764–74.

- Jenkinson, M., Bannister, P., Brady, M., and Smith, S. (2002). Improved optimization for the robust and accurate linear registration and motion correction of brain images. *NeuroImage*, 17(2):825–41.
- Jones, D. K., Knösche, T. R., and Turner, R. (2013). White matter integrity, fiber count, and other fallacies: the do’s and don’ts of diffusion MRI. *NeuroImage*, 73:239–54.
- Jones, D. T., Machulda, M. M., Vemuri, P., McDade, E. M., Zeng, G., Senjem, M. L., Gunter, J. L., Przybelski, S. A., Avula, R. T., Knopman, D. S., Boeve, B. F., Petersen, R. C., and Jack, C. R. (2011). Age-related changes in the default mode network are more advanced in Alzheimer disease. *Neurology*, 77(16):1524–31.
- Jovicich, J., Marizzoni, M., Sala-Llonch, R., Bosch, B., Bartrés-Faz, D., Arnold, J., Benninghoff, J., Wiltfang, J., Roccatagliata, L., Nobili, F., Hensch, T., Tränkner, A., Schönknecht, P., Leroy, M., Lopes, R., Bordet, R., Chanoine, V., Ranjeva, J.-P., Didic, M., Gros-Dagnac, H., Payoux, P., Zoccatelli, G., Alessandrini, F., Beltramello, A., Bargalló, N., Blin, O., and Frisoni, G. B. (2013). Brain morphometry reproducibility in multi-center 3T MRI studies: a comparison of cross-sectional and longitudinal segmentations. *NeuroImage*, 83:472–84.
- Kanwisher, N. (2010). Functional specificity in the human brain: a window into the functional architecture of the mind. *Proceedings of the National Academy of Sciences of the United States of America*, 107(25):11163–70.
- Kim, H. (2011). Neural activity that predicts subsequent memory and forgetting: a meta-analysis of 74 fMRI studies. *NeuroImage*, 54(3):2446–61.
- Laird, A. R., Eickhoff, S. B., Rottschy, C., Bzdok, D., Ray, K. L., and Fox, P. T. (2013). Networks of task co-activations. *NeuroImage*, 80:505–14.
- Laird, A. R., Lancaster, J. L., and Fox, P. T. (2005). BrainMap: the social evolution of a human brain mapping database. *Neuroinformatics*, 3(1):65–78.
- Le Bihan, D. (1991). Molecular diffusion nuclear magnetic resonance imaging. *Magnetic resonance quarterly*, 7(1):1–30.
- Le Bihan, D. (2003). Looking into the functional architecture of the brain with diffusion MRI. *Nature reviews. Neuroscience*, 4(6):469–80.
- Lee, M. H., Smyser, C. D., and Shimony, J. S. (2013). Resting-state fMRI: a review of methods and clinical applications. *AJNR. American journal of neuroradiology*, 34(10):1866–72.
- Li, S. C., Lindenberger, U., and Sikström, S. (2001). Aging cognition: from neuromodulation to representation. *Trends in cognitive sciences*, 5(11):479–486.
- Logothetis, N. K. (2003). The underpinnings of the BOLD functional magnetic resonance imaging signal. *The Journal of neuroscience*, 23(10):3963–71.
- Logothetis, N. K., Pauls, J., Augath, M., Trinath, T., and Oeltermann, A. (2001). Neurophysiological investigation of the basis of the fMRI signal. *Nature*, 412(6843):150–7.
- Lustig, C., Snyder, A. Z., Bhakta, M., O’Brien, K. C., McAvoy, M., Raichle, M. E., Morris, J. C., and Buckner, R. L. (2003). Functional deactivations: change with age and dementia of the Alzheimer type. *Proceedings of the National Academy of Sciences of the United States of America*, 100(24):14504–9.
- Madden, D. J., Costello, M. C., Dennis, N. a., Davis, S. W., Shepler, A. M., Spaniol, J., Bucur, B., and Cabeza, R. (2010). Adult age differences in functional connectivity during executive control. *NeuroImage*, 52(2):643–57.
- Madden, D. J., Gottlob, L. R., Denny, L. L., Turkington, T. G., Provenzale, J. M., Hawk, T. C., and Coleman, R. E. (1999). Aging and recognition memory: changes in regional cerebral blood flow associated with components of reaction time distributions. *Journal of cognitive neuroscience*, 11(5):511–20.
- Mattay, V. S., Fera, F., Tessitore, A., Hariri, A. R., Berman, K. F., Das, S., Meyer-Lindenberg, A., Goldberg, T. E., Callicott, J. H., and Weinberger, D. R. (2006). Neurophysiological correlates of age-related changes in working memory capacity. *Neuroscience letters*, 392(1-2):32–7.
- Matthews, P. M., Filippini, N., and Douaud, G. (2013). Brain structural and functional connectivity and the progression of neuropathology in Alzheimer’s disease. *Journal of Alzheimer’s disease : JAD*, 33 Suppl 1:S163–72.

- Meunier, D., Achard, S., Morcom, A., and Bullmore, E. (2009). Age-related changes in modular organization of human brain functional networks. *NeuroImage*, 44(3):715–23.
- Miller, S. L., Celone, K., DePeau, K., Diamond, E., Dickerson, B. C., Rentz, D., Pihlajamäki, M., and Sperling, R. A. (2008). Age-related memory impairment associated with loss of parietal deactivation but preserved hippocampal activation. *Proceedings of the National Academy of Sciences of the United States of America*, 105(6):2181–6.
- Minear, M. and Park, D. C. (2004). A lifespan database of adult facial stimuli. *Behavior research methods, instruments, & computers*, 36(4):630–3.
- Moreno*, F., Sala-Llloch*, R., Barandiaran, M., Sánchez-Valle, R., Estanga, A., Bartrés-Faz, D., Sistiaga, A., Alzualde, A., Fernández, E., Martí Massó, J. F., López de Munain, A., and Indakoetxea, B. n. (2013). Distinctive age-related temporal cortical thinning in asymptomatic granulin gene mutation carriers. *Neurobiology of aging*, 34(5):1462–8.
- Mori, S. and Zhang, J. (2006). Principles of diffusion tensor imaging and its applications to basic neuroscience research. *Neuron*, 51(5):527–39.
- Nagel, I. E., Preuschhof, C., Li, S.-C., Nyberg, L., Bäckman, L., Lindenberger, U., and Heekeren, H. R. (2011). Load modulation of BOLD response and connectivity predicts working memory performance in younger and older adults. *Journal of cognitive neuroscience*, 23(8):2030–45.
- Nichols, T. E. and Holmes, A. P. (2002). Nonparametric permutation tests for functional neuroimaging: a primer with examples. *Human brain mapping*, 15(1):1–25.
- Onoda, K., Ishihara, M., and Yamaguchi, S. (2012). Decreased functional connectivity by aging is associated with cognitive decline. *Journal of cognitive neuroscience*, 24(11):2186–98.
- Owen, A. M., McMillan, K. M., Laird, A. R., and Bullmore, E. (2005). N-back working memory paradigm: a meta-analysis of normative functional neuroimaging studies. *Human brain mapping*, 25(1):46–59.
- Palacios, E. M., Sala-Llloch, R., Junque, C., Fernandez-Espejo, D., Roig, T., Tormos, J. M., Bargallo, N., and Vendrell, P. (2013). Long-term declarative memory deficits in diffuse TBI: correlations with cortical thickness, white matter integrity and hippocampal volume. *Cortex*, 49(3):646–57.
- Palacios, E. M., Sala-Llloch, R., Junque, C., Roig, T., Tormos, J. M., Bargallo, N., and Vendrell, P. (2012). White matter integrity related to functional working memory networks in traumatic brain injury. *Neurology*, 78(12):852–60.
- Palacios*, E. M., Sala-Llloch*, R., Junque, C., Roig, T., Tormos, J. M., Bargallo, N., and Vendrell, P. (2013a). Resting-state functional magnetic resonance imaging activity and connectivity and cognitive outcome in traumatic brain injury. *JAMA neurology*, 70(7):845–51.
- Palacios*, E. M., Sala-Llloch*, R., Junque, C., Roig, T., Tormos, J. M., Bargallo, N., and Vendrell, P. (2013b). White matter/gray matter contrast changes in chronic and diffuse traumatic brain injury. *Journal of neurotrauma*, 30(23):1991–4.
- Park, D. C., Polk, T. A., Park, R., Minear, M., Savage, A., and Smith, M. R. (2004). Aging reduces neural specialization in ventral visual cortex. *Proceedings of the National Academy of Sciences of the United States of America*, 101(35):13091–5.
- Park, D. C. and Reuter-Lorenz, P. (2009). The adaptive brain: aging and neurocognitive scaffolding. *Annual review of psychology*, 60:173–96.
- Park, H.-J. and Friston, K. (2013). Structural and functional brain networks: from connections to cognition. *Science*, 342(6158):1238411.
- Peña Gómez, C., Sala-Llloch, R., Junqué, C., Clemente, I. C., Vidal, D., Bargalló, N., Falcón, C., Valls-Solé, J., Pascual-Leone, A., and Bartrés-Faz, D. (2012). Modulation of large-scale brain networks by transcranial direct current stimulation evidenced by resting-state functional MRI. *Brain stimulation*, 5(3):252–63.
- Pereira, J. B., Junqué, C., Bartrés-Faz, D., Martí, M. J., Sala-Llloch, R., Compta, Y., Falcón, C., Vendrell, P., Pascual-Leone, A., Valls-Solé, J., and Tolosa, E. (2013). Modulation of verbal fluency networks by transcranial direct current stimulation (tDCS) in Parkinson's disease. *Brain stimulation*, 6(1):16–24.

- Petersen, R. C., Roberts, R. O., Knopman, D. S., Boeve, B. F., Geda, Y. E., Ivnik, R. J., Smith, G. E., and Jack, C. R. (2009). Mild cognitive impairment: ten years later. *Archives of neurology*, 66(12):1447–55.
- Pihlajamäki, M. and Sperling, R. A. (2009). Functional MRI assessment of task-induced deactivation of the default mode network in Alzheimer’s disease and at-risk older individuals. *Behavioural neurology*, 21(1):77–91.
- Power, J. D., Schlaggar, B. L., Lessov-Schlaggar, C. N., and Petersen, S. E. (2013). Evidence for hubs in human functional brain networks. *Neuron*, 79(4):798–813.
- Preacher, K. and Hayes, A. (2008). Asymptotic and resampling strategies for assessing and comparing indirect effects in multiple mediator models. *Behavior Research Methods*, 40(3):879–891.
- Raichle, M. E., MacLeod, A. M., Snyder, A. Z., Powers, W. J., Gusnard, D. A., and Shulman, G. L. (2001). A default mode of brain function. *Proceedings of the National Academy of Sciences of the United States of America*, 98(2):676–82.
- Raichle, M. E. and Mintun, M. A. (2006). Brain work and brain imaging. *Annual review of neuroscience*, 29:449–76.
- Rajah, M. N. and D’Esposito, M. (2005). Region-specific changes in prefrontal function with age: a review of PET and fMRI studies on working and episodic memory. *Brain*, 128(Pt 9):1964–83.
- Rami, L., Sala-Llloch, R., Solé-Padullés, C., Fortea, J., Olives, J., Lladó, A., Peña Gómez, C., Balasa, M., Bosch, B., Antonell, A., Sanchez-Valle, R., Bartrés-Faz, D., and Molinuevo, J. L. (2012). Distinct functional activity of the precuneus and posterior cingulate cortex during encoding in the preclinical stage of Alzheimer’s disease. *Journal of Alzheimer’s disease : JAD*, 31(3):517–26.
- Reuter-Lorenz, P. and Cappell, K. a. (2008). Neurocognitive aging and the compensation hypothesis. *Current Directions in Psychological Science*, 17:177–182.
- Rottschy, C., Langner, R., Dogan, I., Reetz, K., Laird, A. R., Schulz, J. B., Fox, P. T., and Eickhoff, S. B. (2012). Modelling neural correlates of working memory: a coordinate-based meta-analysis. *NeuroImage*, 60(1):830–46.
- Rubinov, M. and Sporns, O. (2010). Complex network measures of brain connectivity: uses and interpretations. *NeuroImage*, 52(3):1059–69.
- Sadaghiani, S. and Kleinschmidt, A. (2013). Functional interactions between intrinsic brain activity and behavior. *NeuroImage*, 80:379–86.
- Sala-Llloch, R., Arenaza-Urquijo, E. M., Valls-Pedret, C., Vidal-Piñeiro, D., Bargalló, N., Junqué, C., and Bartrés-Faz, D. (2012a). Dynamic functional reorganizations and relationship with working memory performance in healthy aging. *Frontiers in human neuroscience*, 6(June):152.
- Sala-Llloch, R., Bosch, B., Arenaza-Urquijo, E. M., Rami, L., Bargalló, N., Junqué, C., Molinuevo, J.-L., and Bartrés-Faz, D. (2010). Greater default-mode network abnormalities compared to high order visual processing systems in amnesic mild cognitive impairment: an integrated multi-modal MRI study. *Journal of Alzheimer’s disease : JAD*, 22(2):523–39.
- Sala-Llloch, R., Fortea, J., Bartrés-Faz, D., Bosch, B., Lladó, A., Peña Gómez, C., Antonell, A., Castellanos-Pinedo, F., Bargalló, N., Molinuevo, J. L., and Sánchez-Valle, R. (2013). Evolving brain functional abnormalities in PSEN1 mutation carriers: a resting and visual encoding fMRI study. *Journal of Alzheimer’s disease : JAD*, 36(1):165–75.
- Sala-Llloch, R., Junqué, C., Arenaza-Urquijo, E. M., Vidal-Piñeiro, D., Valls-Pedret, C., Palacios, E. M., Domènech, S., Salvà, A., Bargalló, N., and Bartrés-Faz, D. (2014). Changes in whole-brain functional networks and memory performance in aging. *Neurobiology of aging*, 35(10):2193–202.
- Sala-Llloch, R., Peña Gómez, C., Arenaza-Urquijo, E. M., Vidal-Piñeiro, D., Bargalló, N., Junqué, C., and Bartrés-Faz, D. (2012b). Brain connectivity during resting state and subsequent working memory task predicts behavioural performance. *Cortex*, 48(9):1187–96.
- Salthouse, T. a. (2011). Neuroanatomical substrates of age-related cognitive decline. *Psychological bulletin*, 137(5):753–84.

- Schölvinck, M. L., Maier, A., Ye, F. Q., Duyn, J. H., and Leopold, D. A. (2010). Neural basis of global resting-state fMRI activity. *Proceedings of the National Academy of Sciences of the United States of America*, 107(22):10238–43.
- Schwindt, G. C. and Black, S. E. (2009). Functional imaging studies of episodic memory in Alzheimer’s disease: a quantitative meta-analysis. *NeuroImage*, 45(1):181–90.
- Seeley, W. W., Crawford, R. K., Zhou, J., Miller, B. L., and Greicius, M. D. (2009). Neurodegenerative diseases target large-scale human brain networks. *Neuron*, 62(1):42–52.
- Segura, B., Ibarretxe-Bilbao, N., Sala-Llonch, R., Baggio, H. C., Martí, M. J., Valldeoriola, F., Vendrell, P., Bargalló, N., Tolosa, E., and Junqué, C. (2013). Progressive changes in a recognition memory network in Parkinson’s disease. *Journal of neurology, neurosurgery, and psychiatry*, 84(4):370–8.
- Sheline, Y. I. and Raichle, M. E. (2013). Resting state functional connectivity in preclinical Alzheimer’s disease. *Biological psychiatry*, 74(5):340–7.
- Sheline, Y. I., Raichle, M. E., Snyder, A. Z., Morris, J. C., Head, D., Wang, S., and Mintun, M. a. (2010). Amyloid plaques disrupt resting state default mode network connectivity in cognitively normal elderly. *Biological psychiatry*, 67(6):584–7.
- Shulman, G. L., Fiez, J. A., Corbetta, M., Buckner, R. L., Miezin, F. M., Raichle, M. E., and Petersen, S. E. (1997). Common Blood Flow Changes across Visual Tasks: II. Decreases in Cerebral Cortex. *Journal of cognitive neuroscience*, 9(5):648–63.
- Smith, S. M. (2002). Fast robust automated brain extraction. *Human brain mapping*, 17(3):143–55.
- Smith, S. M., Fox, P. T., Miller, K. L., Glahn, D. C., Fox, P. M., Mackay, C. E., Filippini, N., Watkins, K. E., Toro, R., Laird, A. R., and Beckmann, C. F. (2009). Correspondence of the brain’s functional architecture during activation an. *Proceedings of the National Academy of Sciences of the United States of America*, 106(31):13040–5.
- Smith, S. M., Miller, K. L., Salimi-Khorshidi, G., Webster, M., Beckmann, C. F., Nichols, T. E., Ramsey, J. D., and Woolrich, M. W. (2011). Network modelling methods for FMRI. *NeuroImage*, 54(2):875–91.
- Smith, S. M., Vidaurre, D., Beckmann, C. F., Glasser, M. F., Jenkinson, M., Miller, K. L., Nichols, T. E., Robinson, E. C., Salimi-Khorshidi, G., Woolrich, M. W., Barch, D. M., Ugurbil, K., and Van Essen, D. C. (2013). Functional connectomics from resting-state fMRI. *Trends in cognitive sciences*, 17(12):666–82.
- Song, J., Birn, R., Boly, M., Meier, T. B., Nair, V. A., Meyerand, M. E., and Prabhakaran, V. (2014). Age-related Reorganizational Changes in Modularity and Functional Connectivity of Human Brain Networks. *Brain connectivity*.
- Sorg, C., Riedl, V., Mühlau, M., Calhoun, V. D., Eichele, T., Läer, L., Drzezga, A., Förstl, H., Kurz, A., Zimmer, C., and Wohlschläger, A. M. (2007). Selective changes of resting-state networks in individuals at risk for Alzheimer’s disease. *Proceedings of the National Academy of Sciences of the United States of America*, 104(47):18760–5.
- Spaniol, J., Davidson, P. S. R., Kim, A. S. N., Han, H., Moscovitch, M., and Grady, C. L. (2009). Event-related fMRI studies of episodic encoding and retrieval: meta-analyses using activation likelihood estimation. *Neuropsychologia*, 47(8-9):1765–79.
- Spaniol, J. and Grady, C. (2012). Aging and the neural correlates of source memory: over-recruitment and functional reorganization. *Neurobiology of aging*, 33(2):425.e3–18.
- Sperling, R. (2011). Potential of functional MRI as a biomarker in early Alzheimer’s disease. *Neurobiology of aging*, 32 Suppl 1:S37–43.
- Sperling, R. A., Laviolette, P. S., O’Keefe, K., O’Brien, J., Rentz, D. M., Pihlajamaki, M., Marshall, G., Hyman, B. T., Selkoe, D. J., Hedden, T., Buckner, R. L., Becker, J. A., and Johnson, K. A. (2009). Amyloid deposition is associated with impaired default network function in older persons without dementia. *Neuron*, 63(2):178–88.
- Sporns, O. (2013a). Structure and function of complex brain networks. *Dialogues in clinical neuroscience*, 15(3):247–62.

- Sporns, O. (2013b). The human connectome: origins and challenges. *NeuroImage*, 80:53–61.
- Tavor, I., Yablonski, M., Mezer, A., Rom, S., Assaf, Y., and Yovel, G. (2014). Separate parts of occipito-temporal white matter fibers are associated with recognition of faces and places. *NeuroImage*, 86:123–30.
- Tomasi, D. and Volkow, N. D. (2012). Aging and functional brain networks. *Molecular psychiatry*, 17(5):471, 549–58.
- Tulving, E. (1987). Multiple memory systems and consciousness. *Human neurobiology*, 6(2):67–80.
- Turner, G. R. and Spreng, R. N. (2012). Executive functions and neurocognitive aging: dissociable patterns of brain activity. *Neurobiology of aging*, 33(4):826.e1–13.
- Tzourio-Mazoyer, N., Landeau, B., Papathanassiou, D., Crivello, F., Etard, O., Delcroix, N., Mazoyer, B., and Joliot, M. (2002). Automated anatomical labeling of activations in SPM using a macroscopic anatomical parcellation of the MNI MRI single-subject brain. *NeuroImage*, 15(1):273–89.
- van den Heuvel, M. P., Mandl, R. C. W., Kahn, R. S., and Hulshoff Pol, H. E. (2009). Functionally linked resting-state networks reflect the underlying structural connectivity architecture of the human brain. *Human brain mapping*, 30(10):3127–41.
- Vannini, P., Hedden, T., Becker, J. A., Sullivan, C., Putcha, D., Rentz, D., Johnson, K. A., and Sperling, R. A. (2012). Age and amyloid-related alterations in default network habituation to stimulus repetition. *Neurobiology of aging*, 33(7):1237–52.
- Vannini, P., Hedden, T., Huijbers, W., Ward, A., Johnson, K. A., and Sperling, R. A. (2013). The ups and downs of the posteromedial cortex: age- and amyloid-related functional alterations of the encoding/retrieval flip in cognitively normal older adults. *Cerebral cortex*, 23(6):1317–28.
- Vannini, P., Lehmann, C., Dierks, T., Jann, K., Vitanen, M., Wahlund, L.-O., and Almkvist, O. (2008). Failure to modulate neural response to increased task demand in mild Alzheimer’s disease: fMRI study of visuospatial processing. *Neurobiology of disease*, 31(3):287–97.
- Vannini, P., O’Brien, J., O’Keefe, K., Pihlajamäki, M., Laviolette, P., and Sperling, R. A. (2011). What goes down must come up: role of the posteromedial cortices in encoding and retrieval. *Cerebral cortex*, 21(1):22–34.
- Vidal-Piñero, D., Martin-Trias, P., Arenaza-Urquijo, E. M., Sala-Llonch, R., Clemente, I. C., Mena-Sánchez, I., Bargalló, N., Falcón, C., Pascual-Leone, A., and Bartrés-Faz, D. (2014a). Task-dependent activity and connectivity predict episodic memory network-based responses to brain stimulation in healthy aging. *Brain stimulation*, 7(2):287–96.
- Vidal-Piñero, D., Valls-Pedret, C., Fernandez-Cabello, S., Arenaza-Urquijo, E. M., Sala-Llonch, R., Solana, E., Bargallo, N., Junque, C., Ros, E., and Bartrés-Faz, D. (2014b). Decreased Default Mode Network connectivity correlates with age-associated structural and cognitive changes. *Frontiers in Aging Neuroscience*, 6(256).
- Vincent, J. L., Snyder, A. Z., Fox, M. D., Shannon, B. J., Andrews, J. R., Raichle, M. E., and Buckner, R. L. (2006). Coherent spontaneous activity identifies a hippocampal-parietal memory network. *Journal of neurophysiology*, 96(6):3517–31.
- Wager, T. D. and Smith, E. E. (2003). Neuroimaging studies of working memory: a meta-analysis. *Cognitive, affective & behavioral neuroscience*, 3(4):255–74.
- Wang, L., Laviolette, P., O’Keefe, K., Putcha, D., Bakkour, A., Van Dijk, K. R. A., Pihlajamäki, M., Dickerson, B. C., and Sperling, R. A. (2010). Intrinsic connectivity between the hippocampus and posteromedial cortex predicts memory performance in cognitively intact older individuals. *NeuroImage*, 51(2):910–7.
- Woolrich, M. W., Ripley, B. D., Brady, M., and Smith, S. M. (2001). Temporal autocorrelation in univariate linear modeling of fMRI data. *NeuroImage*, 14(6):1370–86.
- Zalesky, A., Fornito, A., Harding, I. H., Cocchi, L., Yücel, M., Pantelis, C., and Bullmore, E. T. (2010). Whole-brain anatomical networks: does the choice of nodes matter? *NeuroImage*, 50(3):970–83.
- Zhang, H.-Y., Chen, W.-X., Jiao, Y., Xu, Y., Zhang, X.-R., and Wu, J.-T. (2014). Selective Vulnerability Related to Aging in Large-Scale Resting Brain Networks. *PLoS one*, 9(10):e108807.

- Zhang, Y., Brady, M., and Smith, S. (2001). Segmentation of brain MR images through a hidden Markov random field model and the expectation-maximization algorithm. *IEEE transactions on medical imaging*, 20(1):45–57.
- Zubiaurre-Elorza, L., Soria-Pastor, S., Junque, C., Sala-Llonch, R., Segarra, D., Bargallo, N., and Macaya, A. (2012). Cortical thickness and behavior abnormalities in children born preterm. *PloS one*, 7(7):e42148.